



UNIFORMED SERVICES UNIVERSITY, SCHOOL OF MEDICINE GRADUATE PROGRAMS
 Graduate Education Office (A 1045), 4301 Jones Bridge Road, Bethesda, MD 20814



DISSERTATION APPROVAL FOR THE DOCTORAL DISSERTATION IN THE EMERGING
 INFECTIOUS DISEASES GRADUATE PROGRAM

Title of Dissertation: "Novel Insights into Fur Regulation in *Helicobacter pylori*"

Name of Candidate: Jeremy Gilbreath
 Doctor of Philosophy Degree
 January 10, 2013

DISSERTATION AND ABSTRACT APPROVED:

DATE: 1-10-13
 Dr. Anne E. Jerse
 DEPARTMENT OF MICROBIOLOGY AND IMMUNOLOGY
 Committee Chairperson

1/22/13
 Dr. Scott Merrell
 DEPARTMENT OF MICROBIOLOGY AND IMMUNOLOGY
 Dissertation Advisor

1-10-13
 Dr. Alison D. O'Brien
 DEPARTMENT OF MICROBIOLOGY AND IMMUNOLOGY
 Committee Member

1-10-13
 Dr. Saibal Dey
 Department of BIOCHEMISTRY AND MOLECULAR BIOLOGY
 Committee Member

1-10-13
 Dr. Kevin McIver
 DEPARTMENT OF CELL BIOLOGY AND MOLECULAR GENETICS
 University of Maryland
 Committee Member

The author hereby certifies that the use of any copyrighted material in the thesis manuscript entitled:

“Novel Insights into Fur Regulation in *Helicobacter pylori*”

is appropriately acknowledged and, beyond brief excerpts, is with the permission of the copyright owner.

2013
Jeremy J. Gilbreath
Emerging Infectious Diseases Graduate Program
Department of Microbiology and Immunology
Uniformed Services University
01/07/2013

Abstract

Title of Dissertation:

Novel Insights into Fur Regulation in *Helicobacter pylori*

Jeremy J. Gilbreath, Doctor of Philosophy, 2013

Thesis directed by:

D. Scott Merrell, Ph.D.

Associate Professor, Department of Microbiology and Immunology

Arguably one of the most successful bacterial pathogens, *Helicobacter pylori* colonizes the gastric mucosa of over half of the world's population. As a result of inhabiting this dynamic and tumultuous niche, *H. pylori* must be able to continually adapt to changes in the gastric environment. Many of these adaptive responses are controlled at the transcriptional level by relatively few regulatory proteins; one such protein is the ferric uptake regulator (Fur). In *H. pylori* Fur is a global regulator that is important for initial colonization as well as survival within the gastric niche. *H. pylori* Fur is unique in the extent to which it regulates gene expression; to date no other Fur protein has been shown to activate and repress transcription in both the iron bound (Fe-Fur) and apo (apo-Fur) forms. As such, many aspect of Fur regulation in *H. pylori* are not well understood. We characterized Fe-Fur activation of the *H. pylori oorDABC* genes and demonstrated a need for the distally located Fur box for this activation. Analysis of the *oorDABC* promoter sequence highlighted the possibility of a novel mechanism of Fur-mediated

activation; we hypothesized that Fur competes for binding with another regulatory protein and activates transcription by an anti-repression mechanism. In order to gain insight into how *H. pylori* Fur is able to function in both the iron-bound and *apo* forms, we combined random and site-specific mutagenesis strategies to identify Fur residues important for both Fe-Fur and *apo*-Fur function. Using these strategies, we identified 25 mutations that altered Fe-Fur repression and eight mutations that affected *apo*-Fur repression. Four of these mutations also affected levels of the Fur protein in the cell. From these transcriptional studies, we selected five representative mutations for further study. Of those selected, we were able to successfully purify the wildtype (WT) and three mutant proteins (E5A, A92T, and H134Y). We evaluated these proteins for secondary structure and overall protein fold, the ability to bind iron, oligomerize and bind target DNA sequences in both the fully metallated and *apo* forms. These results showed that these mutated regions play distinct functional roles in Fe-Fur and *apo*-Fur regulation. Taken together, these studies provided novel mechanistic insight into Fe-Fur activation, as well as Fe-Fur and *apo*-Fur repression.

Novel Insights into Fur Regulation in *Helicobacter pylori*

By

Jeremy J. Gilbreath

Dissertation submitted to the Faculty of the
Emerging Infectious Diseases Graduate Program
of the Uniformed Services University of the Health Sciences

F. Edward Hébart School of Medicine

in partial fulfillment of the
requirements for the degree of
Doctor of Philosophy 2013

Acknowledgements

Table of Contents

Approval sheet	i
Copyright Statement	ii
Abstract	iii
Title Page	v
Acknowledgements	vi
Table of Contents	vii
Table of Tables	xii
Table of Figures	xiv
Chapter One: Introduction	17
<i>Helicobacter pylori</i>	17
History and Taxonomy	17
Epidemiology, Disease, and Treatment	19
Niche-specific adaptations and virulence factors	22
Iron uptake, storage, and Fur-mediated gene regulation	26
Iron uptake and storage	26
Fur regulation	27
Iron-bound and <i>apo</i> -Fur regulation	29
Fur Structure	38
Controversy and gaps	44
Goal and Specific Aims	45
Chapter Two: <i>Fur</i> Activates Expression of the 2-Oxoglutarate Oxidoreductase Genes (<i>oorDABC</i>) in <i>Helicobacter pylori</i>	47
Abstract	47
Introduction	48
Materials and Methods	51
Bacterial strains and growth conditions	51
RNA extraction, cDNA synthesis and real-time PCR	54
<i>oorDABC</i> gene junction PCR	55

Primer extension and transcriptional start site (TSS) mapping	55
Construction of P _{oorDABC} ::cat reporter plasmids and strains	56
rFur purification.....	57
rFur fluorescence anisotropy	57
Statistical analyses	59
Results.....	59
The <i>oorDABC</i> genes are co-transcribed as an operon	59
Expression of the <i>oorDABC</i> genes is activated by Fur under iron-replete conditions	60
Fur specifically binds to the putative Fur box in the <i>oorDABC</i> promoter region	64
The Fur box upstream of the <i>oorDABC</i> core promoter is essential for transcriptional activation.....	67
Discussion	70
Acknowledgements.....	79
Chapter Three: <i>Random and Site-Specific Mutagenesis of the Helicobacter pylori Ferric Uptake Regulator Provides Insight into Fur Structure-Function Relationships</i>	80
Abstract.....	80
Introduction.....	81
Results.....	86
Random mutagenesis and manganese selection	86
Screen for altered Pfr expression.....	88
Selection of residues for site-specific mutagenesis	89
Transcriptional analysis of <i>amiE</i> regulation	89
Fur Western blot analysis	99
Purification of recombinant Fur proteins.....	101
Secondary structure content and thermal denaturation.....	104
Iron binding studies	107
DNA binding assays	113
Discussion	116
Materials and Methods.....	132
Strains and growth conditions	132
Random mutagenesis of the <i>H. pylori fur</i> gene	135

Site-specific Fur mutant strains	140
Manganese selection	140
Screen for altered Pfr expression	141
RNA isolation, cDNA synthesis, and quantitative real-time PCR	141
Western blot analysis	142
Recombinant Fur expression strains and protein purification	143
Circular dichroism (CD) spectroscopy	143
Atomic absorption spectrophotometry	144
Oligomerization assays	144
Fluorescence anisotropy	145
Fur protein homology modeling	146
Statistical analysis	146
Acknowledgements	147
Chapter Four: Discussion	148
The logic of gains in Fur function	150
Fe-Fur Activation: an under-appreciated regulatory mechanism	152
The complexity of the <i>H. pylori</i> regulatory network	158
Regulation by small RNAs	160
Iron-bound and <i>apo</i> -Fur box sequences and Fur:DNA interactions	161
Metal ion selectivity <i>in vivo</i>	163
The role of iron and Fur regulation during infection	165
Dissecting the roles of Fe-Fur and <i>apo</i> -Fur regulation <i>in vivo</i>	168
Conclusion	169
References	170
Appendix A: Enterobacterial Common Antigen Mutants of Salmonella enterica serovar Typhimurium Establish a Persistent Infection and Provide Protection Against Subsequent Lethal Challenge	204
Abstract	204
Introduction	205
Materials and Methods	209
Bacterial strains, plasmids, and growth conditions	209

Construction of <i>wecA</i> ::Gm mutant strains	209
Complementation of the <i>wecA</i> mutation.....	212
<i>In vitro</i> characterization of <i>wecA</i> ::Gm and <i>wecA</i> complementation strains	213
Electron microscopy	214
Motility assays	214
<i>In vivo</i> characterization experiments	215
Bacterial load at systemic sites	216
<i>In vivo</i> attenuation and complementation of the <i>wecA</i> mutation	216
Immunization and lethal challenge studies.....	216
Statistical analyses	217
Results.....	217
<i>In vitro</i> characterization of <i>S. Typhimurium wecA</i> mutant strains	217
<i>wecA</i> mutant strains are attenuated <i>in vivo</i>	222
<i>wecA</i> mutant strains establish a persistent infection.....	226
Oral immunization protects against a subsequent oral challenge.....	227
Intraperitoneal immunization protects against subsequent intraperitoneal or oral challenge	233
Discussion	233
References	247
Appendix B: A Core Microbiome Associated with the Peritoneal Tumors of <i>Pseudomyxoma Peritonei</i>	259
Abstract	259
Introduction.....	261
Materials and Methods.....	263
PMP patients	263
DNA extraction, V6 PCR, and sequencing	263
V6 sequence processing and analysis	264
<i>In situ</i> hybridization (ISH) studies.....	265
Culturing and identification of PMP isolates and <i>in vitro</i> characterization.....	267
Clinical trial study design	268
Results.....	268

Sequence analysis and identification of a core PMP Microbiome	268
Direct detection of selected members of the PMP microbiome	278
Isolation and identification bacterial strains associated with PMP	281
Antibiotic treatment efficacy	281
Discussion	288
Acknowledgments	292
References	317

Table of Tables

Table 1. Strains and plasmids used in this study	52
Table 2. Oligonucleotides used in this study	53
Table 3. The <i>oorDABC</i> Fur box is required for activation	71
Table 4. Summary of regulatory phenotypes observed by qRT-PCR	100
Table 5. Summary of Fluorescence anisotropy data	117
Table 6. Summary of mutant protein characterization	121
Table 7 Strains and plasmids used in this study	136
Table 8. Oligonucleotides used in this study	138
Table 9. Bacterial Strains and plasmids used in this study	210
Table 10. Serotyping and ECA Passive Hemagglutination (PHA)	219
Table 11. Oral immunization with ECA mutants and subsequent oral challenge at Day 30 with wildtype <i>S. Typhimurium</i> strains	230
Table 12. Oral Immunization with ECA negative and subsequent oral challenge at Day 45 with wildtype TML strains	232
Table 13. Intraperitoneal immunization with ECA negative and subsequent challenge at Day 30 with wildtype TML strains	234
Table 14. ISH probes used in this study	266

Table 15. PMP Core Microbiome Classifiable at the Genus Level	277
Table 16. Culturable bacteria isolated from PMP tissue samples	282
Table 17. (S1) Core microbiome by patient	295
Table 18. (S2) Sample-by-sample breakdown of OTUs detected	297

Table of Figures

Figure 1. Overview of Fur regulation.....	31
Figure 2. Autoregulation of <i>H. pylori fur</i>	34
Figure 3. Structure of <i>H. pylori</i> Fe-Fur	40
Figure 4. Structure of <i>C. jejuni apo-Fur</i>	43
Figure 5. Transcriptional start site (TSS) mapping and identification of <i>oorDABC</i> promoter elements	62
Figure 6. Mapping of the <i>oorD</i> TSS and promoter structure	66
Figure 7. rFur binds specifically to the <i>oorDABC</i> Fur box	69
Figure 8. Proposed Model of Fur dependent activation of <i>oorDABC</i> expression.....	78
Figure 9. Distribution of random and site-specific mutations across the coding region of <i>H. pylori</i> Fur.	91
Figure 10. Transcriptional regulation of <i>amiE</i> under iron replete and iron-depleted conditions as measured by qRT-PCR.....	94
Figure 11. Transcriptional regulation of <i>pfr</i> under iron replete and iron-depleted conditions as measured by qRT-PCR.....	97
Figure 12. The relative levels of Fur in each mutant strain were measured by Western blot and compared to Fur levels in the wildtype.....	103

Figure 13. Secondary structure and thermal denaturation profiles obtained by circular dichroism (CD) spectroscopy.	106
Figure 14. The ability of the WT and each mutant Fur protein to bind iron (Fe ²⁺) as measured by atomic absorption spectrophotometry.	109
Figure 15. The ability of WT and each mutant protein to oligomerize as determined by <i>in vitro</i> cross-linking.....	112
Figure 16. The ability of the WT and mutant proteins to bind DNA sequences from the <i>amiE</i> and <i>pfr</i> promoters as determined using fluorescence anisotropy.	115
Figure 17. Structural representation of <i>H. pylori</i> Fe-Fur (A) and <i>apo</i> -Fur (B) dimers. ...	125
Figure 18. (S1) Overlay of the modeled <i>H. pylori apo</i> -Fur structure (blue) with <i>C. jejuni apo</i> -Fur (red)	134
Figure 19. Proposed modes of Fe-Fur activation in <i>H. pylori</i>	155
Figure 20. <i>In vitro</i> characterization of <i>wecA</i> mutant and complementation strains of <i>Salmonella</i> serovar Typhimurium	221
Figure 21. Attenuation and complementation of the TML <i>wecA</i> mutant strain.....	225
Figure 22. Bacterial load in systemic sites of infection.....	229
Figure 23. Electron micrograph of gross cell structure of <i>Salmonella</i> strains	242
Figure 24. Swarming (A-D) and Swimming (E-H) motility of <i>Salmonella</i> strains.	244

Figure 25. Percent survival for individual dose groups used for <i>in vivo</i> complementation of the <i>wecA::Gm</i> mutation.....	246
Figure 26. Distribution of prominent bacterial phyla.....	271
Figure 27. β -diversity between PMP communities.....	274
Figure 28. Core set of sequences found in all PMP patients.....	276
Figure 29. Direct detection of bacterial taxa in PMP tissue by ISH.....	280
Figure 30. Bacteria isolated from PMP tissue associates with MUC2.....	284
Figure 31. Patient survival after antibiotic treatment.....	287
Figure 32. (S1) Observed richness in PMP samples.....	294

Chapter One

Introduction^a

Helicobacter pylori

History and Taxonomy

Helicobacter pylori (*H. pylori*) is a unique and highly successful pathogen that has evolved to thrive within the seemingly inhospitable environment of the gastric mucosa. As a result of thousands of years of coevolution with its human host, this remarkable organism has adapted to a lifestyle of extremes. From the dramatic changes in environmental pH and nutrient availability, to the constant onslaught of the host innate and adaptive immune systems, *H. pylori* has a remarkable ability to quickly respond to changes in the environment. Because of these adaptive mechanisms and the ability to persist for the life of the host, this organism has become the subject of great scientific and medical curiosity since it was first discovered over 30 years ago.

Shortly after the year 1900, there were several reports that described the presence of bacteria associated with the stomach mucosa, as well as “spirochaetes” or spiral shaped organisms associated with gastric tissue specimens (51, 135). In the early 1980’s these organisms were repeatedly observed in endoscopic biopsy specimens by Dr. Robin

^aExerpts taken from the review article: Gilbreath, J.J., Cody, W.L., Merrell, D.S., and Hendrixson, D.R. 2011 Change is Good: Variations in Common Biological Mechanisms in the Epsilonproteobacterial Genera *Campylobacter* and *Helicobacter*. *Microbiol Mol Biol Rev.* **75**(1):84-132

Warren, which prompted efforts to culture these bacteria. Using microaerophilic growth conditions and prolonged incubation periods (up to 5 days), Drs. Robin Warren and Barry Marshall were ultimately able to isolate these organisms in pure culture. Because of the similarities between these new bacteria and known *Campylobacter* spp., Warren and Marshall initially named the bacteria *Campylobacter pyloridis* (*C. pyloridis*) (102, 103, 169). For their discovery and initial characterization of *C. pyloridis* as the etiologic agent of gastritis and gastric ulcers, Warren and Marshall were ultimately awarded the Nobel Prize in Physiology or Medicine in 2005. Although morphologically similar, it was subsequently determined that *C. pyloridis* was evolutionarily distant from the *Campylobacter* spp. As a result, *C. pyloridis* was later renamed *Helicobacter pylori* and grouped into a distinct clade within the epsilonproteobacteria (ϵ -proteobacteria).

Members of the ϵ -proteobacteria represent a physiologically and ecologically diverse group of organisms that are quite evolutionarily distinct from the more commonly studied proteobacteria such as *E. coli* and *Salmonella* spp. One common factor shared by the ϵ -proteobacteria is that the niches they inhabit are often found in extreme, geographically-distinct environments. From the high temperature and pressure of deep-sea hydrothermal vents, to the highly acidic gastric mucosa, or microbial mats found in sulfidic caves and springs, survival in these environments clearly requires a unique repertoire of cellular processes that make the ϵ -proteobacteria unique (57, 114, 132, 145). Despite the nearly ubiquitous nature of this class of bacteria, the ϵ -proteobacteria remain one of the most understudied groups of bacterial species. Taxonomically, the ϵ -proteobacteria can be grouped into two orders: the Nautiliales and the Campylobacterales. One of the most commonly studied genera within the ϵ -

proteobacteria is the *Helicobacter* spp., which are members of the order Campylobacterales.

The *Helicobacter* genus consists of 18 different species and can be divided into two major categories, gastric and non-gastric *Helicobacter* spp., with the latter group including enterohepatic *Helicobacter* spp. As a whole, these bacteria colonize a variety of host mammal species, both wild and domestic (117, 146). Although both groups are Gram-negative, spiral-shaped microaerophiles, these bacteria employ biological systems that are specific for their respective niches and are highly adapted to their host environments. By far the most recognized *Helicobacter*, *H. pylori* is the prototypical member of the gastric *Helicobacter* species and is the major human pathogen of this genus.

Epidemiology, Disease, and Treatment

Arguably one of the most successful human pathogens, *H. pylori* chronically colonizes approximately half of the world's population (16, 56). In developing countries, the prevalence of *H. pylori* infection can be greater than 80%, whereas the number of people colonized in developed countries is typically under 40% (133). Recently developed or developing countries typically have higher infection rates than developed countries, and there is an inverse relationship between *H. pylori* infection and socioeconomic status. This seemingly high prevalence is likely the result of a long-lived association with the human host. In fact, phylogeographic studies suggest that *H. pylori* has colonized humans for ~58,000 years, a period of time which coincides with the latest human migration out of Africa (98). Given the presence of gastric *Helicobacter* spp. in a

variety of other animals, it is hypothesized that these bacteria are ancestral in mammals and that these gastric inhabitants may have co-evolved with mammals throughout evolutionary history. This hypothesis is supported by the observation that *H. pylori* has a reduced genome size (roughly 1.6 Mb), a phenomenon commonly seen in endosymbiotic organisms. Because no environmental reservoirs have been discovered for *H. pylori*, transmission to humans is thought to occur via person-to-person contact primarily at a young age (64, 65, 86, 96, 122). Transmission is believed to often occur from parent to child, as infected children often share the same strain as their parents. Though the exact route of transmission is not yet known, there is at least some evidence that supports oral-oral and/or fecal-oral spread. Once established, *H. pylori* infection may persist for the life of the individual in the absence of antibiotic intervention.

Persistent *H. pylori* infection is commonly associated with outcomes that range from asymptomatic carriage and mild gastritis to several types of more severe disease (16, 61, 119-121, 151, 152). *H. pylori* is the etiologic agent of both gastric and duodenal ulcers; 75% of gastric ulcers and 90% of all duodenal ulcers are the result of infection with *H. pylori* (61). The site of ulcer formation is thought to depend on which site(s) within the stomach that the bacteria colonize. For example, *H. pylori*-induced gastritis more frequently progresses to duodenal ulceration if the bacteria colonize the antral region of the stomach, whereas colonization of the corpus more frequently leads to gastric ulcer formation (150). Infection with this pathogen is also associated with the development to two types of cancer: mucosa-associated lymphoid tissue (MALT) lymphoma and gastric adenocarcinoma (16, 119-121, 152). In the case of MALT lymphoma, the disease usually begins as nonatrophic pangastritis, followed by infiltration

of lymphocytes and subsequent lymphoid follicle formation (176). *H. pylori* induced gastric adenocarcinoma usually originates from gastric ulcers and progresses through intestinal dysplasia and metaplasia. As a result of this correlation with cancer, *H. pylori* is classified as a carcinogen by both the World Health Organization and the International Agency for Research on Cancer (24), a distinction not shared by any other bacteria. Though not completely understood, the extent of host disease development is dependent on a combination of host and bacterial genetic factors, as well as several environmental factors. For example, polymorphisms in host immune factors that result in increased pro-inflammatory cytokine levels are frequently associated with increased risk of gastric cancer development in *H. pylori* infected individuals. In addition, *H. pylori* strains with specific polymorphisms in genes that encode virulence factors or iron uptake systems have been associated with more severe disease (81, 82, 84, 85)

Because of the morbidity associated with *H. pylori* infection and the correlation between colonization and gastric cancer development, the dominant medical practice has been to eradicate *H. pylori* from patients who are colonized. Standard treatment typically includes administering three drugs: clarithromycin (500 mg twice daily), a proton pump inhibitor (PPI) to reduce gastric acidity, and amoxicillin (1000 mg twice daily); alternatively the triple therapy can be given with metronidazole (400-500 mg twice daily) substituted for amoxicillin (73). However, there is increasing evidence that *H. pylori* strains are becoming more resistant to this treatment regimen. In cases where triple therapy is ineffective, a quadruple therapy (the standard triple therapy plus bismuth), or second line drugs such as fluoroquinolones and rifamycins may be used (73). Perhaps not surprisingly, this increase in antimicrobial resistance in *H. pylori* strains has led to a

decrease in the success rate of treating *H. pylori* infections. Accordingly, much attention has been given to the colonization factors and virulence mechanisms employed by this organism, with the hope that unraveling the secrets of *H. pylori* pathogenesis will shed light on alternative therapeutic options.

Niche-specific adaptations and virulence factors

The ability to successfully colonize the human stomach is largely the result of evolutionary adaptations that allow *H. pylori* to overcome several limiting factors (36). First, and perhaps foremost, the pH of the gastric lumen can be as low as 2-2.5. One strategy *H. pylori* employ to avoid the low pH of the stomach is to maintain a close association with host epithelial cells. These interactions are mediated by several bacterial outer membrane proteins (OMPs) including the adhesins BabA, SabA, AlpA and AlpB (6, 140). Whereas both BabA and SabA recognize host Lewis antigens present on host epithelial cells (6, 100) AlpA and AlpB bind to host laminin (140). Strains that lack these OMPs are less competitive *in vivo*, which suggests a role for these proteins in establishing and/or maintaining a persistent infection. Although the bacteria preferentially colonize near the gastric epithelium and within free mucin where the pH is close to neutral, peristalsis and stirring of stomach contents can transiently expose *H. pylori* to the highly acidic gastric lumen. To help alleviate this pH related stress, the bacteria produce an extracellular urease enzyme that catalyzes the formation of ammonia from urea and helps increase the extracellular pH and to maintain intracellular pH homeostasis (55, 112). Additionally, *H. pylori* possess polar flagella and environmentally regulated chemotactic systems that allow the bacteria to burrow into the gastric mucin and away

from stressful conditions. Taken together, these types of evolutionary adaptations contribute to the ability of *H. pylori* to persist within the host.

Other limiting factors to persistence within the human host are the innate and adaptive immune responses. However, the immune response to *H. pylori* is relatively weak as compared to other bacterial pathogens (36). This lower degree of immunogenicity is the result of several unique features found on bacterial cell surface molecules. For example, in contrast to other bacterial pathogens, the *H. pylori* flagellin protein is poorly recognized by TLR5 (94) and the lipopolysaccharide (LPS) on the surface of the bacteria has modifications that reduce immunogenicity (95). Many *H. pylori* strains also express components of LPS that mimic host Lewis blood group antigen structures (4, 5). Another example of immune evasion involves the use of lipid glucosylation, which reduces uptake by host phagocytes (177). These types of host mimicry allow the bacteria to persist without triggering an immune response strong enough to clear the infection.

In addition to the adaptive mechanisms that facilitate persistence *in vivo*, *H. pylori* produces two *bona fide* virulence factors that directly affect host cells and contribute to its lifestyle. The first of these factors is encoded by the cytotoxin-associated gene A (*cagA*). Perhaps the most well studied of the *H. pylori* virulence factors, CagA, is encoded within the *cag* pathogenicity island; this genomic region was likely introduced by horizontal gene transfer and also encodes for a type four secretion (T4S) system, which is required for CagA translocation into host cells (29). After injection into host cells, the CagA protein is phosphorylated and exerts effects on multiple host cell-signaling pathways (reviewed in (85)). These alterations in signaling interfere with

several aspects of cellular function including polarization, proliferation, and differentiation (reviewed in (85)). Once inside the host cell, CagA is localized to the plasma membrane where a specific motif (EPIYA) within the C-terminus of the protein is phosphorylated; the amino acid sequence and number of EPIYA motifs within this region is thought to be highly important for CagA-mediated cellular changes (77, 78). Overall, given the dramatic host changes that CagA induces, it is perhaps not surprising that CagA production is linked to the more severe types of *H. pylori* disease (18, 89).

Another important virulence factor produced by *H. pylori* is the vacuolating cytotoxin, VacA. Similar to CagA, VacA is a key component of *H. pylori* virulence that also targets multiple host cell signaling pathways (reviewed in (85)). Unlike CagA, however, this toxin leaves the bacterial cell via the autosecretory pathway and inserts into the host cell membrane rather than being injected directly into the host cell cytoplasm. After insertion, VacA may also be endocytosed into the host cell, and then affect multiple cellular signaling pathways (reviewed in (85)). Once inside the host cell, VacA can interact with mitochondria and induce apoptosis, and also facilitates vacuole formation within the host cell (66, 88). Another key feature of VacA activity is the ability to act as an immunomodulatory molecule. VacA has been shown to disrupt phagosome maturation (183), inhibit MHC class II-dependent antigen presentation, and to interfere with antigen presentation and proliferation in B cells (113). Furthermore, intoxication with VacA can inhibit cytotoxic and helper T cell proliferation and interferes with cellular signaling in macrophages and neutrophils as well (141, 157). Clearly, both CagA and VacA have enormous impact on host cells in close proximity to *H. pylori* by helping to facilitate persistent colonization and evasion of the host immune system.

Another limiting factor for living within the stomach is nutrient availability. Although there appears to be little to no competition for nutrients from other microbes, *H. pylori* is continually forced to compete with the host. As a result, *H. pylori* utilizes multiple mechanisms to obtain nutrients from host cells. One such strategy is the induction of tissue inflammation; induction of inflammatory cytokines leads to death of host cells (37), which likely then leak their contents into the gastric lumen. The importance of inflammation to persistent colonization is evidenced by the multiple ways that *H. pylori* stimulates a pro-inflammatory response within the host. For example, in addition to CagA translocation, the *H. pylori* type T4S system can also deliver fragments of peptidoglycan, which ultimately activate the transcription factor NF- κ B and drive expression of multiple pro-inflammatory factors (164). Similarly, the T4S needle is capable of inducing production of the pro-inflammatory cytokine IL-8 (38). Other mechanisms of nutrient acquisition require the activity of the bacterial toxins CagA and VacA. In addition to the cellular changes described above, insertion of the VacA toxin into the host cell membrane creates anion channels, which allow nutrients to exit the cell and increase cellular permeability (118). This increased permeability provides *H. pylori* with access to other essential nutrients such as bicarbonate, urea, nickel, and iron (118). Similarly, one of the downstream effects of CagA activity is also important for iron acquisition. This toxin has been shown to usurp trafficking of iron-containing transferrin and enhance the ability of *H. pylori* to obtain this molecule (153). The fact that *H. pylori* utilizes multiple strategies to obtain iron highlights the importance of this metal to the biology of this organism.

Iron uptake, storage, and Fur-mediated gene regulation

Iron uptake and storage

Iron is one of the most abundant elements on the planet and is a basic requirement for life. In bacteria, iron plays a critical role in processes such as metabolism, electron transport, oxidative stress response, and regulation of gene expression (63, 74, 83, 104, 108). Although iron is essential for most bacteria, it also catalyzes free radical formation through Fenton chemistry ($\text{Fe}^{2+} + \text{H}_2\text{O}_2 \rightarrow \text{Fe}^{3+} + \text{OH}\cdot + \text{OH}^-$), which results in cellular damage. As such, homeostasis between iron acquisition and storage is crucial for bacterial survival. However, the ability to achieve the proper balance of iron homeostasis is complicated by the environment in which bacteria live. For instance, in anaerobic or acidic environments such as the stomach, iron is found in its soluble ferrous form (Fe^{2+}) and can be readily acquired by most microbes that thrive in these situations. *H. pylori* encodes a single ferrous iron transport protein (FeoB), which has been shown to be required for colonization (163). These findings highlight the importance of ferrous iron uptake to *H. pylori* colonization and survival.

As mentioned above, *H. pylori* is almost exclusively in competition with the host for nutrients such as iron. As a result, this bacterium employs several systems that facilitate uptake of host-derived iron containing molecules. In mammalian hosts, extracellular iron is temporarily stored by high-affinity chelating molecules such as heme, transferrin, and lactoferrin. Other than iron bound to hemoglobin (within erythrocytes), the primary mammalian iron carrier protein is transferrin (for a review on mammalian iron homeostasis see (3)). However, at mucosal surfaces specifically, lactoferrin is the

major iron-chelating molecule (80). During infection, these iron-containing molecules represent a readily available iron source for bacteria. Consequently, *H. pylori* has evolved the ability to obtain iron from host lactoferrin, transferrin, hemoglobin, and heme (48, 80, 139, 175). In addition to these iron uptake systems, the *H. pylori* genome also encodes multiple *fec* genes, which facilitate ferric citrate uptake (9, 39, 155) from the extracellular environment. Acting in concert, these iron uptake systems allow *H. pylori* to efficiently obtain this essential nutrient from the host. Once inside the bacterial cell, the majority of free iron is stored in a prokaryotic ferritin molecule, Pfr. The importance of this non-heme iron storage molecule is illustrated by the fact that *H. pylori* strains require Pfr for survival under iron starvation conditions and for efficient colonization (166). *H. pylori* also utilizes a bacterioferritin-like protein, NapA, that can also bind iron (156, 167). However, because NapA binds less iron than Pfr and also binds DNA, it is hypothesized that this molecule serves to protect DNA from iron-catalyzed free radical damage rather than in simple iron storage. Given ability of *H. pylori* to efficiently take up and utilize iron from many host-derived molecules and environmental sources, clearly these processes are crucial to survival and persistence within the host.

Fur regulation

Regardless of how iron is obtained, maintaining the balance between sufficient iron and levels that lead to iron toxicity is crucial, and therefore this balance must be tightly regulated. In bacteria, the primary regulatory checkpoint in iron homeostasis is iron uptake, and expression of genes encoding factors involved in this process is regulated at the transcriptional level. The major transcription factor responsible for this

regulation is the ferric uptake regulator, Fur, which utilizes iron as a co-factor (7, 74). Described in *E. coli* over 25 years ago (74). Fur is a histidine rich ~17 kDa homodimeric metalloprotein that contains two distinct functional domains: an N-terminal domain responsible for DNA binding and a C-terminal domain that mediates oligomerization of the protein (148). Classically, Fur functions by binding to promoters of iron-regulated genes at a conserved binding sequence known as the Fur box (40, 62, 63). These DNA sequences typically overlap the -10 and -35 regions of Fur regulated promoters so that Fur binding prevents the association of RNAP, and represses transcription (Figure 1).

Initial reports in *E. coli* indicated that the consensus Fur binding sequence was a 19-bp palindromic DNA sequence, GATAATGATAATCATTATC (40). Subsequent analysis of Fur-DNA interactions revealed that the functional *E. coli* Fur binding sequence actually consists of three or more hexameric repeats of a GATAAT sequence (62). The specific model of Fur:DNA interaction has since been further refined by Baichoo and Helmann, who suggested that Fur dimers interact with a specific 15-bp inverted heptamer repeat (7-1-7) (8). The 7-1-7 inverted repeat model of Fur:DNA interaction essentially includes the basic components of both the 19-bp and GATAAT models. This type of highly conserved Fur binding sequence has been described for all members of the Fur protein family to date.

Perhaps not surprisingly, in the well-studied bacterial species, the majority of Fur-regulated promoters are associated with genes involved in iron homeostasis or genes encoding iron-containing proteins. For example, in Gram-negative species such as *E. coli* and *V. cholerae*, genes that are regulated by classic Fe-Fur repression include those involved in siderophore biosynthesis (20, 108), iron uptake and transport, and energy

coupling mechanisms (108). However, in many cases Fur also directly and indirectly regulates many other genes with diverse functions, including genes linked to colonization, virulence, and stress adaptation (58, 67, 72, 108, 128, 134). Clearly, this regulatory protein plays an important role in the biology of many bacterial pathogens.

Iron-bound and apo Fur regulation

In contrast to well-studied species such as *E. coli*, Fur regulation in *H. pylori* is a complex story that has not yet been fully unraveled. While the sequence of *H. pylori* Fur is relatively similar to that of well-studied pathogens such as *E. coli*, it is functionally quite different (14, 26, 44-46). Similar to Fur regulation in *E. coli*, *H. pylori* Fur can act as a classic transcriptional repressor, utilizing iron as a co-factor (13). However, unlike Fur in most other organisms, *H. pylori* Fur has also been shown to act as an *apo*-repressor, as well as an activator in both the iron-bound and *apo*- forms (2, 39, 44, 46, 58, 59, 67). Iron-bound Fur repression in *H. pylori* is similar to that seen in many other organisms; Fur is thought to bind to Fur boxes as a dimer, and repress transcription in an iron-dependent manner. Similarly, recent evidence suggests that *apo*-Fur may also act as a dimer (23), though this hypothesis requires further functional testing (Figure 1).

Figure 1. Overview of Fur regulation

Classic Fe-Fur repression (left panel) occurs when excess iron becomes available; Fur monomers dimerize and bind Fur box sequences, repressing transcription. Fe-Fur activation (middle panel, left side) occurs in a similar manner, except transcription is activated rather than repressed. *apo*-Fur activation (middle panel), and *apo*-Fur repression (right panel) are depicted. *apo*-Fur regulation occurs under iron-depleted conditions; although the oligomeric state of *apo*-Fur and the *apo*-Fur box are not clearly understood, the *apo* form of Fur is able to activate (middle panel, right side) and repress transcription (right panel). Figure was modified from (29).

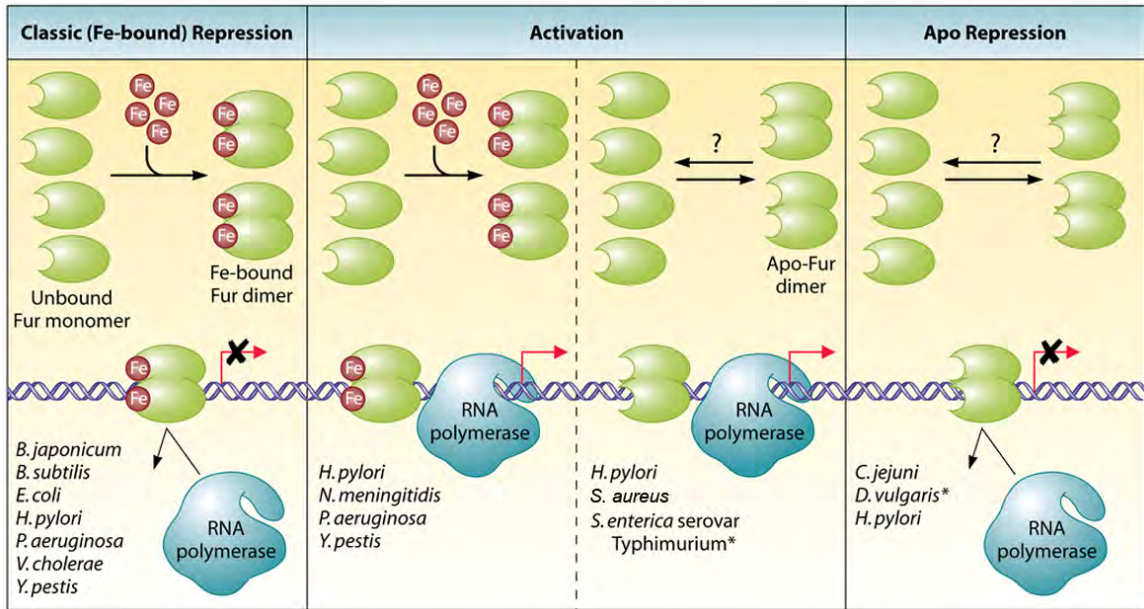


Figure 1: Overview of Fur regulation

As seen in other bacteria, in *H. pylori* Fur regulates a wide variety of genes that encode for diverse functions. One highly complex example of iron-responsive regulation found among genes in the *H. pylori* Fur regulon is that of the *fur* promoter itself (Figure 2). As seen in *E. coli*, expression of the *fur* promoter in *H. pylori* is autoregulated (44). This iron-responsive autoregulation provides the bacteria with a sensitive mechanism to control iron levels within the cell (44, 46). *H. pylori fur* is transcribed from its own promoter, which has three distinct Fur boxes (44). The Fur box with the highest binding affinity under iron-replete conditions (box I) overlaps the -35 region of the promoter, consistent with Fe-Fur repression due to inhibition of RNAP interaction at the promoter. An additional Fe-Fur binding site (box II) lies further downstream (+19 to -13) and may provide stronger or more complete repression in conditions where high concentrations of iron are present in the cell. The third Fur binding site (box III) is located between the -87 and -104 nucleotides, and is bound by *apo*-Fur. In contrast to the repression seen by Fur binding to boxes I and II, *apo*-Fur binding to box III results in the activation of *fur* expression (45). The combination of both Fe-Fur repression and *apo*-Fur activation in the autoregulation of *fur* expression allows *H. pylori* to tightly control production of this multifunctional regulatory protein. In contrast to the complex regulatory mechanisms that control expression from the *fur* promoter, however, most other known Fur regulated genes in *H. pylori* display either Fe-Fur or *apo*-Fur regulation only.

Similar to other bacterial pathogens, the Fur-mediated regulatory network in *H. pylori* is extensive, and contains genes that serve diverse functions. Transcriptional

Figure 2. Autoregulation of H. pylori fur. The figure shown is reproduced from Gilbreath *et al.*, (69) and is based on the work of Delany *et al.*, (44, 45). **(A)** The relative position of the Fe-Fur and *apo*-Fur binding sites is shown. **(B)** (Top) Under iron replete conditions, Fe-Fur binds the high-affinity site in box I and repressed *fur* expression. (Middle) Under conditions of high/excess iron, Fe-Fur also binds the lower-affinity site in box II, resulting in more complete repression of *fur* expression. (Bottom) In the absence of iron or under iron-restricted conditions, box II is not bound by Fur and *fur* expression is derepressed. In addition, *apo*-Fur binds the target sequences in box III and box I, activating *fur* transcription (44, 45).

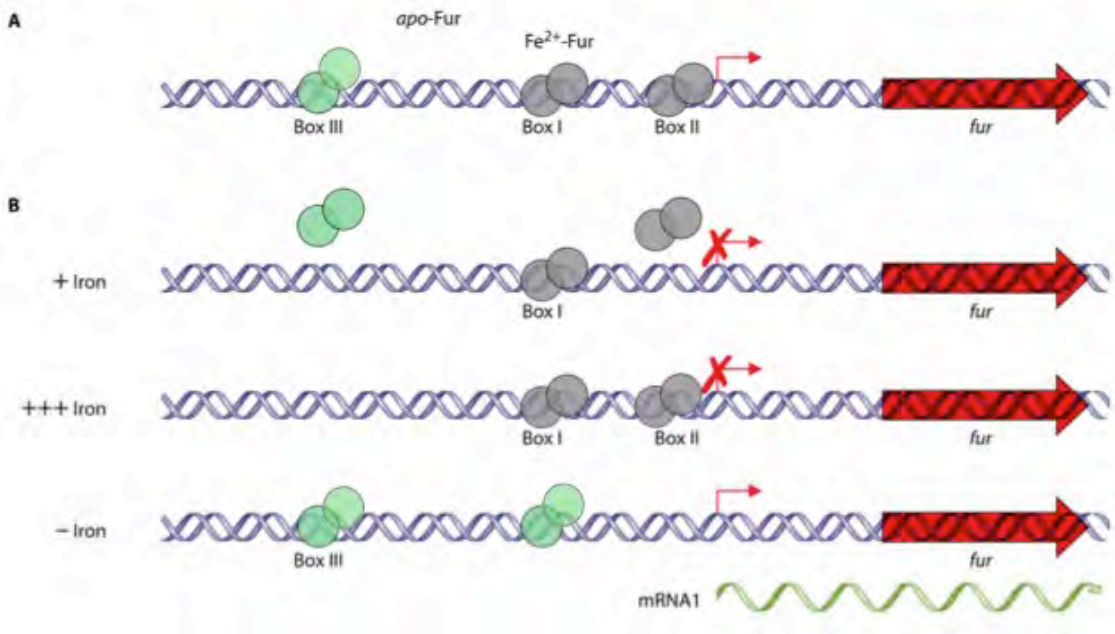


Figure 2: Autoregulation of *H. pylori fur*

profiling identified 97 genes regulated by iron and 43 genes whose expression was Fur-dependent (58). *H. pylori* genes repressed by Fe-Fur include those involved in iron uptake and transport (such as *feoB*, *fecA1*, *fecA2*, *frpB*, *exbB*, and *ceuE*), cellular processes and protein synthesis, as well as many additional genes with unknown or hypothetical functions (58, 67, 110). A subsequent study examined the role of Fur in iron- and acid-responsive regulation (67). In addition to the iron-responsive genes, this study identified more than 90 Fur regulated genes that are differentially regulated in response to pH shock, some of which are directly involved in pH homeostasis. Much like the iron-responsive regulon, the pH responsive genes encode proteins with diverse functions including factors involved in iron uptake (*fecA1*, *fecA2*, *frpB1*), stress adaptation (*amiE*, *pfr*, *katA*), and homologous recombination (*ruvC*) (67). The importance of Fur regulation to pH adaptation is further highlighted by reports that the acid tolerance response (ATR) is Fur dependent (158).

Another important adaptive response that requires Fur-mediated gene regulation is the ability to combat oxidative and nitrosative stress. Genes involved in these stress responses include the superoxide dismutase (*sodB*), catalase (*katA*), alkyl-hydroperoxide reductase (*ahpC*), and the neutrophil activating protein (*napA*), which are all regulated by Fur (58, 67). Collectively, these studies identify a variety of genes encompassing diverse functional categories, and thus highlight the role of Fur as a global regulator that is important for maintaining a persistent infection within the host.

Adding yet another level of complexity to regulation by *H. pylori* Fur is the observation that several genes appear to be upregulated by Fe-Fur (67). Detailed analysis of Fur regulation of the *nifS* promoter suggests that Fur, in fact, can act as a

transcriptional activator. Under iron-replete conditions, Fur was found to protect two distinct regions within the *nifS* promoter (2). Although there are no clear Fur boxes in the *nifS* promoter, the Fur binding regions were reported to be 150 and 200 nucleotides upstream from the transcriptional start, which could be consistent with an orientation of Fur needed to activate transcription. Another set of genes reported to be induced by Fe-Fur encode the 2-oxoglutarate oxidoreductase complex, OorDABC (67). In *H. pylori*, the upstream region of these genes appears to contain a putative Fur box (based on consensus proposed by Merrell *et al.*, (110)), but direct activation by Fur was not demonstrated in that study.

Compared to classical Fe-Fur regulation, relatively little is known about *apo*-Fur regulation. Within *H. pylori*, only two *apo*-Fur regulated genes have been studied in detail: the prokaryotic ferritin, *pfr*, and the superoxide dismutase gene *sodB*. Other *H. pylori* genes putatively repressed by *apo*-Fur include *serB* (encoding a phosphoserine phosphatase), genes involved in energy metabolism such as *hydA* and *hydB*, as well as several genes with unknown or hypothetical function (58). Until very recently, *H. pylori* was the only bacterial species where this type of regulation was directly demonstrated. However, within the last year additional examples of *apo*-Fur regulation have been reported in *C. jejuni* as well as *S. aureus* (47, 72). In *C. jejuni*, *apo*-Fur was shown to repress transcription of the redox protein Dsb (72). Additionally, expression of the efflux transporter NorA is activated by *apo*-Fur in *S. aureus* (47). Despite these findings, *H. pylori* remains the only bacterial species in which Fur regulates gene expression using all four mechanisms: Fe-Fur activation and repression, as well as *apo*-Fur activation and repression (Figure 1).

One of the factors that allow regulatory proteins to regulate certain genes, but not others is the presence protein-specific binding sequences within promoter regions. As such, identification of these binding sequences helps provide a mechanistic understanding of how regulation occurs. Similar to *E. coli*, *H. pylori* Fe-Fur targets promoter regions that contain specific sequences (Fur boxes). The Fe-Fur binding sequence in *H. pylori* (5'-TAATAATcATTATTA-3') has recently been characterized (128) and bears striking similarity to the *E. coli* Fur box sequence. The sequence is a pair of inverted repeats (7-1-7) and is usually located proximal to the core promoter elements. The presence of this sequence or a similar sequence with one or two mismatches is sufficient to confer Fe-Fur repression (128).

Given the relatively paucity of *apo*-Fur regulated genes that have been described in detail, perhaps it is not surprising that little is known about the *apo*-Fur binding sequence. In contrast to the Fe-Fur binding sequence, detailed analysis of *apo*-Fur target sequences in *H. pylori* has only been performed with two promoters, those of *pfr* and *sodB* (encoding the prokaryotic ferritin and superoxide dismutase, respectively) (12, 59). In both instances, *apo*-Fur binds specifically to promoters under metal-depleted conditions. Promoter sequence comparison of these two genes failed to highlight a putative binding sequence and homology to the proposed Fe-Fur consensus is not seen (28, 59). This difference is perhaps not surprising given the functional difference of Fe-Fur and *apo*-Fur targeted promoters; furthermore, in light of the recent structural information, the presence or absence of metal co-factors likely results in conformational changes in protein structure that affect DNA binding specificity.

Fur Structure

The recent resolution of the *H. pylori* Fe-Fur structure has shed light on several novel aspects of this protein compared to the structures of other Fur species. Similar to other Fur structures, *H. pylori* Fur is made up of two major domains: an N-terminal DNA binding domain (DBD), and a C-terminal oligomerization domain (Figure 3). The N-terminal domain contains the canonical winged helix motif that facilitates interaction with Fe-Fur target DNA sequences. Also within this domain is an N-terminal 10 amino acid extension, which is not seen in the structures of the *V. cholerae*, or *P. aeruginosa* Fur proteins (129, 143). In *H. pylori*, this extended region stacks against the DNA binding domain, and creates a hydrogen bond network that ties these N-terminal residues to the metal-coordinating residues in the regulatory metal binding site (S2, described below) (49). Another unique structural feature of *H. pylori* Fur is the presence of three metal binding sites, (designated S1, S2, and S3), rather than the two binding sites found in other Fur structures. S1 is a structural metal binding site located near the oligomerization interface that is coordinated by four cysteine residues. In the other Fur structures, disulfide linkages between analogous cysteine residues function in a similar capacity as this metal binding site, making S1 fairly unique to *H. pylori* (49, 165). *H. pylori* Fur also contains another structural metal binding site, S3, which has been described in all Fur proteins to date. Although this site is not absolutely required for DNA binding, metallation at S3 increases affinity for Fe-Fur target DNA in *H. pylori* (49). The

Figure 3. Structure of H. pylori Fe-Fur

A fully metallated Fur dimer is shown. Chain A is shown in blue, and chain B is depicted in cyan. The N-terminal DNA binding domain (DBD) and C-terminal dimerization domain (DD) are shown. Metal ions located in the structural binding sites S1 and S3, as well as the regulatory metal binding site S2 are depicted as grey spheres. Image was generated using the PDB 2XIG and Polyview 3D (130).

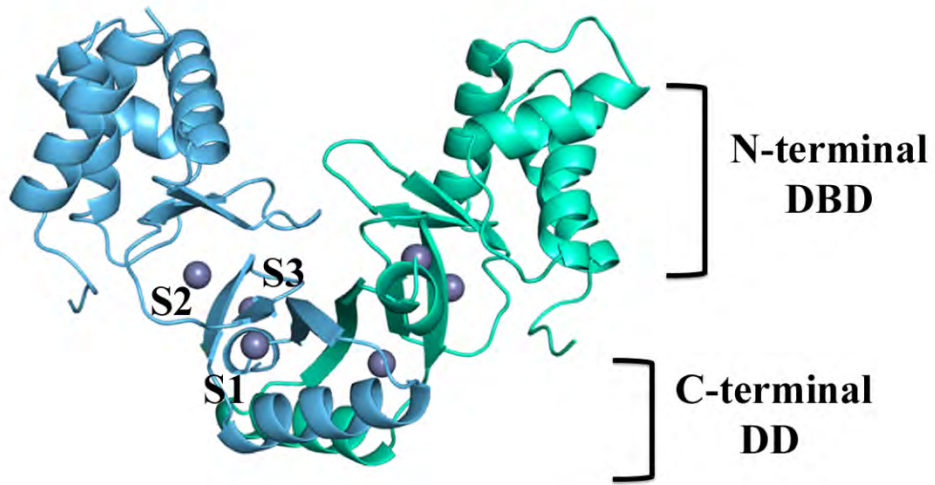


Figure 3: Structure of H. pylori Fe-Fur

regulatory metal binding site in *H. pylori* Fur is S2; the presence or absence of a metal ion at this site distinguishes between the iron-bound (Fe-Fur) and *apo* (*apo*-Fur) forms of the protein. Similar to S3, the S2 site is also conserved among the well-studied Fur proteins (129, 143).

Until very recently, the structural features that distinguish *apo*-Fur from Fe-Fur were a mystery. However, the resolution of *C. jejuni* Fur in its *apo* form has provided valuable insight into how this protein functions without the iron co-factor (23). Given the high degree of similarity between the *C. jejuni* and *H. pylori* Fur proteins, it is likely that this *apo*-Fur structure closely resembles *H. pylori apo*-Fur; thus, the structural features of the *C. jejuni* structure likely translate to *apo*-Fur in *H. pylori* as well. While the overall structure of *apo*-Fur is fairly similar to its Fe-Fur counterparts, there are several major differences. First, the DNA binding domain in the N-terminus of the protein is rotated 180 degrees compared to what has been described for Fe-Fur (129, 143). This rotation places the N-terminal 10 amino acid extension within the “V” shaped DNA recognition region rather than stacked against the outer face of the protein as was described for *H. pylori* Fe-Fur (Figure 4). Another interesting characteristic of the *apo*-Fur structure is the presence of metal ions in the S1 and S3 structural binding sites (23). This finding supports the tenant that these two metal binding sites play a role in maintaining dimeric structure rather than dictating DNA sequence binding specificity. Importantly, there was no metal ion located in the regulatory binding site S2, which confirms the hypothesis that

Figure 4. Structure of C. jejuni apo-Fur

Chain A is shown in cyan, and chain B is depicted in green. The N-terminal DNA binding domain (DBD) and C-terminal dimerization domain (DD) are shown. Metal ions located in the structural binding sites S1 and S3 are depicted as grey spheres. Image was generated using the PDB 4ETS and Polyview 3D (130).

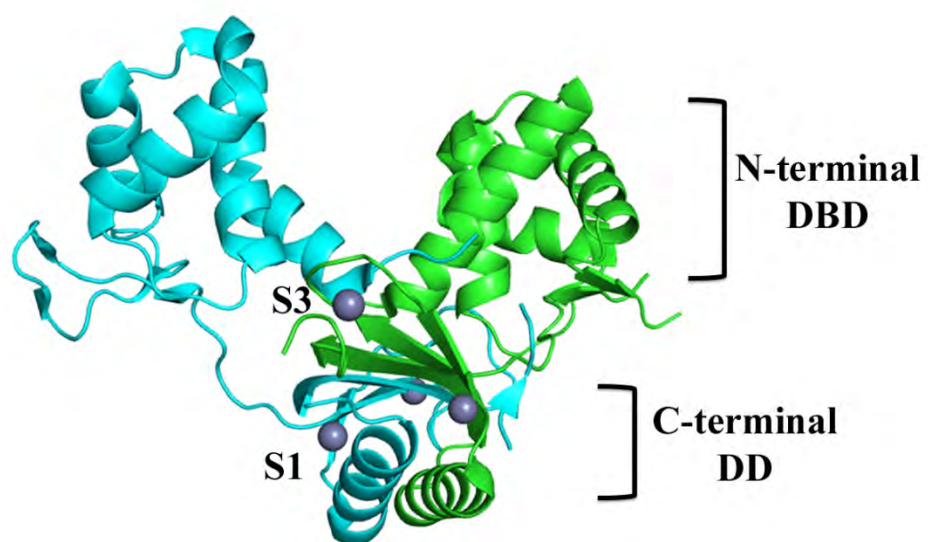


Figure 4: Structure of C. jejuni apo-Fur

the presence or absence of metal at this site determines whether the protein functions as Fe-Fur or *apo*-Fur. Furthermore, when considered in the context of the rotated DNA binding domain, it is likely that metallation at S2 results in the conformational change in the N-terminus that allows the protein to distinguish between Fe-Fur and *apo*-Fur target promoters sequences.

Controversy and gaps

It should be noted that historically, *apo*-Fur regulation has been seen as somewhat controversial, namely due to the previous discovery of Fur-regulated sRNAs such as RyhB. One hypothesis that was previously proposed to explain the apparent regulatory role of *apo*-Fur in *H. pylori* is the existence of a Fur-regulated small RNA (sRNA). Fur-sRNA interactions have been well described in *E. coli*, where RyhB affects expression of several genes previously thought to be Fur regulated (106). However, data supporting the sRNA hypothesis is lacking in *H. pylori* since only a few sRNAs have been studied to date (178, 179) and the published *H. pylori* genomes lack a RyhB homologue (9, 155). This hypothesis seems even less likely given the recent publication of the *C. jejuni apo*-Fur structure (23), and description of *apo*-Fur regulation in additional bacterial species (47, 72). Despite this fact, recent publication of the *H. pylori* primary transcriptome has indicated that a large number of sRNAs exist (142). Based on sequence similarity, several of these putative sRNAs may be regulated by Fur and/or may be involved in regulation of Fur target genes. Further studies will be necessary to determine what, if any, role these putative sRNAs play in iron-responsive and/or Fur-mediated regulation in *H. pylori*.

Although we now have a basic appreciation of the types of regulation performed by *H. pylori* Fur, there are currently significant gaps in our knowledge of how the different forms of this unique regulatory protein function. For example, it remains unclear how Fe-Fur activates transcription, or even whether this type of regulation occurs directly or indirectly. Additionally, little is known regarding how different regions of Fur facilitate the diverse types of regulation employed by *H. pylori*. In light of the *H. pylori* Fe-Fur and the closely related *C. jejuni apo-Fur* structures, it seems reasonable to hypothesize that there are specific amino acid residues within each form of Fur that impact regulation of Fe-Fur and *apo-Fur* regulated genes. However, as very few mutagenesis studies (25, 32) have been performed on *H. pylori* Fur, we currently do not have a clear functional understanding of which are functionally important for each form of the protein. By identifying such regions, or more specifically, which amino acids actively participate in Fe-Fur and/or *apo-Fur* regulation in *H. pylori*, we will gain insight into the regulatory mechanisms employed by this key regulatory protein. Given the unique nature of *H. pylori* Fur, this mechanistic information on the regulatory processes employed by this organism could in turn be used as a framework to better understand other members of this family of regulatory proteins.

Goal and Specific Aims

The overarching goal of this dissertation was to obtain novel insight into Fur mediated regulation in *H. pylori*. This goal was divided into two separate aims: in Aim 1 we characterized Fe-Fur activation of the *oorDABC* genes, which encode for the 2-oxoglutarate oxidoreductase (described in Chapter 2); these studies not only confirmed

that Fe-Fur directly activates transcription at this promoter, but also highlighted a possible mechanism of activation. For Aim 2 we utilized random and site-specific mutagenesis to identify amino acid residues important for Fe-Fur and/or *apo*-Fur function (described in Chapter 3). Based on the phenotypes seen for the mutants obtained in Aim 2, we selected representative mutations, purified wildtype and mutant Fur proteins, and performed detailed biochemical studies to characterize the role of these residues in Fe-Fur and *apo*-Fur function. *En masse*, these studies provide novel insight into the regulatory mechanisms employed by *H. pylori* Fur, and broaden our understanding of Fur regulation in this important pathogen.

Chapter Two

Fur Activates Expression of the 2-Oxoglutarate Oxidoreductase Genes (oorDABC) in Helicobacter pylori

Published as: **Gilbreath, J.J., West, A.L., Pich, O.Q., Carpenter, B.M., Michel, S., and Merrell, D.S.** 2012. Fur Activates Expression of the 2-Oxoglutarate Oxidoreductase Genes (*oorDABC*) in *Helicobacter pylori*. *J Bacteriol.* **194**:6490-6497.

The work presented in this chapter is the sole work of J.J. Gilbreath with the following exceptions: A.L. West and S. Michel performed the fluorescence anisotropy studies, O.Q. Pich created plasmids pDSM430, pDSM815, pDSM833, pDSM845 and strains DSM1079-DSM1082, and Carpenter, B.M. helped with protein purification.

Abstract

Helicobacter pylori is a highly successful pathogen that colonizes the gastric mucosa of ~50% of the world's population. Within this colonization niche the bacteria encounter large fluctuations in nutrient availability. As such, it is critical that this organism regulate expression of key metabolic enzymes so that they are present when environmental conditions are optimal for growth. One such enzyme is the 2-oxoglutarate

(α -ketoglutarate) oxidoreductase (OOR), which catalyzes the conversion of α -ketoglutarate to succinyl-CoA and CO₂. Previous studies from our group suggested that the genes that encode for the OOR are activated by iron-bound Fur (Fe-Fur); microarray analysis showed that expression of *oorD*, *oorA*, and *oorC* were altered in a *fur* mutant strain of *H. pylori*. The goal of the present work was to more thoroughly characterize expression of the *oorDABC* genes in *H. pylori* as well as to define the role of Fe-Fur in this process. Herein we show that these four genes are co-transcribed as an operon, and that expression of the operon is decreased in a *fur* mutant strain. Transcriptional start site mapping and promoter analysis revealed the presence of a canonical extended -10 element but a poorly conserved -35 upstream of the +1. Additionally, we identified a conserved Fur binding sequence ~130 bp upstream of the transcriptional start site. Transcriptional analysis using promoter fusions revealed that this binding sequence was required for Fe-Fur mediated activation. Finally, fluorescence anisotropy assays indicate that Fe-Fur specifically bound this Fur box with a relatively high affinity ($K_d = 200$ nM). These findings provide novel insight into the genetic regulation of a key metabolic enzyme and add to our understanding of the diverse roles Fur plays in gene regulation in *H. pylori*.

Introduction

The Gram-negative pathogen *Helicobacter pylori* colonizes the gastric mucosa of more than half of the world's population (16, 56). While colonization usually results in asymptomatic carriage, a subset of infected individuals may progress to develop a range

of disease states that include gastritis, gastric ulcers, and two types of gastric cancer (16, 56). Because of its unique colonization niche, *H. pylori* is continually faced with dramatic changes in environmental conditions such as pH and nutrient availability. As a result, this organism has evolved very efficient adaptive responses that enable it to persist within the gastric mucosa in spite of these drastic fluctuations. One crucial aspect of the adaptive process involves maintaining tightly controlled regulatory networks that differentially modulate gene expression in response to environmental stimuli.

In *H. pylori*, a key transcriptional regulator that maintains control of many of these adaptive regulatory networks is the ferric uptake regulator (Fur) (39, 58, 67). This regulator is found in many bacterial species and is traditionally associated with the regulation of iron uptake and storage systems. In *H. pylori*, Fur is critical for pH adaptation (15, 67), colonization (22, 67, 111), and mounting adaptive responses to oxidative (26, 28, 58, 67, 69) and nitrosative stress conditions (134). Given the importance of Fur to these essential biological processes, perhaps it is not surprising that *H. pylori* Fur regulates a wide variety of genes that encode for functionally diverse proteins that extend beyond just iron uptake and storage (58, 67). A somewhat unique aspect of Fur regulation in *H. pylori* is the ability to function beyond what is typically seen in other bacteria. Like Fur in other bacterial species, *H. pylori* Fur can function as an iron co-factored transcriptional repressor (Fe-Fur), where iron-dependent binding to specific DNA sequences (Fur boxes) prevents assembly of the transcriptional machinery at the core promoter elements (42, 46, 128). In addition, *H. pylori* Fur can also regulate gene expression in the iron-free or *apo* form of the protein (12, 26, 43, 45, 58). Previous studies have shown that *apo*-Fur can act as both a repressor (12, 26, 58, 59) and as an

activator (45). Furthermore, there is also evidence that Fe-Fur can activate transcription, although to date this regulatory function has only been conclusively demonstrated to occur at a single *H. pylori* promoter (2).

Previous transcriptional profiling experiments conducted by our group (67) identified another set of potentially Fe-Fur activated gene; expression of *oorD*, *oorA*, and *oorC* were decreased in a *fur* mutant strain of *H. pylori*. At the chromosomal level these genes appear to be encoded as part of an operon with *oorB*. The *oorDABC* genes encode a 2-oxoglutarate (α -ketoglutarate) oxidoreductase (OOR) (79) and OOR activity (reversible oxidative decarboxylation of 2-oxoglutarate to form succinyl-CoA and CO₂) has been demonstrated in *H. pylori* using whole cell lysates (79). Additional biochemical studies characterized the *H. pylori* OOR enzyme as an essential oxygen labile heterotetrameric protein consisting of 4 polypeptide subunits of 10 kDa (OorD), 43 kDa (OorA), 33 (OorB), and 24 kDa (OorC) (79). In addition to serving as a source of succinyl-CoA, it has also been proposed that the *H. pylori* OOR enzyme acts to provide NADPH with a respiratory donor electron (79). Thus, the OOR enzyme of *H. pylori* plays a multi-faceted role in central metabolism and energy conservation.

While some of the basic biochemical characteristics of the *H. pylori* OOR enzyme have been described, there is currently little direct information about how expression of the genes that encode the essential enzyme are regulated. Given the importance of the OOR enzyme in the physiology of *H. pylori* and our previous preliminary evidence that suggested Fe-Fur activates expression of these genes (67), herein we characterize transcriptional regulation of the *oorDABC* genes. We show that these genes are co-transcribed as a single operon from a single start site, and that there is a conserved Fur

box distally located upstream of the core promoter elements. Purified Fur bound specifically to this site, and this binding was essential for the Fur-mediated activation of *oorDABC*. These data add to the increasing number of genes regulated by *H. pylori* Fur via non-classical (iron-bound repression) mechanisms and provide potential insight into how sensing changes in environmental cues such as iron availability can initialize changes in intracellular physiology.

Materials and Methods

Bacterial strains and growth conditions

All bacterial strains and plasmids used in this study are listed in Table 1 and oligonucleotides are listed in Table 2. *H. pylori* strains were maintained in brain heart infusion broth (Beckton Dickinson) containing 10% fetal bovine serum (FBS; Gibco) and 20% glycerol at -80°C. *H. pylori* strains were routinely cultured at 37°C under microaerophilic conditions (5% O₂, 10% CO₂, 85% N₂) on horse blood agar (HBA) plates that contained 4% Columbia agar base (Neogen Corp.), 5% defibrinated horse blood (HemoStat Laboratories, Dixon, CA), 0.2% β-cyclodextrin (Sigma), 5 μg/mL amphotericin B (Amersco), 2.5 U/mL polymixin B (Sigma), 5 μg/mL trimethoprim (Sigma), and 10 μg/mL vancomycin (Amersco). Liquid cultures of *H. pylori* were grown in brucella broth that contained 10% FBS and 10 μg/mL vancomycin. *E. coli* strains were maintained in LB with 40% glycerol at -80°C and routinely cultured at 37°C on

Table 1. Strains and plasmids used in this study

Strains and Plasmids		
Strain	Description	Reference
<i>E. coli</i>		
DSM431	BL21 (DE3) Rosetta/pLys <i>Afur</i> (pDSM430) Amp ^r , Kan ^r , Cm ^r	(26)
<i>H. pylori</i>		
DSM1	G27 WT	
DSM300	G27 <i>Afur</i> :: <i>cat</i> Cm ^r	(67)
DSM925	G27 <i>Afur</i> (markerless)	(128)
DSM1079	G27 WT (pDSM845) Kan ^r	This study
DSM1080	G27 <i>Afur</i> (pDSM845) Kan ^r	This study
DSM1081	G27 WT (pDSM833) Kan ^r	This study
DSM1082	G27 <i>Afur</i> (pDSM833) Kan ^r	This study
Plasmid		
pDSM430	pET21A:: <i>fur</i>	(26)
pDSM815	pDSM199:: <i>cat</i>	(128)
pDSM833	pDSM815::P _{oorDABC (-FB)} :: <i>cat</i>	This study
pDSM845	pDSM815::P _{oorDABC} :: <i>cat</i>	This study

Table 2. Oligonucleotides used in this study

Oligonucleotide	Sequence 5' - 3'
oorDA-up	GACAGGAAGGATTTCAAATTCGC
oorDA-dn	CGAGTGGGCATTCCGGTTGATGGG
oorAB-up	GAAAGCAAGCAAAAAGTCGGC
oorAB-dn	GCCCTACCATGCGTGGTGTGAACG
oorBC-up	GCGTCTCAAATGCTAAAATGG
oorBC-dn	GCTGATTTGAGCGACTGAAAGC
oorD-PE	GCGCGACAGCTTTAAAATCCCC
oorD_TSS-up	CGATTAGAGCCGTGGTTTTCC
oorD_TSS-dn	GAAATCCTTCCTGTCAGCCAC
oorD_Fb_up-F	ACCGATAACACCCCTATAACACC
oorD_Fb_up-R	GAAAAAACGCCTCATTAACTTAATTTGAAAGATTAATGTTTTTAA ATGCTCC
oorD_Fb_dn-F	GAGCATTTAAAAAACATTAATCTTTCAAATTAAGGTTAATGAGGCG TTTTTC
oorD_Fb_dn-R	GTCTTCATTCACCCAAACGGC
oorD_EMSA-F	TTCAGCGCGACTTATAAGGAG
oorD_EMSA-R	AGCCCTAGCAATCAAAAATTTGCC
oorD-FA	5FluorT/TTCTAATAATCATTTTTAAAAT
oorD-FA_SCRAM	5FluorT/TTCGTGTGTGTGTGTGAAAT
oorD_qRT-F	CCGTTTGGGTGAATGAAG
oorD_qRT-R	CACGCAACCGATACAACTC
G27_16S-F	ATGGATGCTAGTTGTTGGAGGGCT
G27_16S-R	TTAAACCACATGCTCCACCGCTTG
Cat_qRT-F	ATACCACGACGATTTCCGGCAGTT
Cat_qRT-R	ACTGGTGAAACTCACCAGGGATT

1.5% LB agar plates (MoBio) or in LB broth with shaking at 225 rpm. When applicable, bacterial growth media was supplemented with 25 µg/mL kanamycin (Kan; Gibco), 100 µg/mL ampicillin (Amp; USB Corp.), or 8 µg/mL chloramphenicol (Cm; EMD Chemicals, Inc). The wildtype *H. pylori* strain G27 (9) or genetically modified G27 derivatives were used for all experiments in this study.

RNA extraction, cDNA synthesis and real-time PCR

Exponential phase liquid cultures of *H. pylori* (O.D.₆₀₀ ~0.5) were harvested onto a 0.45 µm filter by vacuum filtration and snap frozen in liquid nitrogen. RNA was isolated using the TRIzol reagent (Invitrogen) as previously described (26). First strand cDNA was synthesized using the Quantitect reverse-transcription kit (Qiagen) according to the manufacturer's instructions. For each cDNA synthesis reaction, a corresponding control reaction with no reverse transcription enzyme was included. Quantitative real-time PCR (qRT-PCR) reactions were performed using a Roto-gene Q instrument (Qiagen) in a total volume of 20 µL; each reaction contained 1X Roto-Gene SYBR Green RT-PCR master mix (Qiagen), 3 pmol each of the forward and reverse primers as indicated, and 1 µL of cDNA or NoRT control reaction as template. Cycling conditions included an initial activation step of 5 minutes at 95°C, followed by 35 cycles of denaturing at 95°C for 10 seconds, annealing at 50°C for 20 seconds, and extension at 72°C for 30 seconds. SYBR Green fluorescence was measured during each extension step. Relative gene expression was calculated as $2^{-(\Delta\Delta C_t)}$ using 16S as the internal reference gene. A post-run melt curve analysis was performed to ensure specificity of

amplification. Three biologically independent replicates of each experiment were performed.

oorDABC gene junction PCR

To detect each of the *oorDABC* gene junctions, a qualitative reverse transcription PCR was performed using GoTaq master mix (Promega), 3 pmol each of the forward and reverse primers as indicated, and 1 μ L of cDNA (or NoRT control reaction), which was synthesized using exponential phase RNA from wildtype G27. Each reaction was incubated for 5 minutes at 95°C, followed by 25 cycles of denaturation at 95°C for 30 seconds, annealing at 50°C for 30 seconds, and extension at 72°C for 1 minute. PCR products were separated on 1% agarose gels and visualized by staining with ethidium bromide. Each PCR was performed at least twice using biologically independent cDNA templates.

Primer extension and transcriptional start site (TSS) mapping

Primer extension reactions were performed using 10 pmol of γ -³²P labeled *oorD*-RT primer, 5 μ g of RNA harvested from exponential phase wildtype or *Afur* liquid cultures, and the AMV reverse-transcription kit (Promega) according to the manufacturer's instructions. Dideoxy sequencing reactions were initiated using the γ -³²P labeled *oorD*-RT primer and the Sequenase PCR amplicon sequencing kit (USB) according to the manufacturer's instructions. Primer extension and sequencing reaction products were resolved by polyacrylamide gel electrophoresis. After electrophoresis, gels were exposed to phosphor screens and subsequently scanned using an FLA-

multifunctional scanner (Fuji-film). Image analyses were performed using the Multi-gauge software package (Fuji-film). TSS mapping experiments were performed at least twice with comparable results.

Construction of $P_{oorDABC}::cat$ reporter plasmids and strains

To evaluate the importance of the putative Fur box in the expression of the *oorDABC* promoter, we created plasmid-based transcriptional fusions to the chloramphenicol acetyl-transferase reporter gene (*cat*). A 151bp region of the *oorDABC* promoter containing the putative Fur box (TAATAATcATTTTTA) was PCR amplified using the primers PoorD-F and catEC-3', digested with BamHI and PstI and directionally cloned upstream of the promoterless *cat* reporter in pDSM815 (128) to create pDSM845 (pDSM815:: $P_{oorDABC}::cat$). This reporter plasmid is derived from pTM117 (27), which was developed by and has been successfully used as a transcriptional reporter by our group (128). Similarly, to create the *oorDABC* promoter fusion without the Fur box, the *oorD_5'(-)* and *oorD_3'(-)* primers were used to amplify the portion of the *oorDABC* immediately downstream of the Fur box. This amplified fragment was then digested using BamHI and PstI and subsequently cloned into pDSM815 to create pDSM833 (pDSM815:: $P_{oorDABC(-FB)}::cat$). Each promoter fusion plasmid was then transformed into the wildtype G27 strain DSM1 and the markerless G27 *fur* deletion strain DSM925 (128) to create strains DSM1079 (WT + pDSM845), DSM1080 (Δfur + pDSM845), DSM1081 (WT + pDSM833), and DSM1082 (Δfur + pDSM833). Transformants were selected on HBA plates that contained 25 μ g/mL kanamycin and plasmid integrity was verified by restriction digest, PCR, and sequencing.

rFur purification

Recombinant native *H. pylori* Fur was purified as described previously (26). Briefly, an *E. coli fur* deletion strain (26) containing the *H. pylori* rFur expression plasmid pDSM430 (26) was grown to mid-exponential phase in LB broth and *fur* expression was induced with 100 mM IPTG (isopropyl-D-thiogalactopyranoside; Sigma) overnight at 30°C. Cells containing rFur were harvested by centrifugation and mechanically disrupted using a French pressure cell (Amicon). rFur was purified from pressed cell lysates by fast-protein liquid chromatography. Cell lysates were first passed through a HiTrap SP column for cation exchange-based purification using a salt gradient of 25mM to 500 mM NaCl. Fractions containing rFur were collected and then passed through a Sephacryl-200 column for size-exclusion purification. Peak fractions were collected and stored in 50mM sodium phosphate, 500 mM NaCl, pH 8.0 at 4°C.

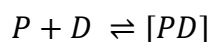
rFur fluorescence anisotropy

Fluorescence anisotropy was used to measure the DNA recognition and binding properties of rFur and the putative *oorDABC* Fur box. Fluorescently labeled DNA that contained either the wildtype *oorDABC* Fur box (*oorD-FA*) or scrambled Fur box sequence (*oorD-FA_SCRAM*) (Table 2) were incubated with increasing concentrations of Fur. Measurements were taken on an SS PC-1 spectrofluorimeter configured in the L format with an excitation wavelength of 495 nm and an emission wavelength of 519 nm. The band pass for the excitation was 2 nm and 1 nm for emission. In a typical

experiment, a 15 nM solution of fluorescently labeled DNA in 30 mM Tris, 120 mM KCl, 16 mM DTT, 1 mM MnCl₂, 20% glycerol, 5 mM Bovine Serum Albumin (BSA) at pH 8.0 was added to a 0.5 cm PL Spectrosil far-UV quartz window fluorescence cuvette (Starna Cells) (52). The anisotropy of the free DNA oligonucleotide was measured. rFur protein was then titrated into the cuvette from a stock solution containing 30 mM Tris, 120 mM KCl, 16 mM DTT, 1 mM MnCl₂ and 20% glycerol at pH 8.0 in a stepwise fashion and the resultant change in anisotropy was recorded. The protein was added until the anisotropy values reached a plateau, which indicated saturation. The data were analyzed by converting the anisotropy, r , to the fraction bound, F_{bound} (the fraction of Fur bound to DNA at a given DNA concentration), using the equation (91) :

$$F_{bound} = \frac{r - r_{free}}{(r_{bound} - r)Q + (r - r_{free})}$$

where r_{free} is the anisotropy of the fluorescein-labeled oligonucleotide, r_{bound} is the anisotropy of the DNA-protein complex at saturation, and Q is the quantum yield ratio of the bound to free form and is calculated from the fluorescence intensity changes that occur ($Q = I_{bound}/I_{free}$). F_{bound} was plotted against the protein concentration, treating Fur as a dimer, and fit using a one site binding model:



$$K_d = \frac{[P][D]}{[PD]}$$

$$F_{bound} = \frac{P_{total} + D_{total} + K_d - \sqrt{(P_{total} + D_{total} + K_d)^2 - 4P_{total} D_{total}}}{2D_{total}}$$

where P is the protein (Fur) concentration and D is the DNA concentration. Each data point from the fluorescence anisotropy assay represents the average of 31 readings taken over a time course of 100 s. Each titration was carried out in triplicate.

Statistical analyses

To assess the statistical significance of the differences in relative gene expression from the native *oorDABC* promoter identified by qRT-PCR, a Student's *t* test was performed on log₁₀ transformed fold change data. Differences in relative gene expression from the plasmid based *cat* promoter fusions were determined using a paired Student's *t*- test on normalized *cat* transcript levels.

Results

The oorDABC genes are co-transcribed as an operon

Previous transcriptional profiling studies using wildtype and *fur* mutant strains of *H. pylori* suggested that expression of *oorD*, *oorA*, and *oorC* were decreased in a *fur* mutant strain of *H. pylori* (67). At the chromosomal level, these genes appear to be encoded as part of an operon with *oorB* (Figure 5A). Furthermore, the proteins produced from the *oorDABC* genes are thought to function together in a single multi-subunit enzyme (79); genes encoding components that work together in this fashion are often expressed as a single transcriptional unit (180). Therefore, we hypothesized that the *oorDABC* genes are co-transcribed as an operon from a single promoter. To test this hypothesis, we designed PCR primers that would allow us to amplify the region that spans each of the gene junctions from genomic DNA (Figure 5B) as well as a cDNA template; amplification from the cDNA template would only occur if the adjacent genes

are co-transcribed. As shown in Figure 5B, we were able to amplify the 295 bp *oorDA*, the 240 *oorAB*, and the 191bp *oorBC* gene junctions. However, we were unable to amplify any of these junctions if no reverse transcriptase was added to the cDNA synthesis reaction. These data indicate that the *oorDABC* genes are in fact co-transcribed and constitute an operon.

Expression of the oorDABC genes is activated by Fur under iron-replete conditions

Given that our previous transcriptional profiling studies suggested that expression of the *oorDABC* genes was activated by Fur under iron-replete conditions (67), and because this type of regulation is different from the classical iron-dependent repression commonly associated with Fur regulation, we sought to further characterize regulation of the *oorDABC* promoter. Initially, we first sought to confirm our previous findings using qRT-PCR, since it is more sensitive than the methods used previously. Rather than measuring expression from each *oor* gene, we opted to use *oorD* expression as a readout for expression from the *oorDABC* promoter since it is the first gene in the operon. Using qRT-PCR, we determined that under iron-replete conditions, expression of *oorD* was ~3.5 fold less in the *fur* mutant strain as compared to the wildtype strain. This difference in expression was significant ($P=0.006$, Student's *t*-test). Thus, in agreement with our previous data (67), maximal transcription from the *oorDABC* promoter requires Fur.

Figure 5. Genetic organization and transcription of the oorDABC operon.

(A) The genes that encode for the individual OOR subunits are organized in an operon.

To determine whether these genes were co-transcribed, primers were designed for the *oorDA*, *oorAB*, and *oorBC* gene junctions. The approximate amplified regions are indicated by the small black bars (not drawn to scale).

(B) PCR amplification of the *oorDA*, *oorAB*, and *oorBC* gene junctions using wildtype *H. pylori* genomic DNA produced amplicons of 295 bp, 240 bp, and 191 bp, respectively.

(C) Qualitative reverse-transcription PCR (RT) of the *oorDA*, *oorAB*, and *oorBC* gene junctions produced amplicons of 295 bp, 240 bp, and 191 bp, indicating that these genes are co-transcribed as

an operon. Control reactions for each reverse-transcription PCR (NoRT) did not produce amplification products, indicating that amplification was specific to the cDNA template.

RT-PCR and NoRT control reactions were performed in duplicate using biologically independent cDNA samples with similar results.

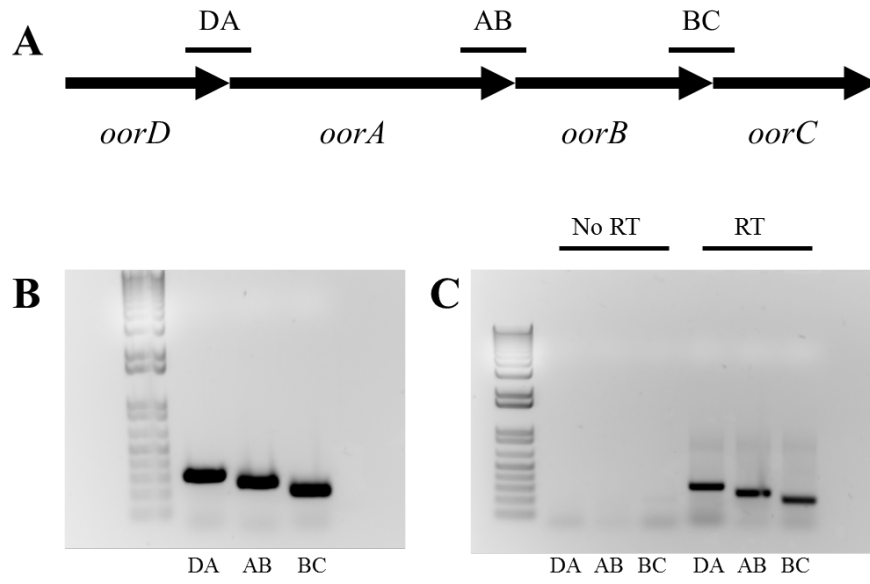


Figure 5. Transcriptional start site (TSS) mapping and identification of oorDABC promoter elements

Given that the *oorDABC* genes are co-transcribed as an operon, and that expression from this promoter is regulated by Fur, we next sought to define the promoter elements of these genes. To this end, we utilized primer extension to map the 5' end of the *oorDABC* transcript and identify the transcriptional start site. As shown in Figure 6A, the primer extension reaction produced a single cDNA product from samples obtained from both the wildtype and *fur* mutant strains. In agreement with our qRT-PCR data, the cDNA product was more abundant in the wildtype strain than in the *fur* mutant, suggesting that Fur activates expression from this promoter (Figure 6A). In both the wildtype and *fur* mutant strains, the +1 was located at a guanine nucleotide located 54 bases upstream of the ATG start codon. Upstream of the transcription start site we identified a well-conserved -10 element (TACAAT) that also contained a TGN motif immediately upstream, which is commonly seen in extended -10 regions (Figure 6B). Extended -10 sequences are found in many *H. pylori* promoters (124, 142) and in this case may be important for efficient *oorDABC* expression as this promoter does not contain a well-conserved -35 sequence. Instead, this region is replaced with a periodic AT-rich sequence that appears to typify many *H. pylori* promoters (124, 142). Further upstream of the core promoter elements, we identified a conserved putative Fur binding site (Figure 6B). This AT rich nearly palindromic sequence (TAATAATCATTTTTTA) is centered ~140 bases upstream of the transcription start site and differs from the core binding site for Fe-Fur by 1 nucleotide (128). Examination of this region in several sequenced *H. pylori* strains showed that this Fur box was highly conserved (data not shown). Of note, the stop codon of the upstream *pabC* gene lies within the 5' end of the putative Fur box; since *pabC* has not been shown to be Fur regulated in previous studies

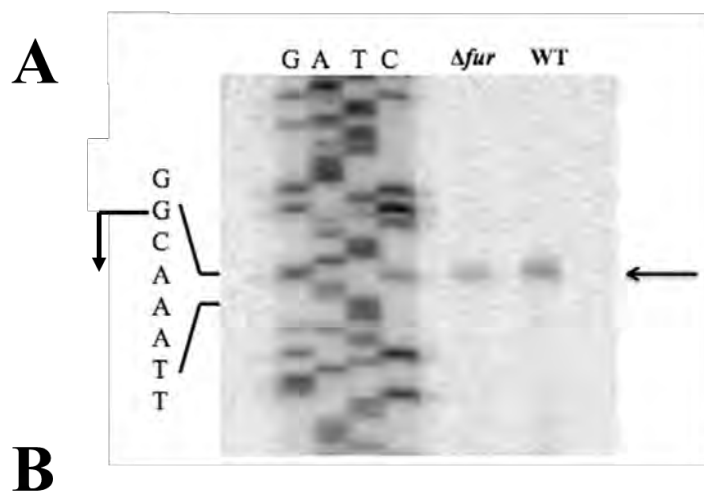
(58, 67), the significance of the location of this Fur box remains unclear. While the binding site for Fur often overlaps the -10 and/or -35 regions for promoters that are repressed by Fur, this is not the case for promoters that are activated by this regulator; Fur typically binds upstream of the core promoter elements for these types of genes (2, 43). Thus, the positioning of the putative Fur binding site in the *oorDABC* promoter is consistent with the notion the Fe-Fur acts as an activator at this promoter.

Fur specifically binds to the putative Fur box in the oorDABC promoter region

Previous work from our lab demonstrated that Fe-Fur binds specifically to a 377 bp region upstream of the *oorD* coding region (67); however, that work did not determine where Fur binding occurred within this fragment. Given our identification of a putative Fur box located in the *oorDABC* promoter region that would have been contained in the larger fragment studied previously, we next sought to determine whether this sequence was in fact the target for Fur interaction. Given that fluorescence anisotropy (FA) has been successfully used to measure the DNA binding properties of metalloregulatory proteins, including Fur (52, 53, 182), we chose to use FA for these studies. To this end, we utilized a fluorescently labeled 23 bp fragment of the *oorDABC* promoter region that contained the putative Fur binding site (*oorD-FA*) as well as a derivation of the same fragment where the conserved Fur binding sequence was scrambled to a GT repeat sequence (*oorD-FA_SCRAM*). For each of these fluorescently labeled templates, we performed binding assays using a range of Fe-Fur concentrations; at concentrations of Fe-Fur where the protein bound the DNA template, the DNA:Fur complex displayed an increased anisotropy. As shown in Figure 7, Fe-Fur bound to the template that contained

Figure 6. Mapping of the oorD TSS and promoter structure.

(A) The *oorD* transcriptional start site (TSS) was mapped using RNA from wildtype and *Δfur* strains of *H. pylori*. First strand cDNA was reverse transcribed from within the *oorD* coding region using the *oorD*-RT primer; only a single band was detected for both strains indicating a single TSS. **(B)** The core promoter region contains a canonical -10 region (underlined) as well as an extended -10 element but does not have a highly conserved -35. However, the region where a typical -35 sequence would lie is indicated for reference (underlined). The putative Fur box (underlined italics) is located ~130 bp upstream of the TSS (+1) which is located 54 bp upstream of the ATG start codon (bolded and italicized).



Fur Box

TTTCTAATAATCAATTTTAAAATTAAGGTTAATGAGGCGTTTTTTCTTTTAAAT

TGAGTAAAAAGTGTTTAGTATTTTCTCATTTC AATTTTAAGTTCCTACTATTAA

-35 -10 +1

AGCATTTTAGATTTTATTA AAAAAGGCTTGCTTACAATTTTAGGCAAATTTTGA

TTGCTAGGGCTTTAAATACAGCTTTTAGCACAAAGGAGAATGAATG

Figure 6. Mapping of the *oorD* TSS and promoter structure

the conserved Fur binding sequence, whereas Fur did not bind to the scrambled sequence to any significant extent. The solution-based anisotropy data obtained using Fe-Fur and the WT DNA template were used to fit an appropriate binding model and calculate a dissociation constant (K_d). The binding affinity of Fe-Fur with the labeled WT DNA template was 200 nM, which is consistent with K_d values for other Fe-Fur target promoters in *H. pylori* (unpublished results).

The Fur box upstream of the oorDABC core promoter is essential for transcriptional activation

While the binding of Fe-Fur to the Fur box in the *oorDABC* promoter region is consistent with Fur dependent activation, we next wanted to ensure that Fur binding to this Fur box was in fact required for transcriptional activation at this promoter. To this end, we utilized plasmid based promoter fusions to determine what, if any, effect loss of the Fur box had on transcription from the *oorDABC* promoter. The first of these fusion reporters contained the full-length wildtype promoter fused to a chloramphenicol acetyl transferase reporter gene (*cat*), while the other plasmid contained a slightly truncated promoter region that did not contain the putative Fur box. Each of these reporters was moved into both wildtype and *fur* mutant strains and the contribution of the putative Fur box to activation of *oorDABC* was quantitated by measuring expression of *cat* by qRT-PCR in three biologically independent experiments (Table 3). First, we compared the levels of *cat* expression from the wildtype *oorDABC* promoter (P_{oorDABC}) and Fur box deletion reporter ($P_{\text{oorDABC}(-\text{FB})}$) fusions in the wildtype and *fur* mutant strain background.

Figure 7. rFur binds specifically to the oorDABC Fur box.

Fluorescently labeled P_{oorDABC} DNA templates with the WT Fur box sequence (closed circles) or with a scrambled Fur box sequence (open triangles) were incubated with increasing concentrations of rFur. Fur binds specifically to the Fur box in the wildtype P_{oorDABC} template, but not to the scrambled sequence. After fitting to an appropriate binding model, the dissociation constant (K_d) was determined to be 200 nM. The Y axis represents the fraction of labeled oligo duplex bound by Fur, and the X axis indicates the concentration of Fur dimer, [Fur]₂.

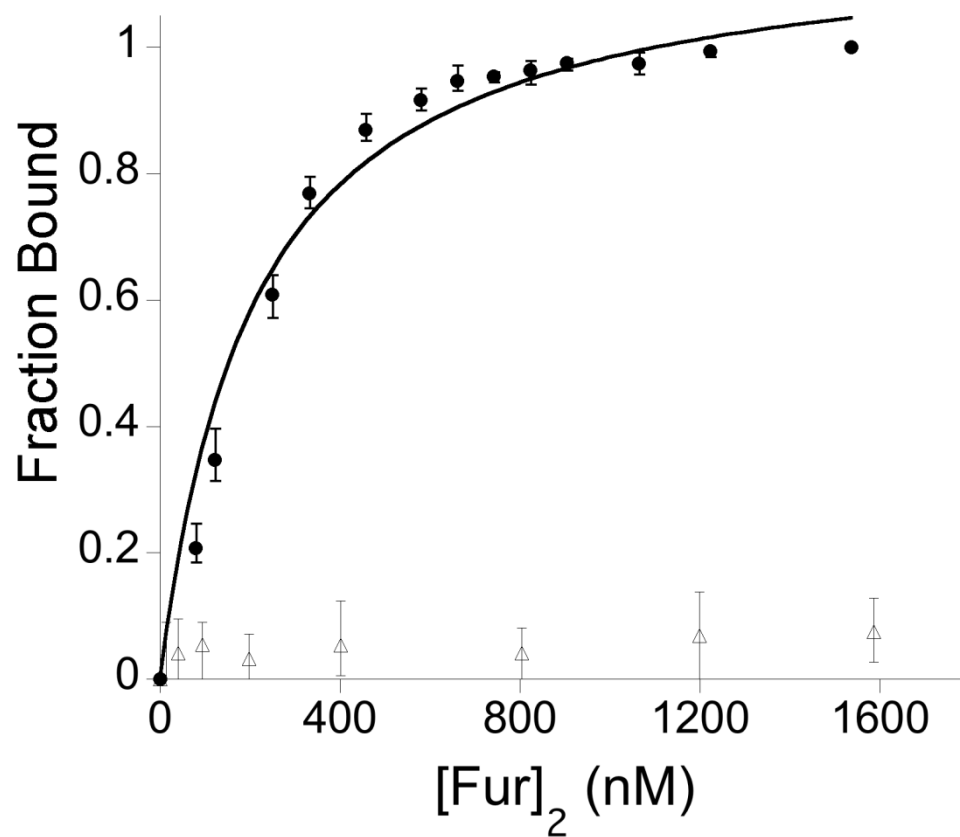


Figure 7. *rFur* binds specifically to the *oorDABC* Fur box

Similar to the qRT-PCR results described above, and as expected if Fur was required for activation of expression, the level of *cat* expression from the wildtype *oorDABC* promoter (P_{oorDABC}) was higher in the wildtype strain than in the *fur* mutant (mean fold activation of 3.7; $p=0.05$, Student's *t*-test) (Table 3). As expected, this difference in *cat* expression was not seen when the reporter plasmids did not contain the Fur box. In contrast, the $P_{\text{oorDABC (-FB)}}$ fusion was expressed at a slightly higher level in the *fur* mutant strain. When the expression of the fusions was compared only within the same strain background, the levels of *cat* expression were dramatically higher in the wildtype strain when the Fur box was present in the fusion (mean fold change of 27.2 fold higher). Since there was a high degree of variability in the degree of increase in reporter expression, this result was not statistically significant, but showed a strong trend towards significance ($p=0.07$). This increased level of expression required Fur, since a similar increase was not seen when these fusions were carried in the *fur* mutant strain; instead, the level of *cat* expression from the $P_{\text{oorDABC (-FB)}}$ fusion was dramatically higher in this strain background (Table 3). Collectively, the results from these experiments confirm our previous finding that *oorDABC* activation is Fur-dependent and provide new evidence that activation requires the Fur box located in the -130 region of this promoter.

Discussion

The ability to survive in the gastric mucosa requires that *H. pylori* be able to efficiently respond to changes in environmental conditions such as pH and fluctuation in nutrients. As with other bacterial pathogens, the major way that *H. pylori* adapts to

Table 3. The *oorDABC Fur* box is required for activation

<i>oorDABC</i> Fold Activation [#]				
	Bio1	Bio2	Bio3	Mean
WT P _{oorD WT} / Δfur P _{oorD WT}	4.8	1.8	4.5	3.7*
WT P _{oorD (-FB)} / Δfur P _{oorD (-FB)}	0.15	2	0.45	0.87
WT P _{oorD WT} / WT P _{oorD (-FB)}	6.7	50	25	27.2
Δfur P _{oorD WT} / Δfur P _{oorD (-FB)}	0.21	0.08	0.07	0.12*

[#]Activation measured as *cat* reporter gene expression in WT or Δfur strains carrying *oorD* reporter plasmids with wildtype or mutated promoter sequences. * indicates statistical significance by Student's *t*-test, $p \leq 0.05$.

Bio1, Bio2, Bio3 indicate biologically independent experiments; WT, wildtype strain; PoorD WT, wildtype promoter; PoorD (-FB), Δfur Box promoter; Δfur , *fur* deletion strain

changes within the host is by altering gene expression in response to external stimuli. However, unlike many other well studied pathogens, *H. pylori* lacks the repertoire of regulatory proteins that usually facilitate these changes. Rather, *H. pylori* alters gene expression using only a handful of dedicated transcriptional regulators (9, 155). As a result, the regulatory proteins that are encoded in the *H. pylori* genome have evolved to function outside of their canonical regulatory roles. One of these regulatory proteins that displays extended function is Fur. Arguably the “master regulator” in *H. pylori*, Fur has been shown to repress and activate transcription in both the iron co-factored and *apo* forms of the protein (2, 12, 26, 39, 42, 45, 46, 58). Of these types of regulation, Fe-dependent activation has been understudied; only *nifS* has previously been shown to be Fe-Fur activated in *H. pylori* (2). Therefore, to extend our knowledge of this type of regulation, herein we characterize the role of Fur in the activation of *oorDABC* expression, which was previously suggested to be activated under iron-replete conditions (2).

The *oorDABC* genes constitute a single transcriptional unit that encodes for a 2-oxoglutarate oxidoreductase (OOR) enzyme. This enzyme catalyzes the formation of succinyl-CoA, which is a major intermediate in carbon metabolism. In addition to generating succinyl –CoA, the oxidative decarboxylation of α -ketoglutarate (2-oxoglutarate) results in the transfer of electrons through the respiratory electron chain via NADPH (79). Thus, OOR function also plays a key role in both amino acid degradation/recycling and in maintaining the energy reserves within the bacterial cell. Since this catalytic step feeds into multiple physiologically important cellular processes, ensuring that this reaction only occurs when conditions are most favorable is critical for

maintaining metabolic homeostasis within the cell. One way of controlling this reaction is to utilize environmental conditions as a signal to transcriptionally regulate the genes that encode the OOR enzyme complex. Given that it functions as a sensor of iron availability, Fur could be considered a surrogate for detection of nutritional availability in the environment: when iron levels are high, it is likely that other nutrients are available as well. Thus, by activating expression of the *oorDABC* genes when iron is abundant, *H. pylori* is able to prime a key component of its central metabolism and maximize efficiency while nutrients are readily available. In contrast, when nutrients are not readily available and iron is depleted, it is less advantageous to continue transcribing the *oorDABC* genes at high levels; thus expression of these genes is reduced to a basal level. While Fur activation at this particular step in carbon metabolism has to yet be described in other organisms, Fur has been shown to activate expression of other metabolic genes in *N. meningitidis* (43). Thus, the utilization of iron availability as a sensor of environmental growth conditions has apparently evolved in other bacterial pathogens.

The mechanism by which Fe-Fur represses transcription has been well-characterized and has been shown to typically involve binding of Fur in the -10 and/or -35 region of the regulated promoter. This binding physically occludes the ability of the RNA polymerase (RNAP) to interact with the promoter and initiate transcription (7, 40, 42, 45, 69). In contrast, the process of Fe-Fur activation occurs significantly upstream of the RNAP binding site. In this regard, Fe-Fur activation mimics activation by another *H. pylori* metalloregulator, NikR, which can also binds upstream of the core promoter elements to activate gene expression (60). For the *oorDABC* promoter, Fur binds a single distal Fur box (TAATAATcTTTTTA) centered ~140 bp upstream of the +1; this binding

sequence is highly conserved, nearly palindromic, and quite similar to the canonical Fe-Fur binding site defined in *H. pylori* and other organisms (8, 128). In addition, the highly conserved nature of this binding sequence among other sequenced *H. pylori* strains suggests that Fur-mediated regulation of *oorDABC* also occurs in these strains. To date, only one other *H. pylori* gene has been shown to be directly activated by Fe-Fur. This gene, *nifS*, encodes a protein involved in iron-sulfur cluster formation and is up-regulated under oxidative stress conditions (2). The *nifS* promoter has been suggested to contain two predicted Fur binding sites; Alamuri *et al.*, used DNase footprinting to show that Fur binds to these two regions that lie ~175 bp and ~225 bp upstream of the +1(2). Interestingly, these reported Fur binding regions do not contain any similarity to the canonical Fe-Fur binding site recently identified for *H. pylori* (128). Fur activation at studied *N. meningitidis* promoters also occurs by binding to distal Fur boxes, (binding sites were typically centered between the -80 and -100 regions) (43). Thus, promoters of Fe-Fur activated genes tend to contain Fur boxes that lie distal to the core promoter elements, perhaps suggesting a similar activation mechanisms at the molecular level.

The obvious question then becomes “how does activation occur mechanistically?” While the answer to this question is not immediately obvious, several possibilities exist. First, Fur could have a direct physical role in recruiting the RNAP complex to the core promoter elements. However, this type of activation seems unlikely given that Fur binds to the distal promoter regions, which would place the protein at such a distance that it would be unlikely to physically interact with RNAP. Second, Fur binding to the distal Fur box may induce a conformational change in the promoter DNA architecture that subsequently enhances either assembly of the RNAP complex or the process of

transcription initiation. Finally, perhaps Fur binding upstream of the *oorDABC* promoter region modulates the function of another regulatory protein. Given that these genes are Fe-Fur activated in this scenario, binding of Fur would most likely block binding of a repressor protein. While we cannot currently rule out the first two mechanisms, previous studies suggest that Fur dependent activation at the *oorDABC* promoter may in fact be the result of competition between two regulatory proteins.

Previous pH-dependent transcriptional profiling of *H. pylori* showed that expression of the OOR genes is activated at low pH (67, 171, 173). This pH-mediated activation is dependent upon the acid responsive regulatory two-component system ArsRS (171). In this system, ArsS serves as the sensor kinase that senses low pH and initiates the phosphorelay that leads to phosphorylation of the response regulator ArsR. ArsR has been shown to regulate expression of numerous genes and appears to have the ability to interact with the promoters of some genes in the non-phosphorylated form while interacting with others only when phosphorylated (126, 127, 171). Previous EMSA assays showed that ArsR directly binds to the *oorDABC* promoter region and that this reaction did not require ArsR phosphorylation (171). Thus, in a normally growing cell at neutral pH, ArsR should exist primarily in the non-phosphorylated state and be able to bind the *oorDABC* promoter. Previous DNase I footprinting experiments using ArsR and ArsR target promoters highlighted an AT rich region that is necessary for binding (50). Within this ArsR binding region, the authors identified two conserved DNA sequences (ATCATT and ATTAAA) that are important for binding (50). Mutation of the ATCATT sequence abrogated ArsR binding, whereas mutation of the ATTAAA sequence reduced binding affinity. As shown in Figure 8B, the Fur binding sequence we

identified in the *oorDABC* promoter region also contains the requisite ArsR core binding sequence (ATCATT), and this sequence directly overlaps with the Fur box. Additionally, the secondary binding sequence (ATTAAA), with one nucleotide difference, is found slightly downstream from the Fur box. Thus, taken together these data support a proposed model wherein Fur and ArsR compete for binding at the *oorDABC* promoter; binding of Fur to the promoter would block binding of the ArsR protein, which likely acts as a repressor at this promoter. Thus, the Fur-mediated activation of *oorDABC* expression likely occurs via an anti-repression mechanism (Figure 8). This model could also explain the higher level of expression we observed when the $P_{\text{oorDABC (-FB)}}$ fusion was carried in the *fur* mutant strain; deletion of the Fur box also removes the sequence required for ArsR-mediated repression. Thus, the levels of *oorDABC* expressed are higher (Table 3). Since the Fur and ArsRS regulons share many genes in common and the proteins have similar binding sequences, it is possible that this type of regulatory is a common phenomenon in *H. pylori*. Indeed, previous studies identified promoters that are subject to regulatory competition. For example, the *exbB* promoter region contains conserved binding sites for both Fur and the nickel-responsive regulator, NikR, and these two proteins bind to overlapping regions within this promoter (41). Thus, competition for binding sites among *H. pylori* regulators does occur, although the extent of competition between these proteins is for the most part underappreciated.

In summary, we have shown Fur-mediated activation of the *oorDABC* genes, which encode the OOR enzyme in *H. pylori* (Figure 5). We found that expression from this promoter occurs from a single start site (Figure 6), and that Fur binds specifically to a conserved Fur box located ~130 bp upstream of the core promoter region (Figure 6).

Figure 8. Proposed Model of Fur dependent activation of oorDABC expression.

(A) Under iron-replete conditions at normal pH, both Fur and ArsR compete for an overlapping binding site within the *oorDABC* promoter region. In the absence of a signal from the ArsR histidine kinase, ArsR may act as a repressor and bind to a region that overlaps the Fur box within the *oorDABC* promoter. When iron is abundant, Fur outcompetes ArsR for binding at this site, which and de-represses *oorDABC* expression and results in increased *oorDABC* transcription. **(B)** Previously identified ArsR core binding sequences (bolded text in boxes) overlap with the Fur box (underlined) identified in this study. The overlap in these regions highlights the possibility of competition between Fur and ArsR.

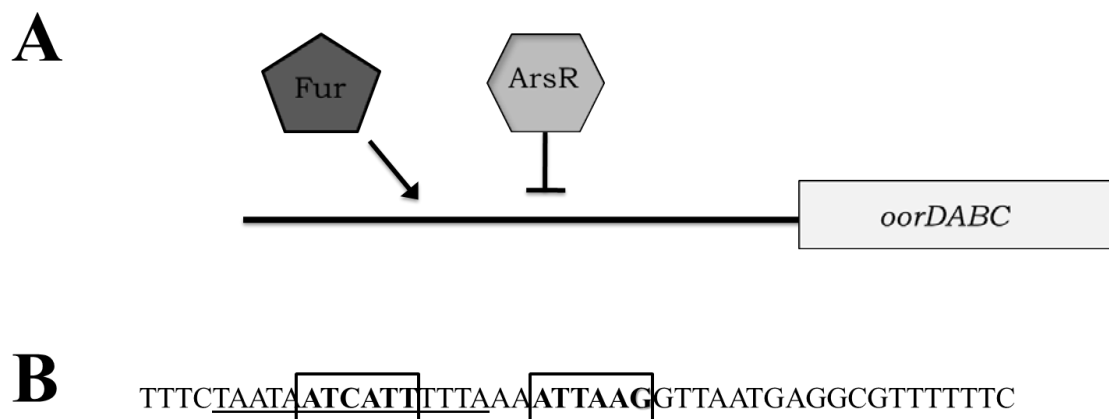


Figure 8. Proposed Model of Fur dependent activation of oorDABC expression.

Furthermore, binding to this Fur box is required for activation of *oorDABC* gene expression (Table 3). These findings add to the growing complexity of Fur regulation in *H. pylori*. Although the precise mechanism of Fe-Fur activation is not yet clear, it likely occurs through an anti-repression mechanism wherein Fur binding blocks binding of ArsR; we are currently investigating the possibility of direct competition between Fur and ArsR as a common regulatory phenomenon in this pathogen.

Acknowledgements

Research in the laboratory of D. Scott Merrell is made possible by grant AI065529 from the NIAID. The contents of this report are the sole responsibility of the authors and do not necessarily represent the official views of the DoD or the NIH.

Chapter Three

Random and Site-Specific Mutagenesis of the Helicobacter pylori Ferric Uptake Regulator Provides Insight into Fur Structure-Function Relationships

Submitted as: **Gilbreath, J.J., Pich, O.Q., Benoit, S.L., Besold, A.N., Maier, R.J., Michel, S.L.J., Maynard, E.L., and Merrell, D.S. 2012.** Random and Site-Specific Mutagenesis of the *Helicobacter pylori* Ferric Uptake Regulator Provides Insight into Fur Structure-Function Relationships. Submitted to *Mol Microbiol*.

The work presented in this chapter is the sole work of J.J. Gilbreath with the following exceptions: O.Q. Pich performed the Pfr-based screen, and qRT-PCR analysis on the mutants obtained from that screen; S.L. Benoit performed the iron-binding studies; A.N. Besold performed the circular dichroism experiments; E.L. Maynard analyzed the fluorescence anisotropy data.

Abstract

The ferric uptake regulator (Fur) of *Helicobacter pylori* is a global regulator that is important for colonization and survival within the gastric mucosa. *H. pylori* Fur is unique in its ability to activate and repress gene expression in both the iron-bound (Fe-Fur) and *apo* forms (*apo*-Fur). In the current study we combined random and site-specific

mutagenesis to identify amino acid residues important for both Fe-Fur and *apo*-Fur function. We identified twenty-five mutations that affected Fe-Fur repression and eight mutations that affected *apo*-Fur repression, as determined by transcriptional analyses of the Fe-Fur target gene *amiE*, and the *apo*-Fur target gene, *pfr*. In addition, four of these mutations also significantly affected levels of Fur in the cell. Based on regulatory phenotypes, we selected several representative mutations to characterize further. Of those selected, we purified the wildtype (WT) and three mutant Fur proteins (E5A, A92T, and H134Y), which represent mutations in the N-terminal extension, the regulatory metal binding site (S2) and the structural metal binding site (S3), respectively. Purified proteins were evaluated for secondary structure by circular dichroism spectroscopy, iron-binding by atomic absorption spectrometry, oligomerization in iron-substituted and *apo* conditions by *in vitro* cross-linking assays, and DNA binding to Fe-Fur and *apo*-Fur target sequences by fluorescence anisotropy. The results showed that the N-terminal, S2, and S3 regions play distinct roles in terms of Fur structure-function relationships. Overall, these studies provide novel information regarding the role of these residues in Fur function, and provide mechanistic insight into how *H. pylori* Fur regulates gene expression in both the iron-bound and *apo* forms of the protein.

Introduction

Helicobacter pylori is a Gram-negative microaerophile that chronically colonizes the gastric mucosa of over half of the world's population (16, 56). While infection always

results in localized inflammation, only a subset of colonized individuals develops overt disease. In severe cases, infection may lead to gastric ulcers, gastric adenocarcinoma, or MALT lymphoma (16, 56). One of the remarkable characteristics of this highly successful pathogen is the ability to survive in the hostile environment of the stomach. Although *H. pylori* normally colonizes within the mucus layer near the gastric epithelium, the bacteria are continuously faced with dramatic fluctuations in pH and changes in the availability of nutrients such as iron. As a result of living in this dynamic niche, *H. pylori* has evolved tightly regulated transcriptional networks that allow the organism to rapidly adapt to changes in the environment.

Despite the importance of regulating gene expression in response to environmental stimuli, the genome of *H. pylori* encodes for relatively few dedicated transcriptional regulators (9, 155). As a result, several of these regulatory proteins have evolved the ability to function in a capacity beyond what is typically seen for their counterparts in other bacterial species. One such protein is the ferric uptake regulator (Fur). Fur belongs to a large family of metalloregulatory proteins and is classically thought of as a repressor of iron uptake systems (reviewed in (93)). Similar to Fur in other bacterial species, *H. pylori* Fur uses ferrous iron (Fe^{2+}) as a co-factor and binds DNA sequences known as Fur boxes to repress transcription (13, 42, 128). However, there are also examples where Fe-Fur Fur acts as a positive regulator, both directly and indirectly (2, 43, 45, 46, 58, 67, 70). Those studies highlight the fact that Fur is more than a repressor of iron uptake systems and instead functions as a global regulator. This global regulatory role is especially apparent in *H. pylori*, where Fur has been shown to regulate a large number of genes required for diverse functions, and has also been shown

to respond not only to intracellular iron levels but also to changes in pH and levels of oxidative and nitrosative stressors(35, 134). One way that *H. pylori* Fur is able to regulate so many genes under different environmental conditions is by repressing and activating gene expression in both the iron-bound (Fe-Fur) and *apo* (*apo*-Fur) forms of the protein (12, 26, 42, 43, 45, 46, 58, 70, 128, 162). This degree of functional diversity is so far unique to *H. pylori* Fur, although there have been reports of Fe-Fur activation in other bacteria, and recently *apo*-Fur repression has been described in *Staphylococcus aureus* and *Campylobacter jejuni* (47, 72). However, *H. pylori* remains the only bacterial species where all four types of Fur regulation have been characterized in detail. Thus, a functional understanding of Fur regulation in this organism could provide valuable information that could expand our understanding of Fur regulation in other bacterial species.

Based on crystallographic data from *Pseudomonas aeruginosa* (129), *Vibrio cholerae* (143), and more recently *H. pylori* (10), progress has been made in understanding the important features of Fe-Fur. The protein is made up of two major domains: the N-terminal domain, which spans amino acids 1-92 in *H. pylori*, contains a canonical winged helix-turned-helix motif (helices α 2- α 4 and sheets β 1- β 2) that facilitates interaction with target DNA, and a C-terminal domain (residues 93-150) that contains several metal coordinating residues and is responsible for dimerization of Fur protomers. A key feature of *H. pylori* Fur is an N-terminal 10 amino acid extension; this region is not seen in the well-studied organisms such as *Escherichia coli*, *P. aeruginosa*, or *V. cholerae* and has only been identified in one other bacterial pathogen to date, *C. jejuni* (23). The structure of *H. pylori* Fur shows that a portion of this extended region

forms helix $\alpha 1$, which stacks against the DNA binding domain and may stabilize this motif. In terms of the C-terminal domain, this region is made up of 3 antiparallel β strands ($\beta 3$ - $\beta 5$) and helices $\alpha 5$ - $\alpha 6$, with helix $\alpha 5$ serving as the dimerization interface.

Also atypical compared to other Fe-Fur structures, the *H. pylori* Fur protein contains three distinct metal binding sites (S1, S2, and S3). S1 is a structural zinc-binding site (10, 165) that is coordinated by four cysteine residues (C102, C105, C142, and C145) found in two CXXC motifs. Metallation at this site stabilizes the three β sheets in this region ($\beta 3$ - $\beta 5$) and is necessary for dimerization (165). S2 is the regulatory binding site; metallation at S2 is responsible for a conformational change in the DNA binding domain that “activates” the protein and facilitates interaction with Fe-Fur target DNA. As the S2 coordination spheres differ in each protomer of the Fur dimer, the exact residues that coordinate the metal ion differ between protomer A and protomer B. In one protomer, the metal ion in S2 is coordinated by H42, E90, H97, and H99; in the other protomer, the ion is coordinated by H42, E90, H97, H99, and E110. In contrast to S2, the S3 site has similar coordination spheres in each protomer of the Fur dimer. Located near the dimerization domain, S3 has a tetrahedral geometry and is coordinated by residues H96, D98, E117, and H134. Previous mutational analysis of the S2 and S3 sites, indicate that S2 is required for Fe-Fur to bind DNA, but S3 is not required; however, metallation of S3 likely increases binding affinity (10).

Until very recently, the structural features of *apo*-Fur have largely remained a mystery. However, the recent publication of the *C. jejuni apo*-Fur structure (23) has finally shed some light on how Fur is able to regulate gene expression in the absence of the iron cofactor. Because *C. jejuni* Fur is most similar to *H. pylori* Fur in terms of

sequence, it is likely that the *C. jejuni apo-Fur* structure is reasonably similar to *H. pylori apo-Fur* (Figure 18 (S1)). Much like its iron-bound counterparts, *C. jejuni apo-Fur* is a dimer and has a canonical winged helix DNA binding domain. However, when compared to the holo-Fur structures (49, 129, 143), the DNA binding domain is rotated 180 degrees. As a result of this rotation, helix $\alpha 1$ is positioned within the DNA binding region, and most likely directly interacts with DNA. In addition to the conformational changes in the N-terminal region of the protein, the metal coordination sites of *C. jejuni apo-Fur* also show some divergence from their metallated counterparts in Fe-Fur. Similar to *H. pylori* Fe-Fur, the S1 site in *C. jejuni apo-Fur* is occupied by a metal ion and is coordinated by two pairs of cysteine residues. Given the similarity of S1 in Fe-Fur and *apo-Fur*, it is likely that this metal ion plays a role in maintaining the dimeric structure for both forms of Fur. The other occupied metal site in the *apo-Fur* structure is S3; while S3 in *H. pylori* Fe-Fur is tetracoordinated by residues H96, D98, E117 and H134, in *C. jejuni apo-Fur* S3 is hexacoordinated with D101, D120, H137 and two water molecules (23). These differences in S3 geometry arise from the rotation of the DNA-binding domain, which renders this site permissive to coordinating water molecules (23). Consistent with the hypothesis that S2 is the regulatory or iron-sensing site within Fur, this site is not occupied in the *apo-* form of the protein.

In the current study, we utilized a combination of random and site-specific mutagenesis to identify residues that are important for iron-bound and *apo-Fur* function in *H. pylori*. We identified 24 mutations via random mutagenesis that affected regulation of the Fe-Fur target gene *amiE* and/or the *apo-Fur* target gene *pfr*. Of the five site-specific *fur* mutations we constructed (R3A, E5A, E8A, R13A, E117R), we identified

two additional residues (E5, E117) that are important for Fur function. Based on the regulatory phenotypes observed in the mutant strains, we selected a subset of these mutations for biochemical studies. Of the five mutations we selected to further characterize, we successfully purified the WT and three mutant proteins (E5A, A92T, and H134Y). These proteins were evaluated for secondary structure content and overall folding, iron binding, oligomerization, and DNA binding in iron-substituted and *apo* conditions. Combined, the results of these studies provide functional insight into Fe-Fur and *apo*-Fur regulation in *H. pylori*.

Results

Random mutagenesis and manganese selection

To identify important residues of *H. pylori* Fur, we opted to initially take a non-biased approach. Using an error-prone PCR-based strategy, we generated a library of ~10,000 random mutant strains; each strain contained ~1 nucleotide change per copy of *fur*, a frequency that was confirmed by sequencing a subset of *fur* genes from the library. We selected this mutation frequency because it was most likely to result in single amino acid changes in the protein. After creating the library, we used a combination of two methods to identify mutations that resulted in a regulatory phenotype. The first strategy was a manganese selection, which has been successfully used to identify key Fur residues in other bacterial species (75, 92, 99). Because manganese acts as a redox stable iron analog, it is thought that strains grown in the presence of excess manganese sense an overabundance of “iron” in the environment. As a result, the bacteria down-regulate

expression of iron uptake systems, which prevents iron from entering the cell. As iron is an essential element for almost all living organisms, shutting down iron uptake in response to the excess manganese in the environment is lethal. By plating the *fur* mutant library on plates that contained 4 mM manganese (manganese (II) chloride), we selected for mutations in *fur* that precluded down-regulation of the iron uptake systems and allowed the mutant bacteria to grow. Aliquots of the mutant library were diluted and plated for single colonies, and 115 manganese resistant (Mn^{R}) colonies were archived. From this pool of 115 mutant strains, we sequenced the *fur* gene to identify mutations that conferred single amino acid changes. We sequenced *fur* from 15-20 strains at a time as a means to determine the saturation point of the mutagenesis. After analyzing the *fur* sequence from 83 Mn^{R} strains we did not detect any new mutations that translated into single amino acid changes and thus, we considered this to be the saturation point. From these 83 strains, we identified 19 single amino acid changes in 15 different residues that conferred a Mn^{R} phenotype. These 15 residues were mostly localized to the C-terminal domain of the Fur protein (Table 5). To ensure the Mn^{R} phenotype was linked to the mutation in *fur*, we next moved each mutation into a clean strain background, re-plated on agar that contained manganese, and re-sequenced *fur* from the newly created strain. In addition, we sequenced the promoter region upstream of *fur* in each strain to ensure that there were no mutations that could affect *fur* expression. For all newly created strains, the Mn^{R} phenotype was transferred with the *fur* mutation, and there were no additional amino acid changes in the coding region or mutations in the *fur* promoter. Thus, we concluded that the ability of each strain to grow in the presence of manganese was linked to the *fur* mutation carried by that strain.

Screen for altered Pfr expression

Although the manganese selection identified multiple residues that appear to be important for Fur function, we considered the fact that performing such a selection under excess metal conditions could bias the results towards identifying mutations that alter metal binding and thus iron-bound repression. This notion was supported by the fact that most of the identified mutations clustered in the C-terminal region of Fur, which contains the vast majority of the metal coordinating residues. To decrease the potential bias of the selection, we also used an alternative strategy to identify mutations that affected *apo*-Fur repression. Based on previous results (12) which showed the *apo*-Fur repressed prokaryotic ferritin protein (Pfr) could easily be visualized by SDS-PAGE followed by Coomassie staining, we designed a visual screen to look for de-repression of the Pfr protein. Using the protocol outlined in the Materials and Methods, we screened ~ 400 individual random *fur* mutant strains. Out of these 400, we identified five strains that displayed altered Pfr levels and contained a single amino acid change in Fur (Table 4). These mutations were distributed across both the C-terminal and N-terminal domains of Fur. Once again, to ensure that the regulatory phenotype was linked to the mutations in *fur*, we moved each mutation into a clean strain background, re-screened the newly created strains for altered Pfr levels, and re-sequenced *fur* and the *fur* promoter. For all five re-created strains, the regulatory phenotype was linked to the mutation in *fur* and there were no additional mutations in the coding or promoter regions.

Selection of residues for site-specific mutagenesis

Because analysis of the distribution of the mutant residues showed that some areas of Fur appeared to be under-represented in our phenotypic assays, we also constructed several site-specific mutations in *fur*. Specifically, we selected four residues in the N-terminal extension (residues 3, 5, 8, and 13) and mutated each of these residues to an alanine (R3A, E5A, E8A, and R13A) (Figure 9 and Table 4). In addition, based on the prediction that changing the charge and size of the side chain at this residue would prevent metallation at this site, we mutated the metal coordinating E117 residue to arginine (E117R). We also created a Cm^R marked control strain (WT_C) to ensure that genetic manipulation of the strains did not affect Fur regulation in some way. These mutations were generated using SOE PCR as described in the Materials and Methods section. Once again, after these site-specific mutant strains were created, we sequenced the *fur* coding sequence and promoter to ensure no additional mutations were present. As a result of our combined mutagenesis approaches, we now possessed 29 *fur* mutations to study in further detail. Additionally, we included the WT, WT_C, and *fur* mutant strains as controls for our future analyses.

Transcriptional analysis of amiE regulation

To determine how the random and site-specific mutations affected iron-bound Fur (Fe-Fur) repression, we quantitated the levels of *amiE* transcript in the mutant strains using qRT-PCR before and after iron chelation; *amiE* is a well-characterized Fe-Fur repressed gene and has been previously used as a reliable readout of Fe-Fur regulation (25, 27). Because *amiE* transcription is normally repressed by Fe-Fur when iron is replete

Figure 9. Distribution of random and site-specific mutations across the coding region of H. pylori Fur. Mutated residues are designated by red letters. The vertical black line denotes the transition from the N-terminal region to the C-terminus (49). Fur amino acids and secondary structure alignment image generated using Polyview-2D: <http://polyview.cchmc.org/> (131).

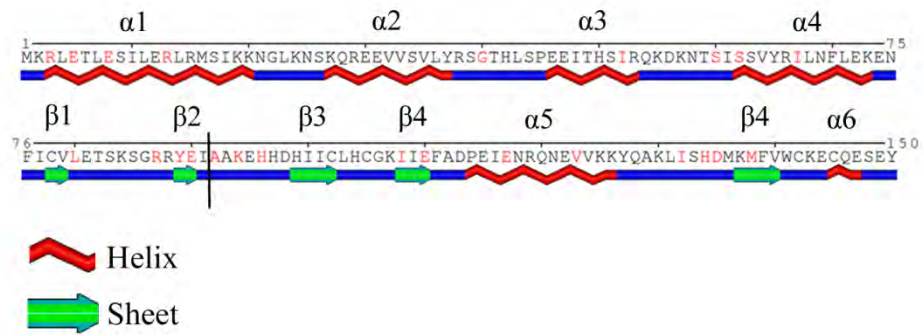


Figure 9. Distribution of random and site-specific mutations across the coding region of *H. pylori* Fur.

(T_0) the addition of the chelating agent should result in the de-repression of *amiE* expression (T_{60}). Thus, we compared changes in the level of *amiE* transcript after iron chelation (T_{60}/T_0). As expected, we saw an increase in *amiE* transcription in the wildtype strain after chelation (Figure 10A). However, in the absence of the Fur protein (the Δfur strain), we saw no change in *amiE* transcription. Seventeen of the mutations identified via the manganese selection showed a phenotype similar to Δfur ; they were not responsive to the change in iron availability. The other two Mn^R strains were responsive to iron, but to a lesser degree than the wildtype strain. All five mutant strains obtained from the Pfr-based screen displayed a significant decrease in iron-responsiveness. However, only a single site-specific mutant strain, E117R, was significantly less responsive to iron chelation.

Given that *amiE* is derepressed in the presence of iron (T_0) in the *fur* mutant, we also compared the basal levels of *amiE* expression in each of the mutant strains to that of the wildtype and Δfur strains. As shown in Figure 10B, several of the mutations identified in the manganese selection resulted in significant de-repression of *amiE* transcription even under iron replete conditions. For example, strains that harbored the L80V, R87Q and Y89C mutations displayed basal levels of *amiE* transcript that were comparable to levels seen in the Δfur strain. Conversely, there were also mutations that did not affect basal levels of expression to a significant degree. The S62T and the E90Q mutations exemplify this scenario, where basal *amiE* levels are comparable to those in the wildtype strain. A similar trend was seen for the mutations obtained from the Pfr-based screen; the

*Figure 10. Transcriptional regulation of amiE under iron replete and iron-depleted conditions as measured by qRT-PCR. (A) Fold increase in amiE transcript levels after chelation. For each strain, relative levels of transcript after chelation were compared to levels prior to chelation (T_{60}/T_0). (B) Relative basal level of amiE transcript in each mutant strain as compared to the wildtype strain (T_0/T_0). In both (A) and (B) the geometric mean of fold differences for at least three biologically independent experiments is shown as grey bars. Error bars indicate one standard deviation above and below the geometric mean. * indicates a statistically significant difference ($P \leq 0.05$, Student's *t* test) when compared to the wildtype strain. WT, wildtype; Δfur , *fur* deletion strain, WT_C, Cm^R wildtype control strain.*

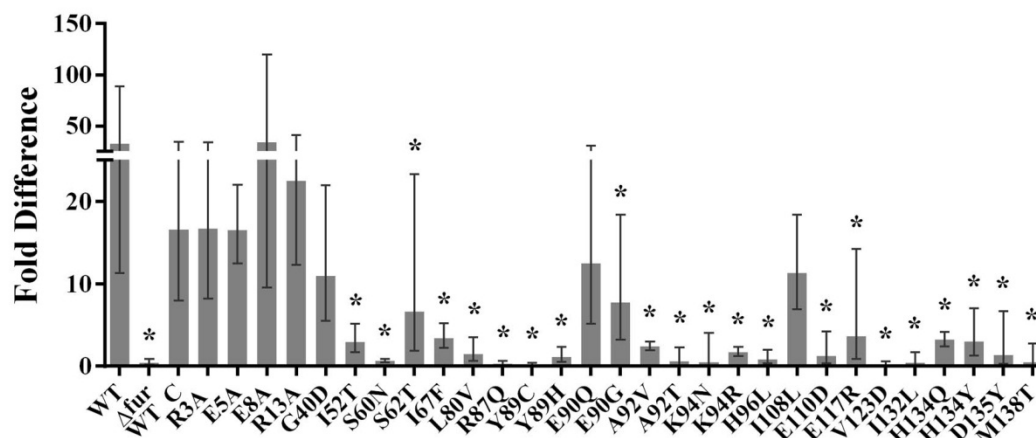
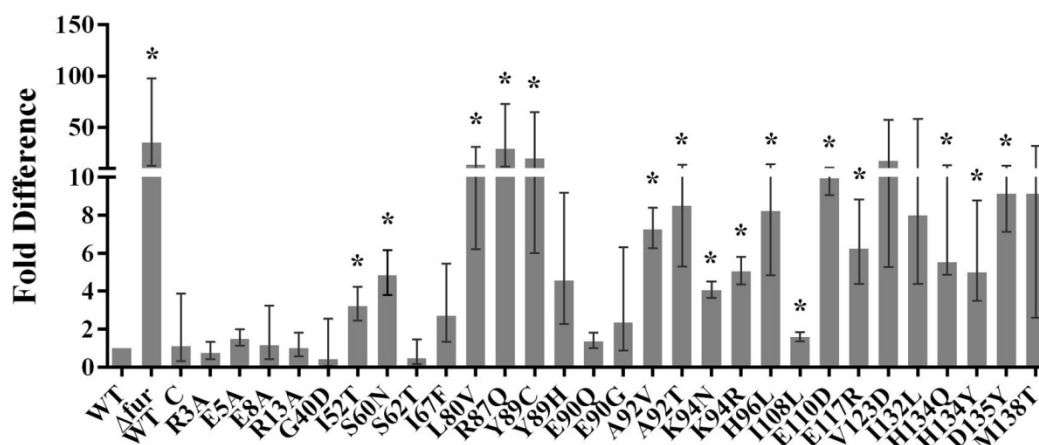
A**B**

Figure 10. Transcriptional regulation of *amiE* under iron replete and iron-depleted conditions as measured by qRT-PCR

I52T and S60N mutations significantly increased basal *amiE* expression, whereas the other three mutations (G40D, I67F, and Y89H) did not. Finally, E117R was the only single site-specific mutation that significantly de-repressed *amiE* expression in iron replete conditions. Based on all of the data shown in Figure 10, we classified each of the mutant strains into three possible categories in terms of Fe-Fur regulation: those with a wildtype phenotype, those with a Δfur phenotype, and those with an intermediate phenotype (Table 4): strains that showed a significant difference in regulation for the T_{60}/T_0 (Figure 10A) and the basal level (Figure 10B) comparisons were considered to be like Δfur , whereas strains that showed a significant difference in only one of the two comparisons were considered to have an intermediate (INT) phenotype. *En masse*, our results suggest that our mutagenesis strategy successfully identified Fur residues important for Fe-Fur dependent regulation.

Transcriptional analysis of pfr regulation

One of the unique characteristics of *H. pylori* Fur is the ability to repress gene expression in the absence of the regulatory iron cofactor. As such, we next sought to determine if any of our random and site-specific mutations altered regulation of the *apo*-Fur repressed gene *pfr* (12). To this end, we used qRT-PCR to compare the levels of *pfr* transcript before and after iron chelation. As an *apo*-Fur repressed gene, expression of *pfr* is decreased after chelation; thus, when iron is removed from the system, there is a decrease in *pfr* transcript levels. As shown in Figure 11A, in the wildtype strain chelation resulted in a decrease in *pfr* transcript from the T_0 to T_{60} timepoint. As expected, this decrease was not seen in the Δfur strain. In contrast to the effects on *amiE* regulation, the

*Figure 11. Transcriptional regulation of pfr under iron replete and iron-depleted conditions as measured by qRT-PCR. (A) Fold decrease in pfr transcript levels after chelation. For each strain, relative levels of transcript after chelation were compared to levels prior to chelation (T_{60}/T_0). (B) Relative post-chelation levels of pfr transcript in each mutant strain as compared to the wildtype strain (T_{60}/T_{60}). In both (A) and (B) the geometric mean of fold differences for three biologically independent experiments is shown as grey bars. Error bars indicate one standard deviation above and below the geometric mean. * indicates a statistically significant difference ($P \leq 0.05$, Student's *t* test) when compared to the wildtype strain. WT, wildtype; Δfur , *fur* deletion strain, WT_C, Cm^R wildtype control strain*

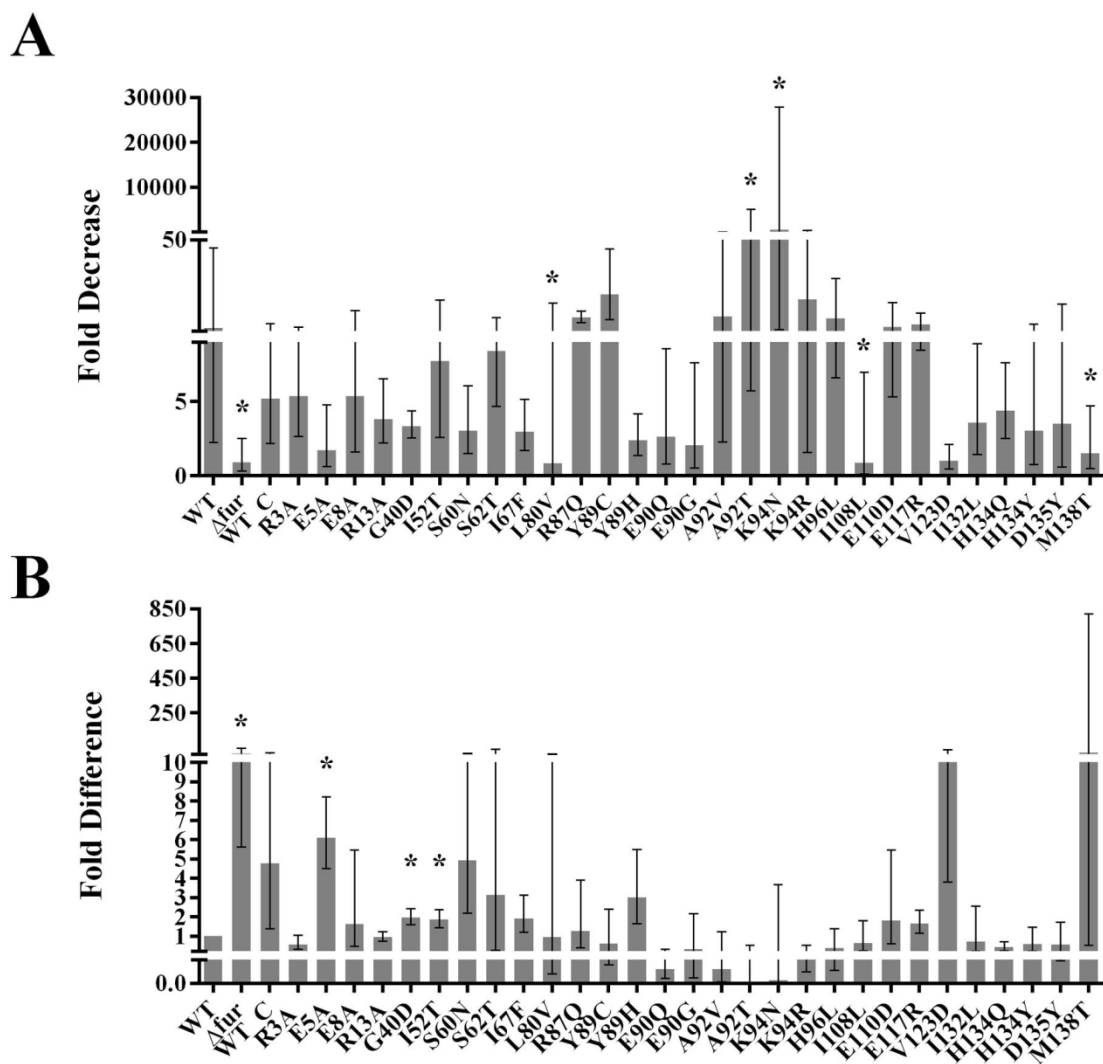


Figure 11. Transcriptional regulation of *pfr* under iron replete and iron-depleted conditions as measured by qRT-PCR.

differences in expression of *pfr* after chelation varied considerably. Of the 19 Mn^R mutant strains, only the L80V, A92T, K94R, and M138T mutations showed a statistically different fold decrease in response to chelation. However, despite considerable variation between experimental repeats, many mutant strains also displayed strong phenotypes. For instance, the V123D mutant strain looked much more like the Δfur strain than the wildtype. Another important feature that was clear after making the T₆₀/T₀ comparisons was the fact that the fold changes observed for several mutant strains (Y89C, A92T, and K94N, for example) was considerably greater than the fold decrease seen in the wildtype strain. Of the five mutations identified in the Pfr-based screen, none resulted in a fold change significantly different than the wildtype strain; however, three of the five showed moderate phenotypes. Similarly, none of the single site-specific mutations resulted in a significantly different fold change after chelation.

In addition to the T₆₀/T₀ comparison, we also compared relative *pfr* transcript levels in each of the mutants to the wildtype strain after chelation (T₆₀), where expression should be repressed by *apo*-Fur. As shown in Figure 11B, in the *fur* deletion strain, *pfr* transcript levels were more abundant (de-repressed) relative to the wildtype strain. Based on this comparison, three mutant strains displayed statistically significant differences in levels of *pfr* at the T₆₀ timepoint; the E5A mutation showed the highest level of derepression. The other two significant differences were observed in the G40D and I52T mutant strains.

Upon closer inspection of the *pfr* levels in the Mn^R strains, we noted that several mutations resulted in hyper-repression at this time point. Importantly, several of these strains carried mutations in or near a metal binding site. For example, the post-chelation

levels of *pfr* transcript in the E90Q, A92T, and K94N mutant strains were lower than the wildtype strain (Figure 11B), which suggests that *apo*-Fur is more abundant or more active in these strains. Similar to the *amiE* transcriptional analysis, we classified each of the mutant strains into four possible categories in terms of *apo*-Fur regulation: those with a wildtype phenotype, those with a hyper-repressed wildtype phenotype, those with a Δfur phenotype, and those with an intermediate phenotype (Table 6). Mutant strains were grouped as described for *amiE* regulation: strains that showed a significant difference in regulation for the T_{60}/T_0 (Figure 11A) and the post-chelation level (Figure 11B) comparisons were considered to be like Δfur , whereas strains that showed a significant difference in only one of the two comparisons were considered to have an intermediate (INT) phenotype. Taken together, our results suggest that our mutagenesis strategy successfully identified Fur residues important for *apo*-Fur dependent repression.

Fur Western blot analysis

One possible factor that could affect Fur-mediated transcriptional regulation is an increased or decreased amount of Fur protein in the cell. Given that Fur in *H. pylori* is autoregulatory, changes in the levels of Fur could occur as a result of altered transcriptional regulation at this promoter, or as the result of alterations in mutant Fur stability. To evaluate the levels of Fur in each of our mutant strains, we used an aliquot of liquid culture taken at the T_0 time point of the iron chelation experiment described above and performed Western blot analyses. For the majority of the mutant strains, the levels of Fur at this time point were similar to that of the wildtype strain (Figure 12). However, in four of the mutant strains the level of Fur was either significantly greater than (I52T,

Table 4. Summary of regulatory phenotypes observed by qRT-PCR

Group	Mutation	Regulatory phenotype	
		<i>amiE</i>	<i>pfr</i>
Manganese Selection	S62T	INT	WT
	L80V	Δfur	WT
	R87Q	Δfur	WT
	Y89C	Δfur	WT
	E90Q	WT	WT*
	E90G	INT	WT
	A92V	Δfur	WT*
	A92T	Δfur	WT*
	K94N	Δfur	WT*
	K94R	Δfur	WT
	H96L	Δfur	WT
	I108N	INT	WT
	E110D	Δfur	WT
	V123D	Δfur	WT
	I132N	INT	WT
	H134Q	Δfur	WT
	H134Y	Δfur	INT
D135Y	Δfur	WT	
M138T	Δfur	WT	
Pfr screen	G40D	INT	INT
	I52T	Δfur	INT
	S60N	Δfur	WT
	I67F	INT	WT
	Y89H	INT	INT
Site-specific	R3A	WT	WT
	E5A	WT	INT
	E8A	WT	WT
	R13A	WT	WT
	E117R	Δfur	WT

WT, phenotype similar to wildtype; Δfur , phenotype similar to *fur* deletion strain; INT, intermediate phenotype;

* indicates hyper-repression after chelation

S60N) or less than (L80V, I132N) the wildtype. We also noted that, although not statistically significant, the Fur levels in the S62T strain were also elevated, and appeared similar to Fur levels in the S60N mutant strain. Thus, in most cases the single amino acid change did not overwhelmingly affect levels of Fur.

Purification of recombinant Fur proteins

In order to better understand at a molecular level how the mutations identified in this study affect the different aspects of Fur function, we selected five mutations to characterize in further detail. Based on the regulatory phenotypes described above, we selected the following mutations: E5A, which is located in the N-terminal extension and showed a wildtype (WT) phenotype for *amiE* regulation and an intermediate (INT) phenotype for *pfr* regulation; A92T, which is located proximal to the S2 site and showed a Δfur -like phenotype for *amiE* and a hyper-repressive phenotype for *pfr*; E117R, which coordinates a metal ion in site S3 and showed a Δfur -like phenotype for *amiE* and WT phenotype for *pfr*; V123D, which is located in the dimerization helix $\alpha 5$ and showed a Δfur -like regulatory phenotype for *amiE* and a WT-like phenotype for *pfr*; H134Y, which is a metal coordinating residue in S3 and showed a Δfur -like phenotype for *amiE* and an INT phenotype for *pfr* regulation. Recombinant expression strains were created for each of these mutations, and native (non-tagged) protein was purified. We were able to successfully purify the WT, E5A, A92T, and H134Y proteins; however, we were unable to obtain soluble protein for the E117R and V123D mutations. As a result, E117R and V123D were not studied further.

*Figure 12. The relative levels of Fur in each mutant strain were measured by Western blot and compared to Fur levels in the wildtype. The geometric mean of fold difference values from three biologically independent experiments are shown by the grey bars, and the error bars indicate one standard deviation above and below the geometric mean. * indicates statistically significant differences ($P \leq 0.05$, Student's t test); when compared to the wildtype strain; WT, wildtype; Δfur , fur deletion strain, WT_C, Cm^R wildtype control strain.*

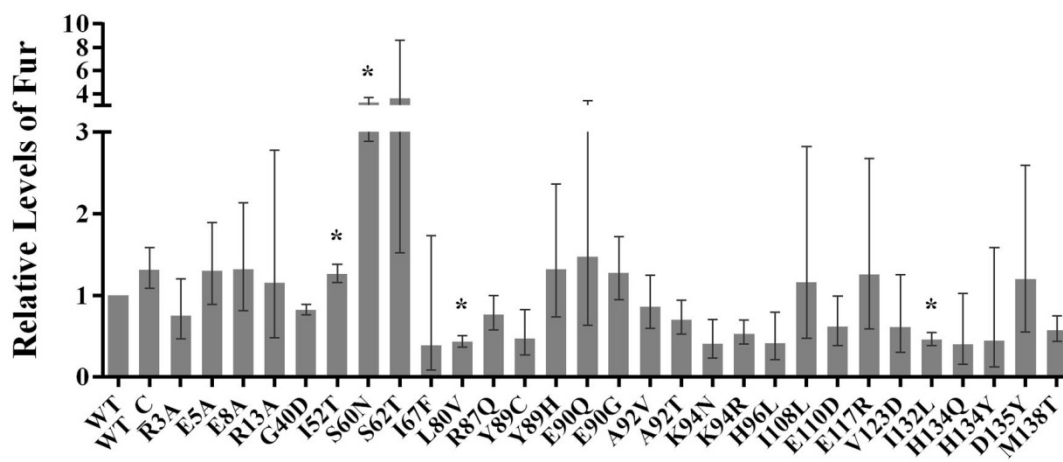


Figure 12. The relative levels of Fur in each mutant strain were measured by Western blot and compared to Fur levels in the wildtype

Secondary structure content and thermal denaturation

Using circular dichroism (CD) spectroscopy, we determined the relative secondary structure content for the WT, E5A, A92T, and H134Y proteins. As shown in Figure 13A, the CD spectra of the WT, E5A, and H134Y proteins were highly similar, which indicated that the E5A and H134Y mutations did not dramatically alter the secondary structure content of these proteins. However, the spectra for the A92T protein did display a slight negative deviation at the lower end of the tested UV range. This shift highlighted the possibility that the A92T mutation altered the secondary structure content of the protein. To compare these changes in secondary structure content more quantitatively, we analyzed the relative differences in CD spectra using CDPro (147). In agreement with the raw CD secondary structure data, only the A92T mutant protein appeared to have notable differences in secondary structure content. This mutation resulted in a ~7% decrease in helical content, as well as a ~3% increase in both turn structure and unstructured regions. To further characterize any structural differences, we also performed thermal denaturation studies to determine whether or not these mutations altered gross protein folding. As shown in Figure 13B, the denaturation profiles for all three mutant proteins were highly similar to that of the WT protein and are indicative of a single unfolding event. Taken together, the CD data indicate that although the secondary structure content of the A92T protein is somewhat different than WT, none of the mutant proteins have notable folding defects. Thus, the regulatory phenotypes seen are most likely due to the effects of the mutations on some aspect of Fur function, rather than differences in overall protein fold.

Figure 13. Secondary structure and thermal denaturation profiles obtained by circular dichroism (CD) spectroscopy. (A) CD spectra were obtained for WT and each mutant protein at room temperature from 190 nm to 250 nm. Each point represents an average of five accumulations. (B) Thermal denaturation studies were performed for WT and each mutant protein from 4°C to 100°C. Readings were taken at a wavelength of 222 nm.

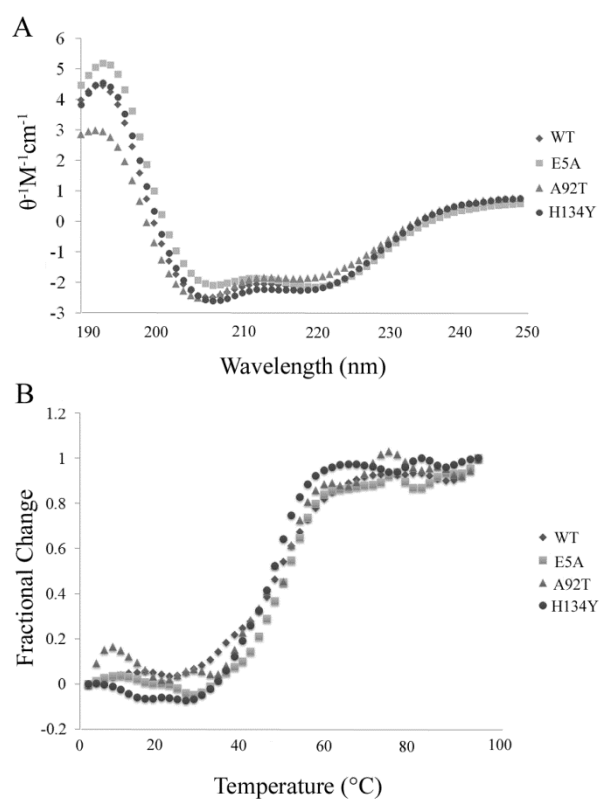


Figure 13. Secondary structure and thermal denaturation profiles obtained by circular dichroism (CD) spectroscopy.

Iron binding studies

To evaluate the effect of the E5A, A92T, and H134Y mutations on the ability of Fur to bind iron, we dialyzed each of the proteins against increasing amounts of iron (Fe^{2+}) under anoxic conditions, and measured the amount of iron bound to each protein by atomic absorption spectrophotometry (Figure 14). As expected, based on previous iron binding studies (25), the WT protein bound three iron ions and binding was saturated after dialyzing against $10\ \mu\text{M}\ \text{Fe}^{2+}$. Similar to the WT protein, the E5A mutant protein also bound three metal ions; however, for this protein, binding saturated at approximately $8\ \mu\text{M}$ iron, which was $2\ \mu\text{M}$ lower than the saturation point of the WT protein. These data suggest that the E5A protein may bind iron more tightly than WT. In contrast, both the A92T and H134Y mutant proteins displayed a clear reduction in iron binding. Even after dialysis against higher concentrations of iron (and up to $25\ \mu\text{M}\ \text{Fe}^{2+}$, data not shown), binding never reached the level observed for the WT and E5A proteins. The fact that neither of these two mutant proteins ever averaged more than 1.5 iron ions per monomer suggests that these two mutations not only affected their respective metal binding sites (S2 adjacent to A92 and S3, which contains H134), but also may have had more distal effects on metal binding.

Oligomerization assays

Another critical facet of Fur regulation is the ability of the protein to form oligomers. As the structures of both Fe-Fur and *apo*-Fur were reported as being dimeric, this characteristic is important for regulation by both forms of the protein (23, 49). To evaluate the ability of the E5A, A92T, and H134Y mutant proteins to form higher order

Figure 14. The ability of the WT and each mutant Fur protein to bind iron (Fe^{2+}) as measured by atomic absorption spectrophotometry. Aliquots of each protein were dialyzed against increasing concentrations of Fe^{2+} (0 to 10 μ M) under anoxic conditions. Each data point represents the mean from at least three replicates and the error bars represent the standard deviation of the mean.

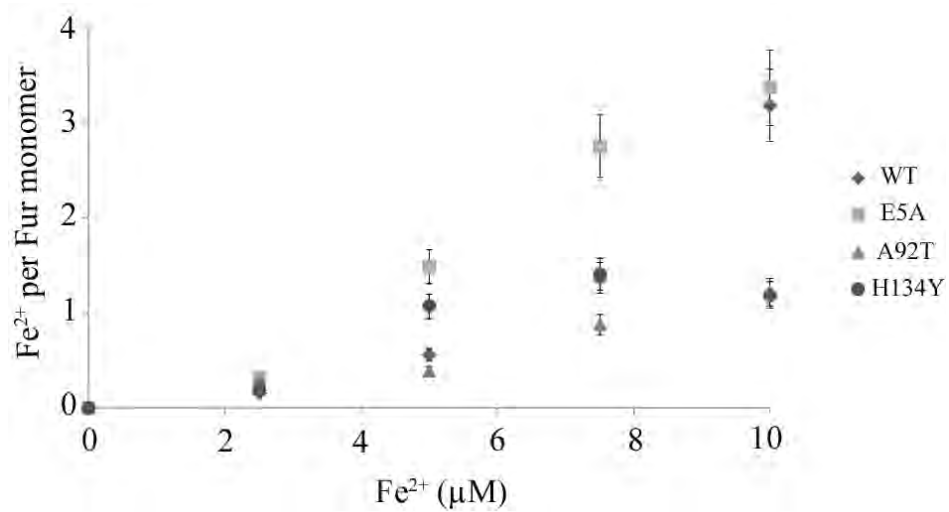


Figure 14. The ability of the WT and each mutant Fur protein to bind iron (Fe²⁺) as measured by atomic absorption spectrophotometry.

structures in both the iron-bound and *apo*- forms, we employed *in vitro* cross-linking assays. Each protein was incubated in an iron-substituted (MnCl_2) or *apo*- binding buffer (25) with and without the crosslinking agent DSS; samples were separated by SDS-PAGE and protein complexes were visualized by SYPRO staining. As depicted in Figure 15A, in the presence of excess metal, all four proteins form higher order oligomers. Compared to the WT Fur, none of the mutant proteins appeared to have a defect in oligomerization under this condition. Interestingly, in the absence of DSS, it appeared that *H. pylori* Fur preferentially exists as a mixture of monomers and oligomers that are larger than the dimer size. Thus, while the basic unit of Fur function may be the dimer, there is a propensity to form higher order oligomers in the presence of excess metal. In contrast, by adding the crosslinking agent, we were able to trap additional oligomeric forms of Fur. In addition to monomers and higher order oligomers, we saw the presence of Fur dimers. These data indicate that in the presence of excess metal the equilibrium seems to be between monomers and higher order oligomers, although dimeric intermediates do occur. While the formation of these oligomers required the presence of metal, this process does not appear to be DNA dependent; the addition of excess Fe-Fur target DNA (the *amiE* promoter) did not visibly alter oligomerization in the presence of excess metal (data not shown).

The recently published structure of *C. jejuni apo*-Fur (23) gave the first indication that this form of the protein existed as a dimer. We next tested the WT and mutant Fur proteins for their ability to oligomerize in *apo*- conditions. At equilibrium, *apo*-Fur appears to exist as a mixture of monomeric and dimeric forms (Figure 15B). In contrast to the excess metal conditions, WT *apo*-Fur does not seem to form a significant number

Figure 15. The ability of WT and each mutant protein to oligomerize as determined by in vitro cross-linking. Oligomerization in iron-substituted conditions (A) or apo (B) conditions were performed in the presence (+) or absence (-) of the crosslinking reagent DSS. Protein complexes were separated by SDS-PAGE and stained with SYPRO Ruby Red. Fur monomers, dimers, and > dimer complexes are indicated by arrows. Predicted molecular weights for Fur complexes are shown.

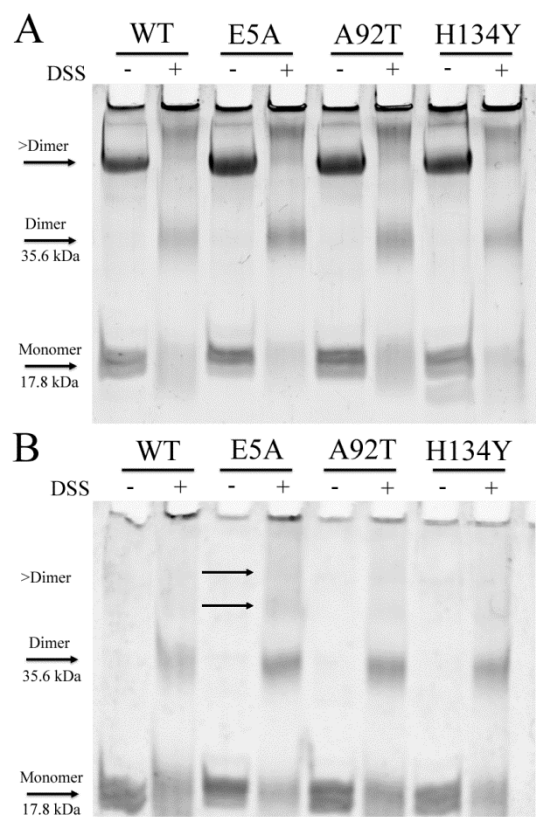


Figure 15. The ability of WT and each mutant protein to oligomerize as determined by in vitro cross-linking

of oligomers larger than the dimer. Thus, it is likely that whatever region of Fur that is responsible for the formation of higher order oligomers (larger than dimer) is not accessible in the *apo*- form of the protein. Similar to the observation made during the iron-substituted Fur oligomerization assays, the addition of target DNA (*pfr* promoter sequence) did not alter the oligomeric form of the protein (data not shown). Compared to the WT protein, the only mutant that displayed a difference in oligomerization in *apo*- conditions was the E5A protein. In the presence of the crosslinking agent, we were able to faintly detect the presence of higher order oligomers that were larger than dimer size (Figure 15B).

DNA binding assays

Finally, we evaluated the ability of the WT and mutant Fur proteins to bind DNA in iron-substituted and *apo*- conditions using fluorescence anisotropy. A summary of the best-fit anisotropy data is shown in Table 5. Under iron-substituted conditions, the WT protein bound the *amiE* oligo duplex with a lower affinity than two of the mutant proteins and with approximately the same affinity as the other mutant (Figure 16A). The order of binding affinity under these conditions was $E5A > H134Y > A92T \geq WT$, with K_d values of 2 ± 1 nM, 6 ± 1 nM, 15 ± 2 nM, and 16 ± 2 nM, respectively. Based on these results, it appears that each of these residues plays a role in Fe-Fur interaction with DNA. To ensure that this interaction was specific, we also performed competition experiments using an unlabeled DNA duplex where the Fur box sequence was mutated to G-T repeats. For these experiments the WT and E5A proteins did not bind the scrambled DNA

*Figure 16. The ability of the WT and mutant proteins to bind DNA sequences from the *amiE* (A) and *pfr* (B) promoters as determined using fluorescence anisotropy. Forward titrations were performed using 50 nM of labeled oligo duplex in either iron-substituted (for *amiE*) or *apo* (for *pfr*) conditions. In both (A) and (B), the curves represent the best fit line and the concentration of Fur dimer (nM) is shown.*

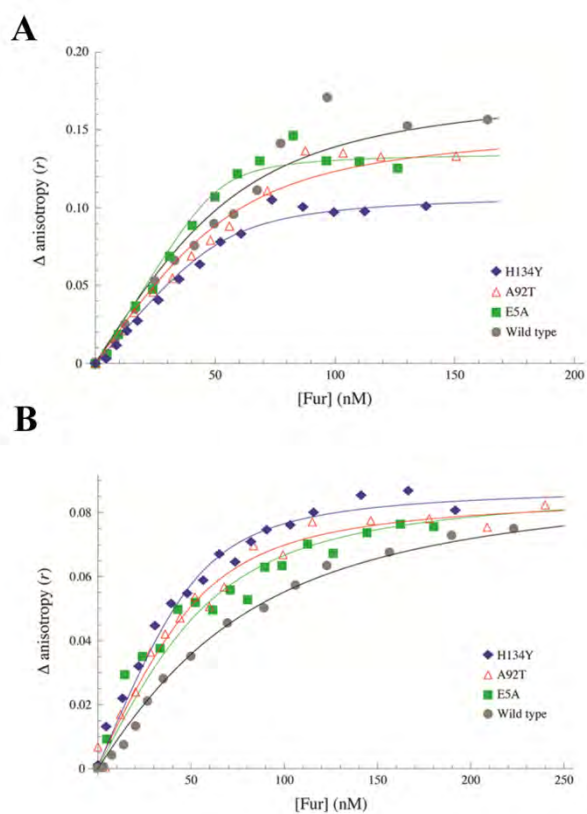


Figure 16. The ability of the WT and mutant proteins to bind DNA sequences from the *amiE* (A) and *pfr* (B) promoters as determined using fluorescence anisotropy.

sequence to a significant degree, while the A92T and H134Y proteins did bind the scrambled template to some extent (data not shown).

Next, we performed similar experiments using the high affinity Fur binding sequence from the *pfr* promoter and *apo*- binding buffer. Similar to the iron-substituted DNA binding assays, the relative binding affinity of the mutant proteins was higher than WT Fur (Table 5 and Figure 16B). Under *apo* conditions the order of binding affinity for the *pfr* promoter sequence was H134 > A92T > E5A > WT, with K_d values of 8 ± 1 nM, 13 ± 1 nM, 19 ± 2 nM, and 43 ± 2 nM, respectively. Once again, we performed competition experiments with an unlabeled DNA oligo duplex that had the putative Fur binding site mutated to G-T repeats. Under *apo* conditions, none of the proteins bound to the unlabeled DNA duplex, which suggests that the binding seen with the wildtype *pfr* promoter sequence was specific (data not shown). Consequently, the binding promiscuity observed for the A92T and H134Y appears to be specific to the fully metallated form of the protein.

Discussion

As highlighted by its importance *in vivo*, Fur mediated regulation is a key component of stress adaptation and gene regulation in *H. pylori* (12, 28, 35, 46, 58, 59, 67, 128, 134, 162). The degree of functional diversity displayed by this pleiotropic regulator is thus far unique. Although Fe-Fur activation and *apo*-Fur regulation have also been reported in a few other bacteria (43, 47, 72), no other bacterial Fur proteins perform all four types of regulation: Fe-Fur repression, Fe-Fur activation, *apo*-Fur activation and

Table 5. Summary of Fluorescence anisotropy data

Oligo Fragment	Fur protein	Kd (\pm error)	R-squared
<i>amiE</i> ; iron-substituted conditions	WT	16 (2) nM	0.998
	E5A	2 (1) nM	0.999
	A92T	15 (2) nM	0.998
	H134Y	6 (1) nM	0.999
<i>pfr</i> ; <i>apo</i> conditions	WT	43 (2) nM	0.999
	E5A	19 (2) nM	0.999
	A92T	13 (1) nM	0.999
	H134Y	8 (1) nM	0.999

Each titration was performed using 50 nM labeled ligand ($L_{tot}=50$ nM); Kd values were rounded to the nearest whole number.

apo-Fur repression. As a result, functional information about *H. pylori* Fur regulation is not only important for understanding regulation in this organism, but also for defining the range of functional capabilities of the Fur family. A previous site-specific mutagenesis study targeted residues that are conserved in several well-studied bacterial species that had been shown to be critical for Fur function in those organisms (25). However, unlike those studies, mutations in the same conserved residues in *H. pylori* Fur did not render the protein completely non-functional. These findings highlight the unique nature of *H. pylori* Fur, and suggested to us that additional methods were required to identify key functional residues in this protein.

In the current study, we employed random and site-specific mutagenesis to identify residues important for Fe-Fur and *apo*-Fur repression. We hypothesized that this type of functional information would provide insight into the contribution of the various regions of the protein to both types of regulation. Using manganese selection, we identified 19 mutations in 15 different residues that conferred a Mn^R phenotype (Figure 9 and Table 4). The majority of these 15 residues were located in the C-terminal half of the protein, which contains the majority of the metal coordinating residues. Due to the role of these residues in metal coordination, it is perhaps not surprising that single amino acid changes in this region resulted in a strong Fe-Fur phenotype. However, it is interesting to note that in other manganese selection studies, the distribution of mutations imparting manganese resistance is quite different. For example, Lam *et al.*, isolated 11 independent Mn^R strains of *V. cholerae* that contained mutations in 10 different amino acid residues (92). In contrast to our findings, those mutations were predominantly located in the N-terminal half of *V. cholerae* Fur, which contains the DNA binding domain of the protein.

H. pylori Fur and *V. cholerae* Fur share 32% identity and 55% similarity (14), thus, the reason for this difference is not completely apparent at the amino acid sequence level. Instead, the difference is likely due to additional levels of regulation seen only with *H. pylori* Fur; the N-terminal domain of *H. pylori* Fur likely undergoes a fairly dramatic conformational change in order to function in the iron-bound or *apo*- form. Because of this requirement for “flexibility,” this region of the protein is likely more permissible to secondary structure perturbation or slight differences in conformation compared to other Fur species.

Despite the apparent plasticity within the N-terminal region of *H. pylori* Fur, by combining multiple mutagenesis strategies, we were able to identify important residues across virtually the entire coding region (Figure 9). Within the N-terminal extension, which is not seen in other Fur species, we specifically mutated residues R3, E5, E8 and R13 (Figure 9 and Figure 17). Of these four, only the E5A mutation affected Fur regulation to any detectable degree (complete phenotype summarized in Table 6). The E5A mutant protein appeared to bind iron tighter than WT Fur, and binding saturated at a lower concentration of Fe^{2+} (Figure 14). Based on the structural description of the N-terminal extension (49), it is possible that this mutation may have shifted the hydrogen bonding network that links these N-terminal residues with residues that coordinate metal binding at S2; Dian *et al.*, also proposed a similar hypothesis regarding the biological role for these residues (49). If this were the case, then we would anticipate that the resulting redistribution of hydrogen bonds could have potentially shifted the coordination sphere of S2, and increased the affinity for the regulatory metal ion. However, as the iron-binding measurements obtained here are not a true measure of binding affinity *per se*, further

studies will be required to test this hypothesis. Consistent with this line of reasoning, a change in binding affinity could also explain the presence of higher order oligomers in the *apo*- cross-linking assay (Figure 15B); given a higher affinity for metal, S2 would be less responsive to chelation. As a result, a portion of the E5A protein might remain as Fe-Fur, which readily forms higher order oligomers. Within the bacterial cell, this shift in the equilibrium between Fe-Fur and *apo*-Fur, where more Fe-Fur is present even after metal chelation, could also explain the defect in *apo*-Fur repressor activity as measured by qRT-PCR (Figure 11B). Additionally, increased iron binding affinity may also explain the higher binding affinity of the E5A protein for the Fe-Fur target sequence in the DNA binding assay. It is possible that metal binding saturation at a lower concentration of metal (8 μ M for E5A vs 10 μ M for WT) could translate to more rapid DNA binding, thus a lower K_d (Table 5).

Interestingly, the relative binding affinity of E5A for the *apo*-Fur target sequence was also higher than the WT protein. Based on the structure of *apo*-Fur in *C. jejuni*, we propose a possible explanation for increased binding under these conditions. In this structure, helix $\alpha 1$ is positioned within the “V” of the DNA binding domain. Given this position, it is possible that altering this residue directly affects how *H. pylori apo*-Fur interacts with target DNA and causes the protein to bind with higher affinity than WT *apo*-Fur. Of note, another *H. pylori* metalloregulator, the nickel-responsive regulator NikR, also contains a unique N-terminus that, when disrupted, affects DNA binding (11). Thus, it is possible that acquisition of additional N-terminal residues that function to mediate specific DNA interactions is a common mechanism for extending the function of regulatory proteins in *H. pylori*.

Table 6. Summary of mutant protein characterization

ASSAY	E5A	A92T	H134Y
<i>amiE</i> qRT	WT	Δfur	Δfur
<i>pfr</i> qRT	INT	WT*	INT
<i>amiE</i> FA	>WT	WT	>WT
<i>pfr</i> FA	>WT	>WT	>WT
Iron binding	WT	<WT	<WT
MnCl oligomerization	WT	WT	WT
<i>apo-</i> oligomerization	>WT	WT	WT

WT, phenotype similar to wildtype; Δfur , phenotype similar to *fur* deletion strain; INT, intermediate phenotype; *indicates hyper-repression at T60; >WT, greater than the wildtype protein; <WT, less than the wildtype protein

Based on these studies collectively, we propose that in Fe-Fur, the E5 residue serves as an anchor point for establishing the S2-stabilizing hydrogen bond network. This hypothesis is indirectly supported by the fact that none of the other mutations made in this region (E3A, E8A, and R13A) had a detectable effect on Fe-Fur or *apo*-Fur repression (Figures 10 and 11). Conversely, in the *apo* form of Fur where helix $\alpha 1$ is positioned to interact with DNA, we propose that E5 serves as a key residue within this helix to facilitate interaction with DNA; once again, mutations in three of the surrounding charged residues did not appear to impact *apo*-Fur function. Thus, within the unique N-terminal extension, E5 appears to play a crucial multi-factorial role in Fur function. Adjacent to the N-terminal extension are helices $\alpha 2$ - $\alpha 4$, which make up the winged helix-turn-helix motif that is involved in DNA binding (49). We identified a single mutation in this region using manganese selection (S62T), but identified four additional mutations (G40N, I52T, S60N, and I67F) using the Pfr-based screen (Figures 9 and 17). Among these $\alpha 2$ - $\alpha 4$ residues, G40 is located at the C-terminal end of helix $\alpha 2$. Given this location, we propose that this mutation affects the conformation of the DNA binding domain, which subsequently alters the ability of Fur to efficiently recognize DNA. However, given that we observed WT-like basal levels of *amiE* (Figure 10B), it is likely that once the Fe-Fur target DNA is recognized, the protein is able to maintain interaction with DNA and repress transcription. Despite the apparent alternative configuration of the helix-turn-helix in *apo*-Fur (23) (Figures 17 and 18 (S1)), the location of this residue is similar in both forms of the protein. However, given the differences in *pfr* expression seen in the G40N strain, it appears that while the *apo* form of this mutant protein might recognize *apo*- target DNA in a manner similar to wildtype Fur, this interaction is not

maintained at the same level as wildtype *apo*-Fur. The I52T and I67F mutations showed similar defects in regulation of *amiE* and *pfr*; neither mutant strain was able to fully repress *amiE* under iron replete conditions. Based on the location of these residues, we propose that this defect is the result of changes in DNA binding affinity for Fe-Fur target DNA. Compared to *amiE* regulation, the regulation of *pfr* in the I52T and I67F mutant strains more closely resembled that of the wildtype strain. The major difference was that neither strain repressed *pfr* expression to as great of an extent as the wildtype. Thus, there may be a slight defect in *apo*- repression due to a change in DNA binding affinity. The final two mutations located within the $\alpha 2$ - $\alpha 4$ region are the S60N and S62T mutations. Despite the close proximity of these two residues and the fact that the levels of Fur were ~3-4 fold higher in these strains as compared to the wildtype (Figure 12), the regulatory phenotypes conferred by these two mutations are quite different. Because the basal levels of *amiE* transcript were increased in the S60N mutant strain and there was no change in these levels after chelation, we hypothesize that the S60N mutation alters the ability of Fe-Fur to bind to DNA and repress transcription. This line of reasoning is consistent with the increased levels of Fur protein in this strain; *fur* expression is autoregulated (repressed by Fe-Fur) so a lack of repression at this promoter would result in higher protein levels. Similarly, the S60N mutation also seems to prevent proper repression of *pfr* expression, as demonstrated by the increased levels of *pfr* transcript after chelation. Conversely, the S62T mutation only demonstrated an effect on iron-bound regulation. In this strain, the basal levels of *amiE* transcript were comparable to wildtype, but showed a lower degree of de-repression after chelation. Thus, the S62T mutation may have increased binding affinity for the *amiE* promoter. While this explanation may seem to be

Figure 17. Structural representation of H. pylori Fe-Fur (A) and apo-Fur (B) dimers.

Residues mutated in this study are highlighted as follows: N-terminal residues 3, 5, 8, and 13 are shown in green; residues 40, 52, 60, 63, and 67 within helices $\alpha 2$ - $\alpha 4$ are shown in blue; $\beta 1$ - $\beta 2$ residues 80, 87, and 89 are shown in magenta; S2 residues 90, 92, 94, 108, and 110 are highlighted in red; S3 residues 96, 117, 132, 134, 135, and 138 are yellow; residue 123 in $\alpha 5$ is highlighted in cyan. From left to right, the structures are rotated as indicated. Images were generated using the Polyview-3D server:

<http://polyview.cchmc.org/polyview3d.html> (130, 131).

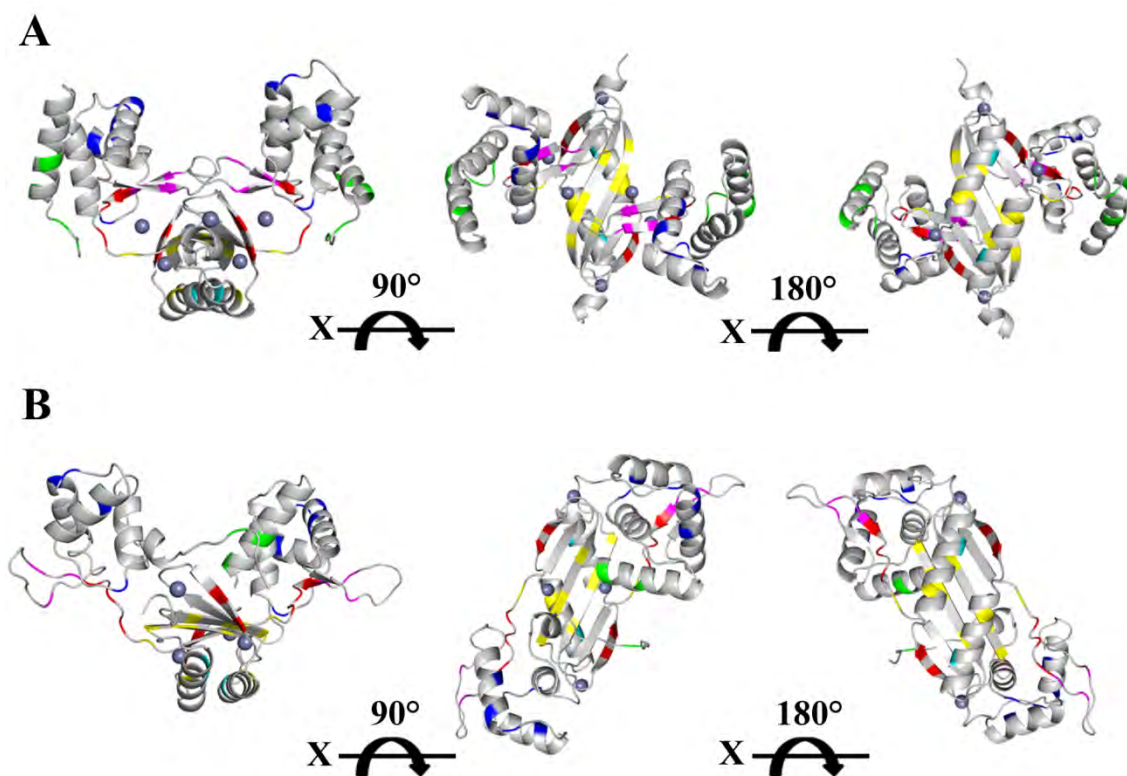


Figure 17. Structural representation of *H. pylori* Fe-Fur (A) and apo-Fur (B) dimers.

contradicted by the higher levels of Fur protein seen in the S62T strain (*i.e. fur* should be repressed similar to *amiE*) it is possible that the location of S62T within the DNA binding helix $\alpha 4$ confers differences in binding affinity to one promoter but not to another. In addition, the nucleotide composition and location of the Fur binding sequence(s) in these two promoters is different, which can directly affect Fur-dependent regulation (128).

At the distal end of the DNA binding domain, we isolated mutations in sheets $\beta 1$ - $\beta 2$ (Figure 17). These mutations (L80V, R87Q, Y89C, and Y89H) all displayed similar regulatory phenotypes and levels of Fur. The basal levels of *amiE* transcript in these strains were higher than the wildtype strain and none were responsive to chelation. Since these four strains were able to regulate *pfr* expression to nearly the same extent as the wildtype strain, it appears that these residues are most important for iron-bound regulation. Given the location of these two sheets near the hinge region that connects the DNA binding domain to the C-terminal domain of the protein, it is possible that these residues may be more important for maintaining the orientation of the DNA binding domain in Fe-Fur, but not necessarily for the *apo* form of the protein.

The S2 metal binding site senses intracellular iron levels, and the presence or absence of a metal ion in this site distinguishes between the iron-bound and *apo* forms of Fur. Using the manganese selection, we obtained mutations in several residues in this region (Figures 9 and 17). Given their location in relation to S2, it is perhaps not surprising that all eight of these mutations (E90Q, E90G, A92T, A92V, K94R, K94N, I108N, and E110D) affected Fur regulation in a similar manner. As a general theme, the basal level of *amiE* transcript in these eight mutant strains was increased compared to the wildtype strain, and metal chelation had little effect on transcript levels (Figure 10).

Conversely, the mutated versions of Fur in these strains were able to regulate *pfr* expression to a higher degree than wildtype. In some cases, such as the A92T and K94N mutant strains, the fold change in *pfr* levels after the chelation treatment was an order of magnitude greater than in the wildtype strain. Comparison of the post-chelation *pfr* levels in this group of mutant strains revealed that mutations in this region of Fur have a tendency to confer a hyper-repressive phenotype. Clues to possible mechanisms for these regulatory defects were provided by the biochemical analysis of the purified A92T mutant protein as a representative of this mutant group (summarized in Table 6). The A92T mutant displayed a significant defect in iron-binding; the protein was only able to bind 1-1.5 metal ions per monomer. Although the A92 residue is not directly involved in coordinating the metal ion in S2, the close proximity of this residue to this site combined with the change in side chain (alanine to threonine) clearly affected the ability of metal to occupy this site. Furthermore, the atomic absorption data indicate that this mutation may affect metallation at S3 as well. This idea is supported by CD spectroscopy (Figure 13A), which detected several changes in overall secondary structure, and the oligomerization assays (Figure 15). As metallation at S1 is required for dimer formation (49, 165), the fact that the A92T protein was able to oligomerize in both the iron-substituted and *apo* forms strongly suggests that the metal ion(s) detected by atomic absorption spectrophotometry occupy S1. On a cellular level, the dramatic reduction in iron binding also explains the constitutive de-repression of *amiE* as well as the hyper-repression of *pfr* that was observed by qRT-PCR (Figures 10 and 11). Because of the defect in iron binding, the vast majority of Fur in the cell at a given time exists as *apo*-Fur. As a result, *amiE* is not repressed even under iron replete conditions (T_0), and higher proportion of

apo-Fur in the cell results in hyper-repression of *pfr*. Finally, the DNA binding assays provided additional clues as to how S2 and the residues proximal to this site affect Fur function. Based on the iron-binding and transcriptional data, we expected that the A92T protein would also be defective in binding DNA under iron-substituted conditions. Instead, the A92T protein bound to the *amiE* oligo duplex with nearly identical affinity as the WT protein (Table 5). However, since this protein also bound to the Fur box scramble sequence to some degree (data not shown), this interaction with the *amiE* promoter fragment is likely non-specific. Thus, this mutation seems to have rendered the A92T mutant protein in a “locked” conformation that allows for non-specific interaction with DNA. This promiscuous binding is specific for iron-substituted conditions, as the A92T protein did not bind the scrambled *pfr* promoter sequence in *apo* conditions (data not shown). Consistent with the hyper-repression of *pfr* observed via qRT-PCR, the binding affinity for the *pfr* oligo duplex was higher than the WT protein (Table 5). Taken together, the analysis of the mutations found in and around S2 indicate that in addition to the metal coordinating residues, the neighboring amino acids such as A92 and K94 are critical for maintaining the proper coordination sphere at S2, and may also indirectly impact metallation at S3.

S3 serves as a structural metal binding site and is occupied in both Fe-Fur and *apo*-Fur. We obtained several mutations in residues that lie within (H96L, E117R, H134Q, H134Y) or directly adjacent to this region (I132N, D135Y, and M138T; Figure 17). These six mutations in or near S3 shared similar regulatory phenotypes. Under iron replete conditions, the basal levels of *amiE* were higher in these mutant strains than the wildtype, and there was no major change in transcript levels after metal chelation. Thus,

these strains had a Δfur -like phenotype for *amiE* regulation. As a group, these mutations had little effect on *pfr* regulation. These strains displayed a wildtype-like fold decrease in *pfr* transcript after chelation, and the relative levels of *pfr* after chelation were similar to the wildtype strain. These findings indicate that despite the fact that S3 is occupied in *apo*-Fur, the residues that are involved in proper metal ion coordination in this form of the protein might be different than that of Fe-Fur. Alternatively, the presence of a metal ion in S3 might not be absolutely required for *apo*-Fur function. The H134Y mutant displayed a greater defect in the ability to respond to chelation as compared to the other mutant strains in this group. *In vitro* analysis of this mutant protein suggested a mechanistic basis for the regulatory phenotypes observed by qRT-PCR (summarized in Table 6). As H134 directly interacts with the S3 metal ion in Fe-Fur, it was not surprising that this mutant protein displayed a significant defect in iron binding. Similar to the A92T mutant, H134Y only bound 1-1.5 iron ions per monomer (Figure 14). Once again, it appears that mutation of this residue has distal effects on metal binding at other sites. Given the lack of a distinct oligomerization defect in either iron-substituted or *apo* conditions (Figure 15), it would appear that this distal effect on metal binding influences S2 rather than S1. Given the apparent requirement for metallation at S3 for both Fe-Fur and *apo*-Fur, this defect in metal binding could explain the lack of *amiE* repression as well as the slight defect in *pfr* regulation. Furthermore, the fact that this mutation only had a slight effect on *pfr* regulation compared to regulation of *amiE* perhaps suggests that H134 plays a more prominent role in metal coordination in S3 of Fe-Fur than in S3 of *apo*-Fur. Based on the DNA binding assays performed in both iron-substituted and *apo* conditions, the H134Y protein displayed a higher affinity for DNA than WT Fur (Figure

16). Not only did this mutant protein bind to the *amiE* and *pfr* oligo duplexes with higher affinity, H134Y also bound to the scrambled *amiE* oligo duplex to some degree (data not shown). These data suggest that the H134Y mutation may have a propensity to bind DNA non-specifically in iron-substituted conditions. These findings are consistent with a previous study that reported non-specific DNA binding of a H134A Fur mutant (25). Thus, under iron-substituted conditions, mutation of this residue may result in a form of the protein that is “locked” in a position that is permissive for DNA binding. While a relatively higher binding affinity was seen with the wildtype version of the *pfr* promoter oligo duplex, the promiscuous binding was not observed under *apo* conditions. These data support the tenant that H134 plays a different role in the iron-bound and *apo* forms of the protein. In the context of *in vivo* regulation of the *amiE* and *pfr* genes, the higher binding affinity seen with the H134Y mutant *in vitro* cannot be clearly explained. However, it is important to consider the fact that this isolated *in vitro* assay may not necessarily translate directly to the way things work within a functional cell. For instance, the DNA binding assays do not take into account the multiple types of metal (Fe^{2+} and Zn^{2+}) that are present *in vivo*, or the fact that *apo*-Fur is known to bind to multiple sites within the native *pfr* promoter with different affinities (12).

We obtained a mutation in one additional residue within the C-terminal domain, V123D, which is located within helix $\alpha 5$ (Figures 9 and 17). This helix serves as an interface for dimerization in both Fe-Fur and *apo*-Fur. As dimerization is important for both types of Fur regulation, it is perhaps not surprising that this mutation resulted in a regulatory phenotype for both *amiE* and *pfr*, despite a lack of statistical significance for the *pfr* phenotype (Figures 10 and 11). Based on the location of this residue, we

hypothesize that this mutation precludes proper dimerization; however, as we were unable to purify the V123D protein due to issues with solubility, we were unable to test this hypothesis in further detail.

One surprising outcome of this study was the fact that no S1 mutations were obtained in either the manganese selection or Pfr-based screen. Given the importance of this site in dimerization (presumably for both types of Fur), it seems that a mutation in this metal binding site would abrogate Fur function to a similar degree as mutations in either S2 or S3 (both of which were obtained by manganese selection). One possible explanation is that because of the essential nature of S1 to proper function, minor structural disruptions in this region may not exert a strong effect; thus, single amino acid substitutions may not be sufficient to eliminate metal binding in S1.

En masse, the *in vivo* and *in vitro* studies detailed herein shed new light on functional features of Fe-Fur and *apo*-Fur regulation in *H. pylori*. When interpreted in the context of the *H. pylori* Fe-Fur (Figure 17) and closely related *C. jejuni apo*-Fur structures (Figures 9 and S1), we can begin to piece together how specific residues or regions of Fur contribute to each type of regulation and how some of these residues contribute to different aspects of function in the iron-bound and *apo* forms of the protein. For example, as proposed by Dian *et al.*, (49), the N-terminal extension apparently plays a role in facilitating metal coordination at S2; furthermore, when interpreted in the context of the *C. jejuni apo*-Fur structure (Figures 17 and 18 (S1)), it is likely that this region is directly involved in binding to *apo*-Fur target DNA. Based on our analysis of the A92T and H134Y mutations, it also appears that maintenance of the S2 site is important for proper metallation at S3, and *vice versa*. To our knowledge, this type of

functional linkage between metal binding sites has not been described for any other Fur protein. In combination with this and other functional studies, we are now poised to address some of the many questions that still remain. For example, it is clear that the N-terminal extension contributes to metal coordination at S2; however, the evolutionary basis of this feature remains a mystery. Did this region evolve to facilitate *apo*-Fur interaction with DNA? Does the hydrogen bonding network that this region forms in Fe-Fur provide metal ion selectivity *in vivo*? While these and many other questions still remain, it is clear that Fur in *H. pylori*, and likely its close relatives, has many unique features that contribute to the regulatory diversity displayed by these organisms.

Materials and Methods

Strains and growth conditions

A complete list of bacterial strains and plasmids used in this study can be found in Table 7. *H. pylori* strains were maintained at -80°C in brain heart infusion broth that contained 10% fetal bovine serum and 20% glycerol. *E. coli* strains were maintained at -80°C in LB broth supplemented with 40% glycerol. *H. pylori* strains were cultured on horse blood agar (HBA) that contained 4% Columbia agar, 5% defibrinated horse blood (HemoStat Laboratories, Dixon, CA), 0.2% β -cyclodextrin, 10 μ g/mL vancomycin, 8 μ g/mL amphotericin B, 2.5 U/mL polymyxin B, and 5 μ g/mL trimethoprim. Liquid *H. pylori* cultures were routinely grown in Brucella broth that contained 10% fetal bovine serum and 10 μ g/mL vancomycin with shaking at 110 rpm. All *H. pylori* cultures were

Figure 18 (S1). Overlay of the modeled H. pylori apo-Fur structure (blue) with C. jejuni apo-Fur (red) (23). The H. pylori structure was modeled as described in the Materials and Methods. Merged structures and images were generated in PyMol. The metal coordinating residues in S1 and S3 are completely conserved between structures. Notably, the major regions appear to be fairly similar with the exception of the N-terminal extension.

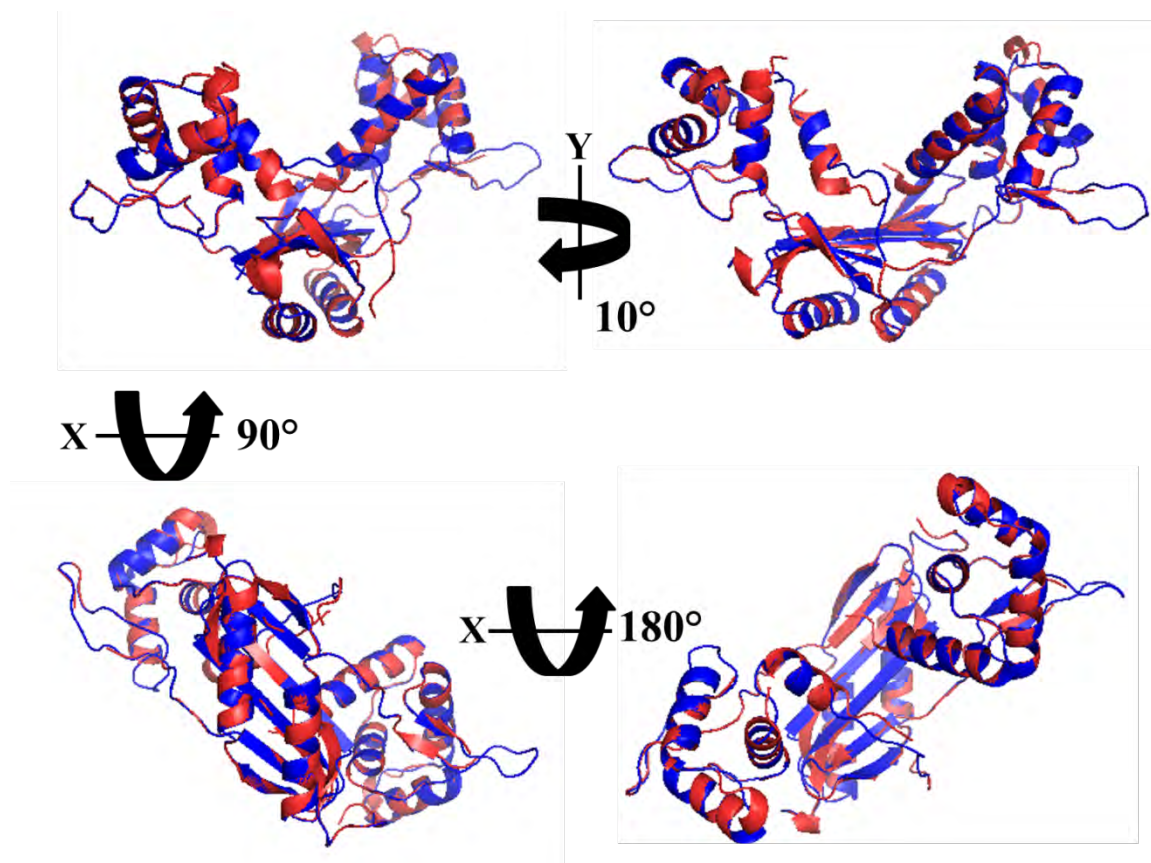


Figure 18. Overlay of the modeled *H. pylori* apo-Fur structure (blue) with *C. jejuni* apo-Fur (red)

grown under microaerophilic conditions (5% oxygen, 10 % carbon dioxide, and 85% nitrogen) in gas evacuation jars. *E. coli* cultures were grown on LB agar plates or in LB broth with shaking at 220 rpm. Bacterial cultures were supplemented with appropriate antibiotics as necessary: ampicillin (Amp), 100 µg/mL; kanamycin (Kan), 50 µg/mL; chloramphenicol (Cm), 50 µg/mL for *E. coli* or 8 µg/mL for *H. pylori*.

Random mutagenesis of the H. pylori fur gene

A library of random *fur* mutations was generated by error-prone PCR using the GeneMorph II Random Mutagenesis Kit (Stratagene) and primers upFur/ATG-F and Fur/cat-R (Table 8). Each PCR was performed in accordance with the manufacturer's instructions so that the resulting amplicons contained 0-2 nucleotide changes per copy. The randomly mutated *fur* amplicons were used to create chloramphenicol resistant Cm^R allelic exchange substrates as follows: the promoter containing upstream region of *fur* was PCR amplified using the Fur-F and upFur/ATG-R primers (Table 8); the *cat* cassette was amplified from strain DSM300 using the Fur/Cat-F and Cat/dnFur-R primers; the downstream region was amplified using the Cat dn/Fur-F and dnFur-R primers (Table 8). Amplicons that contained the *fur* promoter region, mutated coding sequence, *cat* cassette, and downstream region of *fur* were fused together using splicing by overlap extension (SOE) PCR. The resulting allelic exchange substrates were naturally transformed into the wildtype *H. pylori* strain G27. Transformants were selected for on HBA plates that contained 8 µg/mL of chloramphenicol. To ensure we obtained the desired mutation rate, we sequenced the *fur* gene from several transformants and determined that each copy of *fur* did in fact contain between 0-2 randomly distributed nucleotide changes.

Table 7 Strains and plasmids used in this study

Strains and Plasmids		
Strain	Description	Reference
<i>E. coli</i>		
DSM431	BL21 (DE3) Rosetta/pLys <i>Afur</i> (pDSM430) Amp ^R , Kan ^R , Cm ^R	(26)
DSM1197	BL21 (DE3) Rosetta/pLys <i>Afur</i> (pDSM1191) Amp ^R , Kan ^R , Cm ^R	This study
DSM1199	BL21 (DE3) Rosetta/pLys <i>Afur</i> (pDSM11193) Amp ^R , Kan ^R , Cm ^R	This study
DSM1200	BL21 (DE3) Rosetta/pLys <i>Afur</i> (pDSM1194) Amp ^R , Kan ^R , Cm ^R	This study
<i>H. pylori</i>		
DSM1	G27 WT	(9)
DSM300	G27 <i>Afur::cat</i> Cm ^R	(67)
DSM948	G27 Fur R3A; Cm ^R	This study
DSM949	G27 Fur E5A; Cm ^R	This study
DSM950	G27 Fur E8A; Cm ^R	This study
DSM951	G27 Fur R13A; Cm ^R	This study
DSM953	G27 Fur E117R; Cm ^R	This study
DSM954	G27 Fur A92V; Cm ^R	This study
DSM955	G27 Fur A92T; Cm ^R	This study
DSM956	G27 Fur K94N; Cm ^R	This study
DSM957	G27 Fur K94R; Cm ^R	This study
DSM958	G27 Fur H134Q; Cm ^R	This study
DSM959	G27 Fur H134Y; Cm ^R	This study
DSM960	G27 Fur E90Q; Cm ^R	This study
DSM961	G27 Fur E90G; Cm ^R	This study
DSM962	G27 Fur H96L; Cm ^R	This study
DSM963	G27 Fur I108L; Cm ^R	This study
DSM964	G27 Fur D135Y; Cm ^R	This study
DSM965	G27 Fur S62T; Cm ^R	This study
DSM966	G27 Fur M138T; Cm ^R	This study
DSM967	G27 Fur R87Q; Cm ^R	This study
DSM968	G27 Fur I132L; Cm ^R	This study
DSM969	G27 Fur L80V; Cm ^R	This study
DSM970	G27 Fur Y89C; Cm ^R	This study
DSM971	G27 Fur V123D; Cm ^R	This study
DSM972	G27 Fur WT_C; Cm ^R	This study
DSM973	G27 Fur E110R; Cm ^R	This study
DSM1133	G27 Fur S60N; Cm ^R	This study
DSM1134	G27 Fur I52T; Cm ^R	This study
DSM1135	G27 Fur Y89H; Cm ^R	This study
DSM1136	G27 Fur I67F; Cm ^R	This study

DSM1137	G27 Fur G40D; Cm ^R	This study
Plasmid		
pDSM430	pET21b::HpFur WT; Amp ^R	(26)
pDSM1191	pET21b::HpFur E5A; Amp ^R	This study
pDSM1193	pET21b::HpFur A92T; Amp ^R	This study
pDSM1194	pET21b::HpFur H134Y; Amp ^R	This study

Amp^R, ampicillin resistant; Kan^R kanamycin resistant; Cm^R chloramphenicol resistant

Table 8. Oligonucleotides used in this study

Oligonucleotide ^a	Sequence (5'-3') ^b	Reference
SOE PCR		
Fur-F	AAGGCTCACTCTACCCTATTCC	This study
upFur/ATG-R	CCAAAGTTTCTAATCTTTTCATGCTGATATTTCCCTTATCCG	This study
upFur/ATG-F	CGGATAAGGGAAATATCAGCATGAAAAGATTAGAACTTTGG	This study
Fur/cat-F	GAATGCCAAGAGAGTGAATATTAACGCACTACTCTCGACAGAGAG	This study
Fur/cat-R	CTCTCTGTCGAGAGTAGTGCGTTAATATTCCTCTCTTGGCATT	This study
cat/dnFur-R	CTAAGCTTCTCCTTTAAAAATTTTGATAGATTTATGATATAGTGG	This study
Cat/dnFur-F	CCACTATATCATAAATCTATCAAAATTTTAAAGGAGAAGCTTAG	This study
dnFur-R	GGTATTTCTGATGTGGATGG	This study
FurCF (XbaI)	<u>TCTAGAAAGGCTCACTCTACCCTATT</u>	(27)
FurCR (SalI)	<u>GTCGACA</u> AFACTTTACCTGGAAACGC	(27)
R3A-F	GGGAAATATCAGCATGAAAGCCTTAGAAAACCTTGG	This study
R3A-R	CCAAAGTTTCTAAGGCTTTTCATGCTGATATTTCCC	This study
E5A-F	FCAGCATGAAAAGATTAGCTACTTTGGAATC	This study
E5A-R	GATTCCAAAAGTAGCTAATCTTTTCATGCTG	This study
E8A-F	GATTAGAAAACCTTGGCTTCTATTTTAGAGC	This study
E8A-R	GCTCTAAAAATAGAAGCCAAAGTTTCTAATC	This study
R13A-F	CTATTTTAGAGGCTTTGAGGATG	This study
R13A-R	CATCCTCAAAGCCTCTAAAATAG	This study
E117R-F	CCTGAAATTCCGGAACCGCCAGAATG	This study
E117R-R	CATTCTGGCGGTTCCGAATTTCCAGG	This study
Real-time PCR		
G27_16S RT-F	ATGGATGCTAGTTGTTGGAGGGCT	(70)
G27_16S RT-R	TTAAACCACATGCTCCACCGCTTG	(70)
amiE_RT-F	GCGATGATGGAACTACCC	This study
amiE_RT-R	CCCACGCCATAGCTTTTAC	This study
pfr_RT-F	TGAGCATGAGTTCTTGGTGC	This study
pfr_RT-R	AGTCAATTGCACAGGCAC	This study
Fur expression		
HPFur_expression-F (NdeI)	<u>CATATG</u> AAAAGATTAGAACTTTGGAATCTATTT	(26)
HPFur_expression-R (XhoI)	<u>CTCGAG</u> TTATTAATATTCCTCTCTTGG	(26)
E5A-expression-F (NdeI)	<u>GCTACCA</u> TATGAAAAGATTAGCTACTTTGGAATCCATTTT	This study
Fluorescence anisotropy		
amiE-FA_LABEL	5FluorT/GCCCCAATAATCATAATGATTAA	This study
amiE-FA_COMPLEMENT	TTAATCATTATGATTATTGGGGCA	This study
amiE-FA_SCRAM-1	TGCCCCGTGTGTGTGTGTGATTAA	This study
amiE-FA_SCRAM-2	TTAATACACACACACACACGGGGCA	This study
pfr-FA_LABEL	5FluorT/TCATTATCATTATGCTAT	This study

pfr-FA_COMPLEMENT	ATAGCATAAAATGATAATGAA	This study
pfr-FA_SCRAM-1	TTCATTAGTGTGTATGCTAT	This study
pfr-FA_SCRAM-2	ATAGCATAACACTAATGAA	This study

^aImportant restriction enzyme recognition sites shown in parentheses

^bRestriction sites are underlined, mutated codons are in bold italics, and start or stop codons are italicized

Approximately 10,000 Cm^R transformants obtained through numerous independent transformations were pooled and used for the selection and screening procedures described below.

Site-specific Fur mutant strains

The R3A, E5A, E8A, R13A, and E117R mutations were created by SOE PCR using the mutation-specific SOE primers listed in Table 8. Briefly, the FurCF primer was used in combination with each of the mutation-specific reverse primers, and FurCR was used in combination with each of the mutation specific forward primers. These two fragments were spliced together and used to create Cm^R allelic exchange substrates by SOE PCR as described above. Each mutation-bearing substrate was naturally transformed into wildtype G27 and plated on HBA that contained 8 µg/mL chloramphenicol. Proper integration was confirmed by PCR and the presence of the correct mutation was confirmed by sequencing. The *fur* promoter region in each strain was also sequenced to ensure that there were no mutations present.

Manganese selection

Manganese selection has been previously used to identify residues that are important for Fur function (75, 92, 99). Aliquots of the random *fur* mutant library were diluted and plated for single colonies on Brucella broth-based agar plates that contained 10% fetal bovine serum, 10 µg/mL vancomycin, 8 µg/mL amphotericin B, 2.5 U/mL polymyxin B, 5 µg/mL trimethoprim, and 4 mM MnCl₂.

Screen for altered Pfr expression

The *H. pylori* prokaryotic ferritin (Pfr) has been previously shown to be *apo*-Fur repressed (12). Based on the ability to easily visualize Pfr in a stained protein gel, we designed a Pfr-based screen to identify *fur* mutant strains that were deficient in *apo*-repression. Aliquots of the *fur* mutant strain library were diluted and plated on Brucella broth-based plates that contained 10% fetal bovine serum, 10 µg/mL vancomycin, 8 µg/mL amphotericin B, 2.5 U/mL polymyxin B, 5 µg/mL trimethoprim, and 60 µM of the iron chelator 2,2'-dipyridyl (dpp). This concentration of dpp is sufficient to create an iron-depleted condition without completely prohibiting bacterial growth (27). Single colonies were expanded on chelation plates and used to make whole-cell lysates. An equal volume of each lysate was separated via SDS-PAGE and analyzed after staining with Coomassie. The levels of Pfr in each of the random mutant strains were visually compared to both the wildtype and *fur* mutant strains of G27.

RNA isolation, cDNA synthesis, and quantitative real-time PCR

RNA was harvested from liquid cultures under iron-replete and iron depleted conditions. Briefly, an overnight culture of each strain was grown to exponential phase; one half of each culture was harvested by vacuum filtration (T_0) and the other half of the culture was treated with 200 µM dpp to remove iron from the system. After one hour of incubation, the iron-depleted culture was harvested (T_{60}). For each time-point, bacterial cells were snap frozen in liquid nitrogen and stored at -80°C until processed. RNA was purified as previously described (25). cDNA was reverse transcribed from 1 µg of total RNA using the Quantitect reverse transcription kit (Qiagen); for each RNA sample, a

duplicate reaction that contained no reverse transcriptase enzyme was also performed. Levels of target transcripts were determined by quantitative real-time PCR (qRT-PCR) using the Quantitect SYBR Green qPCR kit (Qiagen). Each 20 μ L reaction contained 1X SYBR green master mix, 1 μ L of cDNA template, and 1.5 pmol each of a template specific forward and reverse primer. Cycling conditions included an initial activation step of 15 minutes at 95°C followed by 35 cycles of denaturation at 94°C for 15 seconds, annealing at 50°C for 20 seconds, and extension at 72°C for 30 seconds. For each primer set, post-run denaturation curves were performed to ensure that the reactions only resulted in a single amplicon. Relative gene expression was calculated as $2^{-(\Delta\Delta Ct)}$ using 16S as the internal reference gene. At least three biologically independent replicates were performed for each qRT-PCR experiment. During the course of these experiments, no overt growth defect was observed for any of the mutant strains.

Western blot analysis

H. pylori whole cell lysates were made from aliquots taken during the T₀ time-point of the RNA isolation experiments described above. One milliliter of each culture was pelleted and re-suspended in lysis buffer (25); total protein was quantitated for each lysate using the BCA kit (Pierce). Six micrograms of total protein was separated on 20% SDS-polyacrylamide gels, and Western blots were performed using polyclonal α -*H. pylori* Fur rabbit sera as previously described (25). Three biologically independent blots were performed for each strain.

Recombinant Fur expression strains and protein purification

The *fur* coding region from the A92T and H134Y mutant strains was PCR amplified using the HPFur_expression-F and HPFur_expression-R primers, digested with NdeI and XhoI, and ligated into the appropriately digested pDSM430 expression vector to create plasmids pDSM1193 and pDSM1194, respectively. The coding region from the E5A mutant strain was PCR amplified using the E5A-expression-F and HPFur_expression-R primers and cloned as described above to create plasmid pDSM1191. The presence of the appropriate mutation in each expression plasmid was confirmed by sequencing. The expression plasmids pDSM1191, pDSM1193 and pDSM1194 were each transformed into chemically competent *E. coli Δfur* BL21 (DE3) Rosetta/pLys cells (26) to create strains DSM1197, DSM1199, and DSM1200, respectively. Wildtype (WT) and each of the mutant Fur proteins was purified by FPLC as described previously (26). Briefly, Fur proteins were first passed through a HighTrap SP ion-exchange column using a gradient of 25 mM to 500 mM NaCl. Peak fractions were further purified by size-exclusion on a Sephacryl-200 column. Fur proteins were stored in 50 mM sodium phosphate, 500 mM NaCl, 25% glycerol, pH 8.0.

Circular dichroism (CD) spectroscopy

CD spectra of WT and mutant Fur proteins were analyzed on a Jasco-810 spectropolarimeter. Experiments were performed using a 1 mm path-length-cell at room temperature. Measurements were taken for wavelengths of 190-250 nm with a scan rate of 50 nm per minute. The spectra shown are an average of five accumulations. Samples contained 5 μM protein in 25 mM sodium phosphate, pH 7.5. Thermal denaturation

studies were performed using a 1 mm path-length-cell and 5 μ M of each protein. Protein unfolding was monitored at 222 nm across a temperature range of 4-100°C.

Atomic absorption spectrophotometry

The ability of the WT and mutant Fur proteins to bind iron (Fe²⁺) was determined using graphite furnace atomic absorption mass spectrophotometry as previously described (25). Briefly, 2.5 μ M of each protein was dialyzed against anoxic buffer that contained 50 mM ultrapure NaCl, 10 mM ultrapure sodium formate, the oxygen scavenging enzymes (Oxyrase, OB00-50), and increasing concentrations of ultrapure FeCl₂ · 4H₂O; the dialysis buffer was used at a pH of 7.0. The state of anaerobiosis was verified prior to dialysis using a Clarke-type oxygen electrode. The concentration of iron was measured using a Shimadzu AA-6701F spectrophotometer, and the amount of Fur-bound iron was calculated by subtracting the concentration of iron in protein free buffer from the concentration found in the dialysis bags. The number of iron molecules per monomer of Fur protein was calculated by dividing the amount of Fur-bound iron by the concentration of each Fur protein. Measurements for each sample were repeated until three replicates gave a coefficient of variation of \leq 12%. Data shown represent at least three independent measurements.

Oligomerization assays

To evaluate any potential defects in oligomerization, we assessed the ability of the Fur proteins to form higher order structures using *in vitro* cross-linking. Experiments were performed essentially as described previously (25) with minor changes. Briefly, 2

μg of each protein was combined with 1X *apo*- or MnCl_2 binding buffer (25), and 2 μL of 25 mM disuccinimidyl suberate (DSS, Sigma) and incubated for one hour at room temperature. For each reaction, a no-DSS control reaction was also performed. After incubation, 1X Laemmli buffer was added and samples were boiled for 5 minutes at 95°C. Reactions were separated on 12% SDS-polyacrylamide gels and stained using SYPRO Ruby Red (Invitrogen) according to the manufacturer's recommendation. Each experiment was performed at least twice.

Fluorescence anisotropy

Fluorescence anisotropy was used to measure the binding of wild type and mutant Fur proteins to known binding sites in the Fe-Fur repressed *amiE* promoter and the *apo*-Fur repressed *pfr* promoter. Stock solutions (50 μM) of fluorescently-labeled promoters were prepared by annealing the labeled top-strand oligonucleotide with the unlabeled bottom strand oligonucleotide in 20 mM Tris-HCl, 100 mM NaCl, pH 8.0. Titrations involving the *amiE* Fur box were carried out in iron-substituted binding buffer (30 mM Tris, 120 mM KCl, 16 mM DTT, 1 mM MnCl_2 , 20% glycerol, 480 $\mu\text{g}/\text{mL}$ Bovine Serum Albumin (BSA) at pH 8.0) and titrations involving the *pfr* Fur box were conducted in *apo*-binding buffer (40 mM Tris, 150 mM KCl, 2 mM DTT, 600 $\mu\text{g}/\text{mL}$ BSA, 200 μM EDTA, 24% glycerol, and 0.1 mg/mL sheared salmon sperm DNA at pH 8.0).

A cuvette containing 50 nM labeled DNA was incubated at 20 °C in sample chamber of an ISS PC-1 spectrofluorimeter (ISS, Inc., Champaign, IL) equipped with excitation and emission polarizers configured in the L-format. Anisotropy was recorded using an excitation wavelength of 495 nm and emission wavelength of 526 nm. Band passes for

excitation and emission were set to 8 nm. Purified Fur protein was titrated stepwise into the labeled DNA duplexes until the change in measured anisotropy neared saturation. Each anisotropy value represents the average of 30 measurements recorded with an integration time of 3 seconds. Anisotropy data (change in anisotropy) were analyzed assuming a 1:1 interaction of Fur dimer with the promoter DNA and Fur concentrations are represented in terms of $[Fur_2]$. A single-site binding model was fit to the data using the nonlinear fitting package in Mathematica (Wolfram Research, Inc). Errors in K_d are derived from the residual sum of squares from nonlinear fitting.

Fur protein homology modeling

The *H. pylori* Fur amino acid sequence was modeled against the *C. jejuni apo-Fur* structure (PDB 4ETS) using the SWISS MODEL server (<http://swissmodel.expasy.org>) (138). Chains A and B were modeled separately and then combined into a dimer structure in PyMol. This dimeric structure was used for residue highlighting (Figure 17) and structural overlay images (Figure 18 (S1)). Due to differences in the *H. pylori* and *C. jejuni* primary amino acid sequence, and symmetric differences between the two protomers of the *C. jejuni apo-Fur* structure, chain A of the modeled *H. pylori apo-Fur* structure contains residues 4-146, and chain B contains residues 9-149.

Statistical analysis

Differences in Fur protein levels and levels of *amiE* and *pfr* transcripts were compared using a Student's *t* test on \log_{10} transformed fold changes values as previously described (25). For clarity of presentation, the data are shown in the original scale.

Acknowledgements

Research in the laboratory of D. Scott Merrell is made possible by grant AI065529 from the NIAID. J. Gilbreath is supported by the Robert D. Watkins Graduate Research Fellowship from the American Society for Microbiology and by the Koniag Education Foundation. The authors would like to thank Dr. Jeong-Heon Cha for help in designing the mutagenesis strategy and Dr. James Vergis for help with PyMol. The contents of this report are the sole responsibility of the authors and do not necessarily represent the official views of the DoD or the NIH

Chapter Four

Discussion

Fur regulation in *H. pylori* is a complex story that is not yet fully understood. Among bacteria that have been well characterized, *H. pylori* is the only species in which Fur activates and represses transcription in both the fully metallated (Fe-Fur) and *apo* forms (*apo*-Fur). As a result of this extended functional capacity, the aspects of *H. pylori* Fur regulation that do not fit into the traditional paradigm of Fur acting simply as a repressor of iron uptake systems are not well understood. Accordingly, the goal of this dissertation was to gain a better understanding about how this “traditional” regulatory protein serves a non-traditional role in *H. pylori*. Specifically we sought to better understand Fur-mediated transcriptional activation and to identify amino acid residues in Fur that are important for two types of regulation, Fe-Fur and *apo*-Fur repression.

As described in Chapter two, we characterized Fur regulation of the *oorDABC* promoter as a means to better understand the mechanism of Fe-Fur activation in *H. pylori*. We determined that these four genes are co-transcribed as an operon, and that the level of expression of the operon is decreased in a *fur* mutant strain. Transcription of these genes is initiated from a highly conserved extended -10 motif. Although as with many *H. pylori* promoters, a conserved -35 region is not present. Further upstream of the core promoter region we located a conserved Fe-Fur box that is centered ~140 bases

upstream from the transcriptional start site. Furthermore, we demonstrated that Fur binds to this sequence with a relatively high affinity. Finally, using transcriptional fusions we determined that this Fur box is required for Fur-mediated activation of these genes. Collectively, these data provide novel insight into this understudied aspect of Fur regulation in *H. pylori* and highlight the possibility that Fur interacts with ArsR at this promoter.

The work detailed in Chapter three focused on identification of amino acid residues that are important for Fe-Fur and/or *apo*-Fur repression, with the goal of using this information to better understand *H. pylori* Fur structure-function relationships. Using a combination of random and site-specific mutagenesis strategies, we identified 25 single amino acid mutations that affected Fe-Fur function and 8 mutations that altered *apo*-Fur function; changes were demonstrated by alterations in Fe-Fur repression of the *amiE* gene and *apo*-Fur repression of the *pfr* gene. Based on those transcriptional data, we selected five representative mutations for further study. Of the five selected, we successfully purified recombinant E5A, A92T, and H134Y mutant proteins as well as WT Fur. Each of these proteins was evaluated for secondary structure content and overall fold, as well as the ability to bind iron, form oligomers under iron-substituted and *apo* conditions, and to bind Fe-Fur and *apo*-Fur target DNA sequences. When interpreted in the context of the recent resolution of the *H. pylori* Fe-Fur structure and the *C. jejuni apo*-Fur structure, the functional studies described in Chapter three provide insight into how specific regions of Fe-Fur and *apo*-Fur might facilitate regulation in *H. pylori*.

The logic of gains in Fur function

As a host-restricted pathogen, *H. pylori* has evolved to chronically colonize within the human gastric mucosa. It is hypothesized that throughout the thousands of years that this organism has co-evolved with humans and non-human primates, this symbiont-like lifestyle has resulted in dramatic changes within the bacterial genome (17). As a general theme, organisms that live in restricted niches often fine-tune cellular processes and genomic content over time in order to make the most of their environmental surroundings. As the sole primary inhabitant of the gastric mucosa, *H. pylori* is likely not frequently in direct competition with other microbes for nutrients or colonization space. Rather, the bacteria are only in competition with the human host. As a result, the *H. pylori* genome does not encode for as large of a repertoire of biological systems as many bacterial species that thrive in highly competitive microbial environments (9, 155). These organisms, such as *E. coli*, *Pseudomonas* spp., and *Acinetobacter* spp., contain numerous diverse biological systems, many of which are highly specific for a particular condition or respond to the presence or absence of a particular environmental substrate (1, 19, 115, 123, 144, 149, 159). Because these systems are so specific, many require and utilize dedicated regulatory factors that only respond to a particular stimulus. As a result, the genomes of these organisms often encode for dozens of regulatory proteins (1, 19, 115, 123, 144, 149, 159).

In contrast, as a result of genomic reduction, the genomes of host and niche-restricted organisms often encode for relatively few dedicated transcriptional regulators (9, 155). *H. pylori* exemplifies this case, where the genome of this pathogen in only ~1.6

Mb and contains fewer than 10 regulatory proteins. However, despite the lack of regulatory factors, *H. pylori* must still be able to rapidly and efficiently respond to changes in its environment. As a result, the regulatory proteins utilized by this organism appear to function in extended capacities beyond what is typically seen for analogous proteins in other organisms (34, 45, 46, 160, 161, 170). These differences in functionality can be seen in the expansion of the respective regulons to include genes that are not traditionally regulated by these factors in other bacteria, the ability of individual regulators to respond to multiple environmental conditions, and the ability to regulate genes using mechanisms not commonly seen in other bacterial species (34, 45, 46, 160, 161, 170). One key regulator that displays all three types of functional changes is *H. pylori* Fur (2, 44, 45, 58, 67, 70).

After many years of study in both Gram-negative and Gram-positive bacteria, it has become abundantly clear that Fur is an important regulatory protein that is involved in numerous essential cellular processes (58, 67, 108). Though typically considered a repressor of iron uptake and storage systems, in some bacterial species Fur has evolved to function beyond this restricted regulatory role. To date, no other bacterial Fur protein exemplifies this type of extended regulatory capacity better than that of *H. pylori*, which represses and activates gene expression in both the iron-bound and *apo*- forms of the protein (2, 12, 42-46, 70). As a result of the unique nature of Fur regulation in *H. pylori*, the regulatory models that have previously defined Fur regulation in other bacterial species do not necessarily hold true for *H. pylori*. Thus, there are gaps in our current understanding of many basic features of Fur regulation in this important human pathogen. As a result of the work detailed in this dissertation, we now have a better understanding

of Fe-Fur activation of the *oorDABC* genes, and recognize that local regions within the Fur protein play distinct roles in both Fe-Fur and *apo*-Fur repression. However, given the complexity and unique nature of Fur regulation in *H. pylori*, there is still much to be learned.

Fe-Fur Activation: an under-appreciated regulatory mechanism

One of the least well-characterized types of Fur regulation in *H. pylori* is Fe-Fur activation. Given the fact that only three Fe-Fur activated promoters have been described in *H. pylori* (*oorDABC* (70), *nifS* (2), and *cagA* (128)), it is perhaps not surprising that the mechanisms behind this regulatory process are not well understood. In addition, the apparent differences in how Fe-Fur activation occurs at these three promoters suggests that Fur may activate transcription through multiple mechanisms, which depend on the current environmental conditions.

In general, transcriptional activation can occur through multiple mechanisms, several of which are mediated by regulatory proteins (reviewed in (21)). For example, binding of a regulatory protein to a promoter may help recruit the RNA polymerase (RNAP) complex and enhance transcription; this recruitment can be mediated by direct interaction with RNAP or by recruiting intermediary factors that form a larger protein complex and influence RNAP complex assembly. Alternatively, as in the case of anti-repression, a regulator can dislodge a repressor protein, resulting in de-repression/activation of transcription. A major factor that determines which type of activation occurs at a particular promoter is the location of the regulatory protein binding site. Binding sites that are located proximal to the core promoter elements can be more

likely to facilitate a direct interaction with RNAP. Binding sites that are more distal, relative to the core promoter, can be less likely to have a direct interaction, unless binding results in a change in the promoter DNA architecture. Otherwise, activation from distally located binding sites is perhaps more likely to occur through the recruitment of other factors or by anti-repression.

Given the information regarding Fe-Fur activation at the *oorDABC*, *nifS*, and *cagA* promoters (2, 70, 128), it is not immediately clear which mechanism(s) of Fur-mediated activation occur in *H. pylori*. For *cagA*, the proximal location of the Fur box to the core promoter elements suggests that Fur may directly interact with RNAP (128) (Figure 19). A direct interaction with RNAP at this promoter is indirectly supported by the fact that preliminary *in vitro* transcription data showing that the *cagA* promoter can be activated by the addition of recombinant Fur protein (O.Q. Pich, unpublished results). In contrast, the mechanism(s) of Fe-Fur activation at the *nifS* and *oorDABC* promoters is less clear. At first glance, the fact that the reported Fur binding sites within both promoters are >120 bp upstream of the transcriptional start sites may suggest that Fur does not directly interact with RNAP at these promoters. For this type of interaction to occur, Fur binding would need to result in a bend or fold in the promoter DNA that would bring the Fur protein in close proximity to the core promoter elements. Alternatively, a second DNA binding protein could bind within the promoter region, resulting in the necessary architectural change. Then, once the Fur binding site was more proximally located to core promoter elements, Fur binding could enhance RNAP complex formation, thus activating transcription. Although there are currently no data supporting either of

Figure 19: Proposed modes of Fe-Fur activation in H. pylori. Given the close proximity of the Fur box to the core promoter elements in the *cagA* promoter, we propose that Fur directly interacts with RNAP to activate transcription (**top**). Combined with transcriptional data (67, 70) the distal location and overlap of the *oorDABC* Fur box with a putative ArsR binding site suggests that Fur-mediated activation of these genes is the result of an anti-repression mechanism (70) (**middle**). Given the distal location and lack of a conserved Fe-Fur box in the *nifS* promoter (2), we propose an as of yet unknown mechanism of Fe-Fur activation that is dependent on oxidative stress conditions (**bottom**).

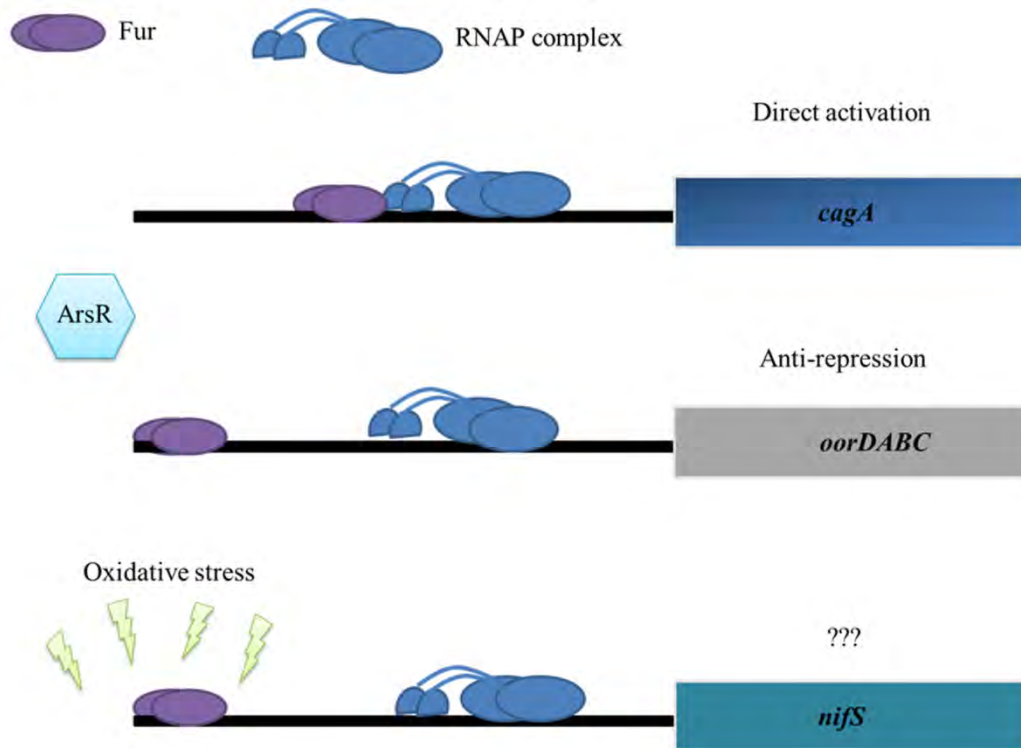


Figure 19. Proposed modes of Fe-Fur activation in *H. pylori*

these hypotheses, the *H. pylori* genome does encode for at least one such architectural DNA binding protein; DNA binding by the histone-like protein (known as HU) has been shown to change DNA topology and supercoiling characteristics (168, 181). Thus, the involvement of an intermediary regulatory DNA binding protein such as HU in Fur-mediated activation cannot be completely ruled out at this point in time. Future studies are needed to test this hypothesis.

Another possible explanation of the Fur-mediated activation seen at the *nifS* and *oorDABC* promoters is the interaction/competition of additional regulators with Fur (Figure 19). As demonstrated by numerous studies, a large number of genes within the *H. pylori* genome are regulated by multiple proteins and in response to various intracellular and environmental signals (101, 136, 161, 170, 172, 173). Furthermore, given the A-T rich nature of the *H. pylori* genome, and the propensity for most of the *H. pylori* regulatory proteins to bind A-T rich sequences, it is attractive to hypothesize that many of these regulatory binding sites overlap within a single promoter. As we proposed for the *oorDABC* promoter in Chapter two, this overlap in binding sequences would result in competition for binding between regulators and could result in transcriptional anti-repression. Although further study is necessary to determine if this type of regulatory mechanism occurs frequently in *H. pylori*, it is interesting to note that like the *oorDABC* promoter, *nifS* has also been shown to be regulated by at least one other regulatory protein (125). Thus, Fe-Fur activation may be the result of competition for binding sites at both the *oorDABC* and *nifS* promoters.

The description of Fe-Fur activation at the *nifS* promoter highlights another possible factor that may contribute to the process of Fur activation. As described by

Alamuri *et al.*, the Fur-mediated activation of the *nifS* promoter occurs in response to oxidative conditions (2). Combined with the fact that the reported Fur binding sites in this promoter do not share any significant degree of similarity with known Fe-Fur binding sequences, this type of response to oxidative stress may indicate that the binding specificity of Fur may change under different intracellular stress conditions. This idea is indirectly supported by data that indicated the Fur regulon increases in size ~4 fold upon exposure to low pH. Thus, there seems to be a precedent for stress-dependent changes in Fur regulation in *H. pylori*. Although there are currently no other reports of Fe-Fur binding to non-canonical binding sequences, at least one other *H. pylori* metalloregulator, NikR, displays altered DNA binding affinity to some promoters in low pH (97). Given these findings, it would be interesting to see if stress conditions also altered DNA binding affinity or promoter specificity of Fur. This type of *in vitro* study could provide insight into the mechanism of Fe-Fur activation at the *nifS* promoter.

Over the past several years, several studies have sought to define the *H. pylori* Fur regulon (39, 58, 67). However, because Fur-specific genome wide transcriptional studies have thus far been limited to only a few conditions (iron replete vs depleted (58) and low pH (67)), it is possible that a subset of Fur regulated genes have been overlooked. If the hypothesis regarding stress conditions and Fur binding specificity were correct, it is possible that Fe-Fur activates additional genes under oxidative, nitrosative, or osmotic stress conditions, which have not yet been examined at a global level. This possibility is supported by the essentiality of Fur to the ability of *H. pylori* to effectively mount adaptive responses to these stress conditions (35, 68, 76, 134). Although the study described in Chapter two does provide novel information about Fur-mediated activation

in *H. pylori*, our results also raise additional questions about the underlying mechanism(s) employed by *H. pylori* Fur. Clearly, much more work is needed to fully elucidate the contribution Fe-Fur activation to *H. pylori* biology.

The complexity of the H. pylori regulatory network

One of the intriguing hypotheses formed during the course of completing the studies described in Chapter Two is the possible existence of regulatory interplay between Fur and the pH responsive regulator ArsR. This type of competition for binding sites between regulators has also been described for other systems in *H. pylori* (22, 41, 161). For example, previous reports have indicated that several *H. pylori* promoters are co-regulated by Fur and the nickel-responsive regulator NikR (41, 161). Under acidic conditions, the number of regulatory circuits that overlap increases to include the Fur, NikR, and ArsR regulons (22). Despite the relatively few genes that were characterized in detail in those previous studies, it is clear that regulatory overlap occurs within *H. pylori* adaptive responses. However, the full extent of these cross-system interactions is likely not fully appreciated since most studies to date have focused on only one regulatory system/regulator at a time. While studying these systems in isolation does provide valuable information, future studies will need to focus on these systems in combination in order to more accurately understand how the regulatory networks of *H. pylori* function and to gain a complete picture of the complexity of transcriptional regulation in this important pathogen.

At the promoter level, regulatory interplay could occur in varying degrees of complexity. For a gene to be regulated by multiple factors, each one must be able to

recognize a specific sequence within the promoter DNA. Both the nucleotide composition of the binding site and the location of these sequences would determine whether or not the respective regulatory proteins would interact at any given promoter. In the simplest scenario, multiple regulators could bind to distinct regions within a single promoter and exert different regulatory effects without directly interacting with one another. While this situation is likely the case for a subset of co-regulated promoters in *H. pylori*, given the extent of overlap between many of the *H. pylori* regulons, it is likely that more complex interactions occur as well.

Both the simplistic and the more complex models of co-regulation can be seen in the regulation of the *exbB* and *nikR* promoters, respectively. In a previous study, Delany *et al.*, identified Fur and NikR binding sites within both of these promoters (41). In the case of *exbB*, DNase footprinting assays indicated that both NikR and Fur occupy distinct sites and can bind simultaneously. As expression from the *exbB* promoter has been shown to be repressed by both Fur and NikR, it is likely that *H. pylori* utilizes both of these regulators to tightly control expression of these genes and ensure that transcription is controlled under multiple environmental conditions. Fine-tuned regulation at this promoter is likely to be important since the ExbB-ExbD-TonB proteins provide the outer membrane with proton motive force, which is important for a variety of energy-dependent processes. Using similar footprinting assays, the authors of that study also showed that within the *nikR* promoter, both NikR and Fur compete for binding at the same site (41). Thus, in response to changes in intracellular metal ion concentrations, *H. pylori* is able to differentially control expression of this gene. Although these data are

strongly suggestive, the full implication of binding competition at this promoter is not known.

Despite the fact that this type of biochemical analysis has only been done for relatively few promoters to date, these studies highlight the potential for multiple modes of co-regulation and regulatory interplay at individual promoters. In order to fully appreciate the complexity of the *H. pylori* regulatory networks, future studies will need to take a combination of genome wide approaches and *in vitro* biochemical studies to understand how the regulatory factors interact globally as well as at a molecular level at individual promoters. Only after completing these types of studies will we be able to completely understand the adaptive responses in *H. pylori* and answer some of the many remaining questions. For example, is there a “master” regulator in *H. pylori*? Among the overlapping regulatory networks, does one regulatory protein “trump” others under certain environmental conditions? Only once these questions have been addressed will we be able to fully appreciate the complexity of transcriptional regulation in *H. pylori*.

Regulation by small RNAs

In addition to regulation by proteins, the recent description of the *H. pylori* primary transcriptome (142) highlights the possibility that these bacteria utilize yet another tier of transcriptional control. In their study, Sharma *et al.*, identified an astonishing number of putative small RNAs (sRNAs). While sRNA species have been shown to function as important regulators in many bacteria, it was previously thought that *H. pylori* did not utilize these molecules for regulation. Because very few of these sRNAs have been characterized, the extent that these nucleic acid species function in a regulatory

capacity remains unclear. However, many of these RNAs appear to be antisense to known Fur regulated genes, which raises an intriguing question: are any of these putative sRNAs or asRNAs Fur regulated? Within the past several years, the role of Fur in regulating sRNAs has become well appreciated in many bacterial pathogens (105-107, 109, 174). However, most of these sRNAs require interaction with the RNA chaperone protein Hfq in order to regulate gene expression. Despite the presence of so many sRNA species, *H. pylori* does not encode an identifiable Hfq homologue, which suggests that these sRNAs could function using novel mechanisms. Additional studies are needed to understand the full extent that these RNA molecules impact regulation in *H.pylori*, and which, if any, of these putative RNAs are Fur regulated. Ongoing studies in our lab suggest that some of these putative sRNAs and asRNAs are in fact Fur regulated (R.C. Johnson and D.S. Merrell, unpublished results); however, it remains to be seen whether these putative Fur regulated sRNAs function on a local or global level in this organism. It is likely that future work in the area of sRNA regulation in *H. pylori* will reveal new and exciting information about how this pathogen regulates gene expression.

Iron-bound and apo- Fur box sequences and Fur:DNA interactions

One of the key factors required for any transcriptional regulatory protein to selectively target specific promoters is the presence of a consensus DNA binding sequence. For the Fur protein, this sequence is commonly referred to as the Fur box. For many years the consensus Fur box sequence in *H. pylori* was unknown. However, recently the Fe-Fur box was determined to be a 7-1-7 inverted repeat motif (5'-TAATAANATTATTA-3') that is similar to the Fur box in other bacteria (128). The

presence of this sequence is necessary and sufficient to impart Fe-Fur regulation in *H. pylori* (128). The absence of this inverted sequence in *apo*-Fur target promoter regions suggests that *apo*-Fur recognizes a different DNA sequence. Given the relative lack of information on *apo*-Fur regulation in general, as well as the relatively few known *apo*-Fur regulated genes, it is perhaps not surprising that the consensus *apo*-Fur box sequence has remained elusive. Preliminary analyses from ongoing studies in our laboratory indicate that there is in fact a conserved *apo*-Fur binding sequence. This sequence (5'-AAATGA-3') is present in the promoters of all known *apo*-Fur repressed genes in *H. pylori* and is required for Fur binding under *apo* conditions (B.M. Carpenter, J.J. Gilbreath, and D.S. Merrell, unpublished results).

Interestingly, the distinct differences between the Fe-Fur and *apo*-Fur binding sequences may suggest possible mechanistic differences in how the different forms of Fur interact with target promoters. Compared to the Fe-Fur box, the *H. pylori apo*-Fur binding sequence is relatively short (only six nucleotides vs 19 for the Fe-Fur box), and does not include a repeated motif. In contrast, the Fe-Fur box contains a 7-1-7 inverted repeat, which is characteristic of binding sequences that are recognized by dimeric DNA binding proteins. Intriguingly, the structural information available for *apo*-Fur in *C. jejuni* (23) combined with the functional data described in Chapter three of this dissertation indicate that *apo*-Fur functions as a dimer. Accordingly, since Fur is a homodimer it stands to reason that each protomer of the dimer should interact with the same DNA sequence. However, based on the proposed consensus *apo*-Fur box, it appears that *apo*-Fur may interact with DNA differently. One possibility is that the symmetry of the two Fur protomers under *apo* conditions may be different in each respective protein chain.

Indeed, the two chains of *H. pylori* Fe-Fur are not symmetric; these differences affect the number of residues that coordinate metal binding in the S2 metal binding site (49). Based on this asymmetry in Fe-Fur, we hypothesize that *H. pylori apo*-Fur may also be asymmetric, which could affect how each protomer of the dimer interacts with target DNA. As a result, only one half of the dimer may actually bind to the consensus DNA sequence. If this hypothesis were correct, we would anticipate that the relative DNA binding affinity for *apo*-Fur to target promoters would be lower than for Fe-Fur target promoters. As shown by our and other's work ((12, 25, 26, 44); B.M. Carpenter, J.J. Gilbreath, D.S. Merrell, unpublished results), *apo*-Fur does seem to bind DNA with less affinity than Fe-Fur in *H. pylori*, thus supporting our hypothesis. While these data are suggestive, it is likely that there are substantial differences in the Fe-Fur:DNA interactions as compared to the *apo*-Fur:DNA interactions. Clearly, further structural studies are needed to clearly understand how *apo*-Fur interacts with target DNA.

Metal ion selectivity in vivo

The primary role of Fur *in vivo* is to regulate iron homeostasis. According to the current dogma, Fur utilizes a regulatory binding site (S2 in *H. pylori*) to “sense” intracellular iron levels and then responds accordingly. To accurately detect iron levels within the cell, Fur must specifically recognize Fe²⁺ ions despite the presence of other metal cations. As Fur can bind several of these ions (Zn²⁺, Mn²⁺, Co²⁺) *in vitro*, and metallation with these ions is sufficient for DNA binding (49), it remains unclear how the protein is able to differentiate between these ligands *in vivo*. Furthermore, the fact that we

were able to use the manganese selection to identify Fur mutations also suggests that Mn^{2+} ions can be used by Fur when concentrations are high enough.

One major factor that affects metal ion responsiveness is metal binding affinity. Briefly, affinity refers to the degree to which a metal is able to act as a ligand for a binding site. In the context of Fur, utilization of one metal ion over another could be the result of differences in metal binding affinities. For example, the affinity for Fe^{2+} in the regulatory metal binding site (S2) may be higher than for other ions such as Zn^{2+} or Mn^{2+} ; in contrast, as Zn^{2+} is thought to occupy S1 *in vivo* (165), this site may have a higher affinity for Zn^{2+} than for Fe^{2+} or Mn^{2+} . The affinity a binding site has for a metal ion is dependent on both the geometry of the coordination sphere and the specific amino acid residues that directly interact with the metal ligand. Given these requirements, an interesting, and thus far unique, aspect of *H. pylori* Fur structure is the asymmetric coordination sphere geometry seen in the regulatory metal binding site (S2) (49). One explanation for this difference in metal ion coordination between Fur protomers is that this specific molecular organization evolved to allow Fur to specifically sense the Fe^{2+} ions rather than other metal ions present in the cell. Although the relative binding affinities for each of the different metal ions present within the *H. pylori* cell have not been determined, it seems likely that the ability of Fur to utilize certain metal ions at each of the S1, S2, and S3 sites is directly related to binding affinity for these ligands. This hypothesis could be tested by measuring the metal binding affinities of various metal ions in each of the metallation sites.

The role of iron and Fur regulation during infection

The success of *H. pylori* within the host is largely determined by the ability to obtain essential nutrients such as iron. In order to maintain a proper balance between persistence and disease pathogenesis, however, the competition between bacteria and the host for these nutrients must be essentially equal. If the host is more competitive, then the colonizing bacteria may be cleared; however, if the bacteria are more competitive, disease may result. An example of where the balance is tipped in favor of the bacterium can be seen in the association of iron-deficiency anemia (IDA) with *H. pylori* infection. Indeed numerous studies have implicated *H. pylori* infection in the development of IDA (30, 31, 33, 54, 90). This link is further supported by the fact that, during *H. pylori* infection, the use of dietary iron supplements does not reverse IDA; however, treating the *H. pylori* infection with antibiotics does eliminate the anemia (31).

More recently, *in vivo* studies using animal models have provided additional evidence that chronic *H. pylori* infection leads to the development of IDA. For example, in a murine infection model, *H. pylori* diminishes host iron stores, as measured by serum ferritin and liver iron levels (87). Similarly, infection with the murine gastric *Helicobacter* species (*H. felis*) also causes IDA in that model (71). Further studies using *H. felis* in an INS-GAS mouse model indicate that chronic gastric *Helicobacter* infection results in reduced levels of serum iron, transferrin saturation, and hyperferritinemia, as well as an increased total iron binding capacity (154), all of which are hallmarks of IDA. Collectively, these studies provide evidence that the competition between *H. pylori* and the host for iron plays a role in determining disease outcome.

In order to maintain intracellular levels of iron that are necessary for growth, *H. pylori* must be able to not only sense when iron levels are low, but also actively obtain iron from the environment. Within the human host, *H. pylori* is able to obtain and utilize free ferrous iron, as well as iron from host-derived hemoglobin, transferrin, and lactoferrin molecules (reviewed in (69)). In addition, *H. pylori* binds the iron-free forms of these host molecules, which is hypothesized to limit host iron utilization (139). To date, all of the components of these iron acquisition systems that have been characterized are regulated by Fur. Thus, Fur regulation is a central component in the ability of *H. pylori* to obtain nutrients that are required for survival within the human host. Recent studies using an *in vitro* polarized epithelial cell model identified an additional mechanism of iron acquisition employed by *H. pylori*. In those studies, Tan *et al.*, showed that the *H. pylori* virulence factor CagA disrupts host transferrin trafficking (153); in CagA intoxicated cells, the transferrin receptor is localized to the apical cell surface rather than the basolateral surface, where it is normally found. Since *H. pylori* primarily colonize along the apical surface of epithelial cells, the re-direction of the transferrin receptor likely makes iron-loaded transferrin more accessible to the bacteria. Interestingly, as described above, studies from our lab showed that expression of CagA is activated in the presence of Fe-Fur (128). Given the role of CagA in iron acquisition, it is perhaps not surprising that the *cagA* gene is regulated by Fur. Collectively, these studies suggest that *H. pylori* may employ a variety of Fur regulated mechanisms to acquire iron *in vivo*, some of which may result from direct interactions with host cells.

A recent report has also provided additional evidence that the competition for iron may be a turning point in disease development. Using Mongolian gerbils that were kept

on an iron depleted diet, Noto *et al.*, demonstrated that the combination of *H. pylori* infection and a low iron diet augments gastric inflammation and accelerates cancer development (116); this model of carcinogenesis may reflect the clinical condition where an infected individual has a pre-existing IDA. Interestingly, subsequent analysis of the protein expression patterns in the *H. pylori* strains that were harvested from these animals indicates that several proteins were over-expressed. Among the proteins identified were CagA, as well as proteins involved in flagellar motility such as FlaA, FlaB, FlgL, and FliD (116). Overexpression of these proteins under iron-depleted conditions may represent a type of stress response in which *H. pylori* actively tries to acquire additional iron. As described above, increased levels of CagA may increase availability of host transferrin on the apical surface of host epithelial cells, and upregulation of flagellar components could ensure that the bacteria are able to respond to nutrient-related chemotactic signals in the environment. However, it should be noted that the overexpression of these proteins was detected after the bacteria were harvested from stomach tissue and allowed to grow *in vitro*. Therefore, these findings may not be entirely representative of the *H. pylori* adaptive response *in vivo*. As such, the role of these proteins under iron depleted conditions *in vivo* remains unclear. As an extension of the studies performed by Noto *et al.*, it would be interesting to use a *fur* mutant strain to examine colonization and disease progression in the iron-depleted Mongolian gerbil. Such studies could provide insight into the importance of Fur and Fur regulation in *H. pylori*-mediated disease progression after the development of IDA. As we begin to characterize the relationship between iron and iron availability within the host and subsequent disease development, there certainly seems to be a strong connection between

iron, Fur regulation, and *H. pylori* mediated disease development. Future studies using the animal models described above will likely aid our understanding of this complex process and may shed light on potential avenues for intervention.

Dissecting the roles of Fe-Fur and apo-Fur regulation in vivo

Numerous studies have identified a role for Fur regulation in numerous adaptive responses *in vitro*, as well as *in vivo* colonization (22, 67) and disease development (111). While these studies highlight the importance of Fur and Fur-mediated regulatory processes *in vivo*, it is important to note that it is unclear whether Fe-Fur regulation and *apo*-Fur regulation are equally important within the host. It is possible that one of these two types of regulation may be more important *in vivo*. Similarly, Fur has been shown to mediate the adaptive response to the acid shock and acid tolerance responses, as well as oxidative, nitrosative, and osmotic stress conditions (35, 134, 136, 158). Once again, it is unclear whether both Fe-Fur and *apo*-Fur function are required for survival under these conditions. Taken together, these data raise an interesting question that does not apply to many other bacteria: can Fe-Fur and *apo*-Fur regulation be separated and studied in isolation? If so, we would then be able to determine the relative contribution of each type of regulation to different stress responses, colonization, and disease development.

Utilizing the recently resolved *H. pylori* Fe-Fur and *C. jejuni apo*-Fur structures (23, 49), and the functional data presented in this dissertation, it may now be possible to design mutations within Fur that confer a Δ Fe-Fur or Δ *apo*-Fur only regulatory system. These mutant strains could then be used in conjunction with wildtype and *fur* deletion strains in co- and single strain infections assays to determine the contribution of Fe-Fur

and *apo*-Fur regulation to initial colonization and establishment of infection within the host. Furthermore, single strain infections in the Mongolian gerbil model of gastric cancer could determine the role for each type of regulation in persistent colonization and disease development. Finally, the Δ Fe-Fur and Δ *apo*-Fur strains could be used to evaluate the role of these two types of regulation in the acid shock and acid tolerance responses, as well as response to oxidative, nitrosative, and osmotic stress conditions. In addition to providing important information regarding regulation in *H. pylori*, as additional species of bacteria are found to utilize *apo*-Fur regulation (e.g. *C. jejuni* (72) and *S. aureus* (47)), *H. pylori* could serve as a model system for understanding Fur regulation across a variety of bacteria.

Conclusion

Despite over 30 years of intense study, there are still many aspects of *H. pylori* biology that are not well understood. As highlighted above, many of these unanswered questions pertain to adaptive responses and transcriptional regulation. As a result of many years of co-evolution within the host niche, these two areas of *H. pylori* biology have become controlled by a relatively small subset of regulatory proteins, including Fur. Compared to Fur in other bacterial species, *H. pylori* Fur has evolved to function in an extended capacity and regulates responses to diverse intracellular and extracellular conditions. Furthermore, *H. pylori* Fur activates and represses gene expression in both the iron-bound and *apo* forms, a level of complexity so far only described in this organism. Despite the recent advances in understanding the regulatory mechanisms of this pleiotropic regulator, there is clearly much more that can be learned about Fur regulation,

the Fur-mediated adaptive responses, and the contribution of Fur to *H. pylori* survival and persistence *in vivo*.

References

1. **Adams, M. D., K. Goglin, N. Molyneaux, K. M. Hujer, H. Lavender, J. J. Jamison, I. J. MacDonald, K. M. Martin, T. Russo, A. A. Campagnari, A. M. Hujer, R. A. Bonomo, and S. R. Gill.** 2008. Comparative genome sequence analysis of multidrug-resistant *Acinetobacter baumannii*. *J Bacteriol* **190**:8053-64.
2. **Alamuri, P., N. Mehta, A. Burk, and R. J. Maier.** 2006. Regulation of the *Helicobacter pylori* Fe-S cluster synthesis protein NifS by iron, oxidative stress conditions, and fur. *J Bacteriol* **188**:5325-30.
3. **Andrews, N. C., and P. J. Schmidt.** 2007. Iron homeostasis. *Annu Rev Physiol* **69**:69-85.
4. **Appelmek, B. J., M. A. Monteiro, S. L. Martin, A. P. Moran, and C. M. Vandenbroucke-Grauls.** 2000. Why *Helicobacter pylori* has Lewis antigens. *Trends Microbiol* **8**:565-70.

5. **Appelmek, B. J., and C. M. Vandenbroucke-Grauls.** 2000. *H pylori* and Lewis antigens. Gut **47**:10-1.

6. **Aspholm-Hurtig, M., G. Dailide, M. Lahmann, A. Kalia, D. Ilver, N. Roche, S. Vikstrom, R. Sjostrom, S. Linden, A. Backstrom, C. Lundberg, A. Arnqvist, J. Mahdavi, U. J. Nilsson, B. Velapatino, R. H. Gilman, M. Gerhard, T. Alarcon, M. Lopez-Brea, T. Nakazawa, J. G. Fox, P. Correa, M. G. Dominguez-Bello, G. I. Perez-Perez, M. J. Blaser, S. Normark, I. Carlstedt, S. Oscarson, S. Teneberg, D. E. Berg, and T. Boren.** 2004. Functional adaptation of BabA, the *H. pylori* ABO blood group antigen binding adhesin. Science **305**:519-22.

7. **Bagg, A., and J. B. Neilands.** 1987. Ferric uptake regulation protein acts as a repressor, employing iron (II) as a cofactor to bind the operator of an iron transport operon in *Escherichia coli*. Biochemistry **26**:5471-7.

8. **Baichoo, N., and J. D. Helmann.** 2002. Recognition of DNA by Fur: a reinterpretation of the Fur box consensus sequence. J Bacteriol **184**:5826-32.

9. **Baltrus, D. A., M. R. Amieva, A. Covacci, T. M. Lowe, D. S. Merrell, K. M. Ottemann, M. Stein, N. R. Salama, and K. Guillemin.** 2009. The complete genome sequence of *Helicobacter pylori* strain G27. J Bacteriol **191**:447-8.

10. **Banerjee, A., and D. N. Rao.** 2011. Functional analysis of an acid adaptive DNA adenine methyltransferase from *Helicobacter pylori* 26695. PLoS One **6**:e16810.

11. **Benanti, E. L., and P. T. Chivers.** 2007. The N-terminal arm of the *Helicobacter pylori* Ni²⁺-dependent transcription factor NikR is required for specific DNA binding. J Biol Chem **282**:20365-75.

12. **Bereswill, S., S. Greiner, A. H. van Vliet, B. Waidner, F. Fassbinder, E. Schiltz, J. G. Kusters, and M. Kist.** 2000. Regulation of ferritin-mediated cytoplasmic iron storage by the ferric uptake regulator homolog (Fur) of *Helicobacter pylori*. J Bacteriol **182**:5948-53.

13. **Bereswill, S., F. Lichte, S. Greiner, B. Waidner, F. Fassbinder, and M. Kist.** 1999. The ferric uptake regulator (Fur) homologue of *Helicobacter pylori*: functional analysis of the coding gene and controlled production of the recombinant protein in *Escherichia coli*. Med Microbiol Immunol **188**:31-40.

14. **Bereswill, S., F. Lichte, T. Vey, F. Fassbinder, and M. Kist.** 1998. Cloning and characterization of the fur gene from *Helicobacter pylori*. FEMS Microbiol Lett **159**:193-200.

15. **Bijlsma, J. J., B. Waidner, A. H. Vliet, N. J. Hughes, S. Hag, S. Bereswill, D. J. Kelly, C. M. Vandenbroucke-Grauls, M. Kist, and J. G. Kusters.** 2002. The

Helicobacter pylori homologue of the ferric uptake regulator is involved in acid resistance. *Infect Immun* **70**:606-11.

16. **Blaser, M. J.** 1998. *Helicobacter pylori* and gastric diseases. *BMJ* **316**:1507-10.

17. **Blaser, M. J.** 1997. The versatility of *Helicobacter pylori* in the adaptation to the human stomach. *J Physiol Pharmacol* **48**:307-14.

18. **Blaser, M. J., G. I. Perez-Perez, H. Kleanthous, T. L. Cover, R. M. Peek, P. H. Chyou, G. N. Stemmermann, and A. Nomura.** 1995. Infection with *Helicobacter pylori* strains possessing *cagA* is associated with an increased risk of developing adenocarcinoma of the stomach. *Cancer Res* **55**:2111-5.

19. **Blattner, F. R., G. Plunkett, 3rd, C. A. Bloch, N. T. Perna, V. Burland, M. Riley, J. Collado-Vides, J. D. Glasner, C. K. Rode, G. F. Mayhew, J. Gregor, N. W. Davis, H. A. Kirkpatrick, M. A. Goeden, D. J. Rose, B. Mau, and Y. Shao.** 1997. The complete genome sequence of *Escherichia coli* K-12. *Science* **277**:1453-62.

20. **Brickman, T. J., B. A. Ozenberger, and M. A. McIntosh.** 1990. Regulation of divergent transcription from the iron-responsive *fepB-entC* promoter-operator regions in *Escherichia coli*. *J Mol Biol* **212**:669-82.

21. **Browning, D. F., and S. J. Busby.** 2004. The regulation of bacterial transcription initiation. *Nat Rev Microbiol* **2**:57-65.

22. **Bury-Mone, S., J. M. Thiberge, M. Contreras, A. Maitournam, A. Labigne, and H. De Reuse.** 2004. Responsiveness to acidity via metal ion regulators mediates virulence in the gastric pathogen *Helicobacter pylori*. *Mol Microbiol* **53**:623-38.

23. **Butcher, J., S. Sarvan, J. S. Brunzelle, J. F. Couture, and A. Stintzi.** 2012. Structure and regulon of *Campylobacter jejuni* ferric uptake regulator Fur define apo-Fur regulation. *Proc Natl Acad Sci U S A* **109**:10047-52.

24. **Cancer, International Agency for Research on** 1994. Infection with *Helicobacter pylori*. Presented at the Monogr Eval Carcinog Risks Hum.

25. **Carpenter, B. M., H. Gancz, S. L. Benoit, S. Evans, C. H. Olsen, S. L. Michel, R. J. Maier, and D. S. Merrell.** 2010. Mutagenesis of conserved amino acids of *Helicobacter pylori* Fur reveals residues important for function. *J Bacteriol* **192**:5037-52.

26. **Carpenter, B. M., H. Gancz, R. P. Gonzalez-Nieves, A. L. West, J. M. Whitmire, S. L. Michel, and D. S. Merrell.** 2009. A single nucleotide change affects fur-dependent regulation of *sodB* in *H. pylori*. *PLoS One* **4**:e5369.

27. **Carpenter, B. M., T. K. McDaniel, J. M. Whitmire, H. Gancz, S. Guidotti, S. Censini, and D. S. Merrell.** 2007. Expanding the *Helicobacter pylori* genetic toolbox: modification of an endogenous plasmid for use as a transcriptional reporter and complementation vector. *Appl Environ Microbiol* **73**:7506-14.

28. **Carpenter, B. M., J. M. Whitmire, and D. S. Merrell.** 2009. This is not your mother's repressor: the complex role of fur in pathogenesis. *Infect Immun* **77**:2590-601.

29. **Censini, S., C. Lange, Z. Xiang, J. E. Crabtree, P. Ghiara, M. Borodovsky, R. Rappuoli, and A. Covacci.** 1996. *cag*, a pathogenicity island of *Helicobacter pylori*, encodes type I-specific and disease-associated virulence factors. *Proc Natl Acad Sci U S A* **93**:14648-53.

30. **Choe, Y. H., S. K. Kim, and Y. C. Hong.** 2000. *Helicobacter pylori* infection with iron deficiency anaemia and subnormal growth at puberty. *Arch Dis Child* **82**:136-40.

31. **Choe, Y. H., J. E. Lee, and S. K. Kim.** 2000. Effect of *Helicobacter pylori* eradication on sideropenic refractory anaemia in adolescent girls with *Helicobacter pylori* infection. *Acta Paediatr* **89**:154-7.

32. **Choi, S. S., P. T. Chivers, and D. E. Berg.** 2011. Point mutations in *Helicobacter pylori's* fur regulatory gene that alter resistance to metronidazole, a prodrug activated by chemical reduction. PLoS One **6**:e18236.
33. **Ciacci, C., F. Sabbatini, R. Cavallaro, F. Castiglione, S. Di Bella, P. Iovino, A. Palumbo, R. Tortora, D. Amoruso, and G. Mazzacca.** 2004. *Helicobacter pylori* impairs iron absorption in infected individuals. Dig Liver Dis **36**:455-60.
34. **Contreras, M., J. M. Thiberge, M. A. Mandrand-Berthelot, and A. Labigne.** 2003. Characterization of the roles of NikR, a nickel-responsive pleiotropic autoregulator of *Helicobacter pylori*. Mol Microbiol **49**:947-63.
35. **Cooksley, C., P. J. Jenks, A. Green, A. Cockayne, R. P. Logan, and K. R. Hardie.** 2003. NapA protects *Helicobacter pylori* from oxidative stress damage, and its production is influenced by the ferric uptake regulator. J Med Microbiol **52**:461-9.
36. **Cover, T. L., and M. J. Blaser.** 2009. *Helicobacter pylori* in health and disease. Gastroenterology **136**:1863-73.
37. **Crabtree, J. E.** 1998. Role of cytokines in pathogenesis of *Helicobacter pylori*-induced mucosal damage. Dig Dis Sci **43**:46S-55S.
38. **Crabtree, J. E., A. Covacci, S. M. Farmery, Z. Xiang, D. S. Tompkins, S. Perry, I. J. Lindley, and R. Rappuoli.** 1995. *Helicobacter pylori* induced interleukin-8

expression in gastric epithelial cells is associated with CagA positive phenotype. *J Clin Pathol* **48**:41-5.

39. **Danielli, A., D. Roncarati, I. Delany, V. Chiarini, R. Rappuoli, and V. Scarlato.** 2006. *In vivo* dissection of the *Helicobacter pylori* Fur regulatory circuit by genome-wide location analysis. *J Bacteriol* **188**:4654-62.

40. **de Lorenzo, V., S. Wee, M. Herrero, and J. B. Neilands.** 1987. Operator sequences of the aerobactin operon of plasmid ColV-K30 binding the ferric uptake regulation (*fur*) repressor. *J Bacteriol* **169**:2624-30.

41. **Delany, I., R. Ieva, A. Soragni, M. Hilleringmann, R. Rappuoli, and V. Scarlato.** 2005. In vitro analysis of protein-operator interactions of the NikR and fur metal-responsive regulators of coregulated genes in *Helicobacter pylori*. *J Bacteriol* **187**:7703-15.

42. **Delany, I., A. B. Pacheco, G. Spohn, R. Rappuoli, and V. Scarlato.** 2001. Iron-dependent transcription of the *frpB* gene of *Helicobacter pylori* is controlled by the Fur repressor protein. *J Bacteriol* **183**:4932-7.

43. **Delany, I., R. Rappuoli, and V. Scarlato.** 2004. Fur functions as an activator and as a repressor of putative virulence genes in *Neisseria meningitidis*. *Mol Microbiol* **52**:1081-1090.
44. **Delany, I., G. Spohn, A. B. Pacheco, R. Ieva, C. Alaimo, R. Rappuoli, and V. Scarlato.** 2002. Autoregulation of *Helicobacter pylori* Fur revealed by functional analysis of the iron-binding site. *Mol Microbiol* **46**:1107-22.
45. **Delany, I., G. Spohn, R. Rappuoli, and V. Scarlato.** 2003. An anti-repression Fur operator upstream of the promoter is required for iron-mediated transcriptional autoregulation in *Helicobacter pylori*. *Mol Microbiol* **50**:1329-38.
46. **Delany, I., G. Spohn, R. Rappuoli, and V. Scarlato.** 2001. The Fur repressor controls transcription of iron-activated and -repressed genes in *Helicobacter pylori*. *Mol Microbiol* **42**:1297-309.
47. **Deng, X., F. Sun, Q. Ji, H. Liang, D. Missiakas, L. Lan, and C. He.** 2012. Expression of multidrug resistance efflux pump gene *norA* is iron responsive in *Staphylococcus aureus*. *J Bacteriol* **194**:1753-62.
48. **Dhaenens, L., F. Szczebara, S. Van Nieuwenhuyse, and M. O. Husson.** 1999. Comparison of iron uptake in different *Helicobacter* species. *Res Microbiol* **150**:475-81.

49. **Dian, C., S. Vitale, G. A. Leonard, C. Bahlawane, C. Fauquant, D. Leduc, C. Muller, H. de Reuse, I. Michaud-Soret, and L. Terradot.** 2011. The structure of the *Helicobacter pylori* ferric uptake regulator Fur reveals three functional metal binding sites. *Mol Microbiol* **79**:1260-75.

50. **Dietz, P., G. Gerlach, and D. Beier.** 2002. Identification of target genes regulated by the two-component system HP166-HP165 of *Helicobacter pylori*. *J Bacteriol* **184**:350-62.

51. **Doenges, J.** 1938. Spirochaetes in the gastric glands of *Macacus rhesus* and humans without definite history of related disease. *Proc Soc Exp Med Sci* **38**:536-538.

52. **Dosanjh, N. S., N. A. Hammerbacher, and S. L. Michel.** 2007. Characterization of the *Helicobacter pylori* NikR-P(ureA) DNA interaction: metal ion requirements and sequence specificity. *Biochemistry* **46**:2520-9.

53. **Dosanjh, N. S., and S. L. Michel.** 2006. Microbial nickel metalloregulation: NikRs for nickel ions. *Curr Opin Chem Biol* **10**:123-30.

54. **DuBois, S., and D. J. Kearney.** 2005. Iron-deficiency anemia and *Helicobacter pylori* infection: a review of the evidence. *Am J Gastroenterol* **100**:453-9.

55. **Dunn, B. E., G. P. Campbell, G. I. Perez-Perez, and M. J. Blaser.** 1990. Purification and characterization of urease from *Helicobacter pylori*. *J Biol Chem* **265**:9464-9.
56. **Dunn, B. E., H. Cohen, and M. J. Blaser.** 1997. *Helicobacter pylori*. *Clin Microbiol Rev* **10**:720-41.
57. **Engel, A. S., N. Lee, M. L. Porter, L. A. Stern, P. C. Bennett, and M. Wagner.** 2003. Filamentous "Epsilonproteobacteria" dominate microbial mats from sulfidic cave springs. *Appl Environ Microbiol* **69**:5503-11.
58. **Ernst, F. D., S. Bereswill, B. Waidner, J. Stoof, U. Mader, J. G. Kusters, E. J. Kuipers, M. Kist, A. H. van Vliet, and G. Homuth.** 2005. Transcriptional profiling of *Helicobacter pylori* Fur- and iron-regulated gene expression. *Microbiology* **151**:533-46.
59. **Ernst, F. D., G. Homuth, J. Stoof, U. Mader, B. Waidner, E. J. Kuipers, M. Kist, J. G. Kusters, S. Bereswill, and A. H. van Vliet.** 2005. Iron-responsive regulation of the *Helicobacter pylori* iron-cofactored superoxide dismutase SodB is mediated by Fur. *J Bacteriol* **187**:3687-92.
60. **Ernst, F. D., E. J. Kuipers, A. Heijens, R. Sarwari, J. Stoof, C. W. Penn, J. G. Kusters, and A. H. van Vliet.** 2005. The nickel-responsive regulator NikR controls activation and repression of gene transcription in *Helicobacter pylori*. *Infect Immun* **73**:7252-8.

61. **Ernst, P. B., and B. D. Gold.** 2000. The disease spectrum of *Helicobacter pylori*: the immunopathogenesis of gastroduodenal ulcer and gastric cancer. *Annu Rev Microbiol* **54**:615-40.

62. **Escolar, L., J. Perez-Martin, and V. de Lorenzo.** 1998. Binding of the fur (ferric uptake regulator) repressor of *Escherichia coli* to arrays of the GATAAT sequence. *J Mol Biol* **283**:537-47.

63. **Escolar, L., J. Perez-Martin, and V. de Lorenzo.** 1999. Opening the iron box: transcriptional metalloregulation by the Fur protein. *J Bacteriol* **181**:6223-9.

64. **Ferguson, D. A., Jr., C. Li, N. R. Patel, W. R. Mayberry, D. S. Chi, and E. Thomas.** 1993. Isolation of *Helicobacter pylori* from saliva. *J Clin Microbiol* **31**:2802-4.

65. **Fiedorek, S. C., H. M. Malaty, D. L. Evans, C. L. Pumphrey, H. B. Casteel, D. J. Evans, Jr., and D. Y. Graham.** 1991. Factors influencing the epidemiology of *Helicobacter pylori* infection in children. *Pediatrics* **88**:578-82.

66. **Galmiche, A., J. Rassow, A. Doye, S. Cagnol, J. C. Chambard, S. Contamin, V. de Thillot, I. Just, V. Ricci, E. Solcia, E. Van Obberghen, and P. Boquet.** 2000. The N-terminal 34 kDa fragment of *Helicobacter pylori* vacuolating cytotoxin targets mitochondria and induces cytochrome c release. *EMBO J* **19**:6361-70.

67. **Gancz, H., S. Censini, and D. S. Merrell.** 2006. Iron and pH homeostasis intersect at the level of Fur regulation in the gastric pathogen *Helicobacter pylori*. *Infect Immun* **74**:602-14.
68. **Gancz, H., and D. S. Merrell.** 2011. The *Helicobacter pylori* Ferric Uptake Regulator (Fur) is essential for growth under sodium chloride stress. *J Microbiol* **49**:294-8.
69. **Gilbreath, J. J., W. L. Cody, D. S. Merrell, and D. R. Hendrixson.** 2011. Change is good: variations in common biological mechanisms in the epsilonproteobacterial genera *Campylobacter* and *Helicobacter*. *Microbiol Mol Biol Rev* **75**:84-132.
70. **Gilbreath, J. J., A. L. West, O. Q. Pich, B. M. Carpenter, S. Michel, and D. S. Merrell.** 2012. Fur Activates Expression of the 2-Oxoglutarate Oxidoreductase Genes (*oorDABC*) in *Helicobacter pylori*. *J Bacteriol* **194**:6490-7.
71. **Gobel, R., E. L. Symonds, S. Kritas, R. N. Butler, and C. D. Tran.** 2006. *Helicobacter felis* infection causes an acute iron deficiency in nonpregnant and pregnant mice. *Helicobacter* **11**:529-32.

72. **Grabowska, A. D., M. P. Wandel, A. M. Lasica, M. Nesteruk, P. Roszczenko, A. Wyszynska, R. Godlewska, and E. K. Jagusztyn-Krynicka.** 2011. *Campylobacter jejuni dsb* gene expression is regulated by iron in a Fur-dependent manner and by a translational coupling mechanism. *BMC Microbiol* **11**:166.
73. **Graham, D. Y., and L. Fischbach.** 2010. *Helicobacter pylori* treatment in the era of increasing antibiotic resistance. *Gut* **59**:1143-53.
74. **Hantke, K.** 1981. Regulation of ferric iron transport in *Escherichia coli* K12: isolation of a constitutive mutant. *Mol Gen Genet* **182**:288-92.
75. **Hantke, K.** 1987. Selection procedure for deregulated iron transport mutants (*fur*) in *Escherichia coli* K 12: *fur* not only affects iron metabolism. *Mol Gen Genet* **210**:135-9.
76. **Harris, A. G., F. E. Hinds, A. G. Beckhouse, T. Kolesnikow, and S. L. Hazell.** 2002. Resistance to hydrogen peroxide in *Helicobacter pylori*: role of catalase (KatA) and Fur, and functional analysis of a novel gene product designated 'KatA-associated protein', KapA (HP0874). *Microbiology* **148**:3813-25.
77. **Higashi, H., R. Tsutsumi, A. Fujita, S. Yamazaki, M. Asaka, T. Azuma, and M. Hatakeyama.** 2002. Biological activity of the *Helicobacter pylori* virulence factor

CagA is determined by variation in the tyrosine phosphorylation sites. Proc Natl Acad Sci U S A **99**:14428-33.

78. **Higashi, H., R. Tsutsumi, S. Muto, T. Sugiyama, T. Azuma, M. Asaka, and M. Hatakeyama.** 2002. SHP-2 tyrosine phosphatase as an intracellular target of *Helicobacter pylori* CagA protein. Science **295**:683-6.

79. **Hughes, N. J., C. L. Clayton, P. A. Chalk, and D. J. Kelly.** 1998. *Helicobacter pylori* *porCDAB* and *oorDABC* genes encode distinct pyruvate:flavodoxin and 2-oxoglutarate:acceptor oxidoreductases which mediate electron transport to NADP. J Bacteriol **180**:1119-28.

80. **Husson, M. O., D. Legrand, G. Spik, and H. Leclerc.** 1993. Iron acquisition by *Helicobacter pylori*: importance of human lactoferrin. Infect Immun **61**:2694-7.

81. **Jang, S., K. R. Jones, C. H. Olsen, Y. M. Joo, Y. J. Yoo, I. S. Chung, J. H. Cha, and D. S. Merrell.** 2010. Epidemiological link between gastric disease and polymorphisms in *VacA* and *CagA*. J Clin Microbiol **48**:559-67.

82. **Jeon, B. H., Y. J. Oh, N. G. Lee, and Y. H. Choe.** 2004. Polymorphism of the *Helicobacter pylori* *feoB* gene in Korea: a possible relation with iron-deficiency anemia? Helicobacter **9**:330-4.

83. **Johnson, D. C., D. R. Dean, A. D. Smith, and M. K. Johnson.** 2005. Structure, function, and formation of biological iron-sulfur clusters. *Annu Rev Biochem* **74**:247-81.
84. **Jones, K. R., Y. M. Joo, S. Jang, Y. J. Yoo, H. S. Lee, I. S. Chung, C. H. Olsen, J. M. Whitmire, D. S. Merrell, and J. H. Cha.** 2009. Polymorphism in the CagA EPIYA motif impacts development of gastric cancer. *J Clin Microbiol* **47**:959-68.
85. **Jones, K. R., J. M. Whitmire, and D. S. Merrell.** 2010. A Tale of Two Toxins: *Helicobacter pylori* CagA and VacA Modulate Host Pathways that Impact Disease. *Front Microbiol* **1**:115.
86. **Kabir, S.** 2004. Detection of *Helicobacter pylori* DNA in feces and saliva by polymerase chain reaction: a review. *Helicobacter* **9**:115-23.
87. **Keenan, J. I., R. A. Peterson, R. Fraser, C. M. Frampton, T. A. Walmsley, R. A. Allardyce, and J. A. Roake.** 2004. The effect of *Helicobacter pylori* infection and dietary iron deficiency on host iron homeostasis: a study in mice. *Helicobacter* **9**:643-50.
88. **Kimura, M., S. Goto, A. Wada, K. Yahiro, T. Niidome, T. Hatakeyama, H. Aoyagi, T. Hirayama, and T. Kondo.** 1999. Vacuolating cytotoxin purified from *Helicobacter pylori* causes mitochondrial damage in human gastric cells. *Microb Pathog* **26**:45-52.

89. **Kuipers, E. J., G. I. Perez-Perez, S. G. Meuwissen, and M. J. Blaser.** 1995. *Helicobacter pylori* and atrophic gastritis: importance of the cagA status. J Natl Cancer Inst **87**:1777-80.
90. **Kurekci, A. E., A. A. Atay, S. U. Sarici, E. Yesilkaya, Z. Senses, V. Okutan, and O. Ozcan.** 2005. Is there a relationship between childhood *Helicobacter pylori* infection and iron deficiency anemia? J Trop Pediatr **51**:166-9.
91. **Lakowicz, J. R.** 1999. Principles of Fluorescence Spectroscopy, 2 ed. Kluwer Academic/Plenum Publishers.
92. **Lam, M. S., C. M. Litwin, P. A. Carroll, and S. B. Calderwood.** 1994. *Vibrio cholerae fur* mutations associated with loss of repressor activity: implications for the structural-functional relationships of fur. J Bacteriol **176**:5108-15.
93. **Lee, J. W., and J. D. Helmann.** 2007. Functional specialization within the Fur family of metalloregulators. Biometals **20**:485-99.
94. **Lee, S. K., A. Stack, E. Katzowitsch, S. I. Aizawa, S. Suerbaum, and C. Josenhans.** 2003. *Helicobacter pylori* flagellins have very low intrinsic activity to stimulate human gastric epithelial cells via TLR5. Microbes Infect **5**:1345-56.

95. **Lepper, P. M., M. Triantafilou, C. Schumann, E. M. Schneider, and K. Triantafilou.** 2005. Lipopolysaccharides from *Helicobacter pylori* can act as antagonists for Toll-like receptor 4. *Cell Microbiol* **7**:519-28.
96. **Leung, W. K., K. L. Siu, C. K. Kwok, S. Y. Chan, R. Sung, and J. J. Sung.** 1999. Isolation of *Helicobacter pylori* from vomitus in children and its implication in gastro-oral transmission. *Am J Gastroenterol* **94**:2881-4.
97. **Li, Y., and D. B. Zamble.** 2009. pH-responsive DNA-binding activity of *Helicobacter pylori* NikR. *Biochemistry* **48**:2486-96.
98. **Linz, B., F. Balloux, Y. Moodley, A. Manica, H. Liu, P. Roumagnac, D. Falush, C. Stamer, F. Prugnolle, S. W. van der Merwe, Y. Yamaoka, D. Y. Graham, E. Perez-Trallero, T. Wadstrom, S. Suerbaum, and M. Achtman.** 2007. An African origin for the intimate association between humans and *Helicobacter pylori*. *Nature* **445**:915-8.
99. **Loprasert, S., R. Sallabhan, W. Whangsuk, and S. Mongkolsuk.** 2000. Characterization and mutagenesis of *fur* gene from *Burkholderia pseudomallei*. *Gene* **254**:129-37.
100. **Mahdavi, J., B. Sonden, M. Hurtig, F. O. Olfat, L. Forsberg, N. Roche, J. Angstrom, T. Larsson, S. Teneberg, K. A. Karlsson, S. Altraja, T. Wadstrom, D.**

Kersulyte, D. E. Berg, A. Dubois, C. Petersson, K. E. Magnusson, T. Norberg, F. Lindh, B. B. Lundskog, A. Arnqvist, L. Hammarstrom, and T. Boren. 2002.

Helicobacter pylori SabA adhesin in persistent infection and chronic inflammation.

Science **297**:573-8.

101. **Marcus, E. A., G. Sachs, Y. Wen, J. Feng, and D. R. Scott.** 2012. Role of the *Helicobacter pylori* sensor kinase ArsS in protein trafficking and acid acclimation. J Bacteriol **194**:5545-51.

102. **Marshall, B. J.** 1983. Unidentified curved bacilli on gastric epithelium in active chronic gastritis. Lancet **i**:1273-1275.

103. **Marshall, B. J., H. Royce, D.I. Annear, et al.** 1984. Original isolation of *Campylobacter pyloridis* from human gastric mucosa. Microbios Letters **25**:83-88.

104. **Mason, J. R., and R. Cammack.** 1992. The electron-transport proteins of hydroxylating bacterial dioxygenases. Annu Rev Microbiol **46**:277-305.

105. **Masse, E., and M. Arguin.** 2005. Ironing out the problem: new mechanisms of iron homeostasis. Trends Biochem Sci **30**:462-8.

106. **Masse, E., and S. Gottesman.** 2002. A small RNA regulates the expression of genes involved in iron metabolism in *Escherichia coli*. *Proc Natl Acad Sci U S A* **99**:4620-5.
107. **Masse, E., H. Salvail, G. Desnoyers, and M. Arguin.** 2007. Small RNAs controlling iron metabolism. *Curr Opin Microbiol* **10**:140-5.
108. **McHugh, J. P., F. Rodriguez-Quinones, H. Abdul-Tehrani, D. A. Svistunenko, R. K. Poole, C. E. Cooper, and S. C. Andrews.** 2003. Global iron-dependent gene regulation in *Escherichia coli*. A new mechanism for iron homeostasis. *J Biol Chem* **278**:29478-86.
109. **Mellin, J. R., S. Goswami, S. Grogan, B. Tjaden, and C. A. Genco.** 2007. A novel fur- and iron-regulated small RNA, NrrF, is required for indirect fur-mediated regulation of the *sdhA* and *sdhC* genes in *Neisseria meningitidis*. *J Bacteriol* **189**:3686-94.
110. **Merrell, D. S., M. L. Goodrich, G. Otto, L. S. Tompkins, and S. Falkow.** 2003. pH-regulated gene expression of the gastric pathogen *Helicobacter pylori*. *Infect Immun* **71**:3529-39.

111. Miles, S., M. B. Piazuelo, C. Semino-Mora, M. K. Washington, A. Dubois, R. M. Peek, Jr., P. Correa, and D. S. Merrell. 2010. Detailed *in vivo* analysis of the role of *Helicobacter pylori* Fur in colonization and disease. *Infect Immun* **78**:3073-82.
112. Mobley, H. L., M. J. Cortesia, L. E. Rosenthal, and B. D. Jones. 1988. Characterization of urease from *Campylobacter pylori*. *J Clin Microbiol* **26**:831-6.
113. Molinari, M., M. Salio, C. Galli, N. Norais, R. Rappuoli, A. Lanzavecchia, and C. Montecucco. 1998. Selective inhibition of Ii-dependent antigen presentation by *Helicobacter pylori* toxin VacA. *J Exp Med* **187**:135-40.
114. Nakagawa, S., K. Takai, F. Inagaki, H. Hirayama, T. Nunoura, K. Horikoshi, and Y. Sako. 2005. Distribution, phylogenetic diversity and physiological characteristics of epsilon-Proteobacteria in a deep-sea hydrothermal field. *Environ Microbiol* **7**:1619-32.
115. Nelson, K. E., C. Weinel, I. T. Paulsen, R. J. Dodson, H. Hilbert, V. A. Martins dos Santos, D. E. Fouts, S. R. Gill, M. Pop, M. Holmes, L. Brinkac, M. Beanan, R. T. DeBoy, S. Daugherty, J. Kolonay, R. Madupu, W. Nelson, O. White, J. Peterson, H. Khouri, I. Hance, P. Chris Lee, E. Holtzapple, D. Scanlan, K. Tran, A. Moazzez, T. Utterback, M. Rizzo, K. Lee, D. Kosack, D. Moestl, H. Wedler, J. Lauber, D. Stjepandic, J. Hoheisel, M. Straetz, S. Heim, C. Kiewitz, J. A. Eisen, K. N. Timmis, A. Dusterhoft, B. Tumbler, and C. M. Fraser. 2002. Complete genome

sequence and comparative analysis of the metabolically versatile *Pseudomonas putida* KT2440. Environ Microbiol **4**:799-808.

116. **Noto, J. M., J.A. Gaddy, J.Y. Lee, M.B. Piazuelo, D.B. Friedman, D.C. Colvin, J., Romer-Gallo, G. Suarez, J. Loh, J.C. Slaughter, S. Tan, D.R. Morgan, K.T.**

Wilson, L.E. Bravo, P. Correa, T.L. Cover, M.R. Amieva, and R.M. Peek Jr. 2013.

Iron deficiency accelerates *Helicobacter pylori*-induced carcinogenesis in rodents and humans. J Clin Invest **123**:1-14.

117. **Owen, R. J.** 1998. *Helicobacter*--species classification and identification. Br Med Bull **54**:17-30.

118. **Papini, E., B. Satin, N. Norais, M. de Bernard, J. L. Telford, R. Rappuoli, and C. Montecucco.** 1998. Selective increase of the permeability of polarized epithelial cell monolayers by *Helicobacter pylori* vacuolating toxin. J Clin Invest **102**:813-20.

119. **Parsonnet, J.** 1994. Gastric adenocarcinoma and *Helicobacter pylori* infection. West J Med **161**:60.

120. **Parsonnet, J., G. D. Friedman, D. P. Vandersteen, Y. Chang, J. H. Vogelman, N. Orentreich, and R. K. Sibley.** 1991. *Helicobacter pylori* infection and the risk of gastric carcinoma. N Engl J Med **325**:1127-31.

121. **Parsonnet, J., S. Hansen, L. Rodriguez, A. B. Gelb, R. A. Warnke, E. Jellum, N. Orentreich, J. H. Vogelman, and G. D. Friedman.** 1994. *Helicobacter pylori* infection and gastric lymphoma. *N Engl J Med* **330**:1267-71.
122. **Parsonnet, J., H. Shmueli, and T. Haggerty.** 1999. Fecal and oral shedding of *Helicobacter pylori* from healthy infected adults. *JAMA* **282**:2240-5.
123. **Perna, N. T., G. Plunkett, 3rd, V. Burland, B. Mau, J. D. Glasner, D. J. Rose, G. F. Mayhew, P. S. Evans, J. Gregor, H. A. Kirkpatrick, G. Posfai, J. Hackett, S. Klink, A. Boutin, Y. Shao, L. Miller, E. J. Grotbeck, N. W. Davis, A. Lim, E. T. Dimalanta, K. D. Potamouisis, J. Apodaca, T. S. Anantharaman, J. Lin, G. Yen, D. C. Schwartz, R. A. Welch, and F. R. Blattner.** 2001. Genome sequence of enterohaemorrhagic *Escherichia coli* O157:H7. *Nature* **409**:529-33.
124. **Petersen, L., T. S. Larsen, D. W. Ussery, S. L. On, and A. Krogh.** 2003. RpoD promoters in *Campylobacter jejuni* exhibit a strong periodic signal instead of a -35 box. *J Mol Biol* **326**:1361-72.
125. **Pflock, M., M. Bathon, J. Schar, S. Muller, H. Mollenkopf, T. F. Meyer, and D. Beier.** 2007. The orphan response regulator HP1021 of *Helicobacter pylori* regulates transcription of a gene cluster presumably involved in acetone metabolism. *J Bacteriol* **189**:2339-49.

126. **Pflock, M., P. Dietz, J. Schar, and D. Beier.** 2004. Genetic evidence for histidine kinase HP165 being an acid sensor of *Helicobacter pylori*. FEMS Microbiol Lett **234**:51-61.
127. **Pflock, M., N. Finsterer, B. Joseph, H. Mollenkopf, T. F. Meyer, and D. Beier.** 2006. Characterization of the ArsRS regulon of *Helicobacter pylori*, involved in acid adaptation. J Bacteriol **188**:3449-62.
128. **Pich, O. Q., B. M. Carpenter, J. J. Gilbreath, and D. S. Merrell.** 2012. Detailed analysis of *Helicobacter pylori* Fur-regulated promoters reveals a Fur box core sequence and novel Fur-regulated genes. Mol Microbiol **84**:921-41.
129. **Pohl, E., J. C. Haller, A. Mijovilovich, W. Meyer-Klaucke, E. Garman, and M. L. Vasil.** 2003. Architecture of a protein central to iron homeostasis: crystal structure and spectroscopic analysis of the ferric uptake regulator. Mol Microbiol **47**:903-15.
130. **Porollo, A., and J. Meller.** 2007. Versatile annotation and publication quality visualization of protein complexes using POLYVIEW-3D. BMC Bioinformatics **8**:316.
131. **Porollo, A. A., R. Adamczak, and J. Meller.** 2004. POLYVIEW: a flexible visualization tool for structural and functional annotations of proteins. Bioinformatics **20**:2460-2.

132. **Porter, M. L., and A. S. Engel.** 2008. Diversity of uncultured Epsilonproteobacteria from terrestrial sulfidic caves and springs. *Appl Environ Microbiol* **74**:4973-7.
133. **Pounder, R. E., and D. Ng.** 1995. The prevalence of *Helicobacter pylori* infection in difference countries. . *Aliment Pharmacol Ther* **9**:33-39.
134. **Qu, W., Y. Zhou, C. Shao, Y. Sun, Q. Zhang, C. Chen, and J. Jia.** 2009. *Helicobacter pylori* proteins response to nitric oxide stress. *J Microbiol* **47**:486-93.
135. **Rosenow, E. C., and A.H. Sandford.** 1915. The bacteriology of ulcer of the stomach and duodenum in man. *J Infect Dis* **17**:210-226.
136. **Sachs, G., D. L. Weeks, Y. Wen, E. A. Marcus, D. R. Scott, and K. Melchers.** 2005. Acid acclimation by *Helicobacter pylori*. *Physiology* **20**:429-38.
137. **Schloss, P. D., S. L. Westcott, T. Ryabin, J. R. Hall, M. Hartmann, E. B. Hollister, R. A. Lesniewski, B. B. Oakley, D. H. Parks, C. J. Robinson, J. W. Sahl, B. Stres, G. G. Thallinger, D. J. Van Horn, and C. F. Weber.** 2009. Introducing mothur: open-source, platform-independent, community-supported software for describing and comparing microbial communities. *Appl Environ Microbiol* **75**:7537-41.

138. Schwede, T., J. Kopp, N. Guex, and M. C. Peitsch. 2003. SWISS-MODEL: An automated protein homology-modeling server. *Nucleic Acids Res* **31**:3381-5.
139. Senkovich, O., S. Ceaser, D. J. McGee, and T. L. Testerman. 2010. Unique host iron utilization mechanisms of *Helicobacter pylori* revealed with iron-deficient chemically defined media. *Infect Immun* **78**:1841-9.
140. Senkovich, O. A., J. Yin, V. Ekshyyan, C. Conant, J. Traylor, P. Adegboyega, D. J. McGee, R. E. Rhoads, S. Slepnev, and T. L. Testerman. 2011. *Helicobacter pylori* AlpA and AlpB bind host laminin and influence gastric inflammation in gerbils. *Infect Immun* **79**:3106-16.
141. Sewald, X., B. Gebert-Vogl, S. Prassl, I. Barwig, E. Weiss, M. Fabbri, R. Osicka, M. Schiemann, D. H. Busch, M. Semmrich, B. Holzmann, P. Sebo, and R. Haas. 2008. Integrin subunit CD18 Is the T-lymphocyte receptor for the *Helicobacter pylori* vacuolating cytotoxin. *Cell Host Microbe* **3**:20-9.
142. Sharma, C. M., S. Hoffmann, F. Darfeuille, J. Reignier, S. Findeiss, A. Sittka, S. Chabas, K. Reiche, J. Hackermuller, R. Reinhardt, P. F. Stadler, and J. Vogel. 2010. The primary transcriptome of the major human pathogen *Helicobacter pylori*. *Nature* **464**:250-5.

143. **Sheikh, M. A., and G. L. Taylor.** 2009. Crystal structure of the *Vibrio cholerae* ferric uptake regulator (Fur) reveals insights into metal co-ordination. *Mol Microbiol* **72**:1208-20.
144. **Smith, M. G., T. A. Gianoulis, S. Pukatzki, J. J. Mekalanos, L. N. Ornston, M. Gerstein, and M. Snyder.** 2007. New insights into *Acinetobacter baumannii* pathogenesis revealed by high-density pyrosequencing and transposon mutagenesis. *Genes Dev* **21**:601-14.
145. **Sogin, M. L., H. G. Morrison, J. A. Huber, D. Mark Welch, S. M. Huse, P. R. Neal, J. M. Arrieta, and G. J. Herndl.** 2006. Microbial diversity in the deep sea and the underexplored "rare biosphere". *Proc Natl Acad Sci U S A* **103**:12115-20.
146. **Solnick, J. V., and P. Vandamme.** 2001. Taxonomy of the *Helicobacter* Genus.
147. **Sreerama, N., and R. W. Woody.** 2000. Estimation of protein secondary structure from circular dichroism spectra: comparison of CONTIN, SELCON, and CDSSTR methods with an expanded reference set. *Anal Biochem* **287**:252-60.
148. **Stojiljkovic, I., and K. Hantke.** 1995. Functional domains of the *Escherichia coli* ferric uptake regulator protein (Fur). *Mol Gen Genet* **247**:199-205.

149. **Stover, C. K., X. Q. Pham, A. L. Erwin, S. D. Mizoguchi, P. Warren, M. J. Hickey, F. S. Brinkman, W. O. Hufnagle, D. J. Kowalik, M. Lagrou, R. L. Garber, L. Goltry, E. Tolentino, S. Westbrook-Wadman, Y. Yuan, L. L. Brody, S. N. Coulter, K. R. Folger, A. Kas, K. Larbig, R. Lim, K. Smith, D. Spencer, G. K. Wong, Z. Wu, I. T. Paulsen, J. Reizer, M. H. Saier, R. E. Hancock, S. Lory, and M. V. Olson.** 2000. Complete genome sequence of *Pseudomonas aeruginosa* PAO1, an opportunistic pathogen. *Nature* **406**:959-64.
150. **Suerbaum, S., and C. Josenhans.** 2007. *Helicobacter pylori* evolution and phenotypic diversification in a changing host. *Nat Rev Microbiol* **5**:441-52.
151. **Swisher, S. C., and A. J. Barbati.** 2007. *Helicobacter pylori* strikes again: gastric mucosa-associated lymphoid tissue (MALT) lymphoma. *Gastroenterol Nurs* **30**:348-54; quiz 355-6.
152. **Talley, N. J., A. R. Zinsmeister, A. Weaver, E. P. DiMagno, H. A. Carpenter, G. I. Perez-Perez, and M. J. Blaser.** 1991. Gastric adenocarcinoma and *Helicobacter pylori* infection. *J Natl Cancer Inst* **83**:1734-9.
153. **Tan, S., J. M. Noto, J. Romero-Gallo, R. M. Peek, Jr., and M. R. Amieva.** 2011. *Helicobacter pylori* perturbs iron trafficking in the epithelium to grow on the cell surface. *PLoS Pathog* **7**:e1002050.

154. **Thomson, M. J., D. M. Pritchard, S. A. Boxall, A. A. Abuderman, J. M. Williams, A. Varro, and J. E. Crabtree.** 2012. Gastric *Helicobacter* Infection Induces Iron Deficiency in the INS-GAS Mouse. *PLoS One* **7**:e50194.
155. **Tomb, J. F., O. White, A. R. Kerlavage, R. A. Clayton, G. G. Sutton, R. D. Fleischmann, K. A. Ketchum, H. P. Klenk, S. Gill, B. A. Dougherty, K. Nelson, J. Quackenbush, L. Zhou, E. F. Kirkness, S. Peterson, B. Loftus, D. Richardson, R. Dodson, H. G. Khalak, A. Glodek, K. McKenney, L. M. Fitzgerald, N. Lee, M. D. Adams, E. K. Hickey, D. E. Berg, J. D. Gocayne, T. R. Utterback, J. D. Peterson, J. M. Kelley, M. D. Cotton, J. M. Weidman, C. Fujii, C. Bowman, L. Watthey, E. Wallin, W. S. Hayes, M. Borodovsky, P. D. Karp, H. O. Smith, C. M. Fraser, and J. C. Venter.** 1997. The complete genome sequence of the gastric pathogen *Helicobacter pylori*. *Nature* **388**:539-47.
156. **Tonello, F., W. G. Dundon, B. Satin, M. Molinari, G. Tognon, G. Grandi, G. Del Giudice, R. Rappuoli, and C. Montecucco.** 1999. The *Helicobacter pylori* neutrophil-activating protein is an iron-binding protein with dodecameric structure. *Mol Microbiol* **34**:238-46.
157. **Torres, V. J., S. E. VanCompernelle, M. S. Sundrud, D. Unutmaz, and T. L. Cover.** 2007. *Helicobacter pylori* vacuolating cytotoxin inhibits activation-induced proliferation of human T and B lymphocyte subsets. *J Immunol* **179**:5433-40.

158. **Valenzuela, M., J. P. Albar, A. Paradela, and H. Toledo.** 2011. *Helicobacter pylori* exhibits a fur-dependent acid tolerance response. *Helicobacter* **16**:189-99.
159. **Vallenet, D., P. Nordmann, V. Barbe, L. Poirel, S. Mangenot, E. Bataille, C. Dossat, S. Gas, A. Kreimeyer, P. Lenoble, S. Oztas, J. Poulain, B. Segurens, C. Robert, C. Abergel, J. M. Claverie, D. Raoult, C. Medigue, J. Weissenbach, and S. Cruveiller.** 2008. Comparative analysis of Acinetobacters: three genomes for three lifestyles. *PLoS One* **3**:e1805.
160. **van Vliet, A. H., F. D. Ernst, and J. G. Kusters.** 2004. NikR-mediated regulation of *Helicobacter pylori* acid adaptation. *Trends Microbiol* **12**:489-94.
161. **van Vliet, A. H., E. J. Kuipers, J. Stoof, S. W. Poppelaars, and J. G. Kusters.** 2004. Acid-responsive gene induction of ammonia-producing enzymes in *Helicobacter pylori* is mediated via a metal-responsive repressor cascade. *Infect Immun* **72**:766-73.
162. **van Vliet, A. H., J. Stoof, S. W. Poppelaars, S. Bereswill, G. Homuth, M. Kist, E. J. Kuipers, and J. G. Kusters.** 2003. Differential regulation of amidase- and formamidase-mediated ammonia production by the *Helicobacter pylori* Fur repressor. *J Biol Chem* **278**:9052-7.
163. **Velayudhan, J., N. J. Hughes, A. A. McColm, J. Bagshaw, C. L. Clayton, S. C. Andrews, and D. J. Kelly.** 2000. Iron acquisition and virulence in *Helicobacter*

pylori: a major role for FeoB, a high-affinity ferrous iron transporter. *Mol Microbiol* **37**:274-86.

164. **Viala, J., C. Chaput, I. G. Boneca, A. Cardona, S. E. Girardin, A. P. Moran, R. Athman, S. Memet, M. R. Huerre, A. J. Coyle, P. S. DiStefano, P. J. Sansonetti, A. Labigne, J. Bertin, D. J. Philpott, and R. L. Ferrero.** 2004. Nod1 responds to peptidoglycan delivered by the *Helicobacter pylori* *cag* pathogenicity island. *Nat Immunol* **5**:1166-74.

165. **Vitale, S., C. Fauquant, D. Lascoux, K. Schauer, C. Saint-Pierre, and I. Michaud-Soret.** 2009. A ZnS(4) structural zinc site in the *Helicobacter pylori* ferric uptake regulator. *Biochemistry* **48**:5582-91.

166. **Waidner, B., S. Greiner, S. Odenbreit, H. Kavermann, J. Velayudhan, F. Stahler, J. Guhl, E. Bisse, A. H. van Vliet, S. C. Andrews, J. G. Kusters, D. J. Kelly, R. Haas, M. Kist, and S. Bereswill.** 2002. Essential role of ferritin Pfr in *Helicobacter pylori* iron metabolism and gastric colonization. *Infect Immun* **70**:3923-9.

167. **Wang, G., Y. Hong, A. Olczak, S. E. Maier, and R. J. Maier.** 2006. Dual Roles of *Helicobacter pylori* NapA in inducing and combating oxidative stress. *Infect Immun* **74**:6839-46.

168. **Wang, G., L. F. Lo, and R. J. Maier.** 2012. A histone-like protein of *Helicobacter pylori* protects DNA from stress damage and aids host colonization. *DNA Repair* **11**:733-40.
169. **Warren, J. R.** 1983. Unidentified curved bacilli on gastric epithelium in active chronic gastritis. *Lancet* **i**:1273.
170. **Wen, Y., J. Feng, D. R. Scott, E. A. Marcus, and G. Sachs.** 2007. The HP0165-HP0166 two-component system (ArsRS) regulates acid-induced expression of HP1186 alpha-carbonic anhydrase in *Helicobacter pylori* by activating the pH-dependent promoter. *J Bacteriol* **189**:2426-34.
171. **Wen, Y., J. Feng, D. R. Scott, E. A. Marcus, and G. Sachs.** 2006. Involvement of the HP0165-HP0166 two-component system in expression of some acidic-pH-upregulated genes of *Helicobacter pylori*. *J Bacteriol* **188**:1750-61.
172. **Wen, Y., J. Feng, D. R. Scott, E. A. Marcus, and G. Sachs.** 2009. The pH-responsive regulon of HP0244 (FlgS), the cytoplasmic histidine kinase of *Helicobacter pylori*. *J Bacteriol* **191**:449-60.
173. **Wen, Y., E. A. Marcus, U. Matrubutham, M. A. Gleeson, D. R. Scott, and G. Sachs.** 2003. Acid-adaptive genes of *Helicobacter pylori*. *Infect Immun* **71**:5921-39.

174. **Wilderman, P. J., N. A. Sowa, D. J. FitzGerald, P. C. FitzGerald, S. Gottesman, U. A. Ochsner, and M. L. Vasil.** 2004. Identification of tandem duplicate regulatory small RNAs in *Pseudomonas aeruginosa* involved in iron homeostasis. Proc Natl Acad Sci U S A **101**:9792-7.
175. **Worst, D. J., B. R. Otto, and J. de Graaff.** 1995. Iron-repressible outer membrane proteins of *Helicobacter pylori* involved in heme uptake. Infect Immun **63**:4161-5.
176. **Wotherspoon, A. C., C. Ortiz-Hidalgo, M. R. Falzon, and P. G. Isaacson.** 1991. *Helicobacter pylori*-associated gastritis and primary B-cell gastric lymphoma. Lancet **338**:1175-6.
177. **Wunder, C., Y. Churin, F. Winau, D. Warnecke, M. Vieth, B. Lindner, U. Zahringer, H. J. Mollenkopf, E. Heinz, and T. F. Meyer.** 2006. Cholesterol glucosylation promotes immune evasion by *Helicobacter pylori*. Nat Med **12**:1030-8.
178. **Xiao, B., W. Li, G. Guo, B. Li, Z. Liu, K. Jia, Y. Guo, X. Mao, and Q. Zou.** 2009. Identification of small noncoding RNAs in *Helicobacter pylori* by a bioinformatics-based approach. Curr Microbiol **58**:258-63.

179. **Xiao, B., W. Li, G. Guo, B. S. Li, Z. Liu, B. Tang, X. H. Mao, and Q. M. Zou.** 2009. Screening and identification of natural antisense transcripts in *Helicobacter pylori* by a novel approach based on RNase I protection assay. *Mol Biol Rep* **36**:1853-8.
180. **Yanofsky, C., T. Platt, I. P. Crawford, B. P. Nichols, G. E. Christie, H. Horowitz, M. VanCleemput, and A. M. Wu.** 1981. The complete nucleotide sequence of the tryptophan operon of *Escherichia coli*. *Nucleic Acids Res* **9**:6647-68.
181. **Ye, F., T. Brauer, E. Niehus, K. Drlica, C. Josenhans, and S. Suerbaum.** 2007. Flagellar and global gene regulation in *Helicobacter pylori* modulated by changes in DNA supercoiling. *Int J Med Microbiol* **297**:65-81.
182. **Zheleznova, E. E., J. H. Crosa, and R. G. Brennan.** 2000. Characterization of the DNA- and metal-binding properties of *Vibrio anguillarum* fur reveals conservation of a structural Zn(2+) ion. *J Bacteriol* **182**:6264-7.
183. **Zheng, P. Y., and N. L. Jones.** 2003. *Helicobacter pylori* strains expressing the vacuolating cytotoxin interrupt phagosome maturation in macrophages by recruiting and retaining TACO (coronin 1) protein. *Cell Microbiol* **5**:25-40.

Appendix A

*Enterobacterial Common Antigen Mutants of Salmonella enterica serovar Typhimurium
Establish a Persistent Infection and Provide Protection Against Subsequent Lethal
Challenge*

Published as: **Gilbreath, J.J., Dodds, J.C., Rick, P.D., Soloski, M.J., Merrell, D.S.,
and Metcalf, E.S.** 2012. Enterobacterial Common Antigen Mutants of *Salmonella
enterica* serovar Typhimurium Establish a Persistent Infection and Provide Protection
Against Subsequent Lethal Challenge. *Infect Immun* **80**:441-450.

The work presented in this chapter is the sole work of J.J. Gilbreath with the following exceptions: M.J. Soloski and P.D. Rick created the *wecA* mutant strain. J.J. Dodds and E.S. Metcalf performed vaccine studies, and D.S. Merrell created the SL1344 *wecA* complementation plasmid.

Abstract

Infection with *Salmonella spp.* is a significant source of disease globally. A substantial proportion of these infections are caused by *Salmonella enterica* serovar Typhimurium (*S. Typhimurium*). Herein we characterize the role of the Enterobacterial common antigen (ECA), a surface glycolipid ubiquitous among enteric bacteria, in *S.*

Typhimurium pathogenesis. Construction of a defined mutation in the UDP- *N*-acetylglucosamine-1-phosphate transferase gene, *wecA*, in two clinically relevant strains of *S. Typhimurium*, TML and SL1344, resulted in strains that were unable to produce ECA. Loss of ECA did not affect gross cell surface ultrastructure, production of LPS, flagella, or motility. However, the *wecA* mutant strains were attenuated in both oral and intraperitoneal mouse models of infection ($p < 0.001$ for both routes of infection, Log-rank test), and virulence could be restored by complementation of the *wecA* gene *in trans*. Despite the avirulence of the ECA-deficient strains, the *wecA* mutant strains were able to persistently colonize systemic sites (spleen and liver) at moderate levels for up to 70 days post-infection. Moreover, immunization with the *wecA* mutant strains provided protection against a subsequent lethal oral or intraperitoneal challenge with wildtype *S. Typhimurium*. Thus, *wecA* mutant (ECA negative) strains of *Salmonella* may be useful as live-attenuated vaccine strains or as vehicles for heterologous antigen expression.

Introduction

Salmonella enterica are enteropathogens that display a broad range of host specificities and are a common cause of gastroenteritis worldwide (46, 48). In the United States alone, non-typhoidal *Salmonella* cause an estimated 1.4 million cases of salmonellosis annually (47-48), which results in up to 50 million dollars per year in medical expenses and work absences (9). More than 2,500 different serotypes of *Salmonella* have been implicated in diarrheal disease (4, 47, 58); however, the majority of enteric salmonellosis cases are caused by a small subset of these serotypes (15, 47, 58),

including *Salmonella enterica* serovar Typhimurium (*S. Typhimurium*). Infection with *S. Typhimurium* can result in a debilitating inflammatory diarrhea that is often accompanied by fever, malaise, vomiting, muscle aches, and abdominal cramps (46). *Salmonella* serotypes that cause diarrheal disease are ingested in contaminated food and water and colonize the small intestine during passage through the digestive tract. Entry into the host intestinal tissue is thought to occur preferentially via antigen sampling microfold (M) cells, although these pathogens can also invade enterocytes. (27). Prior to M cell entry, however, *Salmonella* must first survive/evade host defenses such as the low pH of the stomach, bile salts, and various other innate immune mechanisms (15). A subset of the molecules that permit survival of bacteria in these initial steps in pathogenesis are located on the bacterial cell surface. The expression of these bacterial surface components has also been associated with virulence. Multiple reports have demonstrated that *Salmonella* are less virulent in the absence of cell surface proteins such as OmpS, lipoproteins, and flagella (10, 12, 16, 33, 35, 54). Similarly, attenuation of virulence also occurs in the absence of bacterial surface polysaccharides such as LPS (19). Recently, these studies have been corroborated utilizing a screen for genes that contribute to the ability of *S. Typhimurium* to establish an infection; several of the genes identified are involved in cell surface polysaccharide biosynthesis (13). Moreover, the role of LPS in resistance to antimicrobial effector molecules, systemic disease, and induction of pro-inflammatory cytokines, has been well characterized (8, 18, 21, 24, 34, 53, 56). In contrast, the contribution of other major cell surface polysaccharides to *Salmonella* virulence has not been as clearly delineated.

The cell surface of Gram-negative enteric bacteria contains an additional glycolipid that is ubiquitous among members of the family *Enterobacteriaceae*, the phosphoglyceride-linked Enterobacterial common antigen (ECA_{PG}) (52). The carbohydrate component of ECA_{PG} is a heterotrimeric repeat, $\rightarrow 3$ -D-Fuc4NAc-(1 \rightarrow 4)- β -D-ManNAcA-(1 \rightarrow 4)- α -D-GlcNAc, where Fuc4NAc is 4-acetamido-4,6-dideoxy-D-galactose, MaNAcA is *N*-acetyl-D-mannosaminuronic acid, and GlcNAc is *N*-acetyl-D-glucosamine (17, 51). ECA polysaccharide chains are linked to diacylglycerol through phosphodiester linkage through the potentially reducing terminal GalNAc residue, and the phosphoglyceride anchors the molecules in the outer leaflet of the outer membrane (52). ECA_{PG} accounts for approximately 0.2% of the cellular dry weight of the bacterial cell (52). Two related forms (ECA_{LPS} and ECA_{CYC}) have also been described (17), but ECA_{LPS}, which is linked to the lipid A core region, is only present on a subset of enteric bacteria, and ECA_{CYC} is not surface-expressed (17, 52). The genes involved in ECA_{PG} biosynthesis are chromosomally-encoded in the *wec* gene cluster (also known as *rfe*) (31, 38, 52) and include *wecA-G*, as well as the *wzx*, *wzy*, *wzz* genes that are involved in the addition of the ECA polysaccharide chains to the lipid carrier and transfer of ECA_{PG} to the bacterial cell surface (6, 49). Although the structure and biochemical composition of ECA_{PG} has been well characterized, relatively few studies have investigated the biological function of this major cell surface glycolipid and a conclusive role for ECA_{PG} *in vivo* has yet to be elucidated.

Previous studies suggest that ECA_{PG} (ECA) may contribute to organic acid resistance in Shiga toxin-producing *Escherichia coli* O157:H7 (7). In addition, ECA may play a role in the virulence of *Yersinia enterocolitica* (64), and was shown to be linked to

pustule formation in *Haemophilus ducreyi* infections (5). In the context of *Salmonella*, several intriguing observations have been made: 1) Mayer and Schmidt (36) showed that *S. Typhimurium* ECA does not elicit endotoxin-like activity; 2) passive immunization with anti-ECA antibodies does not protect against salmonellosis (1); 3) ECA plays a role in the resistance of bacteria to host bile salts (40). Moreover, studies in the 1970's, using poorly defined mutations, reported that the virulence of ECA mutant strains of *S. Typhimurium* is attenuated in mice (61). Ramos-Morales, *et al.*, (49) described a role for two ECA specific loci (*wecA* and *wecD*) in bile resistance, as well as virulence. Most recently, a comprehensive study by Chaudhuri *et al.* (13), which identified *S. Typhimurium* genes required for infection of BALB/c mice, showed that among transposon mutations that were ranked by the severity of their attenuation, several genes within the ECA biosynthesis (*wec*) gene cluster, including *wecA*, *wecB*, *wecE*, *wecD*, and *wecC* were found to have high attenuation scores (13). Collectively, these data suggest that ECA may play a broad role in bacterial virulence, and taken together with the studies presented herein, suggest that ECA is important for *Salmonella* pathogenesis.

The results presented in this paper describe a thorough *in vitro* and *in vivo* characterization of ECA mutant strains (*wecA::Gm*) of *S. Typhimurium*. Our studies demonstrate that disruption of the *wecA* locus results in abrogation of ECA production and that the resulting strains are attenuated *in vivo*. Importantly, these *wecA* null strains are not cleared by the host but, establish a persistent infection. Moreover, the *wecA* mutants can protect against a subsequent lethal challenge in a well-established murine model of salmonellosis. Our results highlight the possibility of using ECA negative strains of *Salmonella* as live-attenuated vaccine strains. Furthermore, the capacity of the

ECA mutants to establish a persistent infection suggests the possibility of using ECA negative strains of *S. Typhimurium* as vehicles for heterologous antigen delivery.

Materials and Methods

Bacterial strains, plasmids, and growth conditions

Strains and plasmids used in this study are listed in Table 9. Bacterial stocks were maintained in LB broth + 40% glycerol at -80°C. Bacteria were routinely grown as indicated at 37°C in LB or Trypticase soy (Difco) broth (TSB) or on LB or Trypticase soy agar containing 12.5 µg/mL tetracycline and/or 20 µg/mL gentamicin (Gm) where applicable. Plasmids and PCR products were purified using Qiagen reagents. Growth kinetics were measured in either TSB or minimal N medium (41) supplemented with 0.1% casamino acids.

*Construction of *wecA::Gm* mutant strains*

S. Typhimurium ECA mutant strains (*wecA::Gm*) were constructed in both TML and SL1344 wildtype backgrounds. A 1.5 kb fragment containing the *wecA* gene was PCR amplified from genomic DNA from the wildtype TML strain using primers BRA (5'-TACCCGTAAAGAAGAGCTGCTCACC-3') and BR (5'-CAGCCATAAAGTACGAAACAACCC-3'). This product was cloned into pTOPO-TA to yield plasmid pTA-BRABR1. Insertion of the *wecA* gene was confirmed by restriction. *S. Typhimurium* ECA mutant strains (*wecA::Gm*) were constructed in both

Table 9. Bacterial Strains and plasmids used in this study

Strains and Plasmids		
Strain or Plasmid	Relevant Characteristics	Reference
Plasmids		
pTOPO-TA	Cloning vector	Invitrogen
pTA-BRABR1	pTOPO-TA:: <i>wecA</i>	This Study
pBR322	Cloning vector	Promega
pRL140	pBR322:: <i>wecA</i>	This Study
pUC-Gm	pUC::Gm	This Study
pRL144	pBR322:: <i>wecA</i> ::Gm	This Study
pMAK705 ^{ts}	Temperature sensitive vector; Cm ^R	This Study
pRL145	pMAK705 ^{ts} :: <i>wecA</i> :: Gm	This Study
pACYC184	Complementation vector; Tet ^R	55
pGEM-T Easy	Commercial cloning vector; Amp ^R	Promega
pDSM643	pGEM-T Easy:: <i>wecA</i> ; Amp ^R	This Study
pDSM647	pACYC184:: <i>wecA</i> ; Tet ^R	This Study
<i>E. coli</i> Strains		
Top10	Cloning strain	Laboratory Strain
DH5 α	Cloning Strain	Laboratory Strain
Top10F'	Cloning Strain; F+	Laboratory Strain
PR4131	<i>E. coli</i> DH5 α (pRL140)	This Study
PR4135	<i>E. coli</i> DH5 α (pRL144)	This Study
PR4136	<i>E. coli</i> Top10F' (pRL145)	This Study
<i>S. enterica</i> Strains		
DSM644	Wildtype <i>S. Typhimurium</i> TML	22
DSM645	TML Δ <i>wecA</i> ; Gent ^R	This Study
DSM649	TML Δ <i>wecA</i> (pDSM647) Gent ^R , Tet ^R	This Study
DSM753	Wildtype <i>S. Typhimurium</i> SL1344	62
DSM754	SL1344 Δ <i>wecA</i> ; Gent ^R	This Study
DSM732	SL1344 Δ <i>wecA</i> (pDSM647) Gent ^R , Tet ^R	This Study

TML and SL1344 wildtype backgrounds. A 1.5 kb fragment containing the *wecA* gene was PCR amplified from genomic DNA from the wildtype TML strain using primers BRA (5'-TACCCGTAAAGAAGAGCTGCTCACC-3') and BR (5'-CAGCCCATAAAGTACGAAACAACCC-3'). This product was cloned into pTOPO-TA to yield plasmid pTA-BRABR1. Insertion of the *wecA* gene was confirmed by restriction digestion and sequencing. The 1.5 kb fragment containing the *wecA* gene was liberated from pTA-BRABR1 by EcoRI digestion, and subsequently cloned into the EcoRI site of pBR322 to yield plasmid pRL140. A 800 bp gentamicin (Gm) resistance cassette was liberated from plasmid pUC-GM using XbaI, and then cloned into an SpeI site within the coding region of the *wecA* gene contained within pRL140 to create pRL144 (*wecA*::Gm). A 3.07 kb fragment containing the *wecA*::Gm cassette was then digested from pRL144 using PstI and ClaI and subsequently cloned into the PstI and ClaI sites in pMAK705^{ts} to create plasmid pRL145. pRL145 was electroporated into TML and SL1344 and transformants were selected on LB containing Gm at 30°C. Single colony Gm^R transformants were sub-cultured in Gm and incubated overnight at 44°C to promote plasmid loss; growth would only occur if the *wecA*::Gm cassette had recombined into the bacterial chromosome. Gentamicin-resistant strains were passaged multiple times at 44°C to ensure complete loss of the vector pMAK705^{ts} ::*wecA*::Gm. Gm^R/ Cm^S colonies were then selected and screened by PCR to confirm mutation of *wecA*. To ensure that insertion of the gentamicin resistance cassette into *wecA* did not abrogate expression of the downstream gene (*wzzE*), we performed semi-quantitative reverse transcription PCR for both TML and SL1344 wildtype and *wecA* mutant strains. Expression of *wzzE* in the *wecA* mutant strains was similar to that of the respective wildtype strains digestion and

sequencing. The 1.5 kb fragment containing the *wecA* gene was liberated from pTA-BRABR1 by EcoRI digestion, and subsequently cloned into the EcoRI site of pBR322 to yield plasmid pRL140. A 800 bp gentamicin (Gm) resistance cassette was liberated from plasmid pUC-GM using XbaI, and then cloned into an SpeI site within the coding region of the *wecA* gene contained within pRL140 to create pRL144 (*wecA*::Gm). A 3.07 kb fragment containing the *wecA*::Gm cassette was then digested from pRL144 using PstI and ClaI and subsequently cloned into the PstI and ClaI sites in pMAK705^{ts} to create plasmid pRL145. pRL145 was electroporated into TML and SL1344 and transformants were selected on LB containing Gm at 30°C. Single colony Gm^R transformants were sub-cultured in Gm and incubated overnight at 44°C to promote plasmid loss; growth would only occur if the *wecA*::Gm cassette had recombined into the bacterial chromosome. Gentamicin-resistant strains were passaged multiple times at 44°C to ensure complete loss of the vector pMAK705^{ts}::*wecA*::Gm. Gm^R/ Cm^S colonies were then selected and screened by PCR to confirm mutation of *wecA*. To ensure that insertion of the gentamicin resistance cassette into *wecA* did not abrogate expression of the downstream gene (*wzzE*), we performed semi-quantitative reverse transcription PCR for both TML and SL1344 wildtype and *wecA* mutant strains. Expression of *wzzE* in the *wecA* mutant strains was similar to that of the respective wildtype strains (data not shown). Mutant strains were further characterized as described below.

*Complementation of the *wecA* mutation*

The *wecA* gene and promoter from the wildtype strain TML was PCR amplified using high fidelity Phusion enzyme (Finnzymes, Espoo, Finland) and primers

WecAF1(5'-gcggccgcCCTGACTATCATCGCGACGGC-3') and WecAR1 (5'-ccggcgCATTTTCAGCGCTCACCGCGCG-3'), which incorporate a NotI and SacII site, respectively (restriction enzyme recognition sites denoted by lower case letters). The 1715 base pair product was gel purified, 3'-A overhangs were added, and the full-length fragment was sub-cloned into pGemT-Easy (Promega, Madison, WI) to create plasmid pDSM643. The correct insert size was confirmed by EcoRI digestion, and the digested product was subsequently cloned into the EcoRI site of pACYC184 (55) to create plasmid pDSM647. The complementation plasmid pDSM647 was transformed into *wecA* null strains DSM645 and DSM754 in order to create strains DSM649 and DSM732, respectively. Transformants were selected on 12.5 µg/mL tetracycline and complementation of ECA production was verified as described below.

In vitro characterization of wecA::Gm and wecA complementation strains

Serotyping of wildtype and *wecA* mutant strains was performed with *Salmonella* strain-specific O:4 and O:9 antisera (Difco Laboratories, BD Systems, Sparks, MD) according to the manufacturer's instructions. ECA phenotypes were characterized by passive hemagglutination and immunoblotting. Passive hemagglutination was conducted using a 1:320 dilution of anti-ECA antibody as previously described (50). ECA immunoblotting and LPS/O-antigen silver staining were conducted as follows: whole cell lysates were prepared as previously described (26). Briefly, 2 OD units/mL of overnight culture were pelleted, resuspended in 200 µL of lysis buffer (0.065 M Tris-HCl [pH 6.8], 2% [wt/vol] SDS 5% [vol/vol] β-mercaptoethanol, 10% [vol/vol] glycerol, 0.05% [wt/vol] bromophenol blue), and incubated at 95°C for 15 minutes. Lysates were

cooled to room temperature and treated with 20 μ g proteinase-K (Ambion) at 60°C for 1 hour. Equal volumes of each lysate were subjected to 12% SDS-PAGE using a 4% stacking layer and subsequently stained using the method of Tsai and Frasch (60). For preparation of immunoblots, non-proteinase K treated lysates were prepared as described above and transferred at a constant current of 200 mA for 3 hr using a semi-dry transfer apparatus (Thermo Scientific, Rochester, NY). Membranes were probed with a 1:10,000 dilution of murine anti-ECA monoclonal antibody 898 (1, 26). ECA glycoconjugates were detected using a 1:20,000 dilution of goat anti-mouse IgG conjugated to horseradish peroxidase (Santa Cruz Biotechnology, Santa Cruz, CA). Blots were developed using the SuperSignal West Pico chemiluminescent substrate kit (Thermo Scientific/Pierce) and imaged using a LAS-3000 Intelligent Dark Box with LAS-3000 Lite capture software (Fujifilm, Stamford, CT).

Electron microscopy

Transmission electron microscopy was performed at the Biomedical Instrumentation Center (BIC) of the Uniformed Services University of the Health Sciences. Overnight stationary phase cultures were harvested by centrifugation, fixed with 2% EM grade glutaraldehyde fixation solution, and examined using a Phillips CM100 Electron Microscope without staining.

Motility assays

Swimming and swarming motility assays were performed as previously described (11, 59). Briefly, LB plates containing 0.25% (swimming motility) or 0.5% (swarming

motility) agar were inoculated with a single colony of each strain as indicated. For swimming motility assays, strains were inoculated in the center of each plate and incubated overnight at room temperature. To analyze swarming motility, the LB-based plates contained 0.5% glucose and each strain was inoculated in the center of each plate and incubated overnight at 37°C.

In vivo characterization experiments

Animal experiments were approved by the USUHS Animal Care and Use Committee and were performed in accordance with guidelines set forth by the National Institutes of Health (NIH). *S. Typhimurium* strains were cultured overnight at 37°C in TSB with shaking at 225 RPM. Overnight cultures were diluted ~1:100 and grown to exponential phase (~0.6 optical density at 600 nm). Bacterial cultures were harvested by centrifugation, standardized to a density of 0.6 OD units/mL in isotonic saline, and subsequently diluted to the appropriate dosage as indicated in the text. Doses of bacterial suspensions were administered in isotonic saline at a volume of 0.2 mL for oral gavage or at a volume of 0.5 mL for intraperitoneal (i.p.) injection. Serial dilutions of each inoculum were plated to confirm the dose. Female C57BL/6J mice (Jackson Labs, Bar Harbor, ME) were used for all experiments. For oral infections only, animals were fasted for 4 hours prior to inoculation and for 1 hour post-inoculation. Animals were monitored daily for mortality and onset of end-stage disease symptoms.

Bacterial load at systemic sites

To assess the bacterial load at systemic sites, mice were inoculated with 1×10^4 wildtype or *wecA* null strains as indicated. Spleen and liver tissues were harvested at days 3, 5, 7, 10, 14, 21, 28, 35, 45, 48, 56, 63 and 70 post-infection. Each tissue was homogenized and an aliquot was serially diluted and plated to determine bacterial counts.

*In vivo attenuation and complementation of the *wecA* mutation*

Mice were inoculated with TML wildtype, *wecA* mutant, or *wecA* complemented strains (DSM644, DSM645, and DSM649, respectively) at doses of 1×10^5 , 1×10^6 , or 1×10^7 CFU by oral gavage. I.p. infections were performed using 1×10^2 CFU of each bacterial strain as indicated. Animals were monitored daily for mortality and onset of end-stage disease symptoms. Where indicated, mean time to death (MTD) was calculated as follows: $MTD = \frac{\text{sum of all X values}}{\text{total number of mice dead}}$, where X is the days post-infection multiplied by the number of mice that died that day.

Immunization and lethal challenge studies

Immunizations with *wecA* mutant strains were administered by oral gavage or i.p. injection and were given either 30 or 60 days prior to lethal challenge as detailed in the text for each experiment. Vaccination doses were as indicated in the text for each individual experiment. The post-vaccination oral and i.p. lethal challenges were performed as described above.

Statistical analyses

Statistical analyses for colonization experiments were performed using a two-tailed Student's T-test. Statistical significance of differences in percent survival for oral and i.p. infection experiments was determined using the Kaplan-Meier method and a Log-rank test as indicated in the text.

Results

In vitro characterization of S. Typhimurium wecA mutant strains

Previous studies implicated ECA as a virulence factor of *S. Typhimurium* and indicated that *wecA* mutants are attenuated *in vivo* (40, 51). However, the mutant strains used in those studies were poorly defined (51) or the *in vivo* experiments with those strains were conducted only in competition with the wildtype strain (49). Furthermore, complementation of the mutant strains was not attempted in any of these studies. Thus, the observed mutant phenotypes could not be conclusively linked solely to the absence of ECA expression. Therefore, to clearly delineate the role of ECA as a virulence factor, we analyzed well-defined ECA mutants in a series of *in vitro* and *in vivo* studies. We created isogenic *wecA* mutant strains in two clinically relevant *S. Typhimurium* strain backgrounds, TML (DSM644) (22) and SL1344 (DSM753) (62) as described above. The *wecA* gene encodes a UDP- *N*-acetylglucosamine-1-phosphate transferase and is the first gene in a gene cluster that also encodes the downstream enzymatic components of the ECA biosynthetic pathway. Since *WecA* catalyzes the first step in ECA biosynthesis, we created a non-polar mutation in this gene to eliminate the possibility of changes in the

bacterial cell due to the build-up of ECA intermediates. Deletion of the *wecA* gene resulted in an ECA negative phenotype, as determined by passive hemagglutination (Table 10) and immunoblotting (data not shown). Because components of the ECA biosynthetic pathway are also known to be involved in LPS synthesis in some bacteria (52, 64), and because LPS is important for *Salmonella* colonization (32, 42), we wanted to ensure that non-ECA cell surface polysaccharides were unaltered in our *wecA* mutant strains. To this end, DSM645 (TML *wecA*::Gm) and DSM754 (SL1344 *wecA*::Gm) were serotyped using *S. Typhimurium* O:4 antisera to ensure that our *S. Typhimurium* strains retained expression of the wildtype O:4 antigen (Table 10). In addition, the LPS/O-antigen profile of the *wecA* mutant and wildtype strains was evaluated by silver staining. As depicted in Figure 20A, the *wecA* mutant strains (DSM645 and DSM754) retained LPS profiles indistinguishable from the respective parental wildtype strains. Furthermore, analysis of cell surface structure by transmission electron microscopy revealed no gross abnormalities in the *wecA* mutant strains (Figure 23 (S1)).

To ensure that the ECA negative phenotype of DSM645 and DSM754 was due to mutation of the *wecA* gene, *wecA* complementation strains were constructed as described in the Materials and Methods. Functional complementation of the ECA negative phenotype was observed in both DSM649 (TML *wecA*::Gm + pACYC184::*wecA*) and DSM732 (SL1344 *wecA*::Gm + pACYC184::*wecA*) both by passive hemagglutination (Table 10) and immunoblotting (data not shown). *In vitro* growth of the *wecA* mutant and complementation strains was comparable to the parental wildtype strains (Figures 20B and 20C), with the exception of a slight but reproducible difference in growth of the TML wildtype and mutant strains in rich media; however, the growth kinetics were more

Table 10. Serotyping and ECA Passive Hemagglutination (PHA)

Strain	Genotype	ECA	PHA	Serotyping	
				O:4	O:9
Saline Control		N/A	-	-	-
DSM644	WT	+	+	+	-
TML DSM645	<i>wecA</i> ::Gm	-	-	+	-
DSM649	<i>wecA</i> ::Gm Complemented	+	+	NT	NT
DSM753	WT	+	+	+	-
SL1344 DSM754	<i>wecA</i> ::Gm	-	-	+	-
DSM732	<i>wecA</i> ::Gm Complemented	+	+	NT	NT

NT, not tested; N/A, not applicable

+ indicates hemagglutination; - indicates no hemagglutination

*Figure 20. In vitro characterization of *wecA* mutant and complementation strains of Salmonella serovar Typhimurium. (A) LPS/O-antigen profile of TML wildtype (DSM644), TML *wecA* mutant (DSM645), SL1344 wildtype (DSM753) and SL1344 *wecA* mutant (DSM754) strains. Silver staining was performed as described in Materials and Methods. (B & C) Growth kinetics of TML wildtype (DSM644), TML *wecA* mutant (DSM645) and TML *wecA* complementation (DSM649) strains, and growth kinetics of SL1344 wildtype (DSM753), SL1344 *wecA* mutant (DSM754) and SL1344 *wecA* complementation (DSM732) strains in TSB (panel B) and N minimal media (panel C). Overnight cultures were diluted to an optical density of ~0.1 and incubated at 37°C with shaking. Growth was monitored by absorbance at 600 nm. Data points shown are the average of 2-3 independent experiments and the error bars represent the standard error of the mean.*

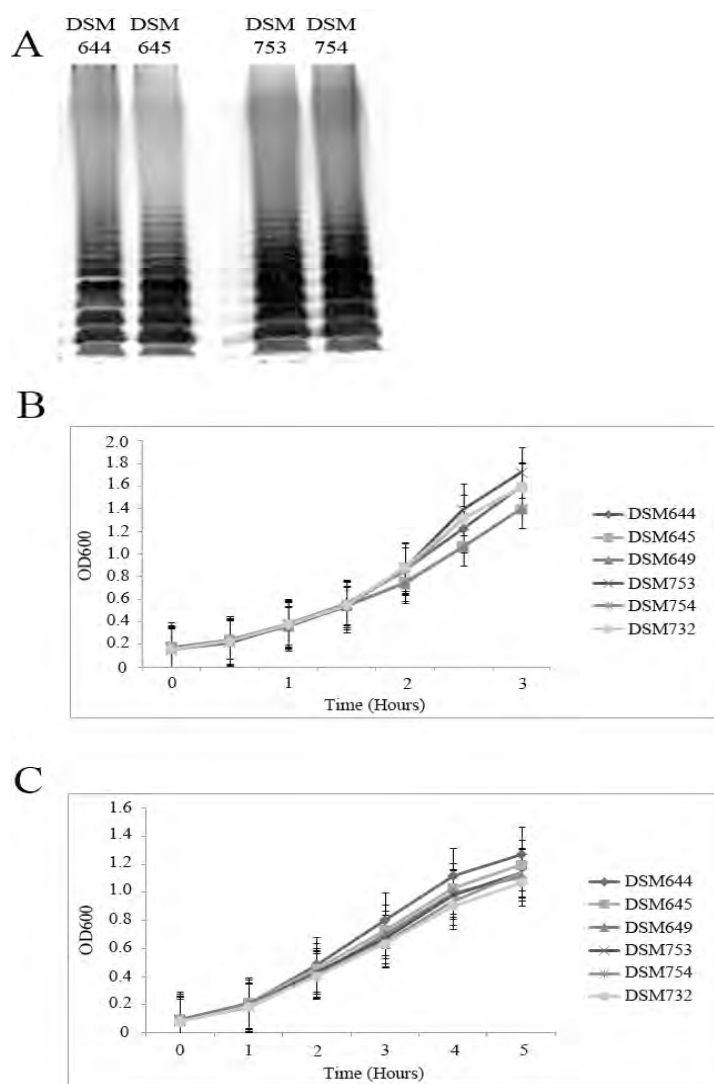


Figure 20. In vitro characterization of wecA mutant and complementation strains of Salmonella serovar Typhimurium

similar in minimal media, which may more accurately represent *in vivo* growth conditions.

Recently, ECA biosynthesis was shown to be a checkpoint for flagellar biosynthesis in another enteric bacterium, *Serratia marcescens* (11). Since previous studies have shown a link between the presence of flagella and virulence in *S. Typhimurium* (10), we sought to determine whether ECA expression was linked to *S. Typhimurium* flagellar biosynthesis. To this end, we determined whether the *S. Typhimurium* *wecA* mutant strains displayed any defects in production of flagella or motility. As shown in Figure 23(S1), the *wecA* mutant strains (DSM645 and DSM754) appear to retain normal numbers and localization of flagella. Furthermore, the *wecA* mutant strains appear to retain wildtype levels of swimming motility (Figure 24(S2)). Similarly, the mutant and complementation strains retained the ability to swarm (Figure 24 (S2)), although in some replicates of the assay, the swarming speeds of the mutant strains appeared slightly slower than the parental wildtype strains when assessed at early timepoints (data not shown). However, after 24 hours of growth the mutant strains were able to swarm to the edge of the plate as well as the wildtype strains. Collectively, our *in vitro* data suggest that the *wecA* null strains are both genetically and functionally isogenic with their respective parental wildtype strains, except for the absence of ECA.

wecA mutant strains are attenuated in vivo

While previous reports implied that ECA may play a role in *S. Typhimurium* virulence (49, 61), those studies utilized poorly-defined mutants, competitive indices, or short-term infection studies. Although those reports were suggestive, we wished to

definitively establish an *in vivo* role for ECA using the more robust single strain model of infection. To this end, we inoculated five C57BL/6 mice per group with 1×10^5 , 1×10^6 , or 1×10^7 CFU of the TML wildtype (DSM644) or *wecA* mutant strain (DSM645) by oral gavage. As depicted in Figure 21A, all 15 of the mice infected with the wildtype TML strain (DSM644) succumbed to infection by day 10, with a mean time to death (MTD) of 7.1 days. The MTD for animals infected with 1×10^5 , 1×10^6 , and 1×10^7 CFU was 7.4, 7.4, and 6.4 days, respectively (Figure 25(S3)). These data are similar to those shown previously with the same strain of *S. Typhimurium* and the same strain of mice (43). In contrast, only 2 of the 15 mice infected with the *wecA* mutant strain DSM645 succumbed to infection (~87% survival) with a MTD of 27.5 days (1 animal infected with 1×10^6 CFU died on day 28 and 1 animal infected with 1×10^7 CFU died on day 27, Figure 25(S3)). This difference in percent survival was highly significant ($p < 0.001$, Log-rank test). In addition, complementation of the *wecA* mutation *in trans* partially restored virulence; 20% of the mice infected with the *wecA* complementation strain (DSM649) survived for the duration of the experiment with a MTD of 13.6 days (Figure 21A). The MTD for animals infected with 1×10^5 , 1×10^6 , and 1×10^7 CFU of DSM649 was 11.5, 18.6, and 12.2 days, respectively. The difference in % survival between the *wecA* mutant and *wecA* complementation strain was also significant ($p < 0.001$, Log-rank test). In addition, the difference in % survival between the wildtype and complemented strains was also significant ($p < 0.001$, Log-rank test), which highlights the fact that only partial complementation was achieved.

We next tested the virulence of the *wecA* mutant strain (DSM645) in the murine single-strain i.p. infection model. C57BL/6 mice were inoculated with 1×10^2 CFU of

*Figure 21. Attenuation and complementation of the TML *wecA* mutant strain. (A)* Groups of 5 C57BL/6 mice were orally inoculated with 10^5 , 10^6 , or 10^7 CFU of the TML wildtype (DSM644), TML *wecA* mutant (DSM645), or TML *wecA* complementation strain (DSM649). Percent survival data for each strain represent combined data from all inoculation doses tested; **(B)** Groups of 8-10 C57BL/6 mice were intraperitoneally inoculated with 10^2 CFU of the TML wildtype (DSM644), TML *wecA* mutant (DSM645), or TML *wecA* complementation strain (DSM649). Percent survival data for each strain represent combined data from two biologically independent experiments. Differences in percent survival between wildtype and *wecA* mutant strains, and *wecA* mutant and complementation strains are statistically significant ($p < 0.0001$, Log-rank test) for both (A) and (B). Percent survival for each of the individual doses are shown in Figure 25(S3).

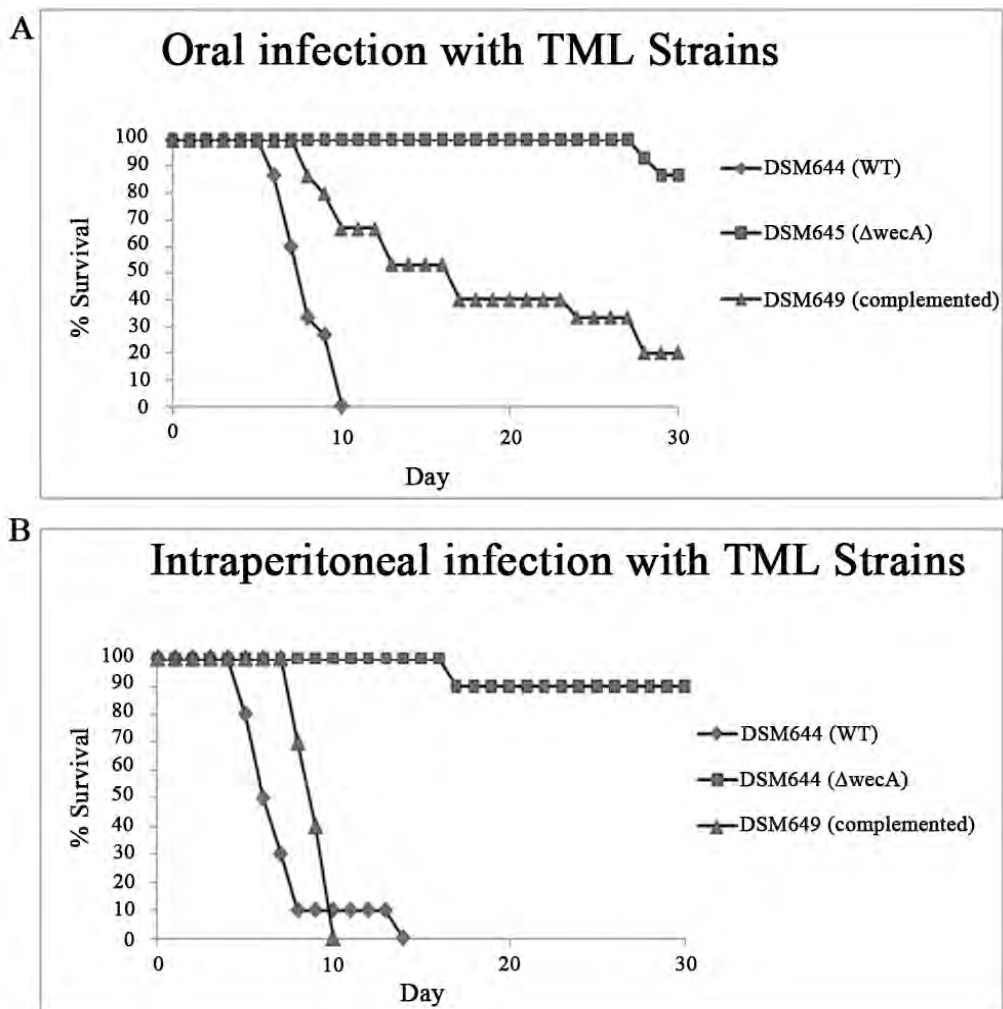


Figure 21. Attenuation and complementation of the TML *wecA* mutant strain

either the wildtype DSM644 or the *wecA* mutant strain DSM645 (Figure 21B). Whereas all of the mice infected with the wildtype strain succumbed to infection (MTD of 5.4 days), only 1 mouse infected with the *wecA* mutant strain died at day 16 post-infection (90% survival). These results were similar to those in the oral infection experiments, where the differences in percent survival were highly significant ($p < 0.001$, Log-rank test). Once again, complementation of *wecA in trans* restored virulence; all mice infected with DSM649 succumbed to infection (MTD of 7.3 days). The difference in survival between the *wecA* mutant and complemented strain was significant ($p < 0.001$, Log-rank test). Similar to the oral infection experiments, the difference in percent survival between the wildtype and complemented strains was also significant ($p = 0.008$, Log-rank test), indicating partial complementation. Collectively, these data indicate that the *wecA* mutant strain is significantly attenuated in both the oral and i.p. single-strain infection models and that the attenuation of virulence is due to the loss of ECA expression since virulence could be at least partially restored upon complementation of the *wecA* mutation.

wecA mutant strains establish a persistent infection

A key component of *Salmonella* virulence is the ability to establish colonization and persist within the host (15, 23, 45). Given the dramatic changes in lethality we observed with the ECA mutant strain, we next sought to determine whether the *wecA* mutant strain retained the ability to efficiently disseminate and colonize within the host. Groups of mice received 1×10^4 TML wildtype (DSM644) or *wecA* mutant (DSM645) strains by oral gavage and were sacrificed at 3-5 day intervals post-infection (Figure 22). The spleen and liver were harvested from each mouse and aliquots of homogenized tissue

were serially diluted and plated to determine bacterial counts. Mice infected with the wildtype TML (DSM644) bacteria succumbed to infection within 10 days post-infection. In contrast, mice infected with the *wecA* mutant strain (DSM645) survived until the experiment was terminated at day 70 post-infection. Moreover, bacterial counts from mice infected with the wildtype bacteria (DSM644) rapidly increased until host death, whereas mice infected with the *wecA* mutant strain (DSM645) displayed a moderate level of persistent infection throughout the duration of the experiment (Figure 22). This persistent infection was accompanied by splenomegally and hepatomegally (data not shown) that often typifies persistent *S. Typhimurium* colonization (40). These data demonstrate that the *wecA* mutant strain of *S. Typhimurium* is able to efficiently colonize mice and establish a persistent infection.

Oral immunization protects against a subsequent oral challenge

Since the virulence of the *wecA* mutant strain was significantly attenuated but the strain was still able to establish a persistent infection, we next sought to determine whether immunization /vaccination with the mutant strains could induce a protective immune response. To this end, mice were orally immunized with 1×10^2 , 1×10^3 , 1×10^4 , 1×10^5 , 1×10^6 , or 1×10^7 CFU of the TML *wecA* mutant strain DSM645. On day 30 post-immunization, the mice were challenged orally with 1×10^3 CFU of the wildtype TML strain DSM644 (Table 11). Of the 78 total mice vaccinated, 66 survived until the day of challenge; of the 66 mice that were challenged with wildtype *S. Typhimurium*, 41 mice (62.1%) were protected for the duration of the experiment (30 days).

Figure 22. Bacterial load in systemic sites of infection

C57BL/6 mice were orally inoculated with 10^4 CFU of the TML wildtype (DSM644) or TML *wecA* mutant (DSM645). Groups of 7-8 mice were sacrificed on days 3, 5, 7, 10, 14, 21, 28, 35, 45, 48, 56, 63, and 70 post infection; Bacterial counts from liver (black symbols) and spleen (gray symbols) were determined by plating serially diluted tissue homogenates, and are shown as the geometric mean \log_{10} CFU per organ. A Student's T-test was used to compare colonization levels of TML wildtype and TML *wecA* mutant strains for each tissue site. * indicates $p < 0.05$ and ** indicates that there were not enough animals remaining to do statistical tests for this time point.

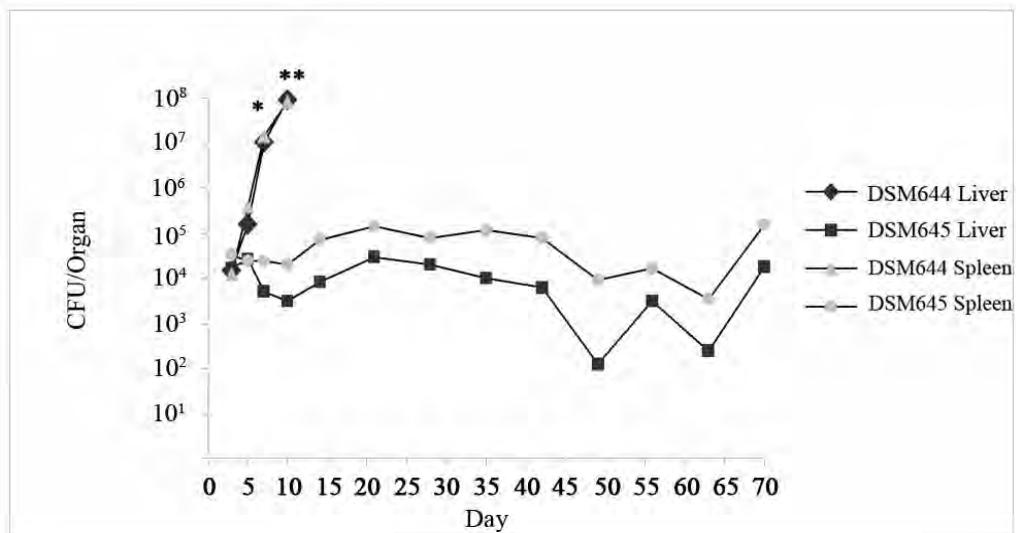


Figure 22. Bacterial load in systemic sites of infection

Table 11. Oral immunization with ECA mutants and subsequent oral challenge at Day 30 with wildtype *S. Typhimurium* strains

Controls								
	Saline	NA	7/7*	DSM644	1.0 X 10 ³	0/7*	0	
	Saline	NA	4/4	DSM644	1.7 X 10 ⁵	0/4	0	
	Saline	NA	4/4	DSM644	1.7 X 10 ⁶	0/4	0	
Immunization				Challenge				
	Strain	Dose	Survived/Total	Strain	Dose	Survived/Total	% Survival	
TML	DSM645	1.0 X 10 ²	3/3	DSM644	1.0 X 10 ³	3/3	100	
	DSM645	1.0 X 10 ³	14/15*	DSM644	1.0 X 10 ³	7/14*	50	
	DSM645	1.0 X 10 ⁴	13/15*	DSM644	1.0 X 10 ³	9/13*	69.2	
	DSM645	1.0 X 10 ⁵	14/15*	DSM644	1.0 X 10 ³	8/14*	57.1	
	DSM645	1.0 X 10 ⁶	11/15*	DSM644	1.0 X 10 ³	7/11*	63.6	
	DSM645	1.0 X 10 ⁷	11/15*	DSM644	1.0 X 10 ³	7/11*	63.6	
		Total:		66/78			41/66	62.1
SL1344	DSM754	1.3 X 10 ⁴	8/8	DSM753	1.7 X 10 ⁵	4/8	50	
	DSM754	1.3 X 10 ⁴	8/8	DSM753	1.7 X 10 ⁶	5/8	62.5	
	DSM754	1.3 X 10 ⁵	7/7	DSM753	1.7 X 10 ⁵	4/7	57.1	
	DSM754	1.3 X 10 ⁵	8/8	DSM753	1.7 X 10 ⁶	6/8	75	
	DSM754	1.3 X 10 ⁶	10/10	DSM753	1.7 X 10 ⁵	6/10	60	
	DSM754	1.3 X 10 ⁶	10/10	DSM753	1.7 X 10 ⁶	6/10	60	
		Total:		51/51			31/51	60.7
Combined Total:			117/129				72/117	61.5

*indicates combined results from 2 independent experiments

DSM644, TML wildtype; DSM645, TML *wecA* mutant; DSM753, SL1344 wildtype; DSM754, SL1344 *wecA* mutant

To ensure that the capacity of the *wecA* mutant strain to protect mice against a subsequent lethal challenge with wildtype bacteria was not *S. Typhimurium* strain-dependent, we conducted a similar experiment with the *S. Typhimurium* wildtype strain SL1344. Mice were orally immunized with 1×10^4 , 1×10^5 , or 1×10^6 CFU of the SL1344 *wecA* mutant strain DSM754; 30 days post-immunization, groups of vaccinated mice were challenged orally with 1×10^5 or 1×10^6 CFU of the SL1344 wildtype strain DSM753. As shown in Table 11, all 51 mice immunized with the SL1344 *wecA* mutant strain survived until the day of challenge. Moreover, 31 of the 51 challenged mice were fully protected against subsequent lethal challenge; the percent survival was similar across all dosage regimens. Although a higher percentage of mice vaccinated with the SL1344 mutant strain survived until the day of challenge, the degree of protection was similar to groups immunized with the TML *wecA* mutant: 62.1% versus 60.7%.

Since the potential to use the *wecA* mutants as live vaccines or vehicles for heterologous antigen delivery would be enhanced if the bacteria persisted in the host for longer than 30 days, we next considered whether the immunity induced by the *wecA* mutant strain would provide protection for longer periods of time. To address this question, BL/6 mice were orally immunized with 1×10^2 , 1×10^3 , 1×10^4 , 1×10^5 , 1×10^6 , or 1×10^7 CFU of the TML *wecA* mutant strain DSM645 on day 0. On day 45 post-immunization the mice were orally challenged with 1×10^4 CFU of the wildtype TML strain DSM644 (Table 12). Twenty-four of the 30 immunized mice (80%) survived until the day of challenge. Of the 24 mice challenged on day 45, 12 survived (50%); the highest degree of protection was seen in the mice immunized with 1×10^6 or 1×10^7 CFU (100%). Taken together, these data indicate that oral immunization with a *wecA* mutant

Table 12. Oral Immunization with ECA negative and subsequent oral challenge at Day 45 with wildtype TML strains

		Controls		
Immunization		Challenge		
Dose	Survived/Total	Dose	Survived/Total	% Survival
Saline	5/5	1.0×10^4	0/5	0
1.0×10^2	4/5	1.0×10^4	0/4	0
1.0×10^3	5/5	1.0×10^4	1/5	20
1.0×10^4	5/5	1.0×10^4	3/5	60
1.0×10^5	3/5	1.0×10^4	1/3	33
1.0×10^6	4/5	1.0×10^4	4/4	100
1.0×10^7	3/5	1.0×10^4	3/3	100
Total:	24/30	Total:	12/24	50

strain of *S. Typhimurium* can induce a protective immune response and that protection may last for at least 45 days post-immunization.

Intraperitoneal immunization protects against subsequent intraperitoneal or oral challenge

To determine whether i.p. immunization with the *wecA* mutant strain could also induce protective immunity, mice were injected with 1×10^1 , 1×10^2 , 1×10^3 , or 1×10^4 CFU of DSM645. On day 30 post-immunization, surviving mice were challenged either with an i.p. lethal dose (1×10^2) or an oral lethal dose (1×10^4) of the wildtype TML strain (DSM644) (Table 13). Thirty-nine of the 40 mice immunized i.p. with either 1×10^1 or 1×10^2 CFU survived until the day of challenge (97.6%); thirty-two of the 39 mice challenged were then fully protected (82.1%) against an intraperitoneal or oral challenge of 1×10^2 or 1×10^4 , respectively. An immunizing dose of 1×10^3 or 1×10^4 CFU of the *wecA* mutant strain was more virulent than the lower immunization doses; only 6 of the 14 mice immunized at these doses survived (42.9%). Clearly, the *wecA* mutant can still be lethal if the immunizing dose is too high.

Discussion

These studies were undertaken to more clearly understand the biological role of one of the major glycolipids on the surface of Gram-negative bacteria, the phosphoglyceride-linked form of Enterobacterial common antigen (ECA_{PG}). Compared with the long history of structure and function studies of other major bacterial surface

Table 13. Intraperitoneal immunization with ECA negative and subsequent challenge at Day 30 with wildtype TML strains

Immunization			Challenge			% Survival
Route	Dose	Survived/Total	Route	Dose	Survived/Total	
ip	Saline	10/10	ip	1.5×10^2	0/10	0
ip	Saline	9/10	Oral	1.0×10^4	0/9	0
ip	1.4×10^1	10/10	ip	1.5×10^2	7/10	70
ip	1.4×10^2	9/10	ip	1.5×10^2	8/9	88.9
ip	1.4×10^3	6/9	ip	1.5×10^2	2/6	30
ip	1.4×10^4	0/5	ip	N/A	N/A	N/A
ip	1.0×10^1	10/10	Oral	1.0×10^4	8/10	80
ip	1.0×10^2	10/10	Oral	1.0×10^4	9/10	90
Total[#]:		45/54	Total[#]:		34/45	75.5

N/A, not applicable
[#] totals exclude animals immunized with saline

glycolipids, such as LPS, definitive studies of ECA function are rare. Although a clear physiological role for the Enterobacterial common antigen has not been determined, ECA has been linked to virulence in several species of bacteria (5, 7, 49, 61). Despite this link to pathogenesis, the function of ECA seems to differ in each species. For example, whereas ECA production in *S. marcescens* is linked to flagellar assembly and motility (11), ECA imparts resistance to organic acids in pathogenic *E. coli* (7). Additionally, while ECA is involved in the swarming motility of *S. marcescens* (11), this phenomenon has not been reported in other Gram-negative bacterial species. Since each of these functions are essential for the survival of these organisms in their respective niches, these data perhaps suggest that although ECA is present in many bacteria, each species has evolved unique ways to utilize ECA or ECA biosynthesis in a manner that is most conducive to survival of the species. Thus, it is possible that Gram-negative bacteria that target different host sites may utilize ECA in different ways. This stipulation is supported by studies that indicate ECA is important in the pathogenesis of bacterial species that colonize very different sites within the host (3, 5, 7, 11, 30, 49). As such, we were interested in determining the role of ECA in *S. Typhimurium* biology.

An early report indicated that an ECA mutant strain of *S. Typhimurium* was attenuated in an intraperitoneal infection model (61); however, due to the limitations in genetic techniques at that time, the mutations responsible for the ECA negative phenotype could not be confirmed as completely isogenic and restoration of virulence by complementation was not achieved. Nevertheless, these data implicate a role for ECA in virulence of *S. Typhimurium*. The role of this molecule in virulence is further supported by the work of Chaudhuri *et al.* and Ramos-Morales *et al.*, who independently reported

that ECA negative strains were attenuated in competitive tail vein and both oral and intraperitoneal short-term infection models (13, 49). Intrigued by these findings, we sought to further evaluate the role of ECA in *S. Typhimurium* pathogenesis.

To this end, we have created genetically defined ECA mutant (*wecA::Gm*) and complementation (Δ *wecA* + pACYC184::*wecA*) strains in both the TML and SL1344 strain backgrounds of *S. Typhimurium* (Table 9). *In vitro* characterization of these strains showed that disruption of the *wecA* gene resulted in the complete loss of ECA production and that ECA production was fully restored in the complementation strains (Table 10 and data not shown). Further *in vitro* characterization showed no major changes in the growth kinetics (Figure 20B and 20C), O-antigen production (Table 10), LPS/O-antigen profile (Figure 20A), or motility (Figure 24(S2)) of the ECA negative strains. Conversely, we found that the ECA mutant strain was severely attenuated *in vivo*; significantly fewer animals were killed by the ECA mutant strain than the wildtype in both the oral and intraperitoneal routes of infection (Figures 21A and 21B). Finally, we determined that either oral or intraperitoneal vaccination with the ECA mutant strain provided protection against subsequent lethal challenge with wildtype *S. Typhimurium*. Interestingly, Ramos-Morales *et al.* previously reported that the intraperitoneal competitive defect in recovery seen with an ECA mutant strain of *S. Typhimurium* was modest as compared to the defect seen during oral infections (49). These results suggested that ECA performs an essential function during oral infection that is less crucial during intraperitoneal infection, or that the presence of ECA on the wildtype bacteria is able to partially complement the ECA mutant phenotype during intraperitoneal but not oral infection. The authors went on to show a role for *S. Typhimurium* ECA in

bile resistance and suggested that bile sensitivity may be responsible for the oral defect (49). Surprisingly, we found that in single strain infections, the ECA mutant strain displayed comparable virulence defects regardless of the route of infection (Figures 21A and 21B). Moreover, we were unable to show increased bile sensitivity with either of our defined *wecA* mutant strains (data not shown). While the reason(s) for the discrepancies between the studies remains unclear, they may be due to the models employed (competitive versus single strain infections) or subtle differences among the *S. Typhimurium* strains used (strain 14028 versus strains TML and SL1344). Regardless, the data clearly indicate that ECA is important for *Salmonella* colonization and virulence, though the actual biological function of ECA remains open to debate.

A key component of *S. Typhimurium* pathogenesis in the murine model of salmonellosis is the ability of this pathogen to disseminate and colonize systemic sites. During oral infection, this process requires that bacteria efficiently cross the intestinal barrier, establish and survive in an intracellular niche, and then disseminate to peripheral sites. Results of our *in vitro* analyses showed no evidence that ECA expression plays a role in bacterial uptake; wildtype and ECA mutant strains both showed similar levels of internalization into INT 407 cells *in vitro* (data not shown). As a consequence of these observations, we postulated that the attenuation of ECA mutant strains was due to the inability of these bacteria to disseminate throughout the host. However, as illustrated in Figure 22, the ECA mutant strain was not only able to colonize systemic sites such as the liver and spleen but was also able to persist for up to 70 days post-infection. Thus, attenuation of the ECA mutants is not due to an inability to properly disseminate within

the host but may be a reflection of the ECA mutant's inability to attain high numbers within the host (Figure 22).

Previous studies have shown that mutations in other genes also lead to the ability of *S. Typhimurium* to establish persistent infections *in vivo*. These genes include (but are not limited to) those associated with metabolic pathways (*e.g.*, *aroD*, *aroA*, *purA*, *purE*, *surA*) and regulatory factors (*ompR*, *rpoS*, *rpoE*, *phoP*). Many strains with mutations in such genes have been considered as potential live vaccine candidates (12, 14, 16, 20, 25, 39, 54, 57). However, for many of these strains, the ability to achieve persistence requires use of an intravenous, intraperitoneal, or highly concentrated oral (10^8 CFU) doses; thus, utilizing these strains as vaccine candidates may be challenging. In contrast, the ECA mutant strain was able to establish a persistent infection with a moderate oral dose of 10^4 CFU; colonization levels for the ECA mutant were approximately 10^3 - 10^4 CFU/spleen and approximately 10^4 - 10^5 CFU/ liver (Figure 22). These colonization values are slightly higher than those reported in the studies using *aroA*, *purA*, and *clpP* mutant strains (35, 44, 63). Given these findings, we hypothesized that higher numbers of persistent bacteria within these organs could result in increased or prolonged immune stimulation within the host and that the ECA mutant might serve as a viable vaccine to protect against subsequent *S. Typhimurium* challenge. Indeed, we found that ECA mutants could provide protection against subsequent lethal challenge by both the oral and i.p. routes of infection. Moreover, this protection lasted as long as 45 days post-vaccination and could be achieved with both the TML- and SL1344-derived ECA mutant strains.

A major consideration in the future development of any live-attenuated vaccine strain is the ability to maintain the delicate balance between attenuation of virulence and optimal immunogenicity. While definitive *in vivo* studies of the role of ECA have been limited, our work clearly demonstrates that ECA mutant strains of *S. Typhimurium* are significantly attenuated in a murine model of infection. In addition, the data presented herein also indicate that ECA negative strains of *S. Typhimurium* can persist for over two months and induce a protective immune response, as indicated by the survival of animals immunized with ECA negative *S. Typhimurium* strains to a lethal challenge (Tables 11, 12 and 13). However, the precise mechanism of attenuation remains unclear. Molecules expressed on the surface of bacterial cells have been shown to serve as pathogen-associated molecular patterns (PAMPS) and are known to act as ligands for immune signaling receptors (2, 28, 37). It is possible that the lack of ECA on the surface of the *wecA* mutant strains alters the initial steps in activation of the host immune response and results in a failure to clear the organisms from systemic sites. Since ECA itself has been shown to be minimally immunogenic (29, 52), ECA mutant strains should retain a similar degree of immunogenicity as wildtype strains. Therefore, given the results presented herein, we propose that ECA mutant strains of *S. enterica* serovar Typhimurium may be good candidates for development of a live-attenuated vaccine against salmonellosis. Furthermore, the ability of the ECA mutant strain to persist at systemic sites suggests the potential to use ECA negative strains as vehicles for heterologous antigen delivery. Future work will focus on characterization of the host immune response to ECA negative strains of *S. Typhimurium* and exploration of the efficiency of these strains as delivery vehicles for heterologous protective antigens.

Acknowledgements

We thank Dr. Tony Maurelli for the gift of the pACYC184 complementation vector, Dr. Suzanne Häubler for the gift of the anti-ECA antibody, Dr. Arif Rahman and Gretchen Guelde for technical expertise, and Dr. Cara Olsen for help with statistical analyses. This work was supported by R073N0, USUHS (E.S.M.) AI42287, NIAID (M.J.S. and E.S.M.), and AI065529, NIAID (D.S.M). J. Gilbreath is supported by the Robert D. Watkins Graduate Research Fellowship from the American Society for Microbiology and the Koniag Education Foundation. The contents of this work are solely the responsibility of the authors and do not necessarily represent the official views of the NIH or the Department of Defense.

Figure 23 (S1). Electron micrograph of gross cell structure of Salmonella strains. Overnight cultures of TML wildtype (A), TML *wecA* mutant (B), SL1344 wildtype (C) and SL1344 *wecA* mutant (D) strains were harvested by centrifugation, fixed, and viewed by transmission electron microscopy. The images shown are representative of numerous similar images. Size bar in lower right-hand corner of each image represents 1 μm .

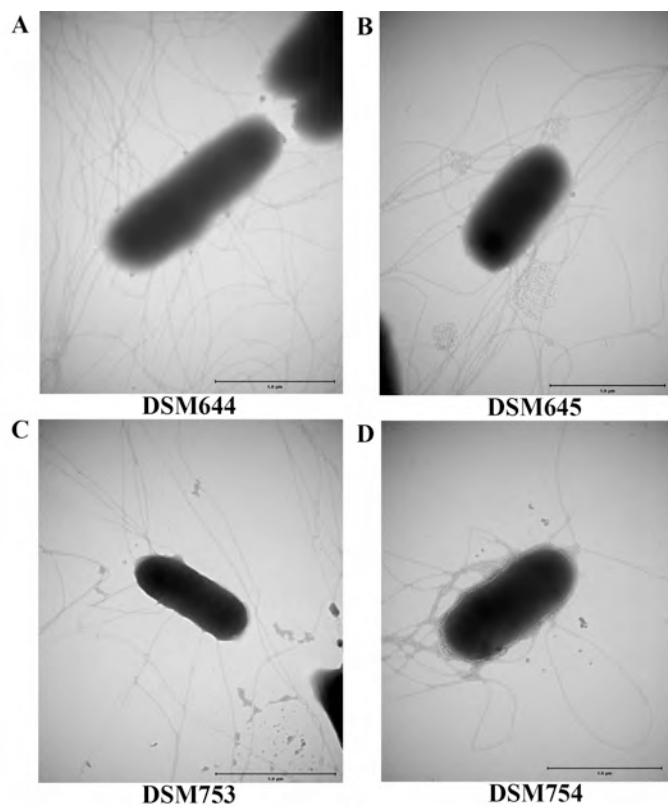


Figure 23 (S1). Electron micrograph of gross cell structure of Salmonella strains

Figure 24(S2). Swarming (A-D) and Swimming (E-H) motility of Salmonella strains. Single colonies (for swimming motility) or toothpick inoculums of liquid culture (for swarming motility) of TML wildtype (A,E), TML *wecA* mutant (B,F), SL1344 wildtype (C,G) or SL1344 *wecA* mutant (D,H) strains were inoculated into 0.5% (swarming motility) or 0.25% LB agar (swimming motility) and incubated overnight. Images shown are representative of duplicate independent experiments.

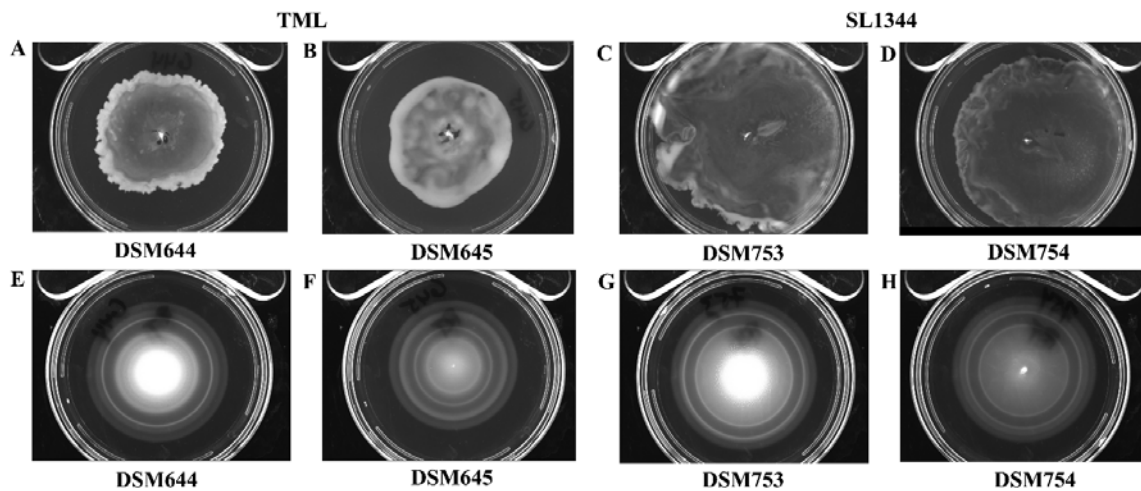


Figure 24 (S2). Swarming (A-D) and Swimming (E-H) motility of Salmonella strains.

*Figure 25 (S3). Percent survival for individual dose groups used for in vivo complementation of the *wecA::Gm* mutation.* Experiments were performed as described in the Materials and Methods. Doses used were 1×10^5 CFU (panel A), 1×10^6 CFU (panel B), or 1×10^7 CFU (panel C).

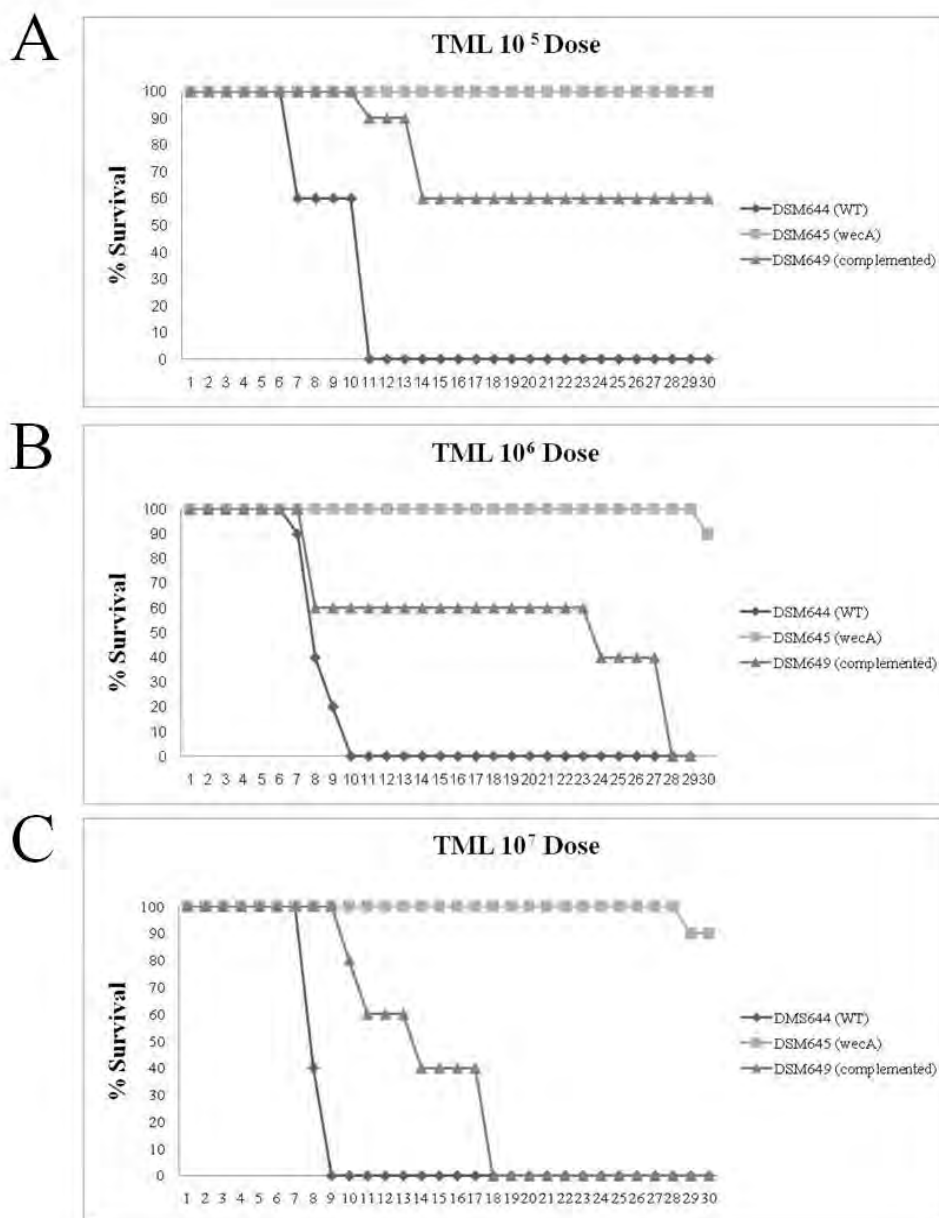


Figure 25 (S3). Percent survival for individual dose groups used for in vivo complementation of the *wecA::Gm* mutation.

References

1. **Albertson, T. E., E. A. Panacek, R. D. MacArthur, S. B. Johnson, E. Benjamin, G. M. Matuschak, G. Zaloga, D. Maki, J. Silverstein, J. K. Tobias, K. Haenftling, G. Black, and J. W. Cowens.** 2003. Multicenter evaluation of a human monoclonal antibody to Enterobacteriaceae common antigen in patients with Gram-negative sepsis. *Crit Care Med* **31**:419-427.
2. **Anderson, K. V.** 2000. Toll signaling pathways in the innate immune response. *Curr Opin Immunol* **12**:13-19.
3. **Bahrani-Mougeot, F. K., E. L. Buckles, C. V. Lockatell, J. R. Hebel, D. E. Johnson, C. M. Tang, and M. S. Sonnenberg.** 2002. Type 1 fimbriae and extracellular polysaccharides are preeminent uropathogenic *Escherichia coli* virulence determinants in the murine urinary tract. *Mol Microbiol* **45**:1079-1093.
4. **Bangtrakulnonth, A., S. Pornreongwong, C. Pulsrikarn, P. Sawanpanyalert, R. S. Hendriksen, D. M. Lo Fo Wong, and F. M. Aarestrup.** 2004. Salmonella serovars from humans and other sources in Thailand, 1993-2002. *Emerg Infect Dis* **10**:131-136.

5. **Banks, K. E., K. R. Fortney, B. Baker, S. D. Billings, B. P. Katz, R. S. Munson, Jr., and S. M. Spinola.** 2008. The enterobacterial common antigen-like gene cluster of *Haemophilus ducreyi* contributes to virulence in humans. *J Infect Dis* **197**:1531-1536.

6. **Barr, K., J. Klena, and P. D. Rick.** 1999. The modality of enterobacterial common antigen polysaccharide chain lengths is regulated by o349 of the *wec* gene cluster of *Escherichia coli* K-12. *J Bacteriol* **181**:6564-6568.

7. **Barua, S., T. Yamashino, T. Hasegawa, K. Yokoyama, K. Torii, and M. Ohta.** 2002. Involvement of surface polysaccharides in the organic acid resistance of Shiga Toxin-producing *Escherichia coli* O157:H7. *Mol Microbiol* **43**:629-640.

8. **Beaty, C. D., T. L. Franklin, Y. Uehara, and C. B. Wilson.** 1994. Lipopolysaccharide-induced cytokine production in human monocytes: role of tyrosine phosphorylation in transmembrane signal transduction. *Eur J Immunol* **24**:1278-1284.

9. **Buzby, J. C., T. Roberts, C.J. Lin, and J.M. MacDonald.** 1996. Bacterial foodborne disease: medical costs & productivity losses. USDA/NAL:Retrieved from: <http://hdl.handle.net/10113/34242>.

10. **Carsiotis, M., D. L. Weinstein, H. Karch, I. A. Holder, and A. D. O'Brien.** 1984. Flagella of *Salmonella typhimurium* are a virulence factor in infected C57BL/6J mice. *Infect Immun* **46**:814-818.

11. **Castelli, M. E., G. V. Fedrigo, A. L. Clementin, M. V. Ielmini, M. F. Feldman, and E. Garcia Vescovi.** 2008. Enterobacterial common antigen integrity is a checkpoint for flagellar biogenesis in *Serratia marcescens*. *J Bacteriol* **190**:213-220.

12. **Chatfield, S. N., C. J. Dorman, C. Hayward, and G. Dougan.** 1991. Role of ompR-dependent genes in *Salmonella typhimurium* virulence: mutants deficient in both ompC and ompF are attenuated in vivo. *Infect Immun* **59**:449-452.

13. **Chaudhuri, R. R., S. E. Peters, S. J. Pleasance, H. Northen, C. Willers, G. K. Paterson, D. B. Cone, A. G. Allen, P. J. Owen, G. Shalom, D. J. Stekel, I. G. Charles, and D. J. Maskell.** 2009. Comprehensive identification of *Salmonella enterica* serovar Typhimurium genes required for infection of BALB/c mice. *PLoS Pathog* **5**:e1000529.

14. **Curtiss, R., 3rd, and S. M. Kelly.** 1987. *Salmonella typhimurium* deletion mutants lacking adenylate cyclase and cyclic AMP receptor protein are avirulent and immunogenic. *Infect Immun* **55**:3035-3043.

15. **Darwin, K. H., and V. L. Miller.** 1999. Molecular basis of the interaction of *Salmonella* with the intestinal mucosa. *Clin Microbiol Rev* **12**:405-428.

16. **Dorman, C. J., S. Chatfield, C. F. Higgins, C. Hayward, and G. Dougan.** 1989. Characterization of porin and ompR mutants of a virulent strain of *Salmonella typhimurium*: ompR mutants are attenuated in vivo. *Infect Immun* **57**:2136-2140.
17. **Erbel, P. J., K. Barr, N. Gao, G. J. Gerwig, P. D. Rick, and K. H. Gardner.** 2003. Identification and biosynthesis of cyclic enterobacterial common antigen in *Escherichia coli*. *J Bacteriol* **185**:1995-2004.
18. **Erridge, C., E. Bennett-Guerrero, and I. R. Poxton.** 2002. Structure and function of lipopolysaccharides. *Microbes Infect* **4**:837-851.
19. **Fadl, A. A., J. Sha, G. R. Klimpel, J. P. Olano, C. L. Galindo, and A. K. Chopra.** 2005. Attenuation of *Salmonella enterica* Serovar Typhimurium by altering biological functions of murein lipoprotein and lipopolysaccharide. *Infect Immun* **73**:8433-8436.
20. **Fang, F. C., S. J. Libby, N. A. Buchmeier, P. C. Loewen, J. Switala, J. Harwood, and D. G. Guiney.** 1992. The alternative sigma factor katF (rpoS) regulates *Salmonella* virulence. *Proc Natl Acad Sci U S A* **89**:11978-11982.
21. **Freudenberg, M. A., S. Tchaptchet, S. Keck, G. Fejer, M. Huber, N. Schutze, B. Beutler, and C. Galanos.** 2008. Lipopolysaccharide sensing an important factor in the innate immune response to Gram-negative bacterial infections: benefits and hazards of LPS hypersensitivity. *Immunobiology* **213**:193-203.

22. **Giannella, R. A., S.B. Formal, G.J. Dammin, and H. Collins.** 1973. Pathogenesis of Salmonellosis: Studies of fluid secretion, mucosal invasion, and morphologic reaction in the rabbit ileum. *J. Clin. Invest.* **52**:441-453.
23. **Haraga, A., M. B. Ohlson, and S. I. Miller.** 2008. Salmonellae interplay with host cells. *Nat Rev Microbiol* **6**:53-66.
24. **Heumann, D., and T. Roger.** 2002. Initial responses to endotoxins and Gram-negative bacteria. *Clin Chim Acta* **323**:59-72.
25. **Hoiseth, S. K., and B. A. Stocker.** 1981. Aromatic-dependent *Salmonella typhimurium* are non-virulent and effective as live vaccines. *Nature* **291**:238-239.
26. **Ilg, K., K. Endt, B. Misselwitz, B. Stecher, M. Aebi, and W. D. Hardt.** 2009. O-antigen-negative *Salmonella enterica* serovar Typhimurium is attenuated in intestinal colonization but elicits colitis in streptomycin-treated mice. *Infect Immun* **77**:2568-2575.
27. **Jones, B. D., N. Ghori, and S. Falkow.** 1994. *Salmonella typhimurium* initiates murine infection by penetrating and destroying the specialized epithelial M cells of the Peyer's patches. *J Exp Med* **180**:15-23.

28. **Kopp, E. B., and R. Medzhitov.** 1999. The Toll-receptor family and control of innate immunity. *Curr Opin Immunol* **11**:13-18.
29. **Kuhn, H. M., U. Meier-Dieter, and H. Mayer.** 1988. ECA, the enterobacterial common antigen. *FEMS Microbiol Rev* **4**:195-222.
30. **Lawlor, M. S., J. Hsu, P. D. Rick, and V. L. Miller.** 2005. Identification of *Klebsiella pneumoniae* virulence determinants using an intranasal infection model. *Mol Microbiol* **58**:1054-1073.
31. **Lew, H. C., H. Nikaido, and P. H. Makela.** 1978. Biosynthesis of uridine diphosphate N-acetylmannosaminuronic acid in rff mutants of *Salmonella typhimurium*. *J Bacteriol* **136**:227-233.
32. **Licht, T. R., K. A. Krogfelt, P. S. Cohen, L. K. Poulsen, J. Urbance, and S. Molin.** 1996. Role of lipopolysaccharide in colonization of the mouse intestine by *Salmonella typhimurium* studied by in situ hybridization. *Infect Immun* **64**:3811-3817.
33. **Lindgren, S. W., I. Stojiljkovic, and F. Heffron.** 1996. Macrophage killing is an essential virulence mechanism of *Salmonella typhimurium*. *Proc Natl Acad Sci U S A* **93**:4197-4201.

34. **Loppnow, H., H. Brade, E. T. Rietschel, and H. D. Flad.** 1994. Induction of cytokines in mononuclear and vascular cells by endotoxin and other bacterial products. *Methods Enzymol* **236**:3-10.
35. **Matsui, H., M. Suzuki, Y. Isshiki, C. Kodama, M. Eguchi, Y. Kikuchi, K. Motokawa, A. Takaya, T. Tomoyasu, and T. Yamamoto.** 2003. Oral immunization with ATP-dependent protease-deficient mutants protects mice against subsequent oral challenge with virulent *Salmonella enterica* serovar typhimurium. *Infect Immun* **71**:30-39.
36. **Mayer, H., and G. Schmidt.** 1979. Chemistry and biology of the enterobacterial common antigen (ECA). *Curr Top Microbiol Immunol* **85**:99-153.
37. **Medzhitov, R., and C. Janeway, Jr.** 2000. Innate immune recognition: mechanisms and pathways. *Immunol Rev* **173**:89-97.
38. **Meier, U., and H. Mayer.** 1985. Genetic location of genes encoding enterobacterial common antigen. *J Bacteriol* **163**:756-762.
39. **Miller, S. I., A. M. Kukral, and J. J. Mekalanos.** 1989. A two-component regulatory system (phoP phoQ) controls *Salmonella typhimurium* virulence. *Proc Natl Acad Sci U S A* **86**:5054-5058.

40. **Monack, D. M., D. M. Bouley, and S. Falkow.** 2004. *Salmonella typhimurium* persists within macrophages in the mesenteric lymph nodes of chronically infected Nramp1+/+ mice and can be reactivated by IFN γ neutralization. *J Exp Med* **199**:231-241.
41. **Nelson, D. L., and E. P. Kennedy.** 1972. Transport of magnesium by a repressible and a nonrepressible system in *Escherichia coli*. *Proc Natl Acad Sci U S A* **69**:1091-1093.
42. **Nevola, J. J., B. A. Stocker, D. C. Laux, and P. S. Cohen.** 1985. Colonization of the mouse intestine by an avirulent *Salmonella typhimurium* strain and its lipopolysaccharide-defective mutants. *Infect Immun* **50**:152-159.
43. **O'Brien, A. D., B. A. Taylor, and D. L. Rosenstreich.** 1984. Genetic control of natural resistance to *Salmonella typhimurium* in mice during the late phase of infection. *J Immunol* **133**:3313-3318.
44. **O'Callaghan, D., D. Maskell, F. Y. Liew, C. S. Easmon, and G. Dougan.** 1988. Characterization of aromatic- and purine-dependent *Salmonella typhimurium*: attention, persistence, and ability to induce protective immunity in BALB/c mice. *Infect Immun* **56**:419-423.

45. **Ohl, M. E., and S. I. Miller.** 2001. Salmonella: a model for bacterial pathogenesis. *Annu Rev Med* **52**:259-274.
46. **Pegues, D. A., E.L. Hohmann, and S.I. Miller.** 1995. *Salmonella*, including *S. typhi*, p. 785-809. In M. J. Blaser (ed.), *Infections of the Gastrointestinal Tract*. Raven Press, New York.
47. **Prevention, C. f. D. C. a.** 1994. *Salmonella* surveillance report-annual summary-1990. Centers for Disease Control and Prevention, Atlanta, GA.
48. **Rabsch, W., H. Tschape, and A. J. Baumler.** 2001. Non-typhoidal salmonellosis: emerging problems. *Microbes Infect* **3**:237-247.
49. **Ramos-Morales, F., A. I. Prieto, C. R. Beuzon, D. W. Holden, and J. Casadesus.** 2003. Role for *Salmonella enterica* enterobacterial common antigen in bile resistance and virulence. *J Bacteriol* **185**:5328-5332.
50. **Rick, P. D., H. Mayer, B.A. Neumeyer, S. Wolski, and D. Bitter-Sueermann.** 1985. Biosynthesis fo Enterobacterial Common Antigen. *J Bacteriol* **162**:495-503.
51. **Rick, P. D., G. L. Hubbard, M. Kitaoka, H. Nagaki, T. Kinoshita, S. Dowd, V. Simplaceanu, and C. Ho.** 1998. Characterization of the lipid-carrier involved in the synthesis of enterobacterial common antigen (ECA) and identification of a novel

phosphoglyceride in a mutant of *Salmonella typhimurium* defective in ECA synthesis. *Glycobiology* **8**:557-567.

52. **Rick, P. D. a. R. P. S.** 1995. Enterobacterial common antigen and capsular polysaccharides, p. 104-112. *In* R. C. C. I. F.C. Neidhardt, J.L. Ingraham, E.C. Lin, K. Low, B. Magasanik, W.S. Reznikoff, M. Riley, M. Schaechter, H.E. Umbarger (ed.), *Escherichia coli* and *Salmonella*: Cellular and Molecular Biology. ASM Press, Washington, D.C.

53. **Rietschel, E. T., T. Kirikae, F. U. Schade, U. Mamat, G. Schmidt, H. Loppnow, A. J. Ulmer, U. Zahringer, U. Seydel, F. Di Padova, and et al.** 1994. Bacterial endotoxin: molecular relationships of structure to activity and function. *FASEB J* **8**:217-225.

54. **Rodriguez-Morales, O., M. Fernandez-Mora, I. Hernandez-Lucas, A. Vazquez, J. L. Puente, and E. Calva.** 2006. *Salmonella enterica* serovar Typhimurium ompS1 and ompS2 mutants are attenuated for virulence in mice. *Infect Immun* **74**:1398-1402.

55. **Rose, R. E.** 1988. The nucleotide sequence of pACYC184. *Nucl. Acids. Res.* **16**:355.

56. **Schletter, J., H. Heine, A. J. Ulmer, and E. T. Rietschel.** 1995. Molecular mechanisms of endotoxin activity. *Arch Microbiol* **164**:383-389.
57. **Sydenham, M., G. Douce, F. Bowe, S. Ahmed, S. Chatfield, and G. Dougan.** 2000. *Salmonella enterica* serovar typhimurium surA mutants are attenuated and effective live oral vaccines. *Infect Immun* **68**:1109-1115.
58. **Tauxe, R. V.** 1996. An update on *Salmonella*. *Health and Environmental Digest* **10**:1-4.
59. **Toguchi, A., M. Siano, M. Burkart, and R. M. Harshey.** 2000. Genetics of swarming motility in *Salmonella enterica* serovar typhimurium: critical role for lipopolysaccharide. *J Bacteriol* **182**:6308-6321.
60. **Tsai, C. M., and C. E. Frasch.** 1982. A sensitive silver stain for detecting lipopolysaccharides in polyacrylamide gels. *Anal Biochem* **119**:115-119.
61. **Valtonen, M. V., U.M. Larinkari, M. Plosila, V.V. Valtonen and P.H. Makela.** 1976. Effect of the Enterobacterial Common Antigen on mouse virulence of *Salmonella typhimurium*. *Infect Immun* **13**:1601-1605.
62. **Wray, C., and W. J. Sojka.** 1978. Experimental *Salmonella typhimurium* infection in calves. *Res Vet Sci* **25**:139-143.

63. **Yamamoto, T., H. Sashinami, A. Takaya, T. Tomoyasu, H. Matsui, Y. Kikuchi, T. Hanawa, S. Kamiya, and A. Nakane.** 2001. Disruption of the genes for ClpXP protease in *Salmonella enterica* serovar Typhimurium results in persistent infection in mice, and development of persistence requires endogenous gamma interferon and tumor necrosis factor alpha. *Infect Immun* **69**:3164-3174.
64. **Zhang, L., J. Radziejewska-Lebrecht, D. Krajewska-Pietrasik, P. Toivanen, and M. Skurnik.** 1997. Molecular and chemical characterization of the lipopolysaccharide O-antigen and its role in the virulence of *Yersinia enterocolitica* serotype O:8. *Mol Microbiol* **23**:63-76.

Appendix B

A Core Microbiome Associated with the Peritoneal Tumors of Pseudomyxoma Peritonei

The work detailed in this Appendix is to be submitted as: **Gilbreath, J.J., Semino-Mora, C., Friedline, C.J., Bodi, K.L., Voohris, A., Sogin, M., McAvory, T., Sardi, A., Dubois, A., Camilli, A., Testerman, T., and Merrell, D.S.** 2012. A Core Microbiome Associated with the Peritoneal Tumors of Pseudomyxoma Peritonei.

The work presented in this chapter is the sole work of J.J. Gilbreath with the following exceptions: C. Semino-Mora performed ISH studies; C.J. Friedline generated the V6-specific SILVA alignment and wrote JAVA programs; H. Liu prepared total DNA from tissue samples; A. Sardi performed tissue collection and the antibiotic clinical study, and T. Testerman isolated strains from PMP tissue.

Abstract

Pseudomyxoma peritonei (PMP) is a rare malignancy characterized by dissemination of mucus-secreting cells throughout the peritoneum. This disease is associated with significant morbidity and mortality, and despite effective treatment

options for early-stage disease, patients with PMP often relapse. Thus, there is a need for additional treatment options to reduce relapse rate and increase long-term survival. A previous study identified the presence of typed as well as non-culturable bacteria associated with PMP tissue, and determined that increased bacterial density was associated with more severe disease. These findings highlight the possibility that these bacteria play a role in the maintenance or progression of PMP disease. To more clearly define the bacterial communities associated with PMP disease, we employed a sequenced-based analysis to profile the bacteria populations found in PMP tumor and mucin in 11 patients. We determined that the types of bacteria present are highly conserved in all PMP patients, irrespective of sampling site (tumor vs. mucin); the dominant phyla are the Proteobacteria, Actinobacteria, Firmicutes, and Bactroidetes. Furthermore, a core set of sequences were found in all 11 patients; these core sequences were classified into >30 groups at the genus level, and contained several taxa that are known to be human pathogens. *In situ* hybridization directly confirmed the presence of bacteria in PMP at multiple taxonomic depths and supported our sequence-based analysis. Furthermore, culturing of PMP tissue samples allowed us to isolate 11 different bacterial strains from 8 independent patients; five *Propionibacterium* spp., two *Corynebacterium* spp., a *Bosea* spp., a *Dermacoccus* spp., an *Amycolatopsis* spp., and an unclassified member of the Chitinophagaceae were isolated. *In vitro* analysis of subset of these isolates suggests that at least some of these strains may interact with the PMP-associated mucin MUC2. Finally, in a pilot clinical study, we provide preliminary evidence that suggests that targeting these bacteria with antibiotic treatment may increase the survival rate of PMP patients. Combined, these data lay the groundwork for obtaining

a better understanding of PMP disease progression and highlight the possibility of using antibiotic therapy as a treatment option for PMP.

Introduction

Pseudomyxoma peritonei (PMP) is a clinical syndrome characterized by the dissemination of mucus-secreting tumors throughout the peritoneal cavity (14, 24, 27). This rare but devastating condition usually arises after rupture of a mucin-producing appendiceal neoplasm and is associated with significant morbidity. Mortality usually results from diffuse spread of mucin within the peritoneum and mechanical obstruction of the intestines. PMP is generally classified into two major categories: diffuse peritoneal adenomucinosis (DPAM) and peritoneal mucinous adenocarcinoma (PMCA) (21, 22, 27). DPAM is the lower grade of PMP disease and refers to an indolent tumor form without cellular atypia and no invasive features. In contrast, PMCA is characterized by severe cellular atypia, poor histologic cellular differentiation, and tissue invasion. When proper treatment is given in a timely manner, the prognosis for patients with DPAM can be good (five year survival rate of ~75%); however, patients with the more severe PMCA do not fare as well (five year survival rate of ~14%) (4). Current therapeutic strategies consist of macroscopic tumor and mucin removal by cytoreductive surgery (CRS) followed by hyperthermic intraperitoneal chemotherapy (HIPEC) (22, 27, 31, 37). However, despite aggressive treatment, the disease frequently relapses and the 10 year survival is only 32% (14, 15, 30). As such, there is a serious need for ways to improve long-term patient outcome.

Within the past several years, it has become increasingly clear that the microbial communities in and on the human body have a far-reaching impact on human physiology and serve to maintain the balance between health and disease states (2, 3, 5, 7, 8, 10, 20, 26, 28, 33, 34). More recently these interactions have been linked to human cancers (3, 20), and have even led researchers to identify particular bacterial species that are enriched in tumor environments as compared to surrounding tissue (3, 20). These insights not only provide novel information about tumor development and subsequent disease progression, but also highlight potential treatment options for these cancers. Using probes designed to recognize both typed and non-culturable bacteria (TNCB), as well as the known bacterial carcinogen *H. pylori*, a recent study observed that there are numerous bacteria associated with the PMP tumors and secreted mucin within the normally sterile peritoneal cavity (30). In PMP tissue, the density of TNCB and *H. pylori* was highest in the more malignant form of PMP; however, the identity of these TNCB was not determined. Taken together, these results suggest that PMP disease progression may be associated with the presence of bacteria within the peritoneum.

We hypothesize that bacteria play a role in the progression or maintenance of PMP disease. In the current study, we utilized high-throughput sequencing of the V6 hypervariable region of the 16S rRNA gene to characterize the bacterial communities associated with tumors and secreted mucin in 11 PMP patients. We identified a highly conserved core group of bacterial taxa that were found in all patients. The core community membership was consistent across all patients tested, although the relative abundance of these bacteria varied from patient to patient. Specific DNA probes and *in situ* hybridization (ISH) was used to directly detect PMP community members across a

range of taxonomic depths. Furthermore, multiple bacterial isolates were obtained by culturing PMP tissue samples under microaerophilic conditions; some of these isolates interact with the PMP-associated mucin MUC-2 as well as host cells *in vitro*. Based on these and previous findings (30), we initiated a pilot clinical study to evaluate the possibility of using antibiotic therapy to target these bacterial communities in the treatment of PMP. Consistent with the hypothesis that these bacteria play a role in PMP disease, our preliminary clinical findings suggest that treating PMP patients with antibiotics early in disease progression may increase long-term survival.

Materials and Methods

PMP patients

This study utilized retrospective PMP patient specimens that were collected peri-operatively at Mercy medical center in Baltimore, MD. Tissue was collected in a sterile surgical suite and stored at -80°C until the samples were ready to process. All procedures were approved by the IRB at all centers involved in this study. Written informed consent was obtained from all patients prior to enrollment in the study.

DNA extraction, V6 PCR, and sequencing

Total genomic DNA (gDNA) was isolated from PMP tissue specimens and stored at -80C. Between 100-200 ng of gDNA was used as template for PCR with a combination of V6-specific primers as previously described (12, 19). The products of 2-3

amplifications from each sample were gel purified and pooled. Pooled amplicons were barcoded, combined into a multiplexed sample and sequenced on an illumina Hi-seq at the Tufts University Core Facility. Raw reads were de-multiplexed, filtered for quality, and barcodes/adapters were removed using Galaxy (13).

V6 sequence processing and analysis

All subsequent sequence analyses were performed using mothur (29). To simplify the dataset, each sample was randomly sub-sampled to a depth of 100,000 reads per sample. Sequences were aligned to a V6-specific, curated database (12) derived from the full-length SILVA alignment. The alignment was screened to remove sequences that were shorter than 56 bp or greater than 72 bp in length, as well as any sequences that contained an ambiguous base call or homopolymer runs of >4 bp. The resulting alignment was then filtered to remove any columns that contained missing information. Reads were pre-clustered so that any sequences that contained a single base pair difference were considered to be the same. Pre-clustered reads were classified using the mothur implementation of the RDP Bayesian classifier (35) using a cutoff of 60% bootstrap support over 100 iterations. Sequences that were classified as mitochondria, cyanobacteria, chloroplasts and sequences that were classified as “unknown,” or “unclassified” at the phylum level were removed from the dataset. The remaining aligned sequences were used to generate a pairwise distance matrix and clustered into operational taxonomic units (OTUs) using average-linkage clustering at an identity of 97%. OTUs were classified using the mothur implementation of the RDP classifier as described above. Prior to α - and β -diversity calculations, we normalized the sequences

from each sample based on the lowest number of OTUs found in any of the samples. As indicated by Good's coverage estimate, this workflow provided ample sample coverage (range of coverage was 0.96 to .99, with a mean coverage of .976).

In situ hybridization (ISH) studies

Probes used for ISH are listed in Table 14. The Actinobacteria, Bacteroidetes, Betaproteobacteria, Gammaproteobacteria, Firmicutes, Rhizobiales, *Pseudomonas*, *Streptococcus*, and Verrucomicrobiales probes were obtained from probeBase (retrieved from: <http://www.microbial-ecology.net/probebase>). The *Propionibacterium*-specific probe was designed using ~50 randomly selected full-length *Propionibacterium* 16S sequences obtained from the RDP database. The specificity of the probe sequence was verified using the ProbeMatch function on the RDP website; the probe sequence used detects ~97% of sequences classified into the *Propionibacterium* genus. Labeling and hybridization procedures were performed as previously described (30). Briefly, formalin-fixed tissue blocks were cut into 5 micron sections; each unstained section was deparaffinized, pre-hybridized, and subsequently treated with denatured probe solution for 18 h at 37°C. The hybridization mixture contained one of the 10 different biotinylated taxa-specific probes. After hybridization, unbound probe was removed by successive washes in decreasing concentrations of SSC (2× SSC for 30 min, 1× SSC for 10 min, 0.5× SSC for 10 min, and 0.1× SSC for 15 min at 60°C). Probes were detected using streptavidin conjugated with fluorescein (FITC). Sections were mounted with Vectashield (Vector Labs, Burlingame, CA), and reactions were observed using a Nikon Eclipse 80i

Table 14. ISH probes used in this study

Probe (Abbreviation)	Taxonomic Depth	Sequence (5'-3')	Target
Actinobacteria (ACT)	Phylum	TATAGTTACCACCGCCGT	23S rRNA
Bacteroidetes (BAC)	Phylum	AGCTGCCTTCGCAATCGG	16S rRNA
Firmicutes (FIR)	Phylum	TGGAAGATTCCCTACTGC	16S rRNA
Betaproteobacteria (BET)	Class	CCCATTGTCCAAAATTCCCC	16S rRNA
Gammaproteobacteria (GAM)	Class	GCCTTCCCACATCGTTT	16S rRNA
Rhizobiales (RHI)	Order	TCGCTGCCCACTGTCACC	16S rRNA
Verrucomicrobiales (VER)	Order	GCTGCCACCCGTAGGTGT	16S rRNA
Pseudomonas (PSE)	Genus	TCTGGAAAGTTCTCAGCA	16S rRNA
Propionibacterium (PRO)	Genus	CACCCATCTCTGAGCACCCCG	16S rRNA
Streptococcus (STR)	Genus	CCACTCTCCCCTTCTGCAC	16S rRNA

microscope with a DS camera, a DS-L2 control unit and an NIS-Elements scope. Control hybridizations for nonspecific binding were performed for all probes used in this study.

Culturing and identification of PMP isolates and in vitro characterization

Aseptically collected surgical specimens were collected and shipped overnight on ice to the LSU Health Sciences Center-Shreveport. As *H. pylori* was previously identified in PMP tissue (30), initial culture conditions were chosen to be suitable for cultivating this organism. Approximately one gram aliquots of tissue material were inoculated into 25 cm² tissue culture flasks with 5 mL of Ham's F12 Nutrient Mixture supplemented with 1% fetal bovine serum, 200 µg/ml β-cyclodextrin, 10 µg/ml trimethoprim, 10 µg/ml vancomycin, 5 µg/ml and 5-fluorocytosine. Cultures were incubated under microaerophilic conditions (5% O₂, 10% CO₂). An additional aliquot of each sample was inoculated into LB broth and incubated in 5% CO₂. Cultures were monitored daily and were subcultured once growth was observed. Each isolate was serially passaged multiple times until the culture was axenic. Full-length 16S rRNA gene sequences were PCR amplified using Fidelitaq high fidelity polymerase (USB) and the 8F and 1492R primers; amplicons were sub-cloned into pGEM-T Easy (Promega). Cloned 16S rRNA genes were sequenced with 1492R and 907R primers. Sequences were classified using the web-based RDP Bayesian classifier (rdp.cme.msu.edu) and the RDP training set 9. Adherence assays were performed by co-culturing selected isolates with HT-29 cells, which produce the PMP-associated mucin MUC2. Interaction with MUC2 was detected by immunohistochemistry. Briefly, *in vitro* MUC2 production was detected using a polyclonal anti-MUC2 antibody; the MUC2::MUC2 antibody conjugates were detected

using biotinylated anti-rabbit antibody and avidin-peroxidase. For each assay, multiple fields were viewed; a representative image is shown in Figure 30.

Clinical trial study design

A pilot clinical study was initiated to evaluate the possible association between bacteria and the development of PMP disease, and to determine the benefit of antibiotic treatment. Beginning in September 2007, a group of 21 patients with PMP was treated with antibiotics in conjunction with the standard cyroreduction surgery and HIPEC treatment with mitomycin C. The treatment group was comprised of 8 patients with DPAM, 11 with PMCA, one patient with both diagnoses, and one patient with no available diagnosis. Based on a recent study (15) patients were divided into two groups: lymph node (LN) positive (seven patients) and LN negative (13 patients). One patient did not have a lymph node assessment. Patients were treated with Prevpac®, which includes lansoprazole, amoxicillin, and clarithromycin. Patient survival was compared using a log-rank statistical test.

Results

Sequence analysis and identification of a core PMP Microbiome

ISH-based studies previously identified the presence of many typed and non-culturable (TNCB) bacteria in tissue samples taken from PMP tumors and secreted mucin (30). That study highlighted the possibility that these bacteria might play a role in PMP

disease progression; thus, these bacteria could possibly be targeted as a novel/ancillary therapeutic option. In order to investigate the presence of these bacteria further, we collected paired tissue samples from 11 PMP patients (11 tumor and 11 mucin samples = 22 total) and used a V6-based analysis to profile the bacterial communities associated with both tumor and secreted mucin.

After clustering sequences into OTUs at a level of 97%, we first examined the community profiles at the phylum level. As shown in Figure 26, the distribution of bacterial phyla between samples was consistent; the most prominent phylum represented in all samples was the Proteobacteria. The relative abundance of the Proteobacteria across the 22 samples ranged from 56.8% to 90.2%, with a mean of 73.0%. Other prominent phyla include the Actinobacteria (3.4% to 19.3%, mean of 10.7%), Firmicutes (1.3% to 17.8%, mean of 6.9%), Bacteroidetes (2.0% to 14.8%, mean of 7.2%), Verrucomicrobia (0.3% to 1.7%, mean of 0.8%), Acidobacteria (0% to 0.6%, mean of 0.3%), TM7 (0% to 0.3%, mean of 0.1%), and OD1 (0% to 0.9%, mean of 0.2%).

The observed richness (number of OTUs) across the individual samples ranged from 388 to 1833, with a mean of 1045. Rarefaction curves for individual tumor and mucin samples are depicted in Figure 32(S1). While the number of OTUs varied between sampled body sites (tumor vs. mucin) in some patients, as a whole, the number of OTUs found in tumor tissue was not significantly different than that found in the free mucin ($P=0.24$, Student's *t*-test). As the microenvironment of tumor tissue may be quite different than free mucin, we asked whether there were any OTUs that were enriched in one type of tissue over the other. Using the *mothur* implementation of Metastats (36), we

Figure 26. Distribution of prominent bacterial phyla. A randomly sub-sampled set of 100,000 sequences were processed using mothur as described in the Materials and Methods. After processing, sequences were classified at a distance of 97%, and classified using the mothur implementation of the RDP classifier. The relative abundance of each phylum is shown as the number of OTUs that were classified in each phylum out of the total number of bacterial OTUs. Numbers indicate patient designations. “T” indicates the sample was taken from tumor tissue, and “M” indicates the sample was from free mucin.

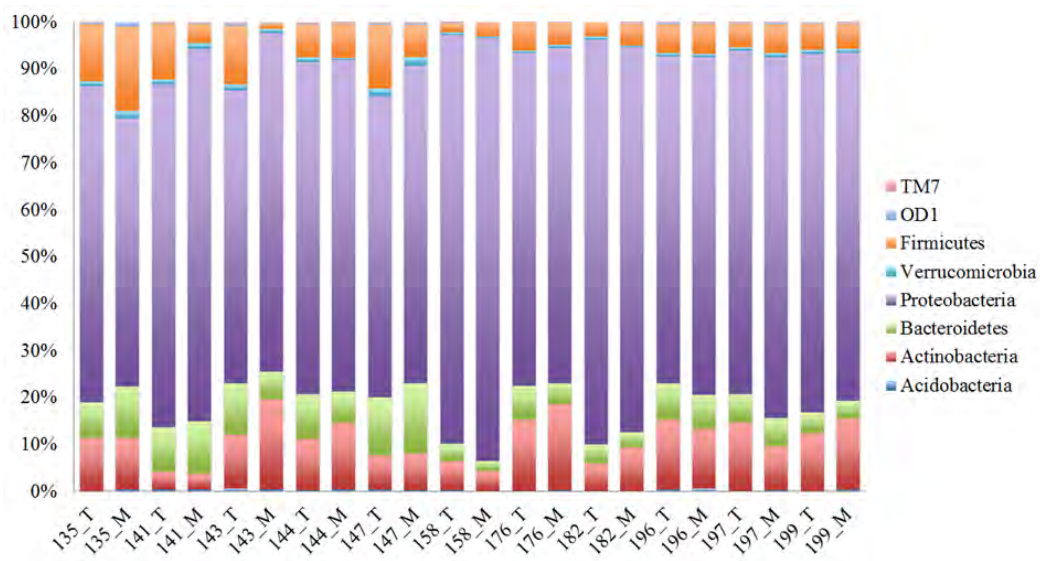


Figure 26. Distribution of prominent bacterial phyla

compared the relative abundance of each OTU from each tissue type. Surprisingly, the number of sequences clustered into each OTU was not significantly different in either site, further highlighting the fact that the bacterial communities in the tumor and mucin tissue sites are highly similar. Given the apparent similarity between the tumor and mucin communities, we combined the sequence sets from the tumor and mucin for each patient. Using these combined datasets, we compared the differences in community membership and relative abundance using the classic Jaccard and thetaYC indices, respectively. As shown in Figure 27, the membership of the communities in each patient displayed a surprisingly high level of similarity. Between patients, the only differences seem to be in terms of relative abundance of community members (Figure 27B) rather than the types of taxa present (Figure 27A).

Given the similarity between the tumor and mucin communities in a given patient, we decided to use the combined tumor and mucin sequence sets for each patient and asked whether there was a core set of sequences that were present in all patients. For a particular sequence to be considered as part of this core microbiome, we took a conservative approach and required that an exact match to a particular sequence be present in all patients. As shown in Figure 28A, there were four phyla represented in the PMP core microbiome; the relative abundance in of each phyla was similar to what was seen for the individual tumor and mucin samples, with the majority of sequences being classified as *Proteobacteria* (77%), followed by *Actinobacteria* (15%), *Firmicutes* (5.7%), and *Bacteroidetes* (2.3%). Within these phyla the core microbiome can be further broken down into 34 different groups that were classifiable at the genus level. The breakdown of sequences is shown in Table 15. The relative abundance of the 10 most prevalent

Figure 27. β -diversity between PMP communities. Heatmaps compare the classic Jaccard (Jclass) dissimilarity indices (**A**) and thetaYC indices (**B**) for bacterial communities found in PMP patients. Calculations were performed using mothur (137).

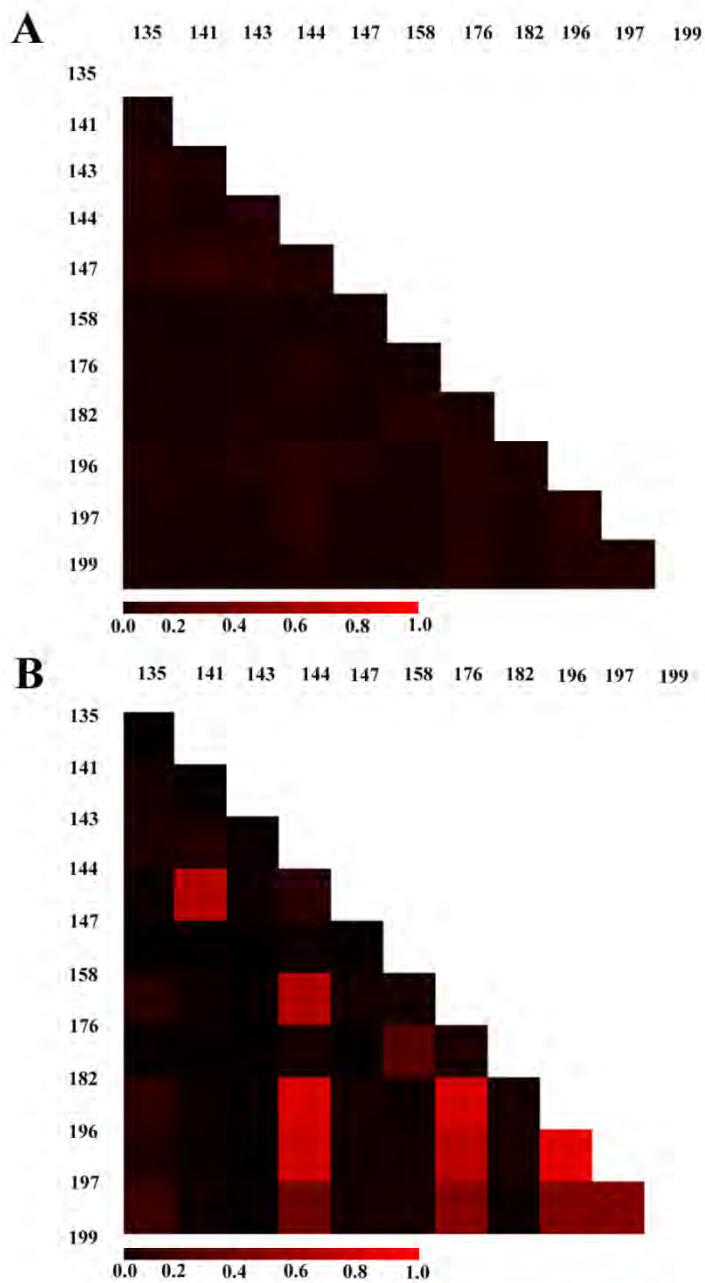


Figure 27. β -diversity between PMP communities

Figure 28. Core set of sequences found in all PMP patients. After combining the tumor and mucin sequence sets for each patient, sequences that were present in all patients were classified at a distance of 97%. The relative abundance of these sequences at the phylum level (**A**) or at the genus level (**B**) is shown.

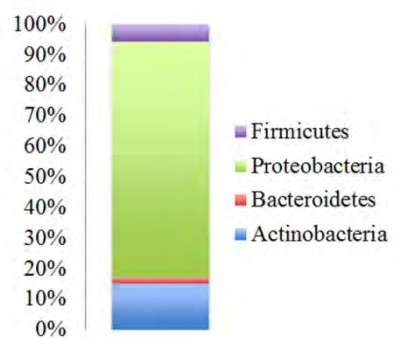
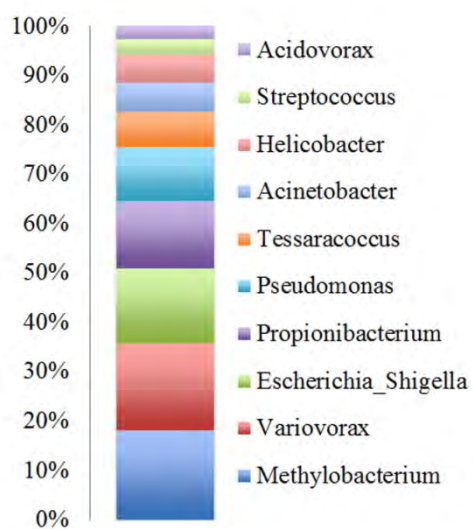
A**B**

Figure 28. Core set of sequences found in all PMP patients.

Table 15. PMP Core Microbiome Classifiable at the Genus Level

Genus	Seqs*
Methylobacterium	106626
Variovorax	104621
Escherichia_Shigella	88823
Propionibacterium	81731
Pseudomonas	64037
Tessaracoccus	41711
Acinetobacter	35628
Helicobacter	33441
Streptococcus	17987
Acidovorax	15911
Moraxella	8777
Sphingomonas	6731
Methylotenera	6097
Haliscomenobacter	5883
Flavobacterium	5483
Polaromonas	5046
Brevibacillus	4674
Stenotrophomonas	4565
Methylophilus	4389
Diaphorobacter	4616
Limnohabitans	4453
Curvibacter	3149
Delftia	2904
Terrimonas	2587
Ralstonia	2372
Bdellovibrio	2288
Flectobacillus	1990
Arcicella	1904
Zoogloea	1663
Microbacterium	1306
Arcobacter	848
Pedobacter	834
Lactococcus	767
Roseomonas	633

*indicates the number of sequences from the core microbiome that were classified

classifiable genera are shown in Figure 28B; while many of these taxa such as *Escherichia*, *Propionibacterium*, *Streptococcus*, and *Helicobacter* are commonly found in humans, some of the taxa represented are more typically categorized as environmental organisms.

Direct detection of selected members of the PMP microbiome

As a complementary approach to our sequencing analysis, we next used DNA probes to detect a subset of the taxa identified in the sequence-based analysis by *in situ* hybridization (ISH). For these experiments we utilized tissue sections from 3 patients that were included in the sequencing study (patients 135, 149, and 196) and two additional patients that were not included in the sequence-based analysis (patients 145 and 244). At the phylum level we were able to detect Firmicutes, Bacteroidetes, and Actinobacteria in tissue specimens from all five patients (Figure 29). Specifically within the Proteobacterial phylum, we detected the presence of Betaproteobacteria and Gammaproteobacteria; at the Order level, we detected the presence of the commonly found human-associated Verrucomicrobiales, as well as the Rhizobiales, which are commonly found within soil environments; using genus-specific probes we verified the presence of *Pseudomonas*, *Propionibacterium* and *Streptococcus* spp., which are known human pathogens (Figure 29). These data support our sequence-based analysis and confirm that members of these taxonomic groups are located directly within or directly associated with the PMP tissue.

Figure 29. Direct detection of bacterial taxa in PMP tissue by ISH

Hybridizations were carried out as described in the Materials and Methods. We detected the presence of each taxonomic group in all five patients tested. Images were selected to show positive hybridization signal, and are not intended to reflect relative abundance within tissue specimens.

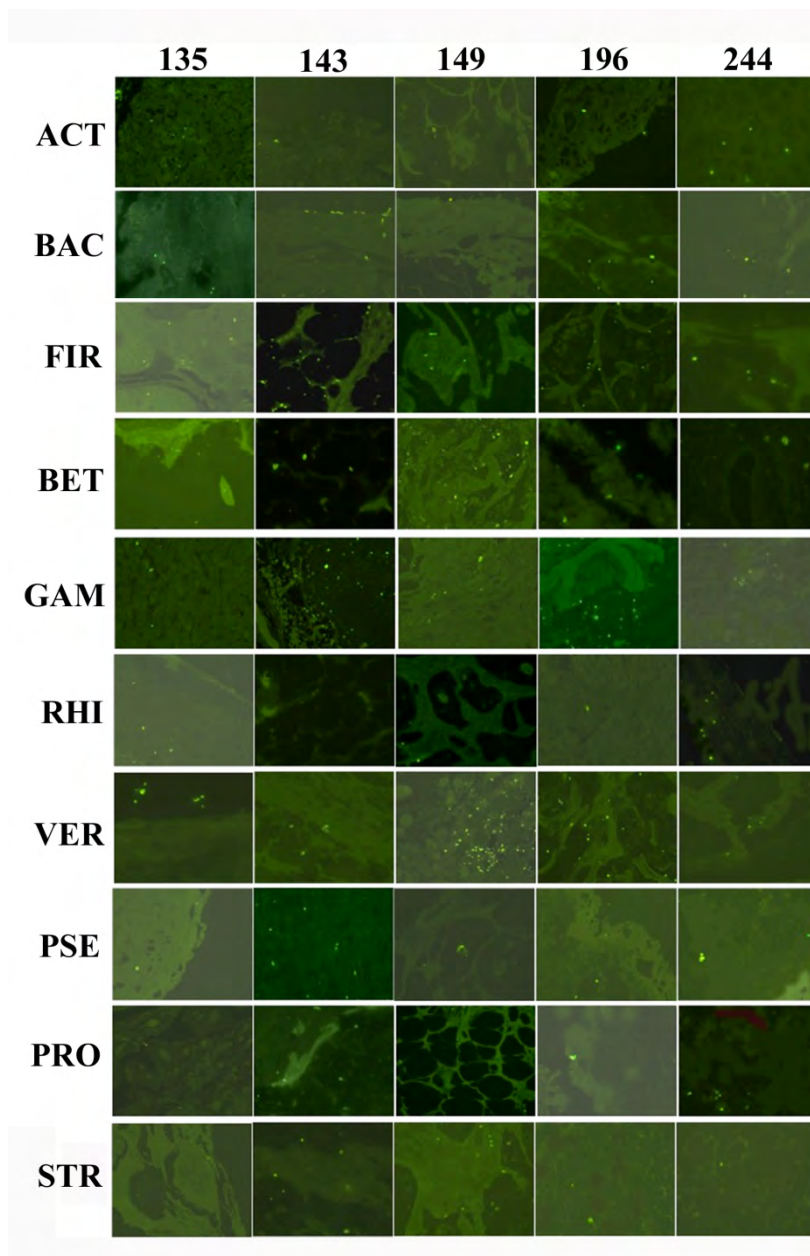


Figure 29. Direct detection of bacterial taxa in PMP tissue by ISH

Isolation and identification bacterial strains associated with PMP

To understand the impact that these bacteria have on disease, it is ultimately important to be able to isolate and study the PMP-associated bacteria. Using microaerophilic conditions, we were able to successfully culture 11 isolates from 8 patients. The identity of these bacterial isolates is shown in Table 16. *In vitro* assays using mucin secreting HT-29 cells indicated that at least some of these organisms are able to adhere to the mucin MUC2, which has been shown to be one of the mucins secreted by PMP cells (Figure 30 and data not shown). Importantly, one of the organisms we were able to culture from multiple patients, a *Propionibacterium spp*, was one of the more prevalent organisms identified in our core microbiome (Figure 28B and Table 15) and was directly detected by ISH (Figure 29). Taken together, these data further support our sequencing results and support a potential role for these bacteria in the maintenance or progression of PMP disease.

Antibiotic treatment efficacy

The ultimate goal of characterizing the bacteria associated with PMP is to determine whether antibiotic treatment might serve as an additional treatment option for patients. To this end, we designed a pilot clinical study to evaluate the efficacy of antibiotic treatment in PMP patients. The previously published five-year survival rate for PMP patients with a PMCA diagnosis is 76% for LN negative individuals, and only 11% for patients that are LN positive (15). Given that we previously identified bacteria in PMP tumors, starting in September 2007 a test group of 21 PMP patients was treated with antibiotics prior to cytoreductive surgery followed by HIPEC using mitomycin. Seventeen of the patients

Table 16. Culturable bacteria isolated from PMP tissue samples

Patient/Strain	Family and Genus level RDP Classification (% bootstrap support)
PMP191F	unclassified_Chitinophagaceae (100), Niastella (70)
PMP191M	Bradyrhizobiaceae (100), Bosea (100)
PMP191C	Dermacoccaceae (100), Dermacoccus (100)
PMP196	Propionibacteriaceae (100), Propionibacterium (100)
PMP213	Propionibacteriaceae (100), Propionibacterium (100)
PMP215	Pseudonocardiaceae (100), Amycolatopsis (100)
PMP219	Propionibacteriaceae (100), Propionibacterium (100)
PMP229	Propionibacteriaceae (100), Propionibacterium (100)
PMP238	Corynebacteriaceae (100), Corynebacterium (100)
PMP267-3	Propionibacteriaceae (100), Propionibacterium (100)
PMP267B	Corynebacteriaceae (100), Corynebacterium (100)

Figure 30. Bacteria isolated from PMP tissue associates with MUC2

Isolate PMP191F (an unclassified Chitinophagaceae) was cultured with MUC2 secreting HCT-29 cells. The rod shaped bacteria interact with cell-associated MUC2 (**A**) as well as secreted MUC2 (**B**). The positive reaction (seen as brown color) for MUC2 staining on the bacterial cells is consistent with interaction or adherence to MUC2. The image shown in panel B is a magnification of the boxed region in panel A.

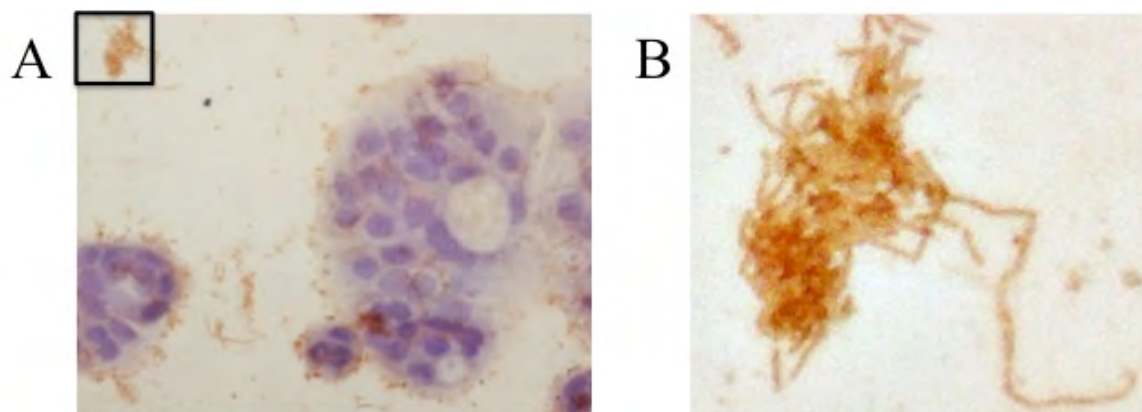


Figure 30. Bacteria isolated from PMP tissue associates with MUC2

received 2 courses of antibiotics, one course 3 weeks prior to surgery and a second course 6-8 weeks following surgery. The four additional patients only received 1 course prior to surgery, since they had difficulty in tolerating the antibiotics used. The antibiotic regimen used was the Prevpac®, which includes lansoprazole, amoxicillin, and clarithromycin. The test group consisted of 8 DPAM patients, 11 PMCA patients, 1 patient with both diagnoses (from separate biopsies), and 1 patient where the diagnosis was not recorded. The test patients can be divided into two major groups based on whether they were LN positive or negative. Thirteen patients were LN negative and 7 patients were LN positive. One patient did not receive a LN assessment. Importantly, survival of LN positive patients within the pilot group that received antibiotic therapy was essentially the same as those that did not receive antibiotics. These results indicate that eliminating bacteria from the affected peritoneal tissue prior to metastasis may improve survival of patients with PMP disease. For the LN negative patients, 6 had PMCA and 7 had DPAM. The LN negative patients who received antibiotics showed longer overall survival than previously recorded in (9). As of September 2012 (4.5 to 5 years after surgery) all 6 antibiotic treated PMCA patients are surviving. The 6 PMCA patients who received antibiotics were included in the study described in (9). If these patients are removed and a logrank statistical test is used to compare survival of the 6 antibiotic PMCA patients to the 37 non-antibiotic PMCA patients remaining in (9), a $P = .078$ is obtained for all 6 surviving patients (Figure 31). Even though this value is not statistically significant, it does indicate a trend that antibiotics could be beneficial. It can be noted that all 7 DPAM patients who

Figure 31. Patient survival after antibiotic treatment

Survival of PMP LN negative patients with or without antibiotic treatment. The red line indicates survival of patients that were treated with antibiotics (Previpac[®]), whereas the black line indicates patients that were not given this treatment.

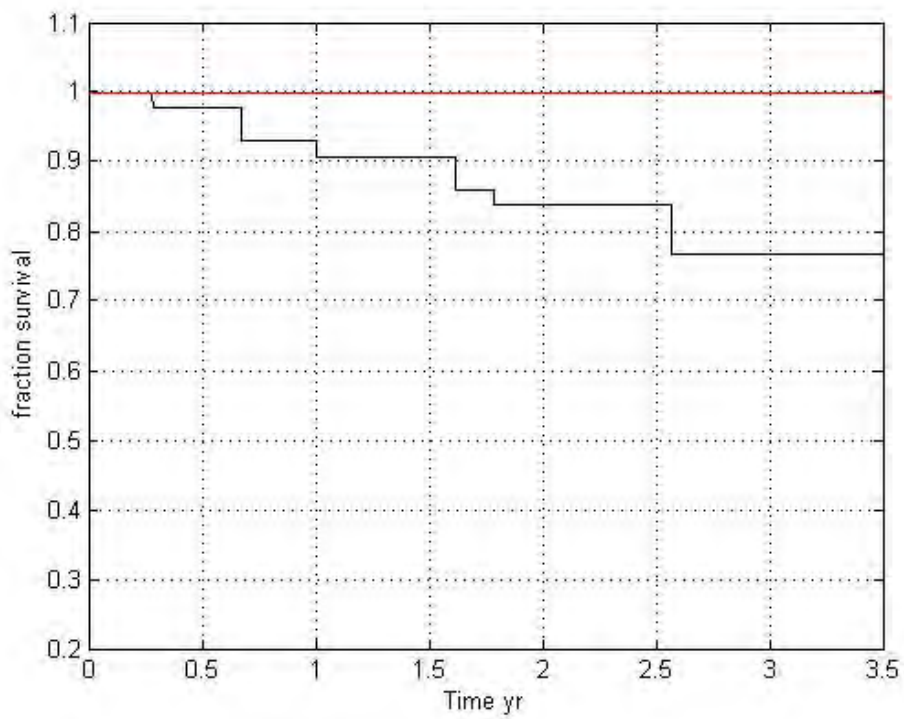


Figure 31. Patient survival after antibiotic treatment

received antibiotics are also surviving as of September, 2012. The results indicate that antibiotics may be beneficial in treating LN negative PMP patients. If the results are correct then they indicate that elimination of bacteria before PMP has had a chance to metastasize can significantly extend overall survival time of LN negative PMP patients.

Discussion

PMP is a rare but serious disease that results in significant morbidity and mortality. As patient outcome is frequently more negative once the disease progresses to the more severe form (PMCA), PMP is most effectively treated prior to this transition. However, despite early intervention, PMP patients experience frequent relapse and the long-term prognosis for PMP patients is somewhat dismal, with only ~30% surviving past the 10 year mark. As such, there is still a great need for novel or supplementary treatment options that will increase patient survival.

In the current study, we identified a core set of bacteria that are present in PMP tumor and mucin tissue. Across the 11 patients in our study, the major difference in the community structures was the relative abundance of each type of bacteria. Interestingly, the dominant phylum present was the Proteobacteria; while this group is commonly found in and on the human body (2, 5, 26, 28), virtually none of the healthy microbiomes described to date are dominated by this phylum. One environment where Proteobacteria do predominate, however, is the microbiome associated with cystic fibrosis (CF) (33). Within the respiratory tract of CF patients, a large proportion of bacteria are Proteobacteria (6, 18). The abundance of Proteobacteria in both PMP and CF is perhaps

the result of similarities in the CF lung environment and PMP tissue in the peritoneum. In both CF and PMP, there is an abundance of mucin/mucus secretion, which may enrich for the Proteobacteria as well as some of the typically “environmental” bacteria found in our sequence-based study (Figure 28B, Table 15, Tables 17(S1) and 18(S2)).

In addition to the dominance of the Proteobacterial phylum, the PMP core microbiome also shares some additional characteristics with that of CF airways. Specifically, there are several non-Proteobacterial genera that are present in both microbiomes. As shown in Figure 28B and Table 15, of those bacteria classifiable at the genus level, one of the more prevalent groups detected in our study was the *Streptococcus* spp. Members of this genus, which includes the *Streptococcus milleris* group (SMG), have been recently shown to be a prominent part of CF disease (33), and are known to be associated with several types of human disease (16, 23, 25, 32). Furthermore, other *Streptococcus* spp., have been shown to increase virulence of other bacterial pathogens such as *P. aeruginosa* (9), which is likely to be found in PMP tissues since members of the *Pseudomonas* genus were found in the PMP core microbiome (Figure 28B, Table 15, Table 17(S1)). A previous study identified the carcinogenic bacterium *H. pylori* in PMP tissue samples, and determined that the density of *H. pylori* could be correlated to PMP disease severity (30). Consistent with this study, we also detected the presence of *Helicobacter* spp. in our core microbiome (Figure 28B, Table 15, Table 17(S1) and 18 (S2)). While the precise role of these bacteria in PMP disease is unclear, *H. pylori* is known to induce a pro-inflammatory environment (1) and secretes oncogenic virulence factors (17) that may contribute to carcinogenesis and/or the maintenance of PMP disease. While our study design did not allow us to confidently

make species level taxonomic classification, the presence of *Streptococcus* spp., *Pseudomonas* spp., *Helicobacter* spp., and other taxonomic groups that contain known human pathogens in the PMP core microbiome highlights the possibility that these bacteria play a role in PMP disease and certainly merits more detailed study.

One attractive feature of performing sequence-based community analyses is the ability to identify possible keystone taxonomic groups or species that are enriched in a particular body site or disease state. Recently, this feature was exploited to identify *Fusobacterium* spp., as being enriched in patients with colorectal cancer (3, 20). However, unlike that study, we did not identify any one bacterial type that was enriched in either of the two sampling sites (tumor and mucin), or in one disease state versus the other (DPAM vs PCMA). This finding perhaps suggests that the combination of all bacterial types present that is important in PMP rather than a single keystone species. Furthermore, the results highlight the importance of studying these organisms as a community in addition to studies using individual bacteria.

In an effort to characterize PMP-associated organisms, we have begun to culture bacteria from PMP samples. To date we have successfully cultured several organisms from multiple patients. Among those species cultured (Table 16), the Firmicute *Propionibacterium* spp. was isolated most frequently. Comparison of 16S sequences from these isolates to completed genomes in Genbank indicates that these *Propionibacterium* spp., are likely to be *P. acnes*. *P. acnes* is commonly found on human skin and has been implicated in several types of human diseases including endophthalmitis and bone infections. Interestingly, a recent *in situ* hybridization-based study found *P. acnes* in

~80% of cancerous prostates (11). In that study, the authors were also able to culture *P. acnes* from cancerous prostates and showed that incubation with this bacterium elicited a strong proinflammatory response in host cells (11); this may be a contributing factor to disease progression. The potential role for the other cultured isolates is less clear. However, preliminary *in vitro* experiments with the unclassified Chitinophagaceae isolate PMP191F indicates that this organism does interact with the PMP-associated mucin, MUC2 (Figure 30).

The presence of a consistent group of bacteria in all PMP patients brings to light one distinct possibility: if these bacteria do play a role in the maintenance of PMP disease or PMP progression, then treatments aimed at clearing this polymicrobial infection should improve patient outcome. We tested this hypothesis in a small pilot clinical study using new patients as well as existing patient data. As shown in the section on antibiotic treatment efficacy, treating PMP patients with a combination of antibiotics (Previpac[®]), improved overall survival. While these findings are exciting and do suggest that antibiotics may be a viable supplementary treatment for PMP, there clearly needs to be additional patients enrolled in a larger clinical study to properly assess the effect of antibiotic treatment on PMP disease.

En masse, the study presented herein characterized a previously unknown aspect of PMP. As a result of our sequence-based analysis, direct detection of bacterial taxa by ISH, and culturing efforts, we have identified a possible novel avenue for treating this deadly disease. While these findings are strongly suggestive, much work needs to be done to better understand the role of bacteria in PMP disease.

Acknowledgments

During the writing of this manuscript, Dr. Andre Dubois passed away unexpectedly. Though ill for a length of time, Dr. Dubois did not want others to be concerned about him and was silent about this fact. Throughout his illness, he worked diligently and passionately on the PMP research. His wisdom, generosity and expertise will be sorely missed by his colleagues and the research community. This work was supported by R0832L, which was funded by Uniformed Services University, as well as funding from the US Military Cancer Institute.

Figure 32 (S1). Observed richness in PMP samples. Rarefaction curves of the observed richness in each of the tumor (**A**) and mucin (**B**) samples. The number of OTUs (y-axis) vs sampling depth (x-axis) is shown.

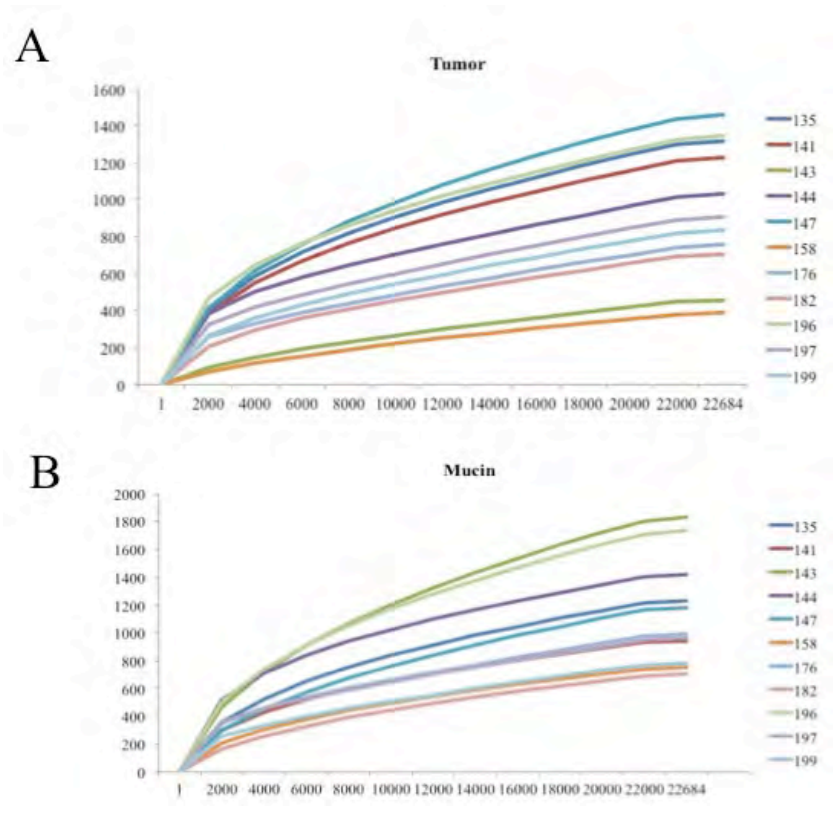


Figure 32. Observed richness in PMP samples

Table 17. (S1) Core microbiome by patient

PMP CORE MICROBIOME													
taxlevel	taxon	total seqs	PMP Patient										
			135	141	143	144	147	158	176	182	196	197	199
1	Bacteria	941151	44786	101360	95784	71326	92474	141553	70443	109509	68398	63308	82210
2	Actinobacteria	142834	3519	2439	16176	18766	4368	4596	19882	11693	20828	19774	20793
3	Actinobacteria	142834	3519	2439	16176	18766	4368	4596	19882	11693	20828	19774	20793
4	Actinomycetales	142834	3519	2439	16176	18766	4368	4596	19882	11693	20828	19774	20793
5	Microbacteriaceae	19392	624	403	14687	552	951	127	584	74	655	439	296
6	Microbacterium	1306	51	184	140	132	235	3	179	1	144	175	62
6	unclassified	18086	573	219	14547	420	716	124	405	73	511	264	234
5	Propionibacteriaceae	123442	2895	2036	1489	18214	3417	4469	19298	11619	20173	19335	20497
6	Propionibacterium	81731	893	1373	440	14357	1027	1912	14289	5331	15151	15135	11823
6	Tessarcoccus	41711	2002	663	1049	3857	2390	2557	5009	6288	5022	4200	8674
2	Bacteroidetes	21145	982	3299	1416	2730	5472	198	1875	300	2164	1720	989
3	Sphingobacteria	15662	655	3029	878	1479	5145	159	1263	246	1361	846	601
4	Sphingobacteriales	15662	655	3029	878	1479	5145	159	1263	246	1361	846	601
5	Saprosiraceae	5883	116	1998	94	159	2979	11	147	75	152	1	151
6	Hallscomenobacter	5883	116	1998	94	159	2979	11	147	75	152	1	151
5	Chitinophagaceae	2587	66	564	76	160	1341	33	57	17	111	37	125
6	Terrimonas	2587	66	564	76	160	1341	33	57	17	111	37	125
5	Cytophagaceae	3894	147	46	307	660	204	83	664	55	840	697	191
6	Arcicella	1904	45	26	148	315	181	46	229	22	437	350	105
6	Flectobacillus	1990	102	20	159	345	23	37	435	33	403	347	86
5	Sphingobacteriaceae	834	2	9	41	141	3	14	305	44	211	49	15
6	Pedobacter	834	2	9	41	141	3	14	305	44	211	49	15
5	unclassified	2464	324	412	360	359	618	18	90	55	47	62	119
6	unclassified	2464	324	412	360	359	618	18	90	55	47	62	119
3	Flavobacteria	5483	327	270	538	1251	327	39	612	54	803	874	388
4	Flavobacteriales	5483	327	270	538	1251	327	39	612	54	803	874	388
5	Flavobacteriaceae	5483	327	270	538	1251	327	39	612	54	803	874	388
6	Flavobacterium	5483	327	270	538	1251	327	39	612	54	803	874	388
2	Proteobacteria	721710	29328	91740	74200	45311	63133	135968	45524	96214	42619	39604	58069
3	Alphaproteobacteria	115437	761	27438	9287	9690	18950	13725	3346	23313	3467	2802	2658
4	Rhizobiales	106626	590	27232	6369	7740	18704	13384	2604	23141	2437	2350	2075
5	Methylbacteriaceae	106626	590	27232	6369	7740	18704	13384	2604	23141	2437	2350	2075
6	Methylbacterium	106626	590	27232	6369	7740	18704	13384	2604	23141	2437	2350	2075
4	Rhodospirillales	633	4	29	7	48	4	33	144	10	185	83	86
5	Acetobacteraceae	633	4	29	7	48	4	33	144	10	185	83	86
6	Roseomonas	633	4	29	7	48	4	33	144	10	185	83	86
4	Sphingomonadales	8178	167	177	2911	1902	242	308	598	162	845	369	497
5	Sphingomonadaceae	8178	167	177	2911	1902	242	308	598	162	845	369	497
6	Sphingomonas	6731	146	113	2910	1685	216	182	497	120	550	176	136
6	unclassified	1447	21	64	1	217	26	126	101	42	295	193	361
3	Betaproteobacteria	275417	4035	51676	8729	17192	34982	31766	12777	63928	13780	12375	24177
4	Burkholderiales	255953	3237	47179	8563	15417	30563	31588	11977	63198	12289	9603	22339
5	Burkholderiaceae	72253	355	39980	763	3400	21647	540	1124	980	1198	756	1510
6	Ralstonia	2372	58	306	153	725	137	180	127	174	181	121	210
6	unclassified	69881	297	39674	610	2675	21510	360	997	806	1017	635	1300
5	Comamonadaceae	145981	2241	3307	6624	9161	4929	30567	6872	61332	9697	7173	4078
6	Acidovorax	15911	660	1752	3650	1800	2866	344	619	681	1483	1069	987
6	Curvibacter	3149	267	186	451	665	326	225	218	16	300	303	192
6	Delftia	2904	32	14	21	623	17	89	1186	9	565	186	162
6	Diaphorobacter	4616	41	1	22	193	7	153	618	478	2296	44	763
6	Limnohabitans	4453	314	378	679	1238	435	174	228	98	399	325	185
6	Polaromonas	5046	144	109	193	752	136	417	285	419	1219	1076	296
6	Variovorax	104621	575	662	1361	3236	865	28999	2689	59409	2787	2947	1091
6	unclassified	5281	208	205	247	654	277	166	1029	222	648	1223	402
5	unclassified	37719	641	3892	1176	2856	3987	481	3981	886	1394	1674	16751
6	unclassified	37719	641	3892	1176	2856	3987	481	3981	886	1394	1674	16751
4	Hydrogenophilales	2865	17	74	2	445	12	6	170	223	276	816	824
5	Hydrogenophilaceae	2865	17	74	2	445	12	6	170	223	276	816	824
6	Hydrogenophilus	2865	17	74	2	445	12	6	170	223	276	816	824
4	Methylophilales	10486	587	2941	101	1043	2883	7	312	197	793	1404	218
5	Methylophilaceae	10486	587	2941	101	1043	2883	7	312	197	793	1404	218
6	Methylophilus	4389	495	499	40	628	301	1	279	145	628	1224	149
6	Methylotenera	6097	92	2442	61	415	2582	6	33	52	165	180	69
4	Rhodocyclales	1663	34	49	10	28	101	103	206	195	141	159	637
5	Rhodocyclaceae	1663	34	49	10	28	101	103	206	195	141	159	637
6	Zoogloea	1663	34	49	10	28	101	103	206	195	141	159	637
4	unclassified	4450	160	1433	53	259	1423	62	112	115	281	393	159
5	unclassified	4450	160	1433	53	259	1423	62	112	115	281	393	159
6	unclassified	4450	160	1433	53	259	1423	62	112	115	281	393	159

Table 17. (S1) (cont.)

	taxon	total seqs	PMP Patient										
			135	141	143	144	147	158	176	182	196	197	199
3	Deltaproteobacteria	2288	12	148	15	283	59	93	354	106	569	448	201
4	Bdellovibrionales	2288	12	148	15	283	59	93	354	106	569	448	201
5	Bdellovibrionaceae	2288	12	148	15	283	59	93	354	106	569	448	201
6	Bdellovibrio	2288	12	148	15	283	59	93	354	106	569	448	201
3	Epsilonproteobacteria	34289	27	6990	975	3467	653	434	4945	521	4355	6873	5049
4	Campylobacterales	34289	27	6990	975	3467	653	434	4945	521	4355	6873	5049
5	Campylobacteraceae	848	11	5	69	142	55	47	138	33	163	57	128
6	Arcobacter	848	11	5	69	142	55	47	138	33	163	57	128
5	Helicobacteraceae	33441	16	6985	906	3325	598	387	4807	488	4192	6816	4921
6	Helicobacter	33441	16	6985	906	3325	598	387	4807	488	4192	6816	4921
3	Gammaproteobacteria	285025	24403	2251	55089	14108	5078	89765	23757	8058	19987	16786	25743
4	Enterobacteriales	107398	693	465	656	1829	1093	88561	3155	1904	1886	2270	4886
5	Enterobacteriaceae	107398	693	465	656	1829	1093	88561	3155	1904	1886	2270	4886
6	Escherichia_Shigella	88823	302	343	360	1660	417	73796	2583	1528	1576	2012	4246
6	unclassified	18575	391	122	296	169	676	14765	572	376	310	258	640
4	Alteromonadales	42103	17755	216	142	2208	282	208	3965	1447	4887	3009	7984
5	Alteromonadaceae	42103	17755	216	142	2208	282	208	3965	1447	4887	3009	7984
6	unclassified	42103	17755	216	142	2208	282	208	3965	1447	4887	3009	7984
4	Chromatiales	424	79	17	17	2208	6	60	1	31	15	107	37
5	unclassified	424	79	17	17	2208	6	60	1	31	15	107	37
6	unclassified	424	79	17	17	2208	6	60	1	31	15	107	37
4	Pseudomonadales	108442	4697	795	53329	2208	2892	559	13472	3489	8495	5474	9205
5	Moraxellaceae	44405	1338	538	839	2208	399	211	12912	2420	7711	4917	8382
6	Acinetobacter	35628	1334	359	832	2208	392	190	11835	2365	6521	3361	4867
6	Moraxella	8777	4	179	7	2208	7	21	1077	55	1190	1556	3515
5	Pseudomonadaceae	64037	3359	257	52490	2208	2493	348	560	1069	784	557	823
6	Pseudomonas	64037	3359	257	52490	2208	2493	348	560	1069	784	557	823
4	Xanthomonadales	4565	67	145	11	2208	88	103	1259	240	951	345	475
5	Xanthomonadaceae	4565	67	145	11	2208	88	103	1259	240	951	345	475
6	Stenotrophomonas	4565	67	145	11	2208	88	103	1259	240	951	345	475
4	unclassified	22093	1112	613	934	2208	717	274	1905	947	3753	5581	3156
5	unclassified	22093	1112	613	934	2208	717	274	1905	947	3753	5581	3156
6	unclassified	22093	1112	613	934	2208	717	274	1905	947	3753	5581	3156
3	unclassified	9254	90	3237	105	2208	3411	185	345	288	461	320	241
4	unclassified	9254	90	3237	105	2208	3411	185	345	288	461	320	241
5	unclassified	9254	90	3237	105	2208	3411	185	345	288	461	320	241
6	unclassified	9254	90	3237	105	2208	3411	185	345	288	461	320	241
2	Firmicutes	53508	10849	3640	3887	4112	19375	730	2815	1229	2513	2147	2211
3	Bacilli	39109	5488	2116	1704	2812	17558	699	1531	1067	2123	2053	1958
4	Bacillales	13232	4716	1855	1344	1609	1706	265	213	283	256	307	678
5	Paenibacillaceae_1	4674	880	726	13	1344	21	204	181	275	205	216	609
6	Brevibacillus	4674	880	726	13	1344	21	204	181	275	205	216	609
5	unclassified	8558	3836	1129	1331	265	1685	61	32	8	51	91	69
6	unclassified	8558	3836	1129	1331	265	1685	61	32	8	51	91	69
4	Lactobacillales	20614	622	142	307	662	14443	320	880	586	992	770	890
5	Lactobacillaceae	777	140	5	35	47	119	31	73	59	116	80	72
6	Lactobacillus	777	140	5	35	47	119	31	73	59	116	80	72
5	Streptococcaceae	18754	434	112	217	583	14191	262	582	438	744	506	685
6	Lactococcus	767	38	29	14	98	58	18	122	29	251	109	1
6	Streptococcus	17987	396	83	203	485	14133	244	460	409	493	397	684
5	unclassified	1083	48	25	55	32	133	27	225	89	132	184	133
6	unclassified	1083	48	25	55	32	133	27	225	89	132	184	133
4	unclassified	5263	150	119	53	541	1409	114	438	198	875	976	390
5	unclassified	5263	150	119	53	541	1409	114	438	198	875	976	390
6	unclassified	5263	150	119	53	541	1409	114	438	198	875	976	390
3	unclassified	14399	5361	1524	2183	1300	1817	31	1284	162	390	94	253
4	unclassified	14399	5361	1524	2183	1300	1817	31	1284	162	390	94	253
5	unclassified	14399	5361	1524	2183	1300	1817	31	1284	162	390	94	253
6	unclassified	14399	5361	1524	2183	1300	1817	31	1284	162	390	94	253

-taxlevel indicates the taxonomic depth of each nomenclature

Table 18 (S2) Sample-by-sample breakdown of OTUs detected

References

1. **Blaser, M. J.** 1990. *Helicobacter pylori* and the pathogenesis of gastroduodenal inflammation. *J Infect Dis* **161**:626-33.
2. **Caporaso, J. G., C. L. Lauber, E. K. Costello, D. Berg-Lyons, A. Gonzalez, J. Stombaugh, D. Knights, P. Gajer, J. Ravel, N. Fierer, J. I. Gordon, and R. Knight.** 2011. Moving pictures of the human microbiome. *Genome Biol* **12**:R50.
3. **Castellarin, M., R. L. Warren, J. D. Freeman, L. Dreolini, M. Krzywinski, J. Strauss, R. Barnes, P. Watson, E. Allen-Vercoe, R. A. Moore, and R. A. Holt.** 2012. *Fusobacterium nucleatum* infection is prevalent in human colorectal carcinoma. *Genome Res* **22**:299-306.
4. **Choudry, H. A., M. E. O'Malley, Z. S. Guo, H. J. Zeh, and D. L. Bartlett.** 2012. Mucin as a therapeutic target in pseudomyxoma peritonei. *J Surg Oncol*.
5. **Costello, E. K., C. L. Lauber, M. Hamady, N. Fierer, J. I. Gordon, and R. Knight.** 2009. Bacterial community variation in human body habitats across space and time. *Science* **326**:1694-7.
6. **Cox, M. J., M. Allgaier, B. Taylor, M. S. Baek, Y. J. Huang, R. A. Daly, U. Karaoz, G. L. Andersen, R. Brown, K. E. Fujimura, B. Wu, D. Tran, J. Koff, M. E.**

Kleinhenz, D. Nielson, E. L. Brodie, and S. V. Lynch. 2010. Airway microbiota and pathogen abundance in age-stratified cystic fibrosis patients. *PLoS One* **5**:e11044.

7. **Dethlefsen, L., M. McFall-Ngai, and D. A. Relman.** 2007. An ecological and evolutionary perspective on human-microbe mutualism and disease. *Nature* **449**:811-8.

8. **Dethlefsen, L., and D. A. Relman.** 2011. Incomplete recovery and individualized responses of the human distal gut microbiota to repeated antibiotic perturbation. *Proc Natl Acad Sci U S A* **108 Suppl 1**:4554-61.

9. **Duan, K., C. Dammel, J. Stein, H. Rabin, and M. G. Surette.** 2003. Modulation of *Pseudomonas aeruginosa* gene expression by host microflora through interspecies communication. *Mol Microbiol* **50**:1477-91.

10. **Eckburg, P. B., and D. A. Relman.** 2007. The role of microbes in Crohn's disease. *Clin Infect Dis* **44**:256-62.

11. **Fassi Fehri, L., T. N. Mak, B. Laube, V. Brinkmann, L. A. Ogilvie, H. Mollenkopf, M. Lein, T. Schmidt, T. F. Meyer, and H. Bruggemann.** 2011. Prevalence of *Propionibacterium acnes* in diseased prostates and its inflammatory and transforming activity on prostate epithelial cells. *Int J Med Microbiol* **301**:69-78.

12. **Friedline, C. J., R.B. Franklin, S.L. McCallister, and M.C. Rivera.** 2012. Microbial community diversity of the eastern Atlantic Ocean reveals geographic differences. *Biogeosci Discuss* **9**:109-150.

13. **Giardine, B., C. Riemer, R. C. Hardison, R. Burhans, L. Elnitski, P. Shah, Y. Zhang, D. Blankenberg, I. Albert, J. Taylor, W. Miller, W. J. Kent, and A. Nekrutenko.** 2005. Galaxy: a platform for interactive large-scale genome analysis. *Genome Res* **15**:1451-5.

14. **Gough, D. B., J. H. Donohue, A. J. Schutt, N. Gonchoroff, J. R. Goellner, T. O. Wilson, J. M. Naessens, P. C. O'Brien, and J. A. van Heerden.** 1994. Pseudomyxoma peritonei. Long-term patient survival with an aggressive regional approach. *Ann Surg* **219**:112-9.

15. **Halabi, H. E., V. Gushchin, J. Francis, N. Athas, R. Macdonald, C. Nieroda, K. Studeman, and A. Sardi.** 2012. Prognostic significance of lymph node metastases in patients with high-grade appendiceal cancer. *Ann Surg Oncol* **19**:122-5.

16. **Hardwick, R. H., A. Taylor, M. H. Thompson, E. Jones, and A. M. Roe.** 2000. Association between *Streptococcus milleri* and abscess formation after appendicitis. *Ann R Coll Surg Engl* **82**:24-6.

17. **Hatakeyama, M.** 2004. Oncogenic mechanisms of the *Helicobacter pylori* CagA protein. *Nat Rev Cancer* **4**:688-94.

18. **Huang, Y. J., E. Kim, M. J. Cox, E. L. Brodie, R. Brown, J. P. Wiener-Kronish, and S. V. Lynch.** 2010. A persistent and diverse airway microbiota present during chronic obstructive pulmonary disease exacerbations. *OMICS* **14**:9-59.

19. **Huse, S. M., L. Dethlefsen, J. A. Huber, D. Mark Welch, D. A. Relman, and M. L. Sogin.** 2008. Exploring microbial diversity and taxonomy using SSU rRNA hypervariable tag sequencing. *PLoS Genet* **4**:e1000255.

20. **Kostic, A. D., D. Gevers, C. S. Pedomallu, M. Michaud, F. Duke, A. M. Earl, A. I. Ojesina, J. Jung, A. J. Bass, J. Taberner, J. Baselga, C. Liu, R. A. Shivdasani, S. Ogino, B. W. Birren, C. Huttenhower, W. S. Garrett, and M. Meyerson.** 2012. Genomic analysis identifies association of *Fusobacterium* with colorectal carcinoma. *Genome Res* **22**:292-8.

21. **Loungnarath, R., S. Causeret, N. Bossard, M. Faheez, A. C. Sayag-Beaujard, C. Brigand, F. Gilly, and O. Glehen.** 2005. Cytoreductive surgery with intraperitoneal chemohyperthermia for the treatment of pseudomyxoma peritonei: a prospective study. *Dis Colon Rectum* **48**:1372-9.

22. **Loungnarath, R., S. Causeret, C. Brigand, F. N. Gilly, and O. Glehen.** 2005. Pseudomyxoma peritonei: new concept and new therapeutic approach. *Ann Chir* **130**:63-9.
23. **Molina, J. M., C. Leport, A. Bure, M. Wolff, C. Michon, and J. L. Vilde.** 1991. Clinical and bacterial features of infections caused by *Streptococcus milleri*. *Scand J Infect Dis* **23**:659-66.
24. **O'Connell, J. T., J. S. Tomlinson, A. A. Roberts, K. F. McGonigle, and S. H. Barsky.** 2002. Pseudomyxoma peritonei is a disease of MUC2-expressing goblet cells. *Am J Pathol* **161**:551-64.
25. **Parkins, M. D., C. D. Sibley, M. G. Surette, and H. R. Rabin.** 2008. The *Streptococcus milleri* group--an unrecognized cause of disease in cystic fibrosis: a case series and literature review. *Pediatr Pulmonol* **43**:490-7.
26. **Ravel, J., P. Gajer, Z. Abdo, G. M. Schneider, S. S. Koenig, S. L. McCulle, S. Karlebach, R. Gorle, J. Russell, C. O. Tacket, R. M. Brotman, C. C. Davis, K. Ault, L. Peralta, and L. J. Forney.** 2011. Vaginal microbiome of reproductive-age women. *Proc Natl Acad Sci U S A* **108 Suppl 1**:4680-7.
27. **Ronnett, B. M., C. M. Zahn, R. J. Kurman, M. E. Kass, P. H. Sugarbaker, and B. M. Shmookler.** 1995. Disseminated peritoneal adenomucinosis and peritoneal

mucinous carcinomatosis. A clinicopathologic analysis of 109 cases with emphasis on distinguishing pathologic features, site of origin, prognosis, and relationship to "pseudomyxoma peritonei". *Am J Surg Pathol* **19**:1390-408.

28. **Scanlan, P. D., F. Shanahan, C. O'Mahony, and J. R. Marchesi.** 2006. Culture-independent analyses of temporal variation of the dominant fecal microbiota and targeted bacterial subgroups in Crohn's disease. *J Clin Microbiol* **44**:3980-8.
29. **Schloss, P. D., S. L. Westcott, T. Ryabin, J. R. Hall, M. Hartmann, E. B. Hollister, R. A. Lesniewski, B. B. Oakley, D. H. Parks, C. J. Robinson, J. W. Sahl, B. Stres, G. G. Thallinger, D. J. Van Horn, and C. F. Weber.** 2009. Introducing mothur: open-source, platform-independent, community-supported software for describing and comparing microbial communities. *Appl Environ Microbiol* **75**:7537-41.
30. **Semino-Mora, C., H. Liu, T. McAvoy, C. Nieroda, K. Studeman, A. Sardi, and A. Dubois.** 2008. Pseudomyxoma peritonei: is disease progression related to microbial agents? A study of bacteria, MUC2 AND MUC5AC expression in disseminated peritoneal adenomucinosis and peritoneal mucinous carcinomatosis. *Ann Surg Oncol* **15**:1414-23.
31. **Shen, P., J. Hawksworth, J. Lovato, B. W. Loggie, K. R. Geisinger, R. A. Fleming, and E. A. Levine.** 2004. Cytoreductive surgery and intraperitoneal

hyperthermic chemotherapy with mitomycin C for peritoneal carcinomatosis from nonappendiceal colorectal carcinoma. *Ann Surg Oncol* **11**:178-86.

32. **Shinzato, T., and A. Saito.** 1995. The *Streptococcus milleri* group as a cause of pulmonary infections. *Clin Infect Dis* **21 Suppl 3**:S238-43.

33. **Sibley, C. D., M. D. Parkins, H. R. Rabin, K. Duan, J. C. Norgaard, and M. G. Surette.** 2008. A polymicrobial perspective of pulmonary infections exposes an enigmatic pathogen in cystic fibrosis patients. *Proc Natl Acad Sci U S A* **105**:15070-5.

34. **Tannock, G. W., K. Munro, H. J. Harmsen, G. W. Welling, J. Smart, and P. K. Gopal.** 2000. Analysis of the fecal microflora of human subjects consuming a probiotic product containing *Lactobacillus rhamnosus* DR20. *Appl Environ Microbiol* **66**:2578-88.

35. **Wang, Q., G. M. Garrity, J. M. Tiedje, and J. R. Cole.** 2007. Naive Bayesian classifier for rapid assignment of rRNA sequences into the new bacterial taxonomy. *Appl Environ Microbiol* **73**:5261-7.

36. **White, J. R., N. Nagarajan, and M. Pop.** 2009. Statistical methods for detecting differentially abundant features in clinical metagenomic samples. *PLoS Comput Biol* **5**:e1000352.

37. **Witkamp, A. J., E. de Bree, M. M. Kaag, G. W. van Slooten, F. van Coevorden, and F. A. Zoetmulder.** 2001. Extensive surgical cytoreduction and intraoperative hyperthermic intraperitoneal chemotherapy in patients with pseudomyxoma peritonei. *Br J Surg* **88**:458-63.